Available online at www.sciencedirect.com
ScienceDirect
Organic Geochemistry 38 (2007) 719–833
Organic Geochemistry
www.elsevier.com/locate/orggeochem

Review

Kerogen origin, evolution and structure

M. Vandenbroucke [a,*], C. Largeau [b,*]

[a] IFP, Geology-Geochemistry-Geophysics Direction, 1-4 Avenue de Bois Preau, 92852 Rueil-Malmaison Cedex, France
[b] UMR CNRS 7618 BIOEMCO, ENSCP, 11 Rue P. et M. Curie, 75231 Paris Cedex 05, France

Received 28 April 2006; received in revised form 27 November 2006; accepted 9 January 2007
Available online 16 January 2007

Abstract

Kerogen, commonly defined as the insoluble macromolecular organic matter (OM) dispersed in sedimentary rocks, is by far the most abundant form of OM on Earth. This fossil material is of prime importance as the source of oil and natural gas; moreover, kerogen can provide essential information on major topics such as past environments, climates and biota. This review reports the main advances in kerogen studies since the comprehensive synthesis edited by Durand [Durand, B. (Ed.), Kerogen, Insoluble Organic Matter from Sedimentary Rocks. Editions Technip, Paris, 1980.]. It is organized into eight sections. The first two are concerned with the successive definitions of kerogen and the definition used here, the different techniques used for kerogen isolation without loss or degradation and basic kerogen analysis. The third and fourth focus on sedimentary OM sources and preservation processes in relation to depositional environment, including sedimentation conditions favourable for kerogen accumulation, and extrapolation to past geological time. Great strides have been made in the latter topics over the last 25 years, owing to a combination of classical studies in organic geochemistry and studies in other domains such as biogeochemistry, oceanography, hydrology and soil science, along with the development of powerful analytical tools. The next two sections deal with the different kerogen classifications by type and kerogen evolution and maturation upon burial in sediments. Structural modelling of coal and kerogen, based on physical and/or chemical structural analysis, is described in the following section. Although, only statistical, the models thus derived provide a synthetic view of the main structural resemblances and differences among various samples in relation to source, maturity or physicochemical properties. Finally, the last section explores some of the advances in kerogen understanding expected for the near future. The review includes a list containing about 500 references.

Contents

* Corresponding authors.
E-mail addresses: mg.vdb@tiscali.fr (M. Vandenbroucke), cllargeau@wanadoo.fr (C. Largeau).

0146-6380/$ - see front matter © 2007 Elsevier Ltd. All rights reserved.
doi:10.1016/j.orggeochem.2007.01.001

1. Introduction

Kerogen is the sedimentary organic matter (OM) which generates petroleum and natural gas. In this respect, many efforts have been devoted to its isolation and to the characterization of its chemical structure and evolution during sediment burial, aiming at a better prediction of oil and gas pools. Great advances have been achieved with respect to the prediction of oil and gas potential and the simulation of petroleum systems. This conceptual definition implies that kerogen and petroleum have complementary characteristics. Accordingly, petroleum (and more generally bitumen) is soluble in the usual organic solvents, whereas kerogen is the sedimentary OM insoluble in these solvents. With kerogen being a complex mixture of organic materials tightly mixed with minerals in sediments, progress in its study has not only been linked to the development of oil exploration via geological sample availability, but also to the huge increase in analytical capabilities during the last 40 years. However, despite the numerous advances made with respect to kerogen knowledge, important points are still far from being elucidated.

Kerogen is a major sink in the global carbon cycle and represents by far the largest OM pool on Earth – 10^{16} tons of C compared to ca. 10^{12} tons in living biomass (Durand, 1980). Accordingly, besides petroleum research, scientists from different disciplines like biogeochemistry, oceanography, hydrology and soil science have been interested in

the processes of OM incorporation into sediments. This has been the source of major advances in kerogen knowledge, such as (i) understanding the relationships between primary productivity, sedimentary OM preservation and planetary driving factors for climatology, (ii) analysis of transportation processes and biochemical alteration of dissolved vs. particulate OM, (iii) contribution of selective preservation of protective tissues to kerogen and (iv) early evolution of OM composition in sediments. The present review describes some of these major advances, realised over the last twenty-five years since the synthesis edited by Durand (1980). Kerogen isolation and bulk characterization are described first in order to define precisely possible limitations in interpretation resulting from various isolation procedures. Other analytical methods are considered only through their applications but are not specifically described. The next section is focussed on kerogen sources and composition, and their variation with geological time and sedimentary environment. The evolution of ideas on mechanisms of OM preservation and the resulting kerogen precursors, which have largely changed since the 1980s, are then discussed. The resulting classifications of kerogen, and their advantages and drawbacks, as well as kerogen transformation during sediment burial, are also presented. Laboratory simulation of maturation using pyrolysis techniques is discussed briefly because laboratory simulation and molecular analysis and quantification of resulting petroleum products have been developed mainly after 1980 (although geological maturation was already largely described in publications from the 1970s). Kinetic modelling of kerogen cracking is not discussed because it is not relevant to the aims of the present review (for more information concerning this topic, see Benson, 1960; Ungerer, 1993; Schenk et al., 1997; Behar et al., 1997, 2003; Burnham and Braun, 1999, and references therein). The last section is focussed on structural modelling of kerogen, in comparison with earlier studies of coal. Finally, future research and expected advances are discussed, including new analytical techniques.

2. Definition of kerogen

2.1. History of successive definitions

2.1.1. Pioneering work

The word kerogen was first coined by Crum Brown (1912; personal communication to Carruthers et al., 1912, p. 143) to describe the OM of a Scottish oil shale that produced a waxy oil upon distillation (keros = wax) and was restricted to organic-rich rocks of economic importance. Recognizing that OM in sedimentary rocks, even at low concentration, can generate oil via artificial pyrolysis or burial for long periods of time, White (1915), then Trager (1924), extended this early definition to all OM in rocks capable of oil generation. At this stage kerogen was considered "a convenient name for the OM from which oil is obtained when rocks containing it are heated" (Down and Himus, 1941). However, some inherent problems arose, as stressed by these latter authors, since OM in sedimentary rocks can comprise both kerogen that has yet to generate oil as well as oil already generated. Later, Breger (1960) proposed a definition based on the chemical composition of organic precursors of kerogen regardless of sediment OM content. Recognizing the main constituents of living OM, he defined those having the best probability of escaping biodegradation to be preserved as kerogen (i.e., lignin, pigments and lipids). He proposed mechanisms by which these functionalized compounds could generate oil. However, this concept still did not address the problem mentioned above regarding the co-occurrence of oil and insoluble compounds in sedimentary rocks.

2.1.2. Present day definitions

The modern definition, by Forsman and Hunt (1958), took this problem into account, and kerogen was defined as the dispersed OM of ancient sediments insoluble in the usual organic solvents, in contrast to extractable OM. This dispersed insoluble material accounts by far for the largest pool of sedimentary OM compared to other forms like coal or gas and more or less soluble fractions such as oil and asphalts (Fig. 1; Durand, 1980).

The definition was later extended by Durand (1980) to all insoluble sedimentary organic material, including not only that dispersed in sedimentary rocks but also "pure" organic deposits such as humic and algal coals, and various asphaltic substances, as well as the insoluble OM in recent sediments and even in soil. The rationale was that all these substances represent various stages in the same transformation process of sedimentary OM upon burial. This definition aimed at accounting for kerogen organic precursors and preservation processes in relation to depositional environment, as well as at highlighting the interrelationship

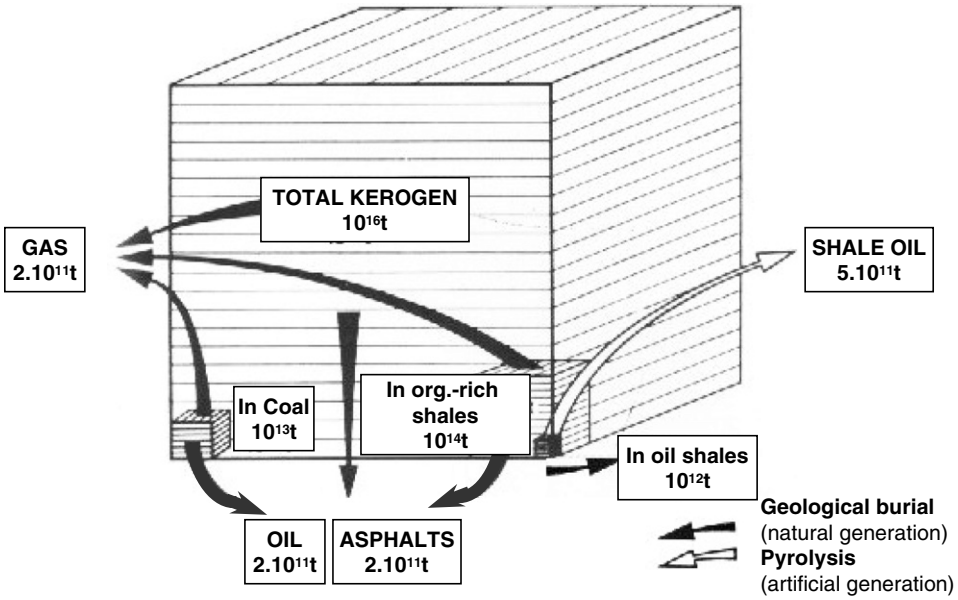

Fig. 1. Comparison of amounts of dispersed kerogen and ultimate resources of fossil fuels. Adapted from Durand (1980).

between kerogen, its precursors and its transformation products. Ambiguities resulting from the modern definition based on solubility are discussed below.

2.1.3. Dependence of definition upon experimental procedure

A major drawback of this pragmatic definition, based on kerogen insolubility in "common organic solvents", contrary to oil or bitumen, is that the amount and chemical structure of both this fraction and the associated soluble fraction differ according to the extraction method used. In fact, there is no established standard protocol regarding solvent characteristics, extraction conditions and solvent to rock proportion. This introduces great variability among different laboratories. Furthermore, extraction is never "complete" and depends not only on the polarity of the solvent but also on the analytical procedure, including sample grinding, and temperature and duration of extraction and stirring. Polar solvents like $CHCl_3$ or C_6H_6/CH_3OH mixtures, used in early studies, have been almost completely abandoned due to their toxicity. Slightly polar solvents with rather low boiling point are generally used, like CH_2Cl_2, sometimes mixed with CH_3OH, because the recovered bitumen contains mainly hydrocarbons, most of which can be extracted efficiently in this way for further analysis. Other more polar compounds, such as resins and asphaltenes, are also extracted, but their yield is highly dependent on extraction conditions. This is also true with solvents of greater polarity frequently used by coal scientists, like pyridine. Pyridine can swell coal structure and afford, in some cases, extraction yields up to 50% by weight, whereas CH_2Cl_2 only extracts a few % of the same coal sample (Van Krevelen, 1993, Chapter 19). The composition and chemical features of kerogen are closely dependent on the solvent used for its isolation and analytical data can be compared only if the same solvent is used. Alternatively, if a special need is perceived with respect to extracting selectively fractions of interest, then solvent choice will be dictated by such needs as, for example, when pyridine is used to maximize extraction from humic coals.

Another problem related to this operational definition is the sequence in the protocol used for the isolation of kerogen. Isolation generally requires chemical destruction of the associated minerals. This is performed on the whole rock, prior to or after organic solvent extraction. In both cases, an additional extraction step is needed after mineral destruction, since hydrogen bonds are broken, or even hydrolysis occur to some extent. Furthermore, the three dimensional structure of kerogen undergoes some change during the removal of the mineral matrix, liberating extractable trapped compounds. Hence, the chemistry of the isolated kerogen will be influenced by the sequence in the protocol used.

2.1.4. Occurrence of other insoluble non-kerogen sedimentary OM

While kerogen is often defined as the potential source of oil and gas, the extended operational definition of Durand (1980) includes other sedimentary OM, isolated on the basis of insolubility, that may or may not be able to contribute to oil or gas formation during its geological history. Two such situations can exist. The first involves mobile allochthonous OM that migrates into a non-reservoir rock (a fracture, for example) and becomes insoluble for some physicochemical reason. This may occur with tars, asphaltites and pyrobitumens that are part of the products generated via maturation and alteration processes and are not themselves the generating substances. These products may be mixed with autochthonous sedimentary OM, confounding a clear unambiguous assignment. The second situation involves the presence of insoluble OM in immature materials. Due to the high content of oxygenated functional groups, part of the OM in recent sediments is only sparingly soluble in many non-oxygenated organic solvents and is sensitive to hydrolysis. Accordingly, the most common solvent for rock extraction, CH_2Cl_2, is not suitable for the separation of soluble and insoluble fractions from such low maturity samples. The extraction method set up by those working on soil OM was thus applied to recent sediments. It is based on the partial solubility of low molecular weight polar substances in acidic or alkaline aqueous solutions (Kononova, 1966; Stevenson and Butler, 1969). Three classes of compounds are usually separated: fulvic acids (soluble in both base and acid solutions), humic acids (base-soluble but acid-insoluble) and finally humin (insoluble in both basic and acidic solutions). Humin from recent sediments should thus be closely related to kerogen in ancient sediments and, consequently, is often called 'protokerogen', but this relationship is not fully understood. In fact, the use of the terms kerogen, humin or protokerogen in the relevant literature, added to different choices of solvent strength, results in ambiguity in the definition and comparison of organic fractions. Moreover, using the same isolation procedure does not mean that humin from recent sediments is similar to humin from soil. Even if soil weathering and river transportation can carry soil OM into aquatic sedimentary environments, the alteration processes during transportation will strongly modify the initial soil OM before its final incorporation into the sediment. Accordingly, whereas humin from recent sediments can be considered as a major constituent of the future kerogen, this is generally not the case for humin from soils, although the extended definition of kerogen by Durand (1980) mentions explicitly the notion of insoluble OM from both recent sediments and soils. An exception to transport should, however, be made for massive humic and algal coals, the sedimentation of which can occur in situ within swamps and shallow lakes from coastal settings, or slowly subsiding basins. In immature coals, humin accounts for the major part of the humic compounds, in sharp contrast to OM from soils, where humic and fulvic acids often predominate. Therefore, we use in the present review the extended definition of Durand (1980) for kerogen, but excluding soil humin.

2.1.5. Consequences of extended definition on distinction between kerogen formation and evolution

The earlier definitions of kerogen, based on petroleum production, did not allow distinction between kerogen formation and kerogen evolution in shallow sediments. In fact, these definitions did not imply any hypothesis about kerogen precursors, formation processes and incorporation into recent sediments as they were related to a further stage in the evolution of sedimentary OM, principally thermal stress at depth. Such a distinction also cannot be achieved using either the definition of Forsman and Hunt (1958) or the extended definition of Durand (1980) based on insolubility. The latter feature is largely related to the macromolecular nature of kerogens and to the solvent used for extraction. However, there is a continuum between living biomass and the fossil macromolecular OM finally preserved in ancient immature sediments as kerogen. Indeed, from the death of photosynthetic organisms to recycling in the water column, sedimentation and finally burial, along with addition of materials from successive populations of heterotrophs, the chemical structure of the macromolecular insoluble OM continuously changes, due to both condensation and degradation reactions. There is still a continuous transformation upon burial between solvent-soluble and solvent-insoluble molecular constituents of the organic debris as soon as they are incorporated into sediments. Therefore, we do not discuss kerogen "formation" per se, because kerogen formation is a continuous process from organism death to the end of metagenesis. Instead, we consider "kerogen origin", i.e. the preservation mechanisms that allow a small percentage of the OM to escape reminerali-

zation and enter the sedimentary cycle, and their consequences for kerogen composition. Kerogen evolution will thus begin with early diagenesis, a transition stage in the first few meters of sediment where bacterial processes are still active. This stage was referred by Tissot and Welte (1978, Chapter 2) as early transformation, but as a part of diagenesis as a whole. It has special importance for the later composition and petroleum potential of kerogen because of changes, sometimes major, in sulfur and oxygen contents. Such changes, largely studied in relation to chemical structure (e.g. Sinninghe Damsté et al., 1998a; Adam et al., 2000), are referred to in the literature in two different ways, either as kerogen "formation" or kerogen "early diagenetic evolution", which has resulted in some confusion. Hence, the reason why in the title of this review we use "kerogen origin" and not "kerogen formation".

2.2. Summary

- Kerogen was first defined by its (a) relationship to petroleum, implying transformation from one into the other, (b) insolubility in organic solvents and (c) occurrence in ancient sedimentary rocks.
- This early definition was extended to OM in recent sediments to account for chemical specificity of organic precursors and preservation mechanisms in relation to depositional environment.
- The operational definition of kerogen, based on insolubility, results in the isolation of an organic fraction that may contain not only genuine sedimentary OM at any stage of its transformation into oil and gas, but also various inert residues unable to form oil or gas.
- With the extension of kerogen definition to recent sediments, OM incorporation into sediments is proposed as the limit between preservation mechanisms vs. evolution processes.

3. Kerogen isolation and bulk characterization

3.1. Isolation

As a result of the generally low concentration of kerogen in sedimentary rocks, the isolation of this dispersed macromolecular OM from associated minerals is a prerequisite for applying many of the analytical techniques first directly used for coal characterization. Several isolation or concentration procedures have been proposed, depending on the desired type of organic isolate and the analysis to be performed. These procedures can be subdivided into physical and chemical methods; detailed reviews can be found in Forsman (1963), Robinson (1969a) and Durand and Nicaise (1980).

3.1.1. Kerogen concentration via physical methods

Physical separation aims at avoiding any chemical alteration of OM during the concentration step. Many physical methods, by analogy with ore concentration techniques, are based either on specific gravity difference between OM (0.9–1.3 for most kerogens) and most minerals (ca. 2.5 for clay and silica, up to 5.0 for pyrite) or on differential wettability by water and hydrocarbons. These methods are applied to finely ground samples, but grinding can generate problems for subsequent microscopic analysis or can promote OM oxidation and loss. Sedimentary OM is tightly associated with minerals via physicochemical interactions or is embedded within mineral grains (Forsman, 1963). When first tested in the 1960s, physical separation appeared incomplete, with highly variable yields depending on kerogen Type and initial concentration, even after repeated processing. Moreover, the resulting kerogen concentrate exhibited a higher aliphatic to aromatic ratio than the total organic fraction, showing that chemical segregation occurred during density fractionation (Smith, 1961). Ultimately, such techniques proved to be useful for separating various macerals for comparing their geochemical features [see, for example, Stankiewicz et al. (1994, 1996)]. As described below, these authors also succeeded in efficiently eliminating pyrite from kerogen by density separation, after chemical destruction of the main minerals.

3.1.2. Kerogen concentration via chemical methods

These methods are based on the destruction of major minerals by non-oxidant acid attack at temperatures between 60 and 70 °C. Treatment is performed under an inert atmosphere to avoid OM oxidation. Reviews of the methods and their application to various rock samples can be found in Forsman and Hunt (1958), Saxby (1970) and Durand and Nicaise (1980). The most common consists in first destroying carbonate, sulfide, sulfate and hydroxides with 6 N HCl. Then, clay minerals, quartz and silicates are eliminated using a mixture

of 40% HF and 6 N HCl (1/2 v/v). Some residual minerals still remain after these treatments, including pyrite and minor heavy oxides such as zircon, rutile and anatase. In addition, newly formed fluorides resulting from the HF treatment, such as ralstonite $Na_xMg_xAl_{2-x}(FOH)_6H_2O$ and other complex fluorides (Robinson, 1969a; Hitchon et al., 1976; Durand and Nicaise, 1980) can be found. These fluorides are difficult to redissolve once precipitated and they interfere with further analysis of kerogen. Therefore, it is important to prevent their formation. According to Durand and Nicaise (1980), the best way to do this is to perform several thorough rinsings with hot deionized water between the acid steps, without filtering the residue to dryness. Moreover, a second 6 N HCl treatment is performed, after the HF/HCl destruction of silicates, in order to eliminate the ions able to form these fluorides. The procedure used at IFP for the preparation of kerogen concentrates and the cell designed for the acid treatment are displayed in Fig. 2. After this treatment, the material, including that recovered on filters and reactor walls is rinsed to neutrality and dried at 100 °C to eliminate residual water. Once dry, the concentrate is homogenized by grinding for subsequent steps in kerogen preparation. As discussed below, kerogen becomes prone to oxidation once minerals have been destroyed. Accordingly, all the above operations are performed under a flow of N_2 and the kerogen concentrate is stored under an inert gas atmosphere before further preparation steps.

Except in the case of very immature sediments, which can lose a few percent of their organic C by HCl hydrolysis during demineralization, the acid treatments do not alter significantly the kerogen structure and do not generate newly formed solvent soluble organic material. The influence of demineralization on a series of coals, starting from lignite, was tested by Larsen et al. (1989). Ion exchange, replacing metals by hydrogen and so changing the hydrogen bonding interactions, was observed. However, the pyridine extract before and after demineralization showed similar yield and molecular weight, indicating that no covalent bonds were created or broken.

A method aimed at preventing possible hydrolysis due to use of a strong acid such as 6 N HCl was

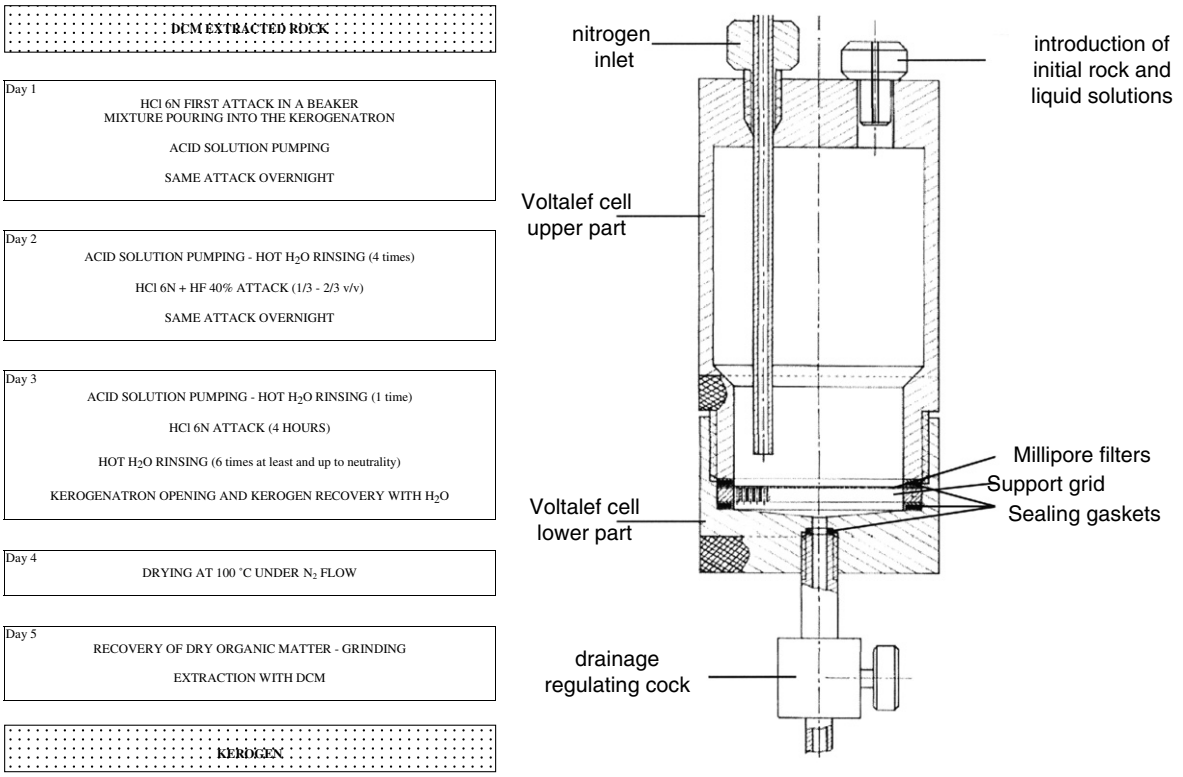

Fig. 2. Analytical flow chart and schematic cross section of a cell resistant to HF and HCl acid treatment, designed for kerogen preparation at IFP (Institut Français du Pétrole) (“kerogenatron”). Adapted from Vandenbroucke (2003).

proposed by Robl and Davis (1993). Considering that HF is sufficiently strong to remove both carbonate and silicates, the authors did not use HCl. It was replaced with boric acid in the mixture with HF so as to form BF_3 in situ and prevent insoluble fluoride precipitation. Comparison of a set of kerogens prepared with this method and with the HF/HCl treatment showed on elemental analysis a little less ash for the former method, but no significant difference in elemental atomic ratios or Fourier transform infra red (FTIR) spectral distribution. In fact, in the HCl/HF treatment used for comparison, the last HCl step described above, needed to avoid formation of insoluble fluorides, was not carried out. This resulted in ralstonite precipitation (Hitchon et al., 1976), thereby increasing the ash content relative to the "IFP" HCl/HF procedure following the ranking and number of acid steps as recommended by Durand and Nicaise (1980).

For recent sediments, whose OM is prone to acid hydrolysis, a multi-step demineralization method with recovery of the dissolved C was proposed by Gélinas et al. (2001). Mineral destruction was performed using dilute acid (1 N HCl and 1 N HCl/HF 10% mixture) at room temperature. Acid solutions and the rinsings from the acid treatment were recovered by centrifugation. Hydrolyzed organic C was recovered from the supernatants after elimination of inorganic ions and freeze drying, and combined with the centrifuged material. Ralstonite was often the major mineral found in the ash. The OM concentrate obtained, with an enrichment factor ranging generally from 2 to 10, and $< 20\%$ C loss even for an initial TOC (total organic carbon) content as low as 0.3%, was suitable for obtaining good quality solid state ^{13}C NMR (nuclear magnetic resonance) spectra.

An additional extraction step with organic solvent is always needed after acid treatment since the recovered OM concentrate still contains residual extractable compounds. The presence of these soluble compounds can be due to one or several of the following reasons: (i) incomplete initial extraction of even finely ground rock because of the existence of still closed or very small pores (Brukner and Vetö, 1983), (ii) initial extraction hindered by physicochemical interaction with minerals and (iii) steric trapping of soluble compounds inside the kerogen matrix. The amount of extract recovered after the acid treatment can be greater in some cases than that obtained directly from the crushed samples. This is particularly true with recent sediments, where oxygenated functional groups are abundant, and with coals where the microporosity is particularly prone to retention (Van Krevelen, 1993, Chapter 7) and where extractable material is tightly trapped in the network of clusters extensively hydrogen bonded to each other within the coal structure (Larsen et al., 1985). The second extract is generally richer in high molecular weight and/or polar compounds than the rock extract (Table 1) and it can be assumed that a major part originates from compounds trapped within the kerogen structure, as shown by comparison of extracts from coal and shale kerogens from the same well at similar depth (Behar and Vandenbroucke, 1988). Such compounds are partly liberated by the unfolding of this structure due to hydrogen bond breaking once minerals have been destroyed. In fact, for kerogen, as for coal, the extraction will never be "complete". Indeed, some studies (Durand et al., 1987; Behar and Vandenbroucke, 1988; Deniau et al., 2004) showed that a number of compounds remain trapped in kerogen macromolecular structures, even after the second extraction step, and are only released by further extraction or thermovaporization.

Pyrite can be a major constituent of kerogen concentrates, particularly from marine sedimentary rocks, where it can amount to more than 40 wt%. It frequently occurs as very small grains protected from physical and chemical elimination by being embedded in the OM. Pyrite elimination is required for certain specific analyses and various methods have been designed for this with greater or lesser success. The use of common oxidative reagents capable of destroying pyrite, such as HNO_3 (often used in palynological studies) is problematic due to OM oxidation by the reagent. Pyrite elimination with dilute HNO_3 and $LiAlH_4$ was used by Saxby (1970), but oxidation of OM functional groups was observed after the first treatment and reduction after the second, as shown by changes in infrared spectra. Durand and Nicaise (1980) used $FeSO_4$ but, besides incomplete pyrite elimination, the results also showed some oxidation of immature OM, as well as sulfur incorporation. $AlCl_3$ treatment (three successive one day treatments at room temperature under N_2) also showed incomplete pyrite elimination, strong OM oxidation and an increase in chlorine content (Table 2).

A technique that seems efficient has been proposed by Acholla and Orr (1993) using acidic $CrCl_2$ under a N_2 flow. Two treatments, with intermediate

Table 1
Composition of C_{14+} dichloromethane extracts (mg/g C and wt%) from rock (EXT-1) and kerogen (EXT-2) according to kerogen type and increasing maturity[a]

Kerogen type[b]	Sample maturity	HI (mg/g C)	SAT-EXT1 (mg/g C)	ARO-EXT1 (mg/g C)	NSO-EXT1 (mg/g C)	SAT-EXT1 (%)	ARO-EXT1 (%)	NSO-EXT1 (%)	SAT-EXT2 (mg/g C)	ARO-EXT2 (mg/g C)	NSO-EXT2 (mg/g C)	SAT-EXT2 (%)	ARO-EXT2 (%)	NSO-EXT2 (%)
I	Onset of oil window	728	62	13	33	57.4	12.0	30.6	6	2	28	16.7	5.6	77.8
I	Top of oil window	487	119	9	35	73.0	5.5	21.5	10	1	45	17.9	1.8	80.4
I	Wet gas window	52	21	5	15	51.2	12.2	36.6	8	1	14	34.8	4.3	60.9
II	Onset of oil window	503	22.2	27.8	68.3	18.8	23.5	57.7	4.1	2.5	32.0	10.6	6.5	82.9
II	Top of oil window	205	39.5	20.7	63.5	31.9	16.7	51.3	3.8	1.6	12.2	21.6	9.1	69.3
II	Wet gas window	30	1.2	2.0	1.7	24.5	40.8	34.7	0.7	1.4	4.0	11.5	23.0	65.6
III	Onset of oil window	337	5.7	15.6	30.5	11.0	30.1	58.9	0.7	4.2	9.7	4.8	28.8	66.4
III	Top of oil window	234	7.1	6.9	16.2	23.5	22.8	53.6	1.7	3.8	5.7	15.2	33.9	50.9
III	Wet gas window	106	0.5	1.1	2.7	11.6	25.6	62.8	0.6	1.0	2.0	16.7	27.8	55.6

[a] Data adapted from Penteado and Behar (2000) and Hill et al. (1999).
[b] Type I: Gomo Fm., Recôncavo Basin, Brasil; Type II: Duvernay Fm., Alta, Canada; Type III: Fruitland Fm. coals, CO, USA. NB: in contrast to different SAT and NSO proportions observed for Types I and II extracts, compositions of Type III rock and kerogen extracts are quite similar due to efficient steric trapping of all types of chemical structure in aromatic network of kerogen.

Table 2
Influence of $AlCl_3$ treatment after kerogen preparation on pyrite elimination and kerogen elemental analysis (wt%)[a]

Kerogen type/maturity[b]	$AlCl_3$	C	H	O	N	S tot	Fe	Cl	Other elements	Pyrite	Atomic ratio	
											H/C	O/C
I/M (GRS)[c]	No	54.38	2.23	6.53	1.29	0.37	0.30	1.24	33.66	0.64	0.492	0.0901
	Yes	39.81	2.54	8.94	0.98	0.55	0.23	3.62	43.33	0.49	0.766	0.1684
II/C (North Sea)	No	23.76	1.99	10.83	0.49	25.08	15.83	0.38	21.64	33.92	1.005	0.3419
	Yes	21.94	1.97	12.55	0.55	23.08	14.20	1.13	24.58	30.43	1.077	0.4290
III/D (North Sea)	No	18.19	1.49	7.94	0.74	29.75	25.9	1.13	14.86	55.50	0.983	0.3274
	Yes	12.98	2.23	13.87	0.49	21.90	17.26	6.52	24.75	36.99	2.062	0.8014
III/D (peat)	No	56.50	4.44	35.80	0.72	0	0	0.55	1.99	0	0.943	0.4752
	Yes	55.37	4.36	35.71	0.75	0	0	0.72	3.09	0	0.945	0.4837

[a] Data (IFP analyses) show for all samples, except peat, that pyrite is incompletely attacked, that Cl and other elements increase (probably because $AlCl_3$ is not totally removed during washing) and that there is a net reduction in C and increase in O, showing that OM is oxidized.
[b] Maturity stage: D (diagenesis), C (catagenesis), M (metagenesis).
[c] GRS, Green River Shale.

grinding, resulted in almost complete removal of pyrite without noticeable alteration of the kerogen, as shown by elemental analysis, infrared and solid state ^{13}C NMR spectra. Although preparation and handling of the reagent is not so easy, this seems by far the best chemical method to date for pyrite removal with minimal kerogen alteration. Another technique based on physical separation of pyrite by density fractionation of kerogen concentrates, has been proposed by Stankiewicz et al. (1994). It is based on the observation that the close intercalation of OM and pyrite requires very efficient grinding before density fractionation. This is achieved by cryogenic treatment of the sample in liquid N_2 before grinding. The idea is that various components of the kerogen concentrate have different expansion rates, which initiates cracking at the boundaries. Then, the sample is finely ground at room temperature under N_2. For density gradient separation by centrifugation, the resulting concentrate is suspended in water with sonication, with a cesium chloride solution having been added. The kerogen and the pyrite are recovered in the aqueous phase and heavy phase, respectively.

3.1.3. Kerogen storage

Kerogen, being an ancient material that has survived extensive natural alteration, is implicitly considered to be highly stable. While this is true as long as it is protected within its mineral matrix, it is not the case for an isolated kerogen. Spontaneous oxidative alteration of coal upon storage and natural weathering of kerogen at outcrops are well documented (e.g. Van Krevelen, 1993, Chapter 21; Nicaise, 1977; see also Table 9 below). In contrast, alteration of isolated kerogen upon laboratory storage is generally underestimated. However such alteration can be extensive even in closed vials, as illustrated by changes in bulk parameters (Table 3) and molecular composition.

Examination of the morphological and chemical features of a Cenomanian black shale showed a major role for the mineral matrix in OM preservation and kerogen stability. Indeed, this ca. 93 Myr old kerogen exhibited extensive alteration in chemical structure, once separated from the mineral matrix, after storage at room temperature in closed vessels for one and two years (Salmon et al., 1997, 2000). Electron microscopy observations on whole

Table 3
Alteration as reflected in elemental analysis (atomic ratio) in a maturity suite of Type II kerogen during storage (10 years)[a,b]

Date 1	Date 2	At H/C 1	At H/C 2	Ratio 2/1	At O/C 1	At O/C 2	Ratio 2/1
March 1992	February 2002	1.28	1.31	1.02	0.084	0.181	2.15
		1.05	1.17	1.11	0.065	0.248	3.82
		0.85	0.97	1.14	0.057	0.190	3.33
		0.60	0.79	1.32	0.070	0.412	5.89
		0.58	0.76	1.31	0.075	0.302	4.03

[a] Closed vials, in the dark without specific precautions regarding vial atmosphere.
[b] Data adapted from Behar et al. (2001).

samples of the shale showed that physical protection resulted from alternation of ca. 100 nm thick organic and clay nanolayers. The rapid oxidative alteration during storage was probably due to oxygen and moisture absorbed from the air before vial filling and could be promoted by UV light. Consequently, it is recommended that freshly isolated kerogen samples be stored as follows: (i) drying and grinding, (ii) removal of residual moisture under vacuum, (iii) filling of the vial with N_2 or Ar, (iv) sealing with a Teflon/rubber septum and (v) storing in the dark.

3.2. Bulk and atomic analyses

3.2.1. Specific gravity

Kerogen specific gravity increases when hydrogen content decreases and is therefore closely related to kerogen Type and maturation. Accordingly, this value is commonly measured for assessing coal and kerogen maturity (Van Krevelen, 1993, Chapter 12). Specific gravity is usually determined with a pycnometer using a gas, generally He, or a liquid like *i*-PrOH. Measurements are made by comparing the volume necessary to fill the calibrated volume of the empty pycnometer and the pycnometer containing the kerogen concentrate. Obtaining kerogen specific gravity requires a correction to account for the amount of pyrite (specific gravity ca. 5) as determined from elemental analysis. This correction is only an approximation because it neglects the usually low amounts of other residual minerals. Moreover, although pyrite is a non-stoichiometric solid corresponding to FeS_n, with n ranging from 1.8 to 2, the approximate weight of pyrite is calculated using $n = 2$ (Read and Watson, 1968). Early data obtained by Forsman and Hunt (1958), using the pycnometer method with *i*-PrOH, indicated a kerogen specific gravity (after ash correction) ranging from 1.2 to 1.5, even for H-rich kerogens. Specific gravity values greater than 1 were also determined by Stankiewicz et al. (1994) for low maturity kerogen concentrates, using the density gradient technique described above. Van Krevelen (1993, p. 362) calculated the specific gravity for coal macerals like exinite, using a group contribution method. In agreement with experimental values, all these calculated specific gravity values were greater than one and, as expected, they varied depending on maceral type and coal rank. In contrast to the above data, we measured kerogen specific gravity values varying from 0.8 to 1.5, using He pycnometry (see Table 4 for selected data). In agreement with the previously observed trends, the values depended on kerogen Type and maturity and showed inverse variation with H content. However, values less than 1 were systematically observed, for all the series of Type II kerogens examined, for samples exhibiting H/C atomic ratios > 1.1. This apparent discrepancy in the range of absolute values compared to the data in the above papers may be due to differences in analytical procedure (use of *i*-PrOH instead of He) and/or in uncertainties related to ash presence and correction for pyrite.

3.2.2. Elemental analysis

The major elements (wt%) in kerogen concentrates are C, H, N, O, S and possibly Fe from pyrite (Himus, 1951). Elemental analysis is considered reliable if the sum of these elements is > 90 wt%. Durand and Monin (1980) cite an average balance of 95% for 427 kerogens. Given this incomplete mass balance due to some residual minerals, and an average oxygen value at 11% on 324 kerogens, it is very important that oxygen be measured directly and not calculated by difference. All determinations should be carried out in duplicate or triplicate according to preset reproducibility criteria, because the amount of sample used for analysis is low (< 1 mg) and kerogen concentrates are sometimes heterogeneous due, especially, to the occur-

Table 4
Examples of specific gravity of Types II and III kerogen measured with He pycnometer (IFP analyses)[a]

Kerogen type	Sample maturity	HI (mg/gC)	T_{max} (°C)	Specific gravity
II	End of diagenesis	532	414	0.814
II	Onset of oil window	439	438	0.995
II	Top of oil window	242	443	1.115
II	Wet gas window	22	479	1.518
III	Onset of oil window	250	435	1.295

[a] Pyrite contribution subtracted from measured specific gravity of kerogen concentrate, using amount of Fe from elemental analysis to calculate pyrite wt%, assuming pyrite specific gravity of 5.

rence of pyrite. C, H and N are determined on one aliquot of the concentrate using thermal conductivity detection of gases produced from combustion at 1000 °C. O is measured on another aliquot by pyrolysis of the kerogen under N_2 flow, transformation of O-containing gases to CO_2, with CO_2 being quantified using coulometry. Total S, including pyritic and organic S, is obtained by oxidation of a third aliquot followed by quantitative coulometry of SO_2. Fe measurement is necessary to calculate the approximate amount of pyrite FeS_2, the organic S being obtained by difference from the measured total S. This analysis is performed on a fourth aliquot: mineralization with a mixture of HNO_3 and H_2SO_4, then quantitation of Fe using atomic absorption. Other minerals resisting acid attack, such as barite, rutile and anatase, can be estimated by the difference between 100% and the sum of the above elements. Ash, after combustion, can also be weighed in order to approximately cross-check the data obtained. However, if pyrite is present, this cross-checking should account for pyrite oxidation during combustion.

Elemental analysis data are used for classifying kerogens in a van Krevelen diagram, as discussed in detail below. The diagram is obtained by plotting the main elements, C, H and O as atomic ratios of H/C vs. O/C, the ratios being calculated by multiplying the weight ratio by the inverse atomic weight ratio of the elements considered. The organic S/C atomic ratio can also be calculated, provided that either pyrite was destroyed during kerogen isolation, or that Fe was analyzed in order to substract pyritic S from total S.

3.2.3. Rock-Eval analysis

Rock-Eval pyrolysis is a well known technique for the rapid geochemical characterization of kerogen in whole rocks, so the apparatus description and its principles are not detailed here (see Espitalié et al., 1985; Espitalié and Bordenave, 1993; Whelan and Thompson-Rizer, 1993; Lafargue et al., 1998; Behar et al., 2001). As indicated in papers by Espitalié and coauthors, Rock-Eval allows rapid and cheap screening analyses to be performed on a large number of samples, in order to select the most representative for detailed geochemical analysis. Briefly, the rock is heated at a programmed temperature rate in a pyrolysis oven under N_2 flow, and hydrocarbonaceous effluents are quantified with a flame ionization detector. A first peak (S1) is due to thermovaporized free compounds and a second peak (S2) to hydrocarbonaceous pyrolysis compounds that mimic those still to be generated by the kerogen upon source rock burial. The amount of CO_2 formed during OM pyrolysis up to 390 °C is measured with a specific detector to provide the S3 peak. If the apparatus is equipped with an oxidation oven, the residual kerogen is then burned at 850 °C under a flow of air and the resulting CO_2 (to provide the S4 peak) is measured. This allows determination of TOC by summing the C content of peaks S1–S4. The main parameters obtained with this technique are the hydrogen index (HI = S2 peak area/TOC), oxygen index (OI = S3 peak area/TOC) and T_{max} (the pyrolysis temperature at the S2 peak maximum). Application to "pure" OM, such as coal and kerogen, requires specific adjustments of the analytical procedure, including decrease in sample weight in order to avoid detector saturation (5–10 mg of kerogen). Moreover the shape of the S2 peak shows that pyrolysis of humic coals and terrestrially-derived kerogens is not complete if the final temperature is 600 °C, as initially used, since the signal does not return to the baseline at the end of pyrolysis. Under these conditions, the HI (a measure of the remaining petroleum potential) is underestimated, as is the TOC content compared to the value obtained using elemental analysis. The final temperature was therefore raised to 800 °C in the newer Rock-Eval 6 apparatus. A very good agreement is thus obtained between TOC values measured with the LECO SC-444 analyzer, the Rock-Eval 6 and elemental analysis (Lafargue et al., 1998; Behar et al., 2001).

Thermogravimetric analysis coupled with mass spectrometry (MS) and applied to reference source rock series (Souron et al., 1977) showed that similar amounts of hydrocarbonaceous products and CO_2 were generated from isolated kerogens or from kerogens still in their host rock. A good correlation was also observed between HI and the H/C atomic ratio of kerogens and coals on one hand, and OI and the O/C atomic ratio on the other hand, as shown in Fig. 3. These observations led Espitalié et al. (1977) to propose the use of the HI vs. OI diagram, measured on whole rocks, instead of the H/C vs. O/C atomic ratio diagram, to help determining kerogen source and maturity. HI consideration alone does not allow Type identification, because the evolution path cannot be defined. The HI vs. OI diagram for rocks takes advantage of the elimination of a specific analytical procedure for isolating kerogen. However it must be used with care because the so called

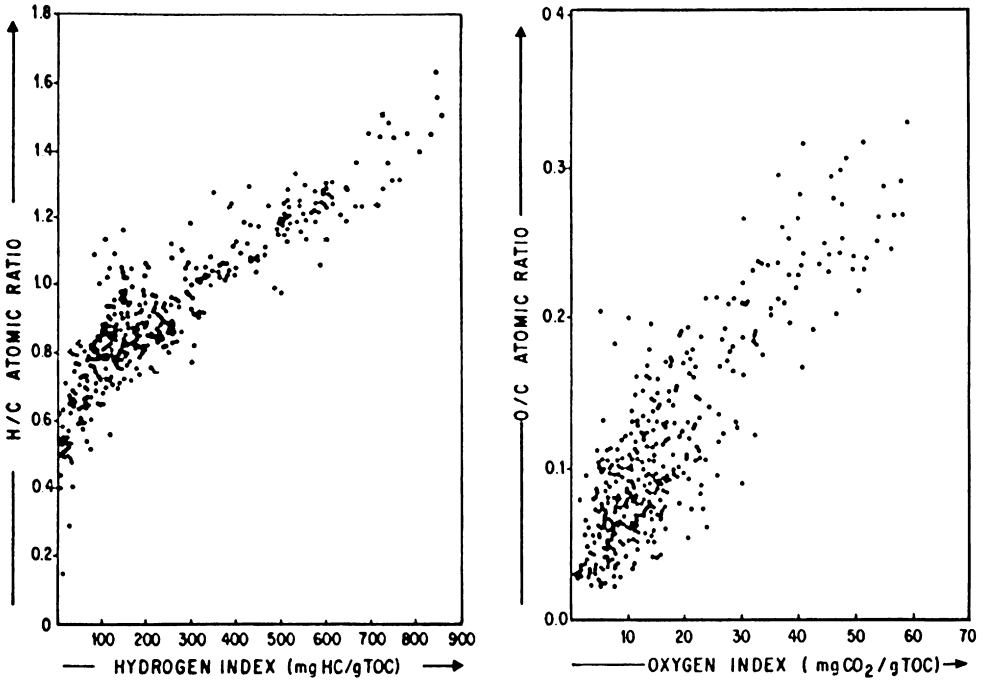

Fig. 3. Correlation between Rock Eval HI and H/C atomic ratio on the left, and Rock Eval OI and O/C atomic ratio on the right, measured on kerogens and coals with TOC > 40 wt%. Adapted from Espitalié et al. (1985).

"matrix effect" (Monin et al., 1980; Espitalié et al., 1984) can substantially lower the HI value, compared to that from the isolated kerogen, for samples with low TOC values (< 1%; Fig. 4). In fact, pyrolysing a rock under a gas flow activates the acid catalytic properties of clays by dehydration, a phenomenon not occurring under geological conditions, and decreases hydrocarbon production by forming coke (Senga-Makadi, 1982). As a result, the correlation using Rock-Eval parameters of whole rocks and elemental atomic ratios of kerogens has a lower correlation coefficient for organic-poor rocks. The diagram plotting HI as a function of T_{max} could bring some information related to evolution paths but, due to analytical uncertainties and restricted T_{max} range for petroleum generation by Types I and II, it is often not reliable. It was observed that the T_{max} of whole rocks having low TOC can be increased compared to that of kerogen by way of retention by minerals of the heavy fraction, the first to be released (Espitalié et al., 1984). Rock-Eval should thus be used as a screening tool, and careful examination of resulting data in terms of non-significant values and possible contamination is necessary before interpretation (Espitalié and Bordenave, 1993, p. 257). It is only after detailed geochemical analysis on samples selected as a result of such screening, that one can securely define the Type of OM and its maturity stage.

3.3. Summary

- Based upon the now largely accepted operational definition of kerogen, various procedures can be used for the isolation of kerogen concentrates. These may introduce differences in kerogen composition as characterized by bulk and molecular methods. It should be noted that, once isolated from its host rock, kerogen is prone to oxidation and should be stored in the dark under an inert gas atmosphere.
- As developed in a later section, bulk analytical techniques such as elemental analysis or Rock-Eval pyrolysis are at the origin of separation of kerogens into main Types characterized by evolution paths. Although spectroscopic methods for kerogen analysis have not been detailed in this section, they are also of primary importance for understanding and quantifying kerogen source and composition in more detail, and are presented through their numerous applications in the following sections.

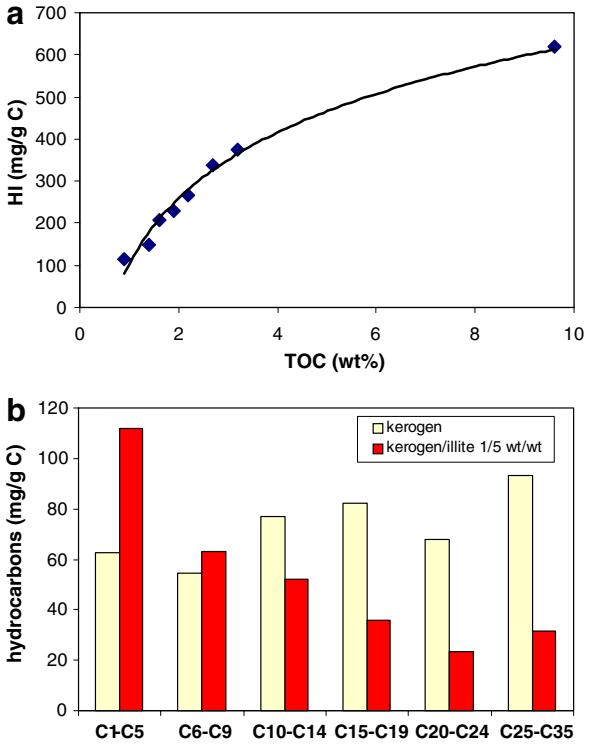

Fig. 4. Influence of illite abundance (“matrix effect”) on amount and composition of effluent during Rock-Eval pyrolysis: (a) HI vs. TOC for mixtures of the same oil shale (initial TOC = 9.6%) with illite for illite/oil shale weight ratios ranging from 0 to 10; HI is reduced from 620 to 115 mg/g C due to increasing coke formation. (b) Pyrolysis-GC effluent of kerogen alone and mixed with illite (1/5 wt/wt) showing catalytic cracking effect on *n*-alkane amount and distribution; pyrolysis effluent quantified with pyrolysis-GC in the C_1–C_{35} range; amount is 437 mg/g C for kerogen alone and is reduced to 318.5 mg/g C for the 1/5 kerogen/illite mixture due to effluent cokefaction, with carbon distribution shifted to shorter chains. Adapted from Senga-Makadi (1982).

4. Biological sources and depositional environment, present and past

In this section, we discuss the processes that lead to OM incorporation into sediments, in order to decipher the relationships between living organisms and kerogens. This requires a multidisciplinary approach, taking into account production in the biosphere, sedimentation processes controlling OM deposition and its amount, microbial effects on OM preservation, and physical and chemical interactions between mineral and organic constituents (Tyson, 1995). Information about past geological times, concerning once-living organisms and environmental conditions, even if it is often incomplete or uncertain, is also required for understanding the observed worldwide occurrence of discrete geological periods with OM-rich sediments, the type of organisms involved in their formation, and the associated environmental conditions. We do not intend to provide a comprehensive synthesis of all these topics. Rather, we will focus on the points that can help to clarify aspects of kerogen incorporation into present day sediments in relation to depositional environment, and in extending this information to the past, especially to the Phanerozoic.

4.1. Biological sources

Because kerogen is the insoluble OM buried in sediments, thus being tightly related to the sedimentary environment, its chemical structure exhibits significant variation depending on sources and depositional conditions. Early studies by Down and Himus (1941) and by Forsman and Hunt (1958) recognized that close correspondence exists between two main kerogen Types and the related end member organic rocks, namely humic coals and bogheads. These materials represent the end points of sedimentary OM deposition when transportation, mineral precipitation and detritic mineral input, alone or combined, are very low.

4.1.1. Primary producers and the carbon cycle

As shown by microscopic studies and extensive chemical analysis including biomarker typing (e.g. Peters and Moldowan, 1993; Peters et al., 2004 and references therein), two main primary producers contributed to sedimentary OM during the Phanerozoic: first, algae and then, terrestrial higher plants that emerged around the Silurian. The organic fraction deposited in lacustrine or marine environments corresponds to residues from these primary producers and from various heterotrophic organisms, including fungi and bacteria that escaped complete mineralization through the whole C cycle. Bacteria are the last living organisms to rework this OM. However, although their input can be traced via specific biomarkers, it is difficult at this time to quantify accurately the bacterial contribution to the final organic content of sediments. The mechanisms of the successive series of transformations from living to sedimentary OM in Quaternary sediments have been described in detail (Heinrichs, 1993 and references therein) and are only mentioned briefly below. Globally, it is generally considered that, most of the time, the OM

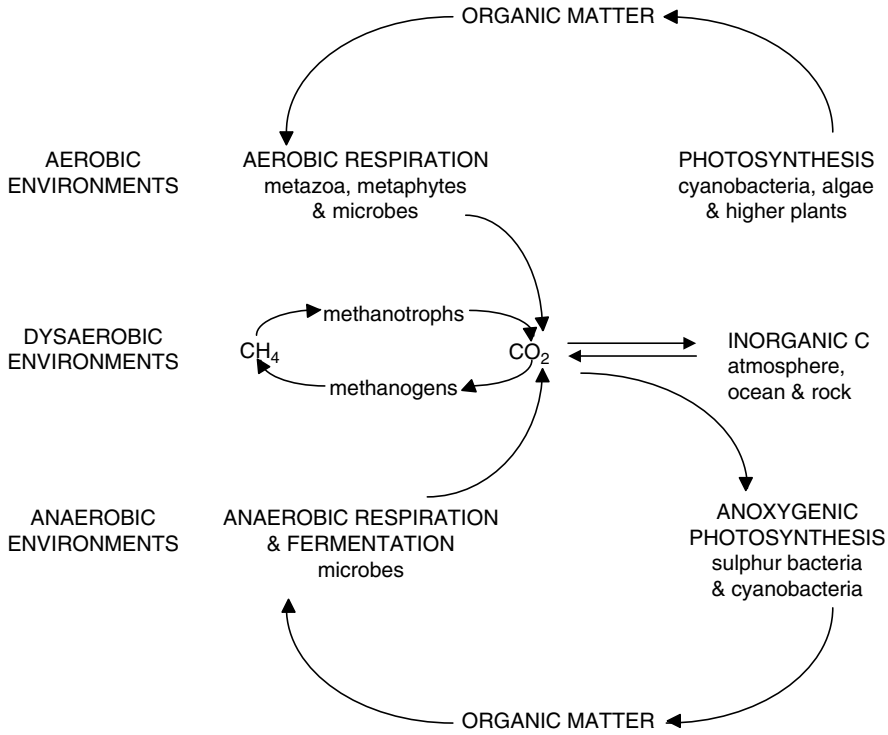

Fig. 5. Interactions between major participants of the carbon cycle. Adapted from Summons (1993).

incorporated into sediments corresponds to only 0.1% to <1% of the whole living biomass of source organisms (Tissot and Welte, 1978).

The first part of the C cycle (Fig. 5) involves the primary producers that are photoautotrophic organisms which transform atmospheric CO_2 or inorganic C (CO_2 and associated CO_3^{2-}) dissolved in water into their own metabolites using solar energy for photosynthesis. Life is thus restricted for these organisms to the photic zone, i.e. the land surface and the upper hundred meters of the water column. Accordingly, the major contributors are phytoplankton in water and higher plants on earth. Primary productivity assessment as a function of the different production sites and their area (Table 5) indicates that continental ecosystems are today more productive than marine ones (Huc, 1980; Summons, 1993).

The second part of the cycle (Fig. 5), which occurs after the death of autotrophs, corresponds to their mineralization through the whole food chain by heterotrophic organisms, that use the energy provided by oxidation reactions to synthesize their own metabolites. The major pathways of C oxidation are oxygen consumption, sulfate reduction, fermentation and methanogenesis (Heinrichs,

Table 5
Present day distribution of primary production in terrestrial and marine environments (after Huc, 1980; Summons, 1993)

Environment	Total production (tons C/year)	Production zone	Total area (10^6 km^2)	Organic productivity (% total production)
Terrestrial	4.8×10^{10}	Desert	68	4
		Grass land	26	13
		Forest	41	65
		Agriculture	14	18
Marine	3.5×10^{10}	Estuary	2	8
		Continental shelf	84	47
		Deep ocean	276	46

1993), while denitrification would generally play a minor role for OM remineralization. A consortium of different bacterial types is necessary to achieve OM degradation, among which hydrolytic and fermentative bacteria are of primary importance. Being the only ones capable of degrading initial biomacromolecules into small units available to other bacteria, they are consequently the first actors in the overall microbial degradation process (Tyson, 1995, p. 50). The OM is thus decomposed by more or less restricted classes of heterotrophs, depending on the environmental conditions and related electron acceptors. These organisms sometimes show great adaptive capacity to survive in aggressive environments, which may be reflected by way of specific biomolecules. For example, gammacerane, often used to correlate crude oils and source rocks, and a biomarker commonly associated with hypersaline environments (de Leeuw and Sinninghe Damsté, 1990), has probably a precursor playing a key role in the regulation of membrane exchanges in halophilic bacteria.

The organic debris settling on surficial sediments is thus the sum of all residues escaping the biological cycle, and incorporates residues of complex bacterial populations, depending on sequential redox horizons in the lacustrine or marine environment (Froelich et al., 1979; Deming and Baross, 1993). Further degradation occurs in the upper sedimentary layers. However, according to Heinrichs (1993), it seems that most of the OM that is buried below 1 m will be preserved. For marine settings, about 70% of the sedimented material would correspond to the detrital rain of particulate OM and about 30% to remains of benthic heterotrophs (including macrofauna, meiofauna and microbial populations) living near the sediment–water interface (Mayer, 1993). The proportion of remains of benthic precursors might be less than 30% when the organic input is predominantly terrestrial because, as discussed below, the presedimentary alteration should be high, and the resulting refractory organic matter is not available for further biodegradation at the sediment–water interface. Moreover, high sedimentation rates, correlated with enhanced OM preservation (Heinrichs, 1993), are frequently observed in depositional environments with a large terrestrial organic input. However, the relationship between high sedimentation rate and high TOC is not straightforward, because it depends on the respective rates of mineral sedimentation and oxic/suboxic bacterial degradation, the balance being in favour of TOC dilution for very high sedimentation rates (Tyson, 1995, pp. 99–118).

4.1.2. Microscopic features of sedimentary OM from millimetre to nanometre scale

A precise description of the morphological features of sedimentary OM can be obtained by microscopic observations at various scales and can afford important information on sources and preservation pathways. This petrographic approach has been used for a long time in coal studies (Hutton, around 1830, as cited by Van Krevelen, 1993, p. 108) and has been proven successful in identifying remains of source organisms in coals. It should be applied systematically to sedimentary OM along with geochemical analysis. Unfortunately, light microscopy (reflectance or transmittance, natural light or UV fluorescence) is often made difficult on polished blocks and thin sections of untreated rocks because of OM dissemination and interference from minerals. With kerogen concentrates, difficulties arise from the presence of sometimes abundant, unrecognizable "amorphous" fractions. However, in addition to these amorphous materials, a number of organic remains such as algal bodies, faecal pellets, spores, pollen and plant debris have been identified via light microscopy (Plate a).

A petrological classification of petroleum source rocks based on two main organic sources, aquatic (algae and bacteria) and terrestrial (mainly lignin-related components) was proposed by Combaz (1980). Terrestrial constituents such as spores, pollen and cuticles, when concentrated into cannel coals, were considered in this classification as a special class named liptobioliths. Other classifications based on the organic fraction alone, analogous to the maceral nomenclature established for coals by Stopes (1935), were proposed by Robert (1979), Alpern (1980), Hutton (1987), Teichmüller (1989) and revised by Taylor et al. (1998, Chapters 4 and 5). Table 6 is a simplified classification of kerogen constituents based on these studies.

Important advances resulted from the use of transmission electron microscopy (TEM) for kerogen examination. Owing to the much higher resolution obtained relative to light microscopy, it appears that a number of kerogens, previously considered as amorphous on the basis of light microscopy observation, contain organic remains with well-defined morphology. Indeed, TEM studies on 60% of a large set of "amorphous" kerogens isolated from source rock and oil shales, ranging in age from

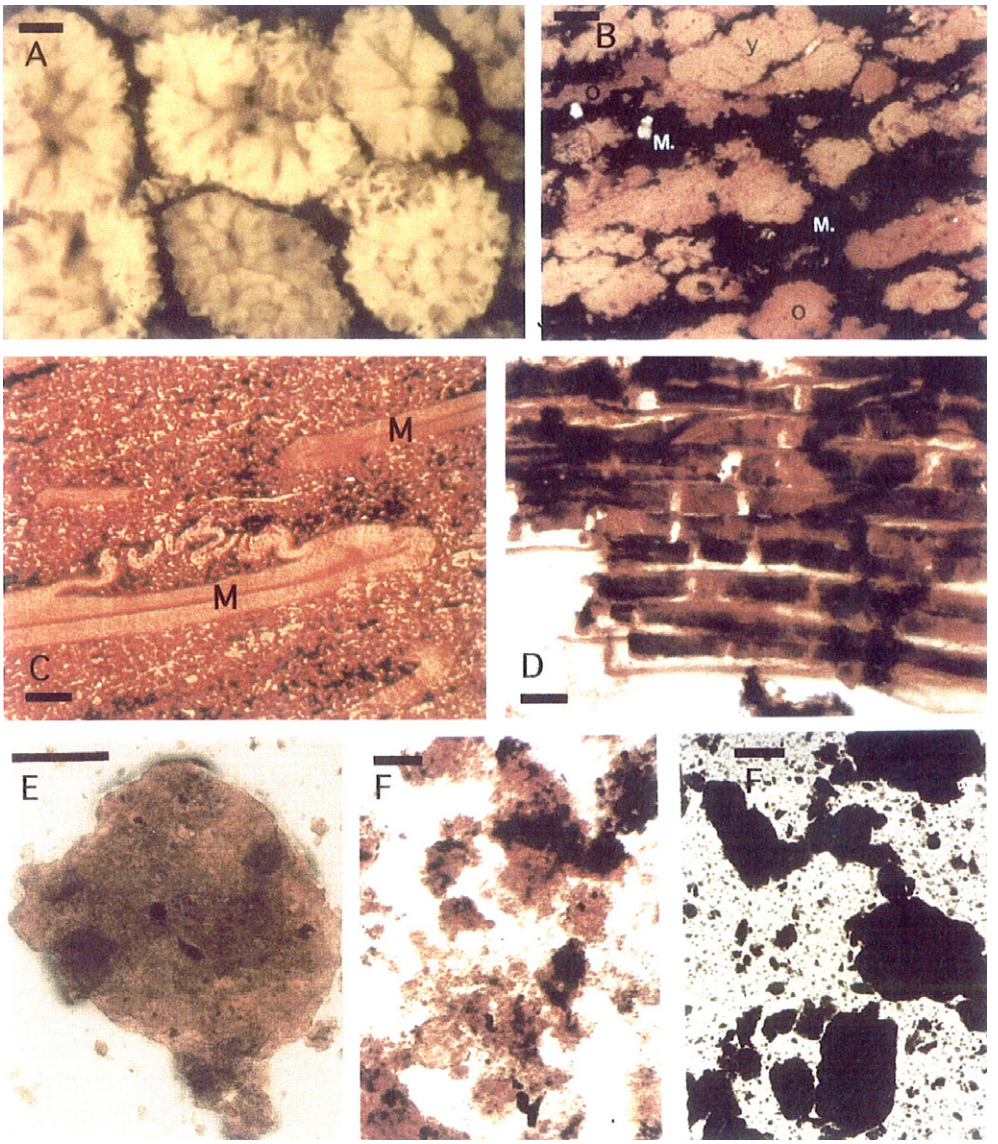

Plate a. Examples of kerogen diversity as revealed by light microscopy. (A) Ermelo Torbanite (Permian-Carboniferous, South Africa); the bulk of this extremely organic-rich deposit is composed of fossil colonies of *Botryococcus* with well preserved morphology. (B) Autun Torbanite (Permian, France) showing yellow (Y) and orange (O) colonies interbedded with an abundant organo-mineral matrix (M). These two types of colonies exhibit substantial differences in chemical composition as revealed by micro-FTIR spectroscopy probably due to differences in colony microenvironment after deposition. (C) Sporinite-rich cannel-coal (Westphalian, UK) dominated by megaspores (M). (D) Woody debris (Maestrichtian, Sahara). (E) Gel-like particles accounting for the bulk of the extremely sulfur-rich kerogen of Orbagnoux (Kimmeridgian, France). (F) Weakly mature (left) and highly mature (right) granular organic matter (Kimmeridgian, North Sea). Scale bars: A (10 μm), B (50 μm), C and D (25 μm), E and F (75 μm). Reprinted with permission from Landais et al. (1993, p. 2532), Copyright (1993) Geochemical Society for B; with permission from Combaz (1980, p. 93), for C, 97 for D, 105 for F, Copyright (1980) Editions Technip for C, D, and F; with permission from Mongenot et al. (1997, p. 335).

Infra-Cambrian to Miocene, revealed the presence of very thin lamellar structures (Largeau et al., 1990a,b). Such very thin structures, termed ultralaminae, are usually 10–60 nm thick and are tightly associated into bundles (Plate b, C and D). These structures, whose origin is discussed below, generally co-occur with a truly amorphous fraction. The relative amounts of ultralaminae and of nanoscopically amorphous OM in kerogen can vary greatly. Thus, some kerogens, like the Rundle Oil Shale

Table 6
Simplified petrographic classification of kerogen constituents (after Robert, 1979; Alpern, 1980)

Maceral	Organoclast (organic microconstituent) (Alpern, 1980)	Source of constituents (Robert, 1979)
Vitrinite	Woody tissues	Primary
Inertinite	Burned organic tissues	Primary
Exinite	Higher plant protective tissues, spores, pollen, resins	Primary
Alginite	Phytoplankton	Primary
Bituminite	Migrated bitumen	Secondary
Faunal relics	Zoobenthos	Primary

(Eocene, Australia) and the Göynük Oil Shale (Oligocene, Turkey), are composed mostly of ultralaminae. In contrast, the kerogen of the Green River Shale contains only a low contribution of such structures and is dominated by amorphous OM (Largeau et al., 1990a; Derenne et al., 1991; Gillaizeau et al., 1996). A combination of morphological and chemical studies showed the occurrence of two main types of nanoscopically amorphous OM in kerogens with different origins (see section on preservation processes). Homogeneous, gel-like kerogen fractions were shown to be related to natural sulfurization (Boussafir et al., 1995; Mongenot et al., 1997, 1999, 2000), whereas degradation–recondensation yields heterogeneous, diffuse and sometimes granular fractions (Zegouagh et al., 1999; Deniau et al., 2001) as shown in Plate b (E and F).

Direct TEM examination of kerogen in rock samples has only been performed on a few samples. Such in situ observations, on a series of rock fragments from the Kimmeridge Clay Formation (Upper Jurassic, UK) selected using light microscopy, provided information on: (i) the correlation of the ultrastructures identified with TEM of the isolated kerogens and the macerals identified with light microscopy on polished rock sections and (ii) the association of these different macerals with minerals at a nanoscopic level (Boussafir et al., 1995).

Parallel TEM and scanning electron microscopy (SEM) observations (secondary electron mode) were performed on some kerogens, chiefly composed of organic microfossils and isolated from organic-rich deposits. These observations revealed that fine morphological features, like the multilayered nature of cell walls, can be retained in ancient kerogen, as observed for the colonies of *Gloeocapsomorpha prisca* that form Kukersite Oil Shale (Ordovician, Estonia; Derenne et al., 1992a), and for Neoproterozoic acritarchs (Ediacarian, Australia; Arouri et al., 1999). Such combined studies also showed large differences in the level of morphological preservation of *Botryococcus* colonies, related to differences in depositional conditions, in various Maar-type oil shales (Pliocene, Hungary; Derenne et al., 1997, 2000). Well preserved *Botryococcus* colonies were also examined with confocal laser scanning fluorescence microscopy in a Paleogene oil shale (Ukraine) and three-dimensional information on colony organization was thus obtained with this new method (Stasiuk, 1999).

A wealth of information can be derived from microscopic observations coupled to spectroscopic pin-point analysis. Thus, transmission micro-FTIR spectroscopy on thin sections allowed identification and characterization of different types of heterogeneity (Fig. 6), both in *Botryococcus* colonies and in the organic matrix, in Permian to Carboniferous Torbanites (organic-rich deposits in which kerogen is chiefly composed of accumulations of *Botryococcus*). Comparison of the FTIR spectra obtained through these pin-point in situ analyses and of the spectra classically obtained on bulk samples showed that the latter afforded significantly biased information on the composition of *Botryococcus* colonies, their oil potential and kerogen maturity (Rochdi et al., 1991; Landais et al., 1993). Transmission micro-FTIR spectroscopy was also used to examine vitrinite and liptinite alteration in a cannel coal under UV irradiation and its relationships with temporal alteration in fluorescence emission spectra of kerogen macerals (Pradier et al., 1992). micro-FTIR examination of macerals in kerogens was also performed using reflectance mode (Lin and Ritz, 1993; Mastalerz and Hower, 1996; Mastalerz et al., 1998; Arouri et al., 1999). Micro-FTIR examination of *Botryococcus* colonies in a series of cannel coals, along with pin-point elemental analysis using an electron microprobe, thus revealed large variations in composition, related to differences in maturation and depositional conditions (Mastalerz and Hower, 1996). Combined Micro-FTIR and X-ray absorption near edge spectroscopy (XANES) were used for observations at the μm scale on various prokaryotic microfossils, including the spatial distribution of alkyl groups and sulfur oxidation state (Foriel et al., 2004).

Elemental mapping with electron dispersive spectrometry (EDS), along with SEM in backscattered electron mode (BSEM), was performed on polished sections of a few rock samples, including

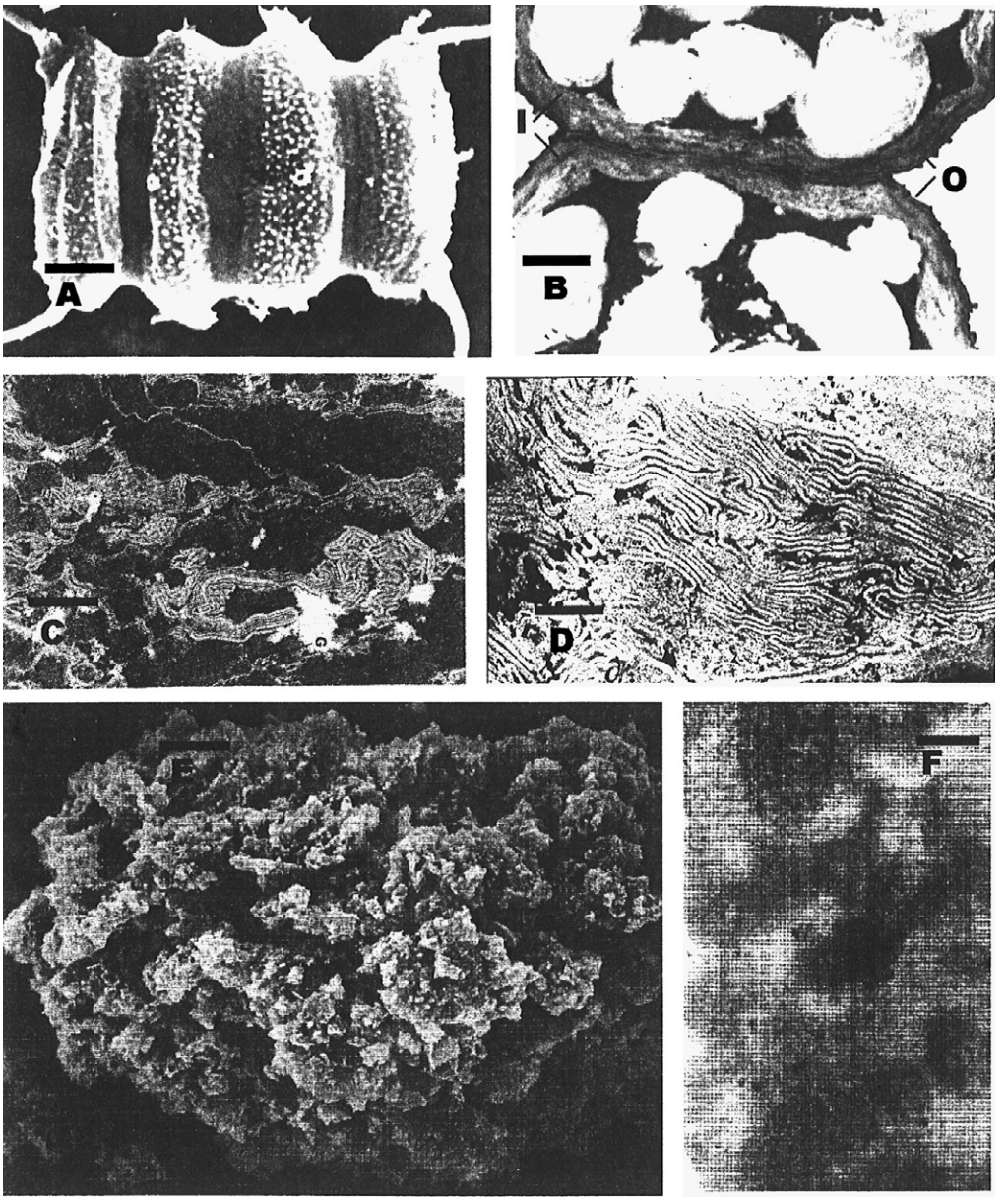

Plate b. A and E scanning electron microscopy, B–D and F transmission electron microscopy. A–D: Observations on the extant green microalga *Scenedesmus quadricauda* and relationship with fossil ultralaminae. (A) Four-celled typical colony of *S. quadricauda*. (B) Ultrathin section showing a partial view of two adjacent cells from a colony, the cells are surrounded by a classical polysaccharidic wall (I) and a very thin algaenan-comprised trilaminar outer wall (O). (C) Typical trilaminar organization of the very thin outer walls is well preserved in the isolated algaenan, however these walls are now somewhat distorted due to the complete elimination of the cell contents and of the thick polysaccharidic inner wall following the drastic hydrolysis aimed at removing all the cell components but the algaenan. (D) Fossil ultralaminae from an ultralaminae-rich deposit (upper Kimmeridgian, Gabon); morphological and chemical similarities indicate that such structures originate from the selective preservation of very thin, algaenan-comprised, microalgal outer walls. (E,F) Kerogen isolated from marine sediments of the North-West African upwelling system showing the granular morphology generally observed in kerogens formed via the degradation–recondensation pathway. Scale bars: A (10 μm), B–D (2 μm), E (100 μm) and F (1 μm). Reprinted with permission from Derenne et al. (1991, p. 1043), for B, 1044 for C, Copyright (1991) Geochemical Society for B and C; with permission from Largeau et al. (1990), p. 892, Copyright (1990) Pergamon Press for D; with permission from Zegouagh et al. (1999, p. 105).

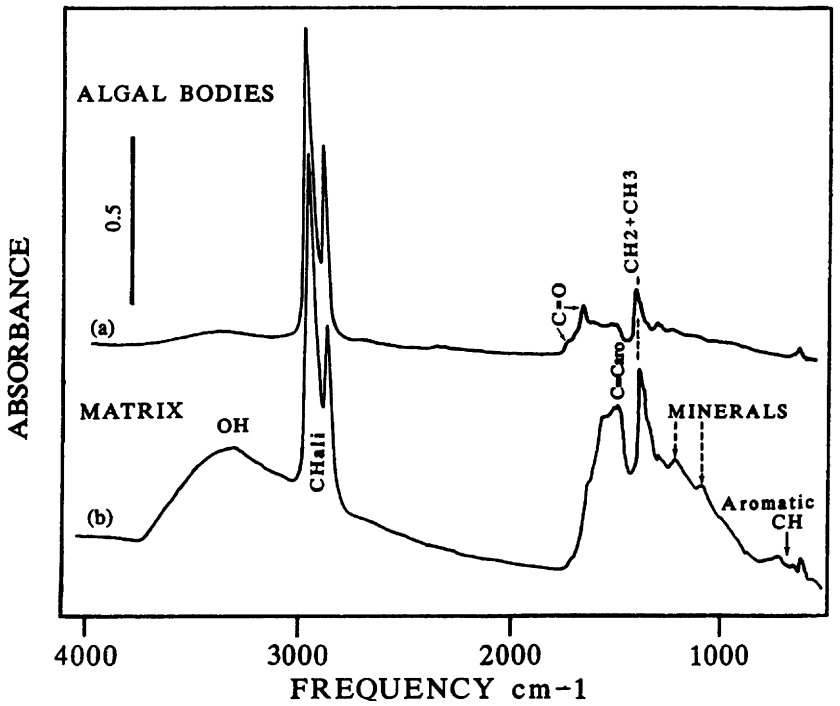

Fig. 6. Transmission micro-FTIR spectra from thin section of a *Botryococcus*-rich oil shale (Carboniferous, Russia) similar to shale illustrated in Plate a (B). The spectra reveal sharp differences in composition between fossil colonies of *Botryococcus* (mostly originating from selective preservation of cell walls made up of algaenan) and organic matrix (mostly originating from degradation–recondensation). Reprinted with permission from Landais et al. (1993, p. 2532).

Kimmeridgian Shales (Dorset, UK; Lallier-Vergès et al., 1993) and extremely sulfur-rich, bituminous laminites (Upper Kimmeridgian, Orbagnoux, France; Mongenot et al., 1997). Elemental mapping of C, Ca and S on the Orbagnoux samples thus showed that the S corresponds almost exclusively to organic S and is homogeneously distributed within the OM (Plate c).

4.2. Changes associated with sedimentation processes

4.2.1. Depositional environment

Sedimentation occurs only in aquatic environments with either fresh or saline water, for example oceanic platforms or inland basins, under variable water depth. Given the relative global areas of present day lacustrine and coastal marine zones, it appears that the major depositional environment for OM is presently coastal marine settings. The emerged land surface, being eroded by meteoric processes, temperature changes, and wind and rain, often makes a major contribution to mineral sedimentary input.

Except for coal beds that are mostly, and in the case of massive veins exclusively, deposited in situ, terrestrial higher plant debris accumulates after transport to aquatic sedimentary systems. These residues have already suffered strong biotic as well as abiotic degradation under oxic conditions in soils, before being transported, first by surface runoff and erosion and then by rivers. During this transport, relatively inert substances like waxes and lignified tissue, or biopolymers such as cutan and suberan, can partly escape oxic degradation (de Leeuw and Largeau, 1993; Hedges and Oades, 1997). Given their strong alteration upon transportation, terrestrial organic remains probably do not suffer major changes through bacterial alteration during further settling and incorporation into the sediment. This is supported by elemental analysis data showing that, even when sedimented in marine environments where sulfate-reducing bacteria thrive, terrestrial OM generally contains very low amounts of sulfur. This is not always the case for humic coals, which may, however, incorporate sulfur into their organic network if a marine transgression occurs during early diagenesis (Chou, 1990; White et al., 1990). This incorporation is possible because immature coals, being deposited in place, have not been submitted to the oxic degradation

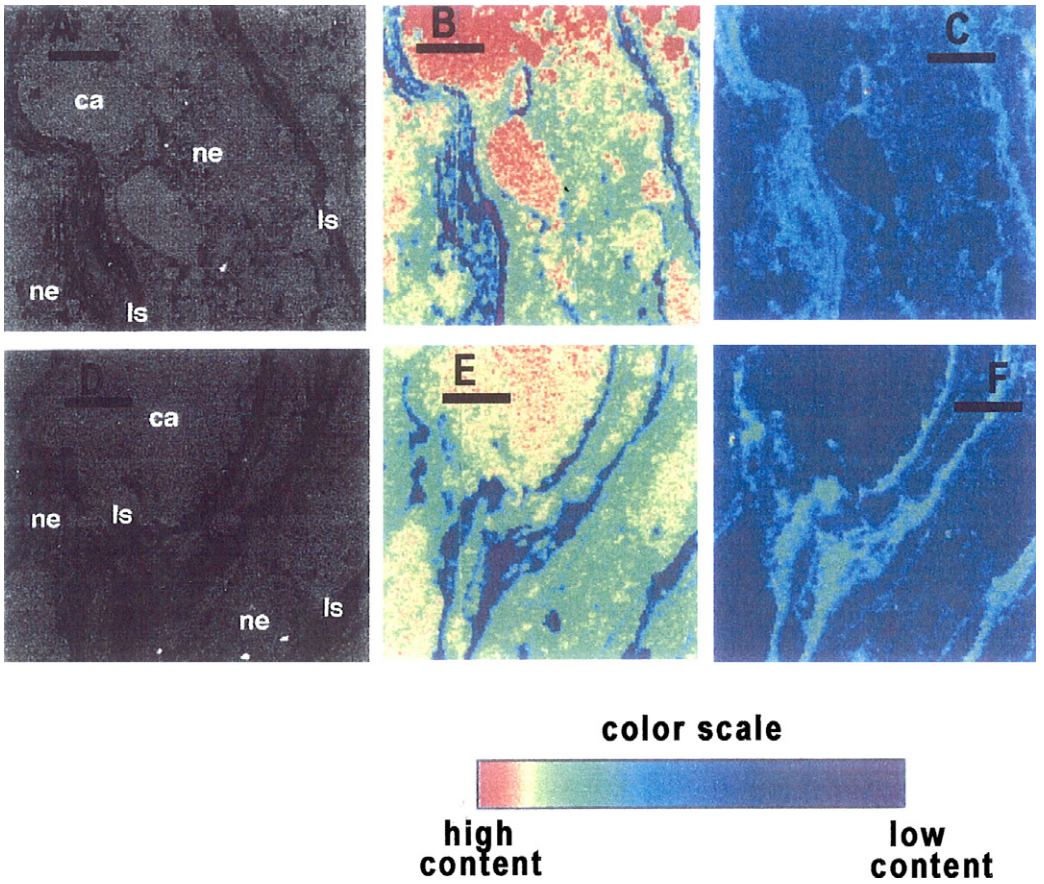

Plate c. BSEM observation (A,D) and elemental mapping of calcium (B,E) and sulfur (C,F) by EDS of polished sections of a typical sulfur-rich sample from the Orbagnoux deposit (upper Kimmeridgian, France) showing that sulfur almost exclusively corresponds to organic sulfur and is homogeneously distributed in the lamellar and diffuse organic matter (maps C and F). ca, pure carbonate; ls, lamellar organic matter; ne, diffuse organic network. Scale bars: (25 μm). Reprinted with permission from Mongenot et al. (1997, p. 336).

associated with pre-depositional transport. Therefore, their chemical structure is probably more labile than that of coal debris transported during land erosion, so that they can incorporate reduced S species from bacterial metabolism. Bacterial alteration in the resulting sulfur-rich coals is clearly indicated by the light isotopic composition of this organic sulfur (Chou, 1990).

In opposition to weak biochemical alteration of terrestrial organic debris once it has arrived at the site of sedimentation, intense reworking of phytoplanktonic OM takes place in aquatic sedimentary systems and bacterial material is added to the organic debris provided by primary producers. The duration of the transportation step in the water column down to the sediment and the water salinity and oxicity thus exert great influence on the amount and composition of the sedimented OM by selecting the various potential consumers, particularly in deep settings in the marine environment. Oxicity may be determinant in lacustrine systems often subject to seasonal or periodic (climate-driven) water stratification (Hollander et al., 1990; Huc et al., 1990). Given its greater density, it appears that particulate OM, among which faecal pellets might bring a major, although disputed, contribution (Tyson, 1995, pp. 42–45), will be much less altered by bacteria than dissolved OM. Moreover, biodegradation of particulate OM by exoenzymes is required before use by bacteria (Deming and Baross, 1993). The main source of sedimented OM is thus the particulate fraction of the total organic input (Tissot and Pelet, 1981; Wakeham and Lee, 1993; Hay, 1995). It was considered that the amount of organic matter settling on the sea floor would depend roughly on the balance between organic productivity, which is limited by nutrient availability, and degradation efficiency, which is thought to

be controlled by the thickness of the oxic zone (Demaison and Moore, 1980). However this interpretation is now disputed in studies showing that variations in OM productivity, associated with climatic changes, might be the main factor controlling the amount finally preserved in sediments (Calvert and Pedersen, 1992). As discussed below, this relationship between increased productivity and increased preservation is also supported by the observation of high atmospheric CO_2 concentrations at given stratigraphic intervals corresponding to major source rock deposition (Berner, 1994; Huc et al., 2005). Moreover, many studies showed that, in environments globally oxygenated at the metre scale, microenvironments hosting active anaerobic bacterial consortia exist at the micron scale (Alldredge and Cohen, 1987). It should be noted that the productivity vs. preservation dispute has not settled down, and most workers (e.g., Tyson, 2005; Huc et al., 2005; van Buchem et al., 2005) now consider productivity, preservation and dilution to be mutually interdependent with respect to the accumulation of organic matter in marine sediments. It has also been hypothetised that the preservation conditions for a given redox state may have changed along geological time and life evolution, due to increased efficiency of the biological degradative mechanisms of consumers (Klemme and Ulmishek, 1991).

A last step in organic-rich sediment formation is related to transport and remobilization of surficial materials. Particle sieving and density fractionation by hydrodynamic currents, or gravity transport mechanisms, redistribute both mineral matter and OM according to the topographic features of the final sedimentation site, as shown in Fig. 7 for Black Sea recent sediments (Huc, 1988). In this example, the maps for primary production in surficial water and bottom water anoxic zone clearly do not reflect the distribution of sedimented OM. In contrast, there is a direct relationship between mineral grain size distribution, associated with centripetal current systems, and OM content that is higher in the least mobile zones. However, it is not clear whether this relationship is due to a similar density sieving effect on smaller and lighter clay and OM particles, or whether there is a physical association between clay minerals and OM resulting in, besides sieving of

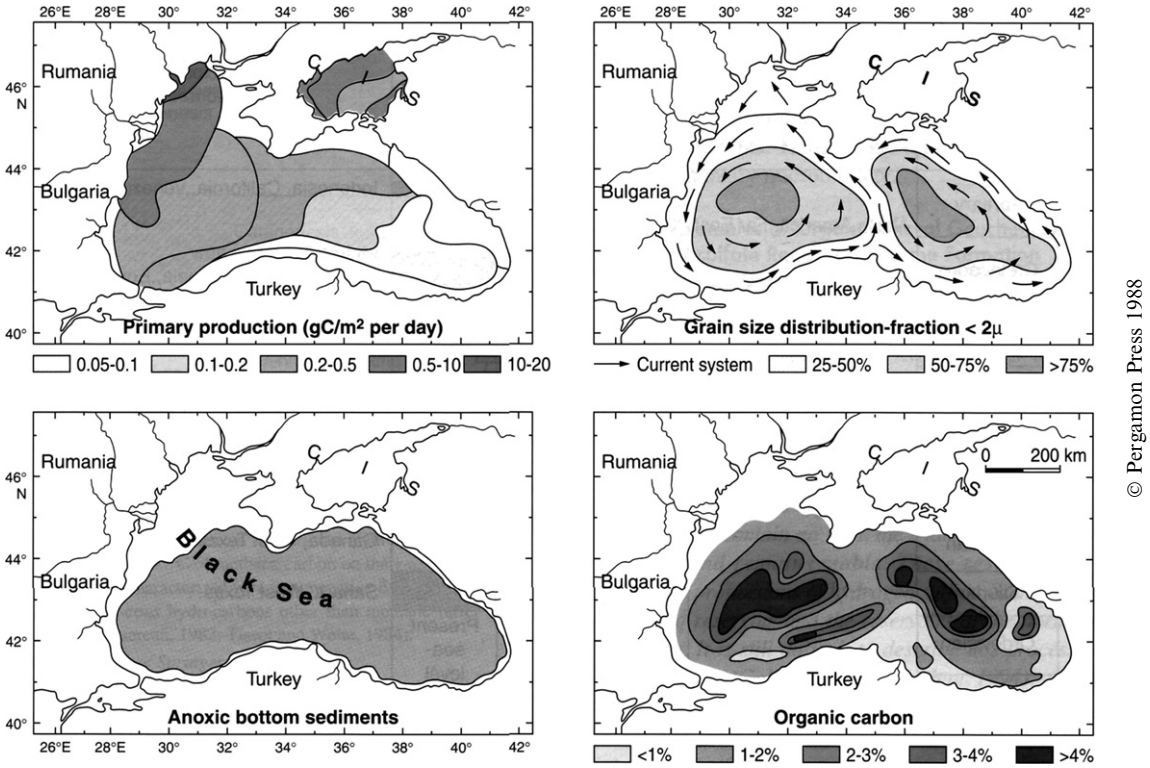

Fig. 7. Influence of transportation on final distribution of sedimented organic matter. Example from Black Sea recent sediment. Comparison between primary production (top, left), grain size distribution (top, right), anoxic bottom conditions (bottom, left), and organic C distribution in bottom sediment (bottom right). Reprinted with permission from Huc (1988, p. 265).

light particles, a better preservation efficiency. Whatever the exact mechanism associating light clay and OM concentration, this hydrodynamic zonation effect, and more generally the influence of the topography of the sediment floor on OM distribution, has been observed in many other examples both for recent and ancient sediments (Huc, 1988; Huc et al., 1990).

Measurements using sediment traps and primary productivity estimates in marine environments have shown that a very low amount (around 0.3%) of the initial living biomass is incorporated into sediments (Summons, 1993). Bacterial OM has thus been considered to represent in some cases a substantial, and even major, contribution to kerogen (Ourisson et al., 1984). However, given the low bacterial biomass in sediments and their highly metabolizable composition, it seems that the bacterial contribution to sedimented OM should represent (most of the time) only a few % of the TOC in surficial sediments (Tyson, 1995, p. 72; Hartgers et al., 1994).

4.2.2. Relationship between organic and mineral sedimentation

As shown below, the distinction between aquatic and terrestrial kerogen is quite closely related to the mineralogical environment of the deposited OM. Aquatic and terrestrial kerogens can thus often be recognized by the composition of the associated minerals. Thus, taking mineralogy into account can be of great help in reconstructing the origin or Type of the sedimented OM in ancient sediments for mature source rocks (Huc, 1990). This reconstruction can be extended at least over the Mesozoic and Cenozoic eras; however, beyond these times, knowledge about ocean position and resulting climates, atmosphere composition and ecosystems becomes much more imprecise. Some examples of this major role of the global environmental selection of related mineral and organic facies are given below (see Tyson, 1995, for a detailed survey).

Aquatic environments are rich in planktonic organisms, among which algae with biologically constructed mineral shells can be abundant. The development of these organisms depends directly on the availability of mineral substances dissolved in water. An example of such algae are diatoms, found in both lacustrine and marine communities since the end of Cretaceous and whose shells are made of silica. A characteristic of the open marine environment is the frequent occurrence among phytoplanktonic organisms of coccolithophoridae with carbonate shells. The detrital input of minerals into marine environments will be limited offshore by transport capacities of winds and streams and only the lightest fraction of detrital minerals, mainly made up of clays, will reach deep sedimentation sites. The sediment mineralogy associated with marine kerogens will thus often vary from almost pure carbonate of biochemical origin (Williams and Barghoorn, 1963) to marls (carbonate plus clays). In marine settings, the association of marine planktonic algae as primary producers with sulfate-containing seawater leads to their biodegradation by sulfate-reducing bacteria (Summons, 1993). Marine kerogens are thus also associated with pyrite if clay minerals are present to release Fe ions (Berner, 1987). In many open marine environments, mineral input to sediments chiefly originates from biological sources and from precipitation reactions triggered by the physicochemical changes occurring in the mixing zone between freshwater and seawater. Under these conditions, the total sedimentation rate will generally be low and the organic to mineral ratio may thus become fairly high. Marine source rocks with TOC $> 10\%$ are not exceptional in the sedimentary record.

Except for coal beds deposited in swamps as massive peats, i.e. under good preservation conditions due to low surface/volume ratio, terrestrial higher plant residues will suffer strong degradation under oxic conditions in soils before being transported by meteoric waters into rivers. However lignin-containing OM and aliphatic protective tissues can partly escape degradation owing to their specific resistance. Weathering phenomena will generally associate these organic residues with detritic minerals such as clays and silts. In view of the continuously oxic conditions prevailing during riverine transport, only terrestrial particulate OM has a chance of arriving at the sea, where it flocculates together with detritic minerals in deltaic systems, due to physicochemical processes induced by the change in salinity. The already strong degradation of terrestrial OM by the time it arrives at its settling place, along with the generally high burial rate in deltaic systems, prevents further extensive bacterial reworking in many cases (Hedges and Oades, 1997). Consequently, even though deposited in a marine environment, terrestrial kerogens are often almost devoid of organic S and are rich in aromatic structures derived from lignin, contain some resistant aliphatic moieties, sometimes mixed with coal debris, and are associated with clay minerals and

silts. The high mineral sedimentation rate due to precipitation resulting from salinity change would normally dilute the OM and lower the organic content of deltaic deposits. However, given the high energy of such environments, an abundant input of large sized organic particles is often observed, and the organic content of these sediments may vary over a short distance from low (around 1%) to very high (almost pure OM) concentrations. In deltaic systems, the source rocks formed in tidal channels are deposited together with organic-lean sands transported as bedloads on the bottom of distributary channels. The seaward progradation of the delta during geological times changes the lateral position or the activity of such channels, making an excellent connection between potential source rocks and reservoirs. Sedimentological study of the Mahakam delta (Allen et al., 1979) showed clearly how such a petroleum system is formed in time and space.

Hypersaline systems exert very specific constraints on the selection of organisms able to survive these particularly aggressive chemical environments. Such evaporitic systems can exist in marine as well as lacustrine environments. Many lacustrine source rocks such as the Eocene Green River shales were characterized at the time of deposition by alkaline waters, often associated with tectonic and volcanic activity, as reflected in the predominance of dolomite over calcite (Kelts, 1988). However, the ionic balance of lake waters varied quickly, depending on geodynamic and climatic changes. It was observed both for ancient and modern lacustrine settings that some blue green algae such as *Spirulina* are specific to alkaline hypersaline lakes. Kelts (1988) also mentions the presence of dense cyanobacterial mats in such environments, where no organisms above unicellular protozoae can survive, but where alkalinity promotes better solubility of CO_2, P and other nutrients, there by supporting high organic productivity.

4.3. Present and past OM accumulation in sediments

4.3.1. Quantitative distribution of kerogen in sedimentary rocks

Kerogen is generally by far the major component of total OM in sedimentary rocks, the remaining part being soluble or volatile products that have not, or not yet, been squeezed out of the rock by compaction. Kerogen amount is conveniently estimated by measuring the organic carbon (OC) content (wt%) of the extracted whole rock, after acid destruction of carbonate and quantification of the CO_2 generated by OM combustion. However, because C is not the only constituent of kerogen and since the C content of kerogen increases with maturity due to sediment burial, kerogen amount is underestimated by OC content, all the more so if sample maturity is low. Kerogen concentration in any sedimentary rock depends on the relative fluxes of organic and mineral constituents. Hence, this concentration not only reflects the organic productivity vs. alteration conditions, but also the general sedimentation pattern at a given geological period.

Global estimates summing, for all known sedimentary rocks, the quantities of the various forms of organic and carbonate carbon were obtained in the 1970s and are reported in Table 7, from the calculated mass of rocks in the Earth's crust and OC data from the literature (Hunt, 1972, 1996). Atmospheric and water dissolved CO_2 are not included in the Table, because it refers only to sedimentary rocks.

It has long been recognized that minerals can significantly influence OM preservation in sedimentary rocks. Table 8A (Hunt, 1972) shows the dependence of OC content on mineralogy. It appears not only that the average OC content of sediments is low, but also that the major part of sedimentary OM is preserved in fine-grained clays and shales. Table 8B illustrates the increase in TOC observed by

Table 7
Organic vs. carbonate C distribution in sedimentary rocks, in 10^{12} tons C (after Hunt, 1996)

Carbon form	Sediment type	Amount in continent, shelf and slope	Amount in oceanic domain	Total
Kerogen C	Clay/shale	8200	700	12,015
	Carbonate	800	1000	
	Sandstone/ siliceous	900	400	
	Coal	15		
Soluble C	Dispersed petroleum[a]		550	556.7
	Reservoired petroleum		6.7	
Mineral C	Shale		9300	64,300
	Carbonate		51,100	
	Sandstone		3900	

[a] Petroleum is taken here to mean all solvent soluble organic C including gas, heavy oil and asphaltic deposits.

Table 8
A: Average organic C content of sedimentary rocks. B: variation in average organic C content with sediment type and grain size (after Hunt, 1996)

Location	Sediment type	Average C (wt%)
A		
Continent, shelf and slope	Clays and shale	0.99
	Carbonate	0.33
	Sandstone	0.28
Oceanic domain	Clays and shale	0.22
	Carbonate	0.28
	Siliceous	0.26
Sediment	Sediment type, grain size	Average C (wt%)
B		
Viking	Siltstone	1.47
Shale	Clay 2–4 μm	1.70
Canada	Clay < 2 μm	5.32
Recent	Sand	0.70
Clastic	Silt	1.0
Sediments	Clay mud	1.6
California	Shelf >100 μm	< 0.2
Sediments	Offshore, 3–9 μm	5–9

several authors for the same mineralogy when grain size decreases (Hunt, 1996). Studies of recent sediments also clearly indicated that a textural control on OM concentration and a TOC increase were systematically observed when the mean particle size of sediments decreased (Suess, 1973; Tanoue and Handa, 1979; Mayer et al., 1985). Further studies illustrated the tight dependence of OM preservation on mineral particle size and surface area and on sediment mineralogy (Mayer, 1994a,b). Results from SPLITT fractionation (split flow, thin cell, lateral transport) of marine sediments, which allows hydrodynamic sorting of particles by size and density (Keil et al., 1994), indicated that the total amount of associated OM depends only on the size class, whereas the mineralogy influences the composition of the adsorbed OM. A major role for minerals in OM protection has also been recognized for soil (e.g. Oades, 1995; Kaiser and Guggenberger, 2000; Schmidt and Noack, 2000; Baldock and Skjemstad, 2000; Kiem and Kögel-Knabner, 2002; Eusterhues et al., 2003). Observations by Poirier et al. (2001) showed conspicuous differences between survival under natural conditions and resistance to laboratory hydrolysis, for the deep layers of a tropical soil. In these layers the OM exhibited a mean ^{14}C age above 8000 years but the bulk was labile when submitted to laboratory hydrolysis after elimination of minerals. Such uncoupling reflects a major role of the mineral matrix for long term OM protection in this soil. In addition, long term protection of proteinaceous materials in biominerals is well documented.

The occurrence of "sorptive protection" in sedimentary OM preservation was inferred from observations on various recent marine sediments. These observations showed positive correlations between TOC and mineral grain surface area (Fig. 8) and sharp increases in mineralization rates, in laboratory degradation experiments with bacteria, after OM desorption from sediments (Mayer, 1994a; Keil et al., 1994; Hedges and Keil, 1995). Furthermore, the observations also revealed preferential association of OM with Ca-rich (smectite, specific surface area >100 m^2/g) rather than with Ca-poor (kaolinite, specific surface area ca. 30–40 m^2/g) clay minerals (see also Ransom et al., 1998). Adsorption of organic compounds as molecular monolayers on to minerals should provide an efficient protection against diagenetic degradation. Potentially labile compounds could thus survive and contribute to kerogen. Over 80% of the surface area of marine sediment grains is accounted for by a few nm wide pores and it was considered that most of the adsorbed OM is concentrated in these mesopores (Mayer, 1994b). Such a location would afford efficient physical protection against microbial degradation due to the very small size of the pores excluding hydrolytic enzymes. Moreover, high OM concentration in the pores should favour subse-

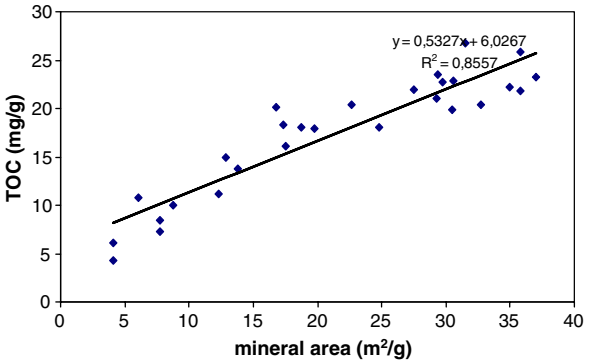

Fig. 8. TOC vs. surface area for sediment sampled in the Gulf of Maine at sediment–water interface, for water depth >75 m. Surface area determined using BET method on N_2 gas adsorption isotherms. Linear regression slope is 0.53 mg TOC m^{-2}. Modified from Mayer (1994a).

quent condensation reactions and hence contribution to protokerogen of low molecular weight, intrinsically labile compounds (Collins et al., 1995). Intimate association between OM and clay minerals was observed in estuarine sediments via high resolution TEM observations and high resolution element mapping using energy filtering TEM (Furukawa, 2000). Further laboratory experiments on OM adsorption/desorption using mesoporous and nonporous minerals supported protection in mesopores (Zimmerman et al., 2004). On the contrary, other observations pointed to preferential association of OM with clay particle edges rather than with mesopores (Mayer et al., 2004). Physical protection by clay minerals can also result, as mentioned in the section on kerogen storage, from the alternation of organic and clay nanolayers (Salmon et al., 2000). Efficient protection of intracrystalline OM, occluded in $CaCO_3$ minerals, was also observed for carbonate sediments (Ingalls et al., 2004). Whatever the implicated process(es), mineral protection should be reflected in the presence of amorphous kerogens intimately associated with the mineral matrix.

OM sedimentology and its interaction with minerals was also clearly evidenced by Belin (1992a,b) via BSEM observations. This technique takes advantage of the spatial resolution of SEM and of the influence of the atomic number contrast between light OM and heavier minerals on the amount of backscattered electrons. The study of more or less carbon-rich samples from twelve well known source rocks varying in age, source and depositional conditions showed two main types of OM distribution in the mineral matrix: as particles or as laminites parallel to the stratification. Beside the pure organic particles of different morphology and size appearing in black on the BSEM micrographs, an organic shapeless intermediate form disseminated within the matrix could also be observed (Belin, 1992b). Micrographs of source rocks displaying these two main types of OM distribution and their relationship with minerals, highlighting the close association of organic particles with pyrite, are shown in Plate d. The influence of the depositional environment on OM morphology (particulate in coastal high energy settings and laminated or structureless in basinal confined low energy settings) has been shown clearly by these studies. Observations on the variability of organo-mineral textures for a given TOC and

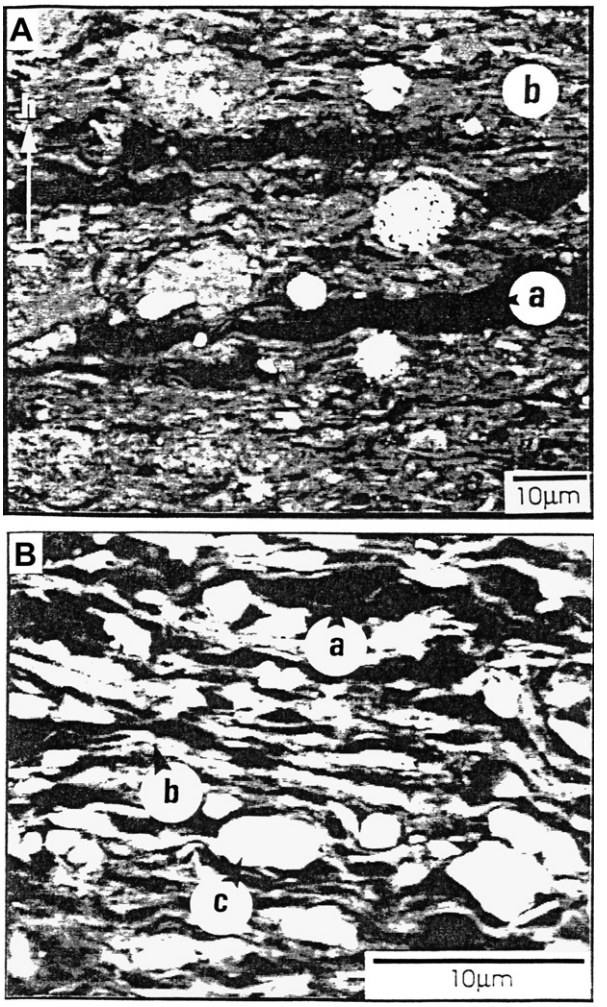

Plate d. Main types of organic matter sedimentology as observed with SEM used in backscattered electron mode. The organic matter appears black due to the low atomic number. (A) Laminated morphology: example of the Toarcian paper Shales from the Paris basin. TOC = 5.3 wt%. The organic matter is made both of elongated algal bodies (a) arranged in laminae, several tens of µm in length, less than 5 µm thick, parallel to bedding, and of small organic particles often less than 2 µm, associated with clay minerals (b). The organic network can be considered as almost continuous. Note the presence of pyrite framboids. The arrow (h) is perpendicular to the bedding. (B) Particulate morphology: example of the Noto formation of the Ragusa basin, Sicily, TOC 17.1 wt%. The organic particles (a) have a more or less round shape, 2–5 µm in diameter; they could originate from faecal pellets or from mechanical erosion of larger organic particles, either algal mats or plant debris. They are dispersed within minerals, clays (b) and quartz (c), the granulometry of which is similar to that of organic matter, indicating that the same depositional mechanism controls both organic and mineral sediment deposition. Reprinted with permission from Belin (1992b).

its consequences in terms of OM adsorption on mineral surfaces or continuity of organic networks, a key factor for oil migration (Durand, 1988; Stainforth and Reinders, 1990), are also important outcomes of this work.

4.3.2. Evolution of OM production and preservation over geological time

Sedimentary cycles were recognized early and attributed to the combined effect of tectonics and sea level variation (Graubau, 1936). It was later observed by petroleum geologists that the abundance of sedimented OM, including coal, depends on sea level change, and that the highest sea level positions correspond to the highest estimated phytoplankton production (Vail et al., 1977; Tissot, 1979). Stratigraphic control on OM production and preservation occurs at different timescales corresponding to four main eustatic cycles (Duval et al., 1998) ranging from first order (duration >50 Ma) to fourth order (duration between 0.01 and 0.5 Ma). In each of these sequences, sea level rise increases the surface area of shallow epicontinental seas, where OM preservation is higher than in the deep ocean. Moreover, increased volcanic activity during continental drifting is responsible for CO_2 release into the atmosphere, which in turn changes the climate and oceanic circulation, promoting primary production (Huc et al., 2005).

On a first order scale (Fig. 9), two periods, from the Silurian to the lower Permian and from the upper Jurassic to the middle Cretaceous, contain more than 80% of the known source rocks. On a second-order scale (duration 3–30 Ma), six stratigraphic intervals, from the early Silurian to the middle Miocene/upper Oligocene (Fig. 10), are characterized worldwide by organic-rich sedimentary rocks accounting for around 90% of the world's initial petroleum resources. However, effective source rocks in terms of petroleum potential only occur in minor zones in these stratigraphic intervals, often not over a few tens of meters thick. The third and fourth order cycles have a local influence at the basin scale, as exemplified by the lower Jurassic and Kimmeridgian organic-rich sedimentary rocks in England (van Buchem and Knox, 1998; van Buchem et al., 2005).

The main factors controlling source rock deposition and kerogen composition through geological time are assumed to be the evolution of climatic conditions associated with atmosphere composition and continent rifting, and the balance between OM

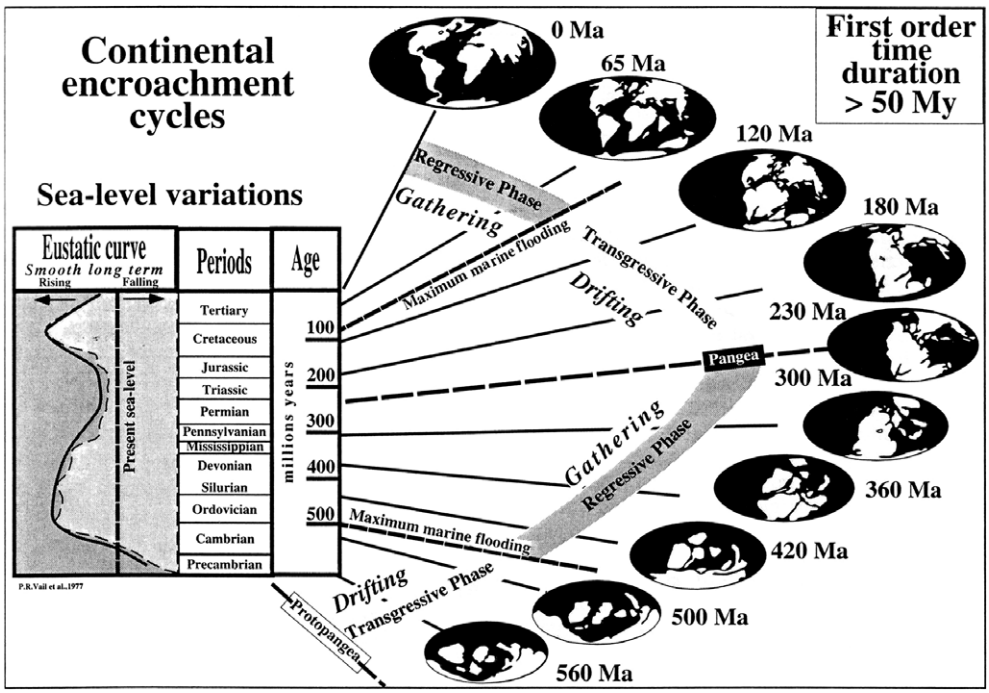

Fig. 9. Continental encroachment cycles and first order eustatic cycles during Phanerozoic: transgressive and regressive phases. Reprinted with permission from Duval et al. (1998, p. 45).

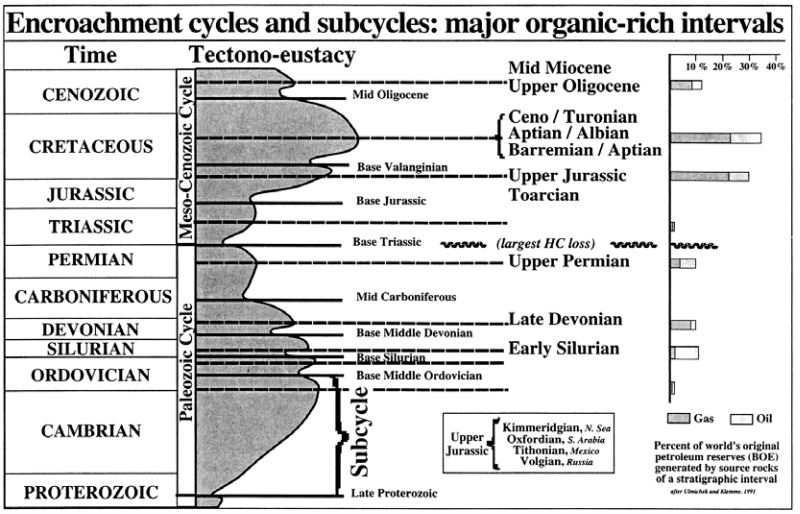

Fig. 10. Continental encroachment subcycles and second order eustatic cycles: major organic-rich intervals. Reprinted with permission from Duval et al. (1998, p. 46).

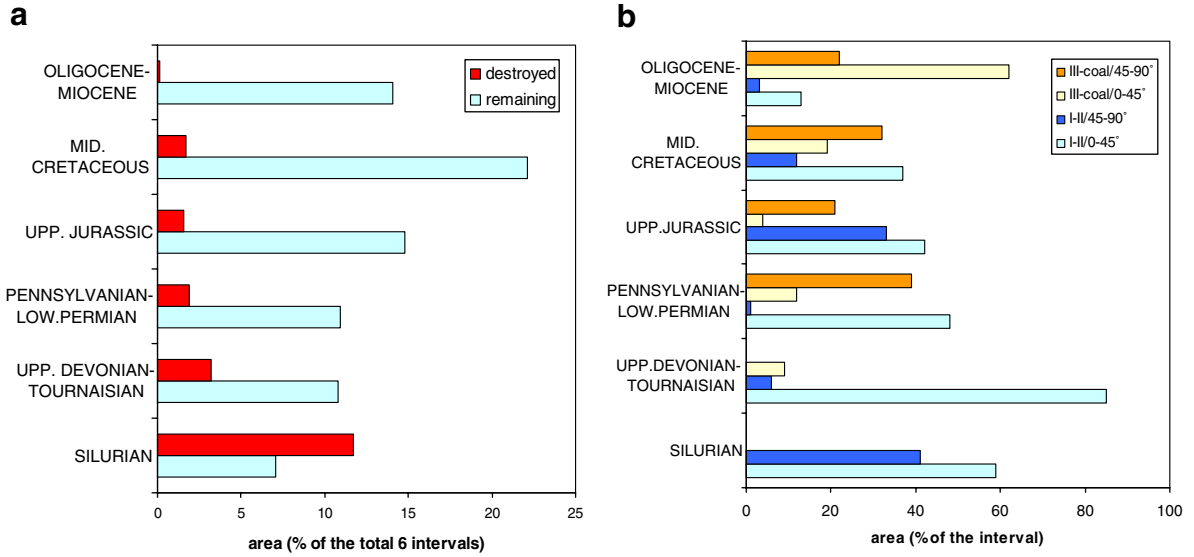

Fig. 11. (a) Source rock area distribution, remaining and presently destroyed by erosion or metamorphism, in % of the six main organic-rich stratigraphic intervals; (b) distribution of Types I/II and III source rocks areas (% of the interval) according to palaeolatitude in each stratigraphic interval. Modified from Klemme and Ulmishek (1991).

primary production and degradation (Klemme and Ulmishek, 1991). The total vs. presently destroyed (i.e. removed by orogenesis) geographical areas in the six major organic-rich stratigraphic intervals and their OM Type are presented respectively in Fig. 11a and b according to the data compiled by these authors. Source rocks containing aquatic lacustrine or marine OM (Types I and II as defined in the section on kerogen Types) have been grouped together because Type I kerogens have provided only ca. 3% of the original reserves of the world's petroleum (Klemme and Ulmishek, 1991). If the age of the source rock has a strong influence on its partial destruction by geological events, it is clear that the total depositional area for C-rich sedimentary rocks is not increasing with the evolution of life. Indeed the areal extension of younger source rocks containing terrestrial deposits (Type III as

defined in the section on kerogen Types) is paralleled by a relative decrease in aquatic OM deposits. It is also clear from Fig. 11b that the climate, using palaeolatitude as a proxy, influences both the bioproductivity and the preservation of sedimented OM, particularly for aquatic remains for which water stratification and resulting anoxia under warm climates favour increased preservation. For terrestrial OM, this is not observed except for the last stratigraphic interval, during which the most prolific sedimentary environments are large tropical and equatorial deltas.

The amount of sedimented OM depends on the balance between primary production by photosynthetic organisms and mineralization by heterotrophs. Therefore, the biological evolution of primary producers cannot be the only factor controlling the organic content of source rocks. Bacteria seem to have reached a high level of diversification very early because many fossil bacteria from lower Proterozoic rocks have their extant morphological analogues. However, this does not mean that their enzymatic set has not changed. The composition of the atmosphere regarding O_2 and CO_2 proportions has changed over geological time. However, it seems that deposition of rich source rocks was possible during the late Proterozoic-early Paleozoic times under dysoxic, or even oxic, conditions, as deduced from the presence of benthic fossils. This observation led Klemme and Ulmishek (1991) to hypothesize that heterotroph evolution towards a better degradative efficiency for OM, associated with diversification of the nature and geographical distribution of primary producers, changed progressively over geological time from environments favourable for marine source rocks to environments favourable for terrestrial source rocks. Indeed, the evolution of terrestrial plants after the Silurian brought a new OM source. However, until the Permian, plants were located on seashores, whereas during the Mesozoic and Tertiary there was a large land expansion and progressive adaptation of plants to more arid or swampy environments owing to a larger development of wax-rich protective tissue (Thomas, 1981; Klemme and Ulmishek, 1991). In contrast, in the marine realm, black shale facies – the dominant marine source rocks in the Cambrian and Ordovician – even when deposited in more or less oxic conditions, became more and more restricted to dysoxic environments in the Silurian, Devonian and early Carboniferous. A parallel increase in benthic fossil number and diversification is observed with increasing water depth. These features suggest better efficiency for marine OM consumption because there is no reason why marine primary productivity should have decreased through geological time. This is reflected in the change observed in the structural forms where major OM accumulations are observed, from open platforms in the Paleozoic to half sags (asymmetric sedimentary bodies composed of the seaward prograding wedges of clastic rocks and carbonate bank sediments) and deltas in the Tertiary.

4.4. Summary

- Kerogens are mainly sourced from plant materials, algae and terrestrial higher plants, and contain an unknown but probably minor amount of bacterial input. From 0.1% to $< 1\%$ of the organic primary productivity from autotrophic organisms is incorporated into sediments, leading to a chemical composition for kerogen strongly different from that of living organisms.
- Kerogen composition depends not only on biological precursors, but also on the chemical and biochemical alteration processes occurring during OM transport to the site of sedimentation, thus leading to a clear-cut difference between marine and terrestrial kerogens. This difference is also observed in the chemical composition and granulometry of associated minerals.
- At the Phanerozoic geological timescale, six stratigraphic intervals, associated with warm climate and high stand water levels, contain 90% of the world's petroleum source rocks.

5. Preservation processes

At the beginning of the 1960s, Forsman (1963, p. 177) had already noted that "It seems fairly safe to assume that kerogen represents the resistant portions of organisms that were deposited with the sediment". It was considered for a long time, in agreement with the insolubility and highly complex chemical structure of kerogen, that seemingly random polycondensation reactions played a major role in the genesis of this fossil macromolecular material. Thus, according to the so-called "degradation–recondensation" pathway, some biodegradation products of biopolymers would recondense progressively, thus escaping mineralization, and

the resulting insoluble product would consist of geopolymers (or more precisely geomacromolecules) that are the direct precursors of kerogen. It was only in the 1980s that the contribution of another process was demonstrated. The so-called "selective preservation" pathway does not require any intermediate condensation step. It also allows for better correspondence with coal formation mechanisms, where selective preservation was an obvious pathway on the basis of microscopic studies. Although selective preservation may account in some cases for the major part of the constituents of a kerogen, its implication strictly depends on the occurrence of organisms containing resistant biomacromolecules in the initial biomass. In contrast to selective preservation, the classical mechanism via degradation–recondensation is expected to occur in any situation and to account for a highly variable proportion of the total kerogen.

5.1. Degradation–recondensation mechanisms

Dead organisms and various excretion products undergo biochemical and physicochemical decomposition during deposition. Among their constituents, the most prone to biodegradation are proteins and carbohydrates that can be broken into water-soluble amino acids and sugars by ubiquitous enzymes and then used very rapidly in the biological cycle. Biodegradation of phenol-containing biomolecules also generates large amounts of water-soluble phenolic compounds. Abiotic recondensation reactions between such degradation products occur spontaneously under conditions similar to those in natural environments. These reactions would form complex (randomized) chemical structures that cannot be biodegraded further since they are no longer recognizable by degradative enzymes. These recombined compounds can thus escape the biological cycle. With humic-like compounds being formed by this type of recondensation reaction, the whole process was thought to be similar to natural humification and so kerogen was supposed to originate, at least in part, from condensation reactions similar to those occurring in humic substance formation (Huc and Durand, 1974). Given their supposed common precursors, therefore, the relationship between kerogen and humic substances in waters, soils and sediments was studied extensively.

Like the definition of kerogen, the definition of humic substances in recent sediments is operational. As mentioned above, the latter are derived from soil science (Kononova, 1966) where humic acids are oxygen-rich, acidic water-soluble compounds extractable with alkali, with the difference between humic and fulvic acids being that the latter are not reprecipitated at pH 2. Humin is the insoluble organic residue from this extraction. Humin can also be isolated using the same method as for kerogen, i.e. acid destruction of the associated minerals, although a few % loss of hydrolysable OC occurs for very immature sediments, and therefore it can be considered as protokerogen (Stuermer et al., 1978).

5.1.1. Basic mechanisms considered for humification

5.1.1.1. Maillard reactions. Spontaneous random condensation of glycine (amino acid formerly named glycocolle) and glucose (reducing sugar), along with CO_2 formation, was observed by Maillard in air-free water at temperatures from ca. 30 to 100 °C for times from minutes to a few days (Maillard, 1912a,b, 1916). The elemental balance of these experiments showed that water was also formed and that condensation increased continuously with time, producing water-insoluble, humic-like yellow, then brown, compounds termed melanoidins. Condensation was observed using different amino acids and reducing (aldehyde- or ketone-containing) sugars, and also starting with hydrolysis products of polypeptides and non-reducing sugars. The reaction mechanism would be as shown in Fig. 12. This reaction was supposed by Maillard to be the origin of soil humus. However, chemical degradation studies (Burges et al., 1964) showed that phenols were very abundant, whereas proteins are minor components among the degradation products of soil humic substances. Nevertheless, this type of condensation could easily occur in humic substances from marine environments, because algal OM generally has a higher protein content than land plants, as shown in Fig. 13 (Huc, 1980).

5.1.1.2. Oxidative condensation of phenols. As phenols can be abundant constituents (up to 30%) of soil humic acids (Burges et al., 1964), condensation of some of their oxidation products, quinones, was proposed as one of the major humification mechanisms in soils, following the reaction scheme described in Fig. 14 (Kononova, 1966; Flaig, 1966). Condensation between oxidation products of various phenols was simulated in the laboratory using H_2O_2 and peroxidase (Schnitzer et al., 1984) or mineral oxides, but substitution position

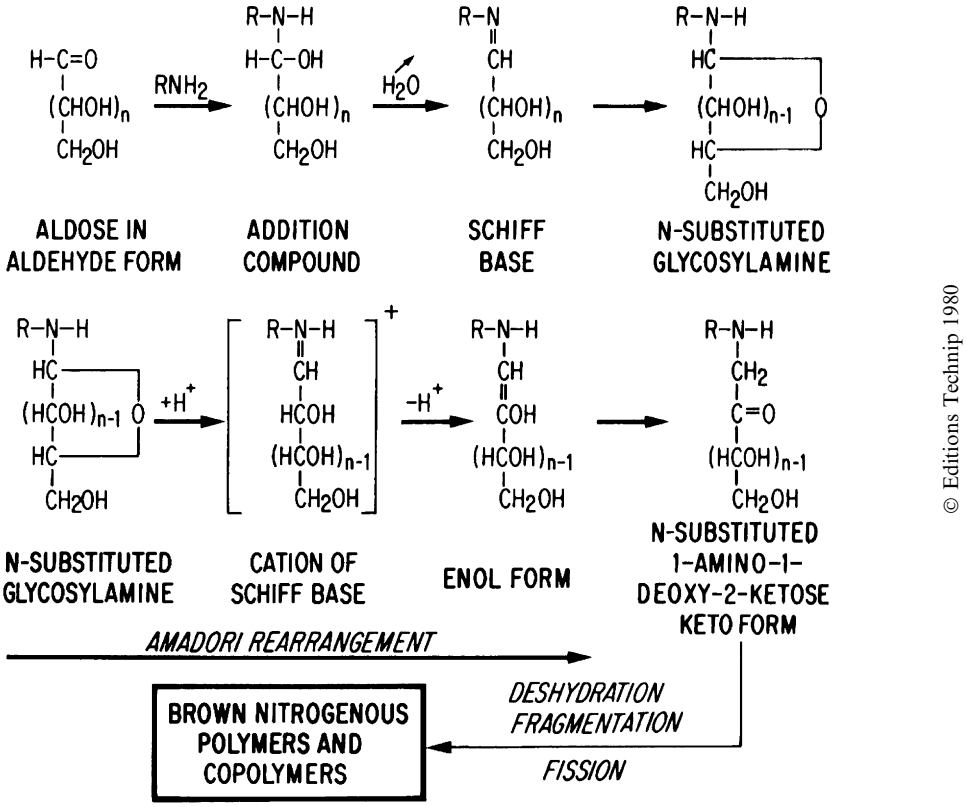

Fig. 12. Reaction mechanism assumed for Maillard reaction: formation of melanoidins via sugar–amine condensation. Reprinted with permission from Huc (1980, p. 457).

appeared to control quinone formation and subsequent condensation (Flaig, 1988).

Nitrogenous compounds, for example amino acids from protein biodegradation, can easily be incorporated during oxidative polymerisation of phenols, accounting for nitrogen occurrence in humic substances. A reaction scheme showing the possible condensation reaction between amino acids and phenols was proposed by Stevenson and Butler (1969); Fig. 15. Amino sugars from bacterial cell walls can also condense with phenols in a similar way (Martin and Haider, 1971). In soils, phenolic compounds can originate from tannins or from lignin degradation by fungi. The microbial biomass - bacteria, yeasts and fungi - can also be a source of phenols, then quinones from aliphatic precursors, as demonstrated by Haider and Martin (1967) and Martin and Haider (1971). This condensation mechanism based on phenols could thus be implicated for humic substances in both soils and sediments. In fact, phenol reactions and the Maillard reaction might be linked into an integrated abiotic humification process catalysed by minerals (Jokic et al., 2004).

5.1.1.3. Oxidative crosslinking of polyunsaturated fatty acids. Paraffinic structures are abundant in dissolved humic substances in open ocean water (mainly fulvic acids), as evidenced by NMR and elemental analysis, whereas organic molecules able to undergo condensation, according to the above mechanisms, occur only in very low concentration. These two features led Harvey et al. (1983) to propose a new condensation pathway, starting from polyunsaturated triglyceryl lipids abundant in marine organisms. The reaction would be initiated by sunlight-mediated autoxidation producing, by way of oxygen cross-linking, oxygen-rich humic products with some aromatic structures and aliphatic chains ending with free terminal carboxyl groups, as shown in Fig. 16.

Synthetic fulvic acids were successfully obtained by Harvey and Boran (1985), using various unsaturated triglycerides in OM-free seawater under sun-

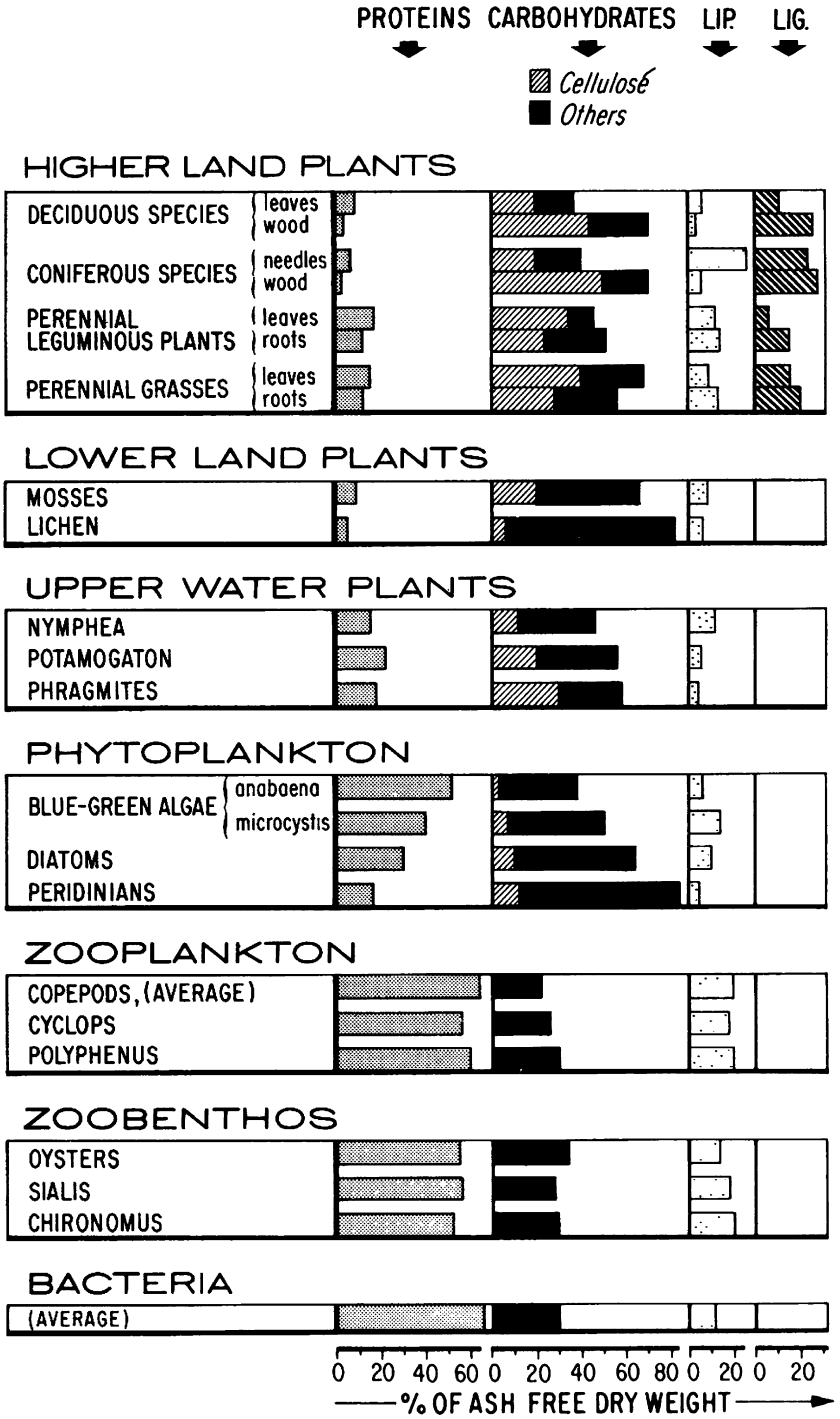

Fig. 13. Composition (dry wt%) of main organic constituents (proteins, carbohydrates, lipids and lignin) from various living organisms. Reprinted with permission from Huc (1980, p. 448).

light. However, several inconsistencies in elemental analysis, nitrogen incorporation and ^{13}C fractionation were observed between these synthetic humic products and natural ones. The main question remains the demonstration of this model for fulvic acid formation in marine environments.

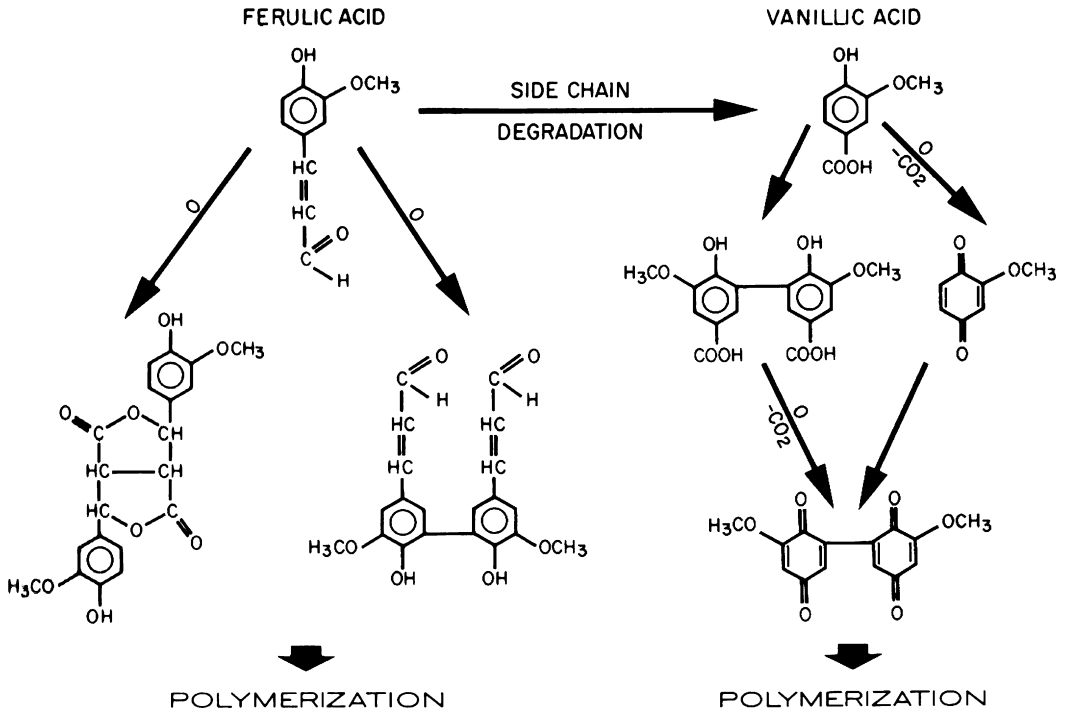

Fig. 14. Possible formation of humic compounds by phenol–phenol oxidative condensation. Reprinted with permission from Huc (1980, p. 456).

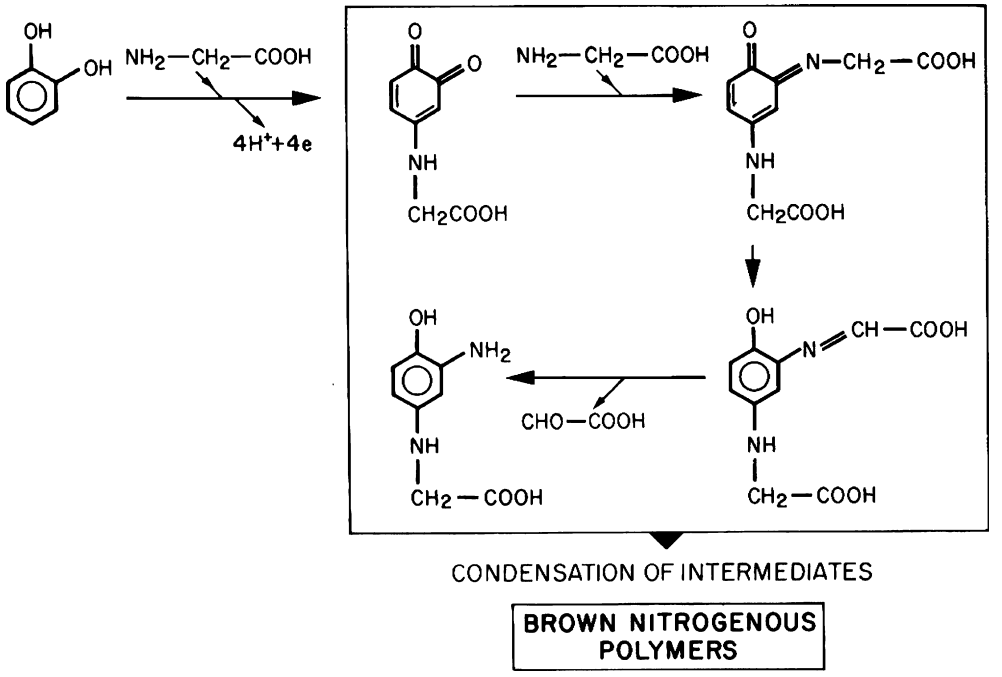

Fig. 15. Reaction mechanism assumed for condensation between amino acids and phenols. Reprinted with permission from Huc (1980, p. 456).

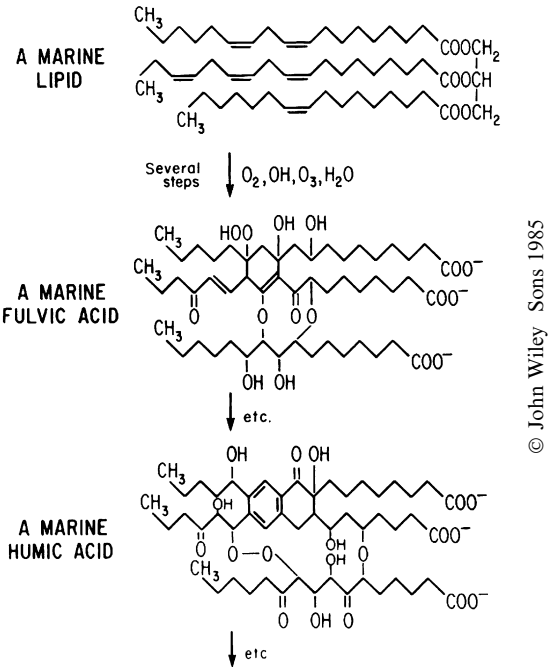

Fig. 16. Cross-linking oxidative reaction mechanism in unsaturated triglyceryl lipids assumed to be at the origin of marine fulvic and humic acids. Reprinted with permission from Harvey and Boran (1985, p. 237).

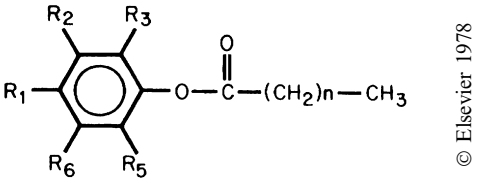

Fig. 17. Hypothetical structure of condensation products of fatty acids with phenols in humic (HA) and fulvic (FA) acids. R_1 = OH or COOH or $COCH_3$; R_2 = H or OH or COOH; R_3 = H or OH or COOH or OCH_3; R_4 = OH esterified to fatty acid; R_5 = H or OH or OCH_3; R_6 = H or $COOCH_3$; n = mainly 14 and 16 for HA and 14, 15, 16 and 18 for FA. Esters could form via any free OH group on the aromatic ring. Reprinted with permission from Schnitzer (1978, p. 45).

5.1.1.4. Esterification between fatty acids and phenols. Even for land derived OM, a substantial amount of paraffinic structures is observed in humin from recent sediments, as shown by solid state ^{13}C NMR (Hatcher et al., 1985). The incorporation of fatty acids, present among other lipids in cuticular waxes and cork saponification products (Van Krevelen, 1993, p. 152), may occur by condensation between fatty acids and phenols. The general structure of the resulting compounds, able to undergo further condensation by other reactions, is shown in Fig. 17 (Schnitzer and Neyroud, 1975). Saponification of humic and fulvic acids releases high amounts of both fatty and phenolic acids. The phenolic to fatty acid molar ratio of 0.76 observed for various humic acids suggests that ester bonds are the main covalent bonds responsible for paraffinic structure incorporation into humic terrestrial materials (Schnitzer, 1978).

As already discussed in Section 2.1.5, we have restricted OM preservation mechanisms to chemical reactions allowing a small part of the OM to escape remineralization during its transport and falling down to the sedimentation site. Accordingly, sulfurization is described for the early diagenesis stage of OM evolution (Section 7.1.2).

5.1.2. Implication of these condensation reactions for sedimentary OM

The prevalent view for OM preservation in sediments in the 1970s was based on biopolymer degradation, followed by random polycondensation, ending with non-biodegradable geopolymers (Nissenbaum and Kaplan, 1972; Welte, 1974) according to Fig. 18.

After the death of primary producers, biopolymers are biodegraded and a small part of these degradation products escape the biological cycle by undergoing increasing polycondensation via the above mechanisms, with successive formation of initially water-soluble, then insoluble compounds. In this scheme, there is a direct relationship between fulvic acids, then humic acids and finally humin and kerogen, as suggested for humin formation in soils (Swain, 1963) and for coals (van Krevelen, 1961; Stach, 1975). This mechanism was also proposed to explain the observed decrease in the amounts of fulvic, then humic acids relative to humin, with increasing burial depth in marine sediments (Huc and Durand, 1977). However, the condensation reactions, although possible under environmental conditions, proceed slowly at natural temperatures. Moreover, the starting biodegradation products, probably in low concentration in the environment, are likely to be mineralized before recondensation (François, 1990).

Polycondensation was not the unique mechanism considered by Tissot and Welte (1978): they explicitely indicated (p. 87) that "a certain part of the organic matter, mostly made of lipids ... never passed through the fulvic or humic acid stage", as shown in Fig. 19. "Lipids" was taken by these authors in the sense of aliphatic insoluble compounds and not in the sense of the common definition implying

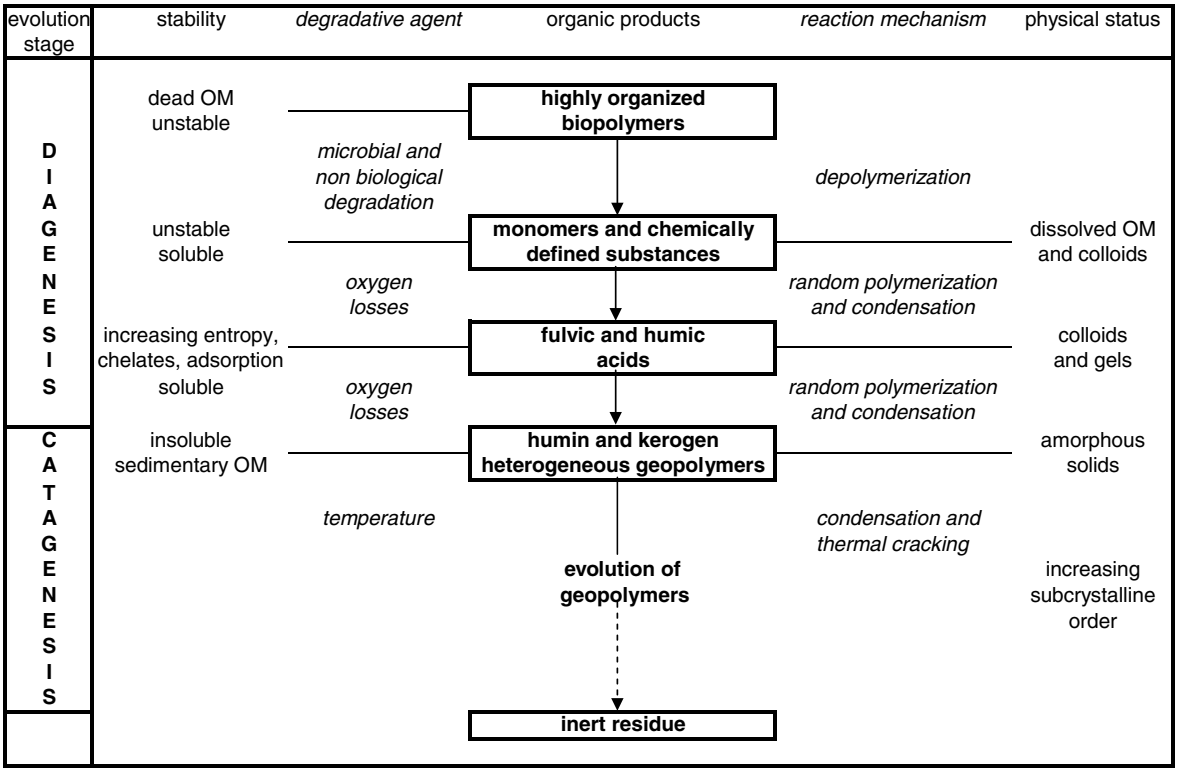

Fig. 18. Schematic pathway of successive transformation of OM from biopolymers to sedimentary OM. Adapted from Welte (1974).

solubility in organic solvent. This has led to a frequent misunderstanding of Fig. 19. Moreover, no information on the nature of these "lipids" and no quantitative estimate of respective contributions of such kerogen precursors was available at that time. It is worth noting that in his definition of sedimentary OM and kerogen, Durand (1980) also mentioned (p. 14) that "sedimentary organic matter was in part comprised of substances of low chemical reactivity which had a protective role against the external medium, among which are for example sporopollenin or chitin".

Pyrolysis gas chromatography (Fig. 20) clearly shows that paraffinic structures occur in substantial amounts in humins and humic acids, whereas this is not the case for fulvic acids, in terrestrial as well as in marine sourced sediments (Vandenbroucke et al., 1985). The same observation was also reported by Ishiwatari (1985) for the alkaline permanganate degradation products from a lacustrine sediment. The author concluded that it is impossible to explain the formation of humic acids and humin by polymerization of fulvic acids. In fact, fulvic acids might be derived from humic acid oxidation and, as proof, fulvic acids were experimentally obtained from humic acids stored in air-containing water (Flaig et al., 1975). Similarly, humic acids could be derived partly from humin oxidation. Indeed, it is a general observation that, in a homogeneous set of samples from a given environment, the humin to humic acid ratio increases with organic carbon (OC) amount. This could be due to better preservation of humin from bacterial reworking, due either to physical inaccessibility or to OM hydrophobicity. An example of this relationship is given in Table 9 for three coaly surficial samples from the Mahakam delta (Vandenbroucke et al., 1987). Increasing transport distance, and hence duration, for the same initial OM, also decreases the amount of OM deposited in surficial sediments and increases the fulvic acid and hydrolysable fraction, reducing the corresponding amount of non-hydrolysable humin, as shown in Table 10 (Vandenbroucke et al., 1985).

Based on the above observations, it was suggested that oxidative degradation reactions, probably mainly due to bacterial reworking, could form fulvic acids from humic acids, and humic acids from humin. In such a process, part of the originally sedimented OC would be progressively eliminated with

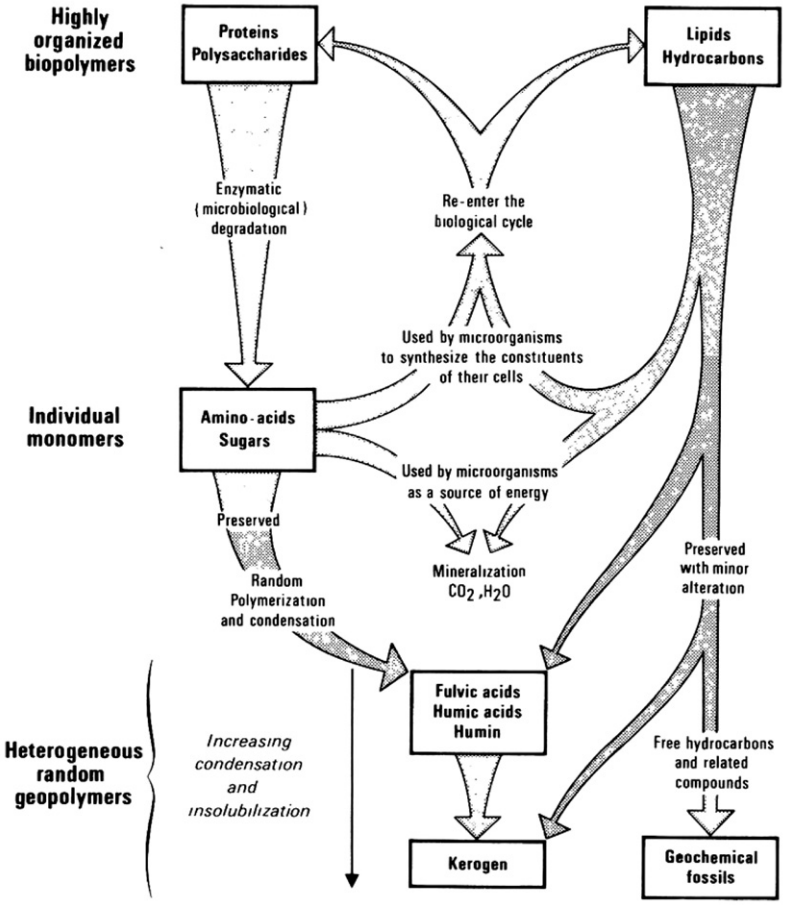

Fig. 19. Fate of organic material during sedimentation and diagenesis, assuming two different paths for incorporation of biopolymer residues into kerogen. Reprinted with permission from Tissot and Welte (1978, p. 90).

increasing burial by mineralization and water solubilization, as shown by direct measurements on resuspended material from sediment traps (Suess, 1980; Weser et al., 1982). Since efficient bacterial oxidation is no longer possible once the sediment is buried more than a few meters, fulvic and humic acid amounts should decrease progressively (Vandenbroucke et al., 1985). Similar conclusions, concerning oxidative degradation from humin to humic compounds, rather than a reverse condensation, were also put forward by Hatcher et al. (1982) to account for the solid state ^{13}C NMR analysis of a series of coalified woods and, by analogy with these observations, for the transformation of humin in aquatic sediments (Hatcher et al., 1985). However, some similarities between analysis of humic acids and humin, together with their parallel defunctionalization with increasing burial, suggest that a presently poorly quantified part of the humic acids might undergo insolubilization and be incorporated into humin. It can thus be expected that the related kerogen fraction would originate essentially from condensation reactions.

5.1.3. The relationship between kerogen and humic substances

The mechanism leading via successive condensation from fulvic acid to humic acid and then humin and kerogen is now strongly disputed, although it is generally agreed that the main precursor of kerogen is humin. Two opposite generic models (Fig. 21) are presently proposed to explain humic substance formation, as discussed by Hedges (1988).

The abiotic condensation model (Fig. 21) is the classical pathway proposed in the 1970s for kerogen formation (Huc and Durand, 1977). In such a model, after the first biodegradation step, producing simple building blocks from biopolymers, these blocks recombine by abiotic reactions that prevent further biodegradation. In parallel, some high

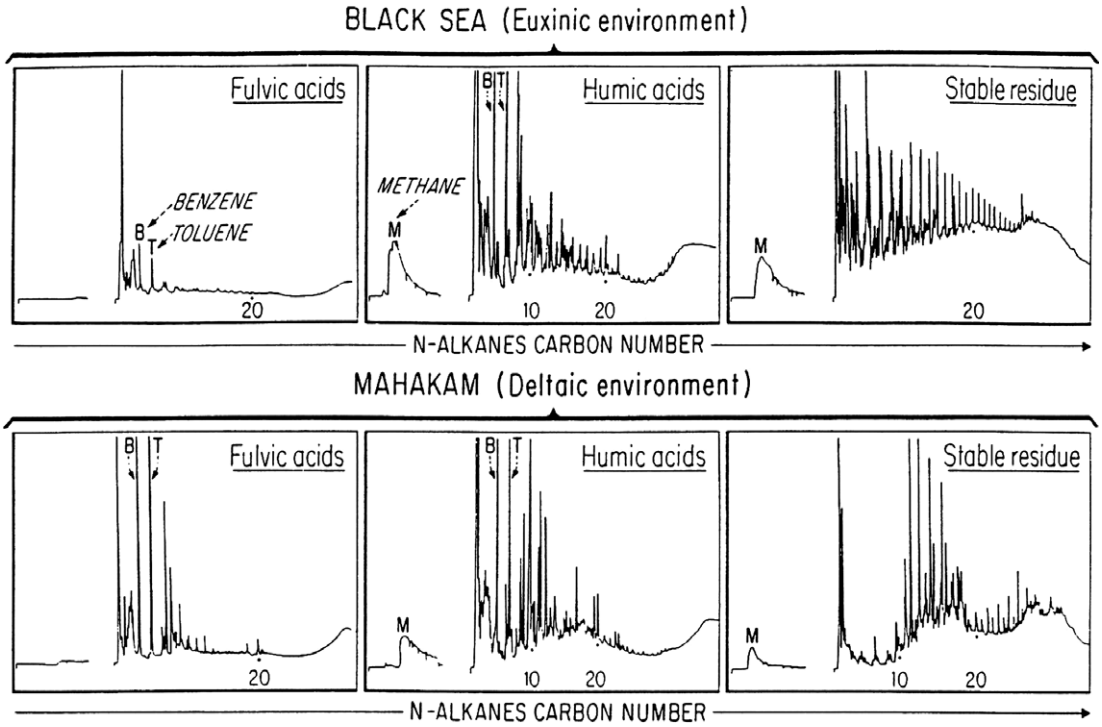

Fig. 20. Pyrolysis-GC of fulvic acids, humic acids and humins (stable residues) isolated from recent sediments with Types II (Black Sea) and III (Mahakam delta) organic precursors. Reprinted from Vandenbroucke et al. (1985, p. 261).

Table 9
Relationship between TOC and humic compound distribution in OM of coals and coaly shales from surficial sediments in Mahakam delta (Indonesia)[a]

TOC (%)	2 N HCl hydrolysate	Fulvic acid (% of TOC)	Humic acid (% of TOC)	Humin (% of TOC)
27.3	1.3	4.9	12.7	81.1
12.4	1.6	6.8	28.6	63.0
2.7	6.3	19.9	25.8	48.0

[a] After Vandenbroucke et al. (1987).

Table 10
Influence of pre-sedimentary alteration on OM composition in surficial samples collected under increasing water depth [a,b]

Water depth (m)	TOC (%)	2 N HCl hydrolysate	Humin hydrolysate	Fulvic acid (% TOC)	Humic acid (% of TOC)	Humin (% of TOC)
1900	2.28	14	25	8	18	35
2500	2.08	11	20	10	39	20
3250	0.91	16	29	16	23	15
3750	0.43	28	23	19	23	7

[a] After Vandenbroucke et al. (1985).
[b] Sampling performed at four stations along Cape Blanc transect, offshore Mauritania.

molecular weight degradation products of biopolymers, showing enough chemical resistance to further biodegradation, would be incorporated as such into humin. Humic substances generated by such a pathway increase in size and complexity, by going from fulvic to humic acids and then via insolubilization to humin. Only one part of humin would thus be concerned with the whole process, the other being

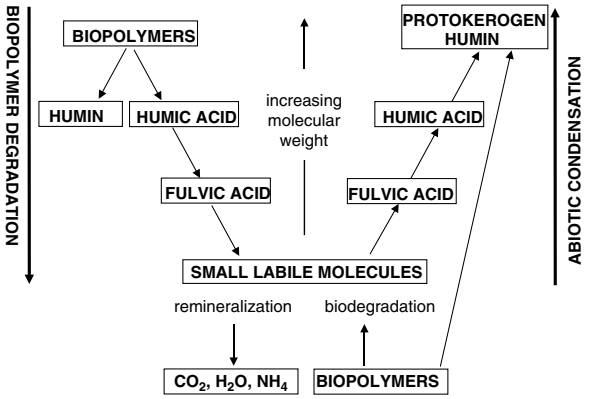

Fig. 21. Schematic representation of biopolymer degradation and abiotic condensation pathways assumed for humic substance formation. Adapted from Hedges (1988, p. 47).

directly inherited from resistant biopolymer-derived macromolecules (Durand, 1980). In this pathway, fulvic and humic acids are, at least in part, intermediates for humin formation, and there is a net gain in humin (protokerogen) with natural evolution upon burial.

The second generic model is the biopolymer degradation model (Fig. 21). Since biopolymer degradation is the initial step in any of the previously discussed schemes, it is assumed to be the main mechanism for humic substance formation. In this pathway, increasing degradation of biopolymers produces humic and then fulvic acids. However, these water-soluble acids would not be the only products generated. On one hand, fulvic acids can be degraded up to the ultimate formation of simple acids in a further step. On the other hand, as for the abiotic condensation model, high molecular weight resistant molecules are incorporated without further degradation into humin. In such a model, humic acid formation is the first stage in the degradation process, fulvic acids derive from further degradation of humic acids and only one part of the humin is concerned with the whole degradation path. Accordingly, fulvic and humic acids do not participate in humin formation and there is a net loss of humin (protokerogen) with natural evolution upon burial.

Humic and fulvic acids are proportionally more abundant than humin and the total amount of sedimented OC decreases when depositional conditions become more degradative. Accordingly, humic acid formation by this "degradative" model could also be a major pathway for marine (Vandenbroucke et al., 1985) as well as terrestrial OM (Hatcher and Spiker, 1988). However, recombination reactions, i.e. the first "condensation" model, could occur when the concentration of reactive chemical species is high enough, for example during the biopolymer degradation step. It can also be hypothesized that during diagenesis the loss of oxygenated functional groups in humic acids promotes their insolubility in water, and thus their incorporation as constituents into the future kerogen.

5.2. Selective preservation pathway

This pathway is based on the production by some living organisms of insoluble biomacromolecules that exhibit a high resistance to chemical and bacterial degradation. These biomacromolecules are generally highly aliphatic and remain almost unaffected by drastic basic and acid laboratory hydrolysis. Such macromolecular components also show a high resistance to attack by microbial hydrolytic enzymes. Thus, they can remain virtually unaffected during deposition while most of the other constituents of the initial biomass are heavily degraded and remineralized. As a result, selective preservation, and hence selective enrichment, of such biomacromolecules takes place during diagenesis.

5.2.1. Selective preservation of materials from algal cell walls

It has been recognized for a long time that different types of biomolecules exhibit large differences in their intrinsic resistance to diagenetic alteration and remineralization. For example, it is well documented that lipids and lignins are less degraded during early diagenesis than proteins and carbohydrates (e.g. Van Krevelen, 1993, Chapter 5). In addition, early studies showed some similarities between the products obtained from alkaline permanganate oxidation of the "kerogen-like" material, isolated from some extant microalgae and bacteria through extraction and acid hydrolysis, and the oxidation products of ancient kerogens of algal origin (Philp and Calvin, 1976). Such similarities were considered as possibly reflecting the contribution of polymeric debris from microalgal and bacterial cell walls as the source of the main building blocks of these kerogens. However, condensation reactions between polymeric debris were still considered as an important part of the whole process leading to kerogen.

A further step towards the recognition of a new pathway resulted from comparison of the solid state ^{13}C NMR spectra of "kerogen-like" substances

(insoluble and resistant to acid hydrolysis) isolated from extant microalgae and from recent sapropelic sediments (Mangrove Lake, Bermuda; Hatcher et al., 1983). Based on the spectral similarities observed and on the predominance of paraffinic carbons, it was considered that "probable kerogen precursors exist in living algae" and suggested that "these materials might survive microbial and chemical decomposition to constitute the source of insoluble kerogen" and that such material is probably

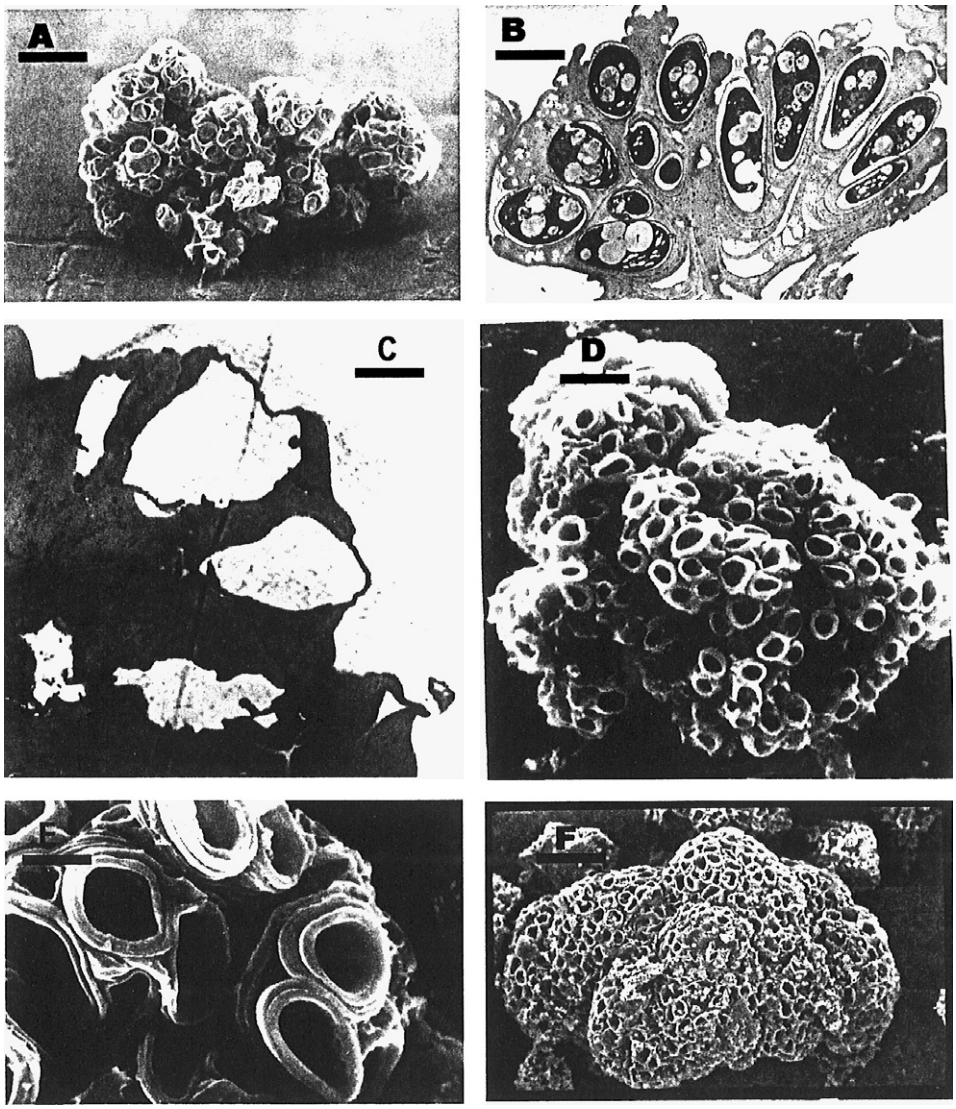

Plate e. Observations of *Botryococcus* by scanning (A, D–F) and transmission (B,C) electron microscopy. A and B: extant green microalga *B. braunii*. Colony exhibiting the "cauliflower" organization typical of the species (A), with the individual cells tightly embedded in thick, algaenan-based, outer walls as illustrated by ultrathin section of a part of a colony (B). Following algaenan isolation the morphology of the outer walls is well retained whereas the cell contents appear as "ghosts" due to complete elimination of all the soluble and hydrolysable constituents (C). Colony from a lacustrine sediment (East Africa, ca. 40,000 yr) (D) and partial view at higher magnification (E). During the first stages of fossilization the cell contents were fully eliminated by diagenetic degradation; in contrast, the algaenan-based thick outer walls were selectively preserved (D,E); diagenesis thus resulted in changes similar to those encountered upon algaenan isolation from extant *B. braunii* through drastic laboratory treatment. Such walls and the typical organization of *Botryococcus* are still well recognizable in ancient sedimentary rocks, for example in *Botryococcus*-rich Pliocene oil shales of Hungary (F) and Permian Torbanites (Plate 1A, 1B). Scale bars: A, D and F (25 μm), B (10 μm), C (2 μm) and E (6 μm). Reprinted with permission from Largeau et al. (1990), Copyright (1990) Elsevier for A and D; with permission from Derenne et al. (1989), Copyright (1989) Pergamon Press for B and C; with permission from Derenne et al. (1997, p. 1881).

"an original component of algae and possibly associated bacteria and is differentially concentrated by selective preservation during diagenesis".

Finally, straightforward evidence of the occurrence of the selective preservation pathway stemmed from parallel morphological and chemical studies of low maturity lacustrine kerogens (Torbanites, Permian) and of the cell walls of the extant, ubiquitous, freshwater green microalga *Botryococcus braunii* (Berkaloff et al., 1983; Largeau et al., 1984, 1986). Extensive extraction of cultured algae, followed by drastic basic and acid hydrolysis, showed a specific composition for the outer walls that build up the matrix of *B. braunii* colonies and are responsible for their typical "cauliflower" organization [Plate e(A)]. Such outer walls were thus shown to (i) contain insoluble, highly aliphatic, non-hydrolysable biomacromolecules and (ii) perfectly retain their morphological features after the above treatment that results in the elimination of all the components of the algal biomass, except this aliphatic resistant material [Plate e(C)]. In addition, comparative studies showed very close chemical composition for the resistant biomacromolecules isolated from extant *B. braunii* and for the kerogen of immature Torbanites, as reflected in FTIR and solid state ^{13}C NMR spectra and pyrolysis products (Largeau et al., 1984, 1986).

Such morphological and chemical similarities demonstrated that the bulk of these kerogens is comprised of virtually unaltered aliphatic insoluble biomacromolecules from *B. braunii* outer walls. Selective preservation was also illustrated by SEM observations of *B. braunii* colonies from recent (ca. 40,000 yr) sediments from Lake Zuquala [Ethiopia; Plate e(D and E)], where cell contents and polysaccharidic inner walls are entirely eliminated, whereas the outer walls are perfectly retained. It thus appeared that diagenetic microbial degradation of *B. braunii* biomass resulted in the same conspicuous changes as the drastic laboratory treatment used for isolation of the resistant material, i.e. total elimination of all components but the aliphatic macromolecular material of outer walls. Kerogen formation in Torbanites mostly results from the selective preservation of the latter material – hence (i) the remarkable preservation of the specific morphology of the colonies, (ii) the highly aliphatic nature of these Type I kerogens and (iii) the extremely high kerogen content of Torbanites, the resistant material being a major component of *B. braunii*. Similar studies showed the occurrence of highly aliphatic, non-hydrolysable, macromolecular material in the outer walls of the extant green microalga *Tetraedron minimum* and formation of the kerogen of the Messel Oil Shale (Eocene, Germany) through the same type of pathway as for Torbanites (Goth et al., 1988).

Subsequent examination of a number of other extant microalgae revealed the presence of non-hydrolysable, highly aliphatic, macromolecular components in the outer walls of vegetative cells (reviewed in Derenne et al., 1992b; Gelin et al., 1999) of a relatively large number of freshwater and marine species. The general term algaenan was coined for this new family of lipid-like biomacromolecules (Tegelaar et al., 1989a) so as to recall their origin and highly aliphatic nature. The term "lipid-like" is used here to emphasize that algaenan is biosynthetically related to lipids, being composed of lipid sub-units, but cannot be considered as lipid due to the insolubility in organic solvents.

In *B. braunii* and *T. minimum*, the algaenan builds up relatively thick outer walls so that the typical morphology of the two organisms is well retained both in the isolated algaenan and the resulting kerogen. In contrast, the other algaenan-containing species generally exhibit much thinner outer walls (ca. 10–30 nm thick). When examined with TEM, these very thin outer walls show a typical trilaminar structure [Plate b(B)], which is generally retained following algaenan isolation. However, the algaenan-containing outer walls are now highly distorted and the initial shape of the cells is no longer recognizable [Plate b(C)]. Comparative morphological and chemical studies with the ultralaminae identified using TEM for a number of

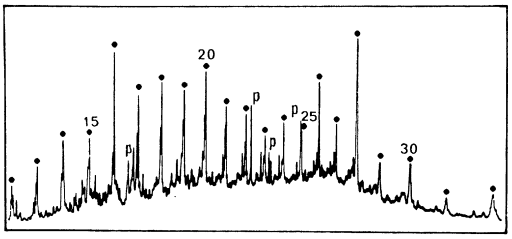

Fig. 22. GC trace of medium polarity fraction (toluene-elution) isolated from off-line pyrolysate at 400 °C of algaenan of *Scenedesmus quadricauda* (microalgal species exhibiting very thin cell walls composed of algaenan), showing abundant presence of C_{12}–C_{32} *n*-alkyl nitriles. Production of nitriles upon pyrolysis is a typical feature of this type of algaenan and of the fossil counterparts formed by selective preservation (ultralaminae illustrated in Plate b). Reprinted with permission from Derenne et al. (1991, p. 1046).

lacustrine and marine kerogens [Plate b(D)] demonstrated that the corresponding kerogen fractions were formed via the selective preservation of such algaenan (Largeau et al., 1990a,b; Derenne et al., 1991, 1992c,d; Gillaizeau et al., 1996). The chemical correlation between these extant and fossil materials was based, in particular, on the presence of long chain *n*-alkylnitriles in the pyrolysates (Fig. 22), whereas such nitrogen-containing pyrolysis products were not detected in the case of the ''thick'' algaenans of *B. braunii* and *T. minimum* and of derived kerogens. The major role of the selective preservation of algaenan in the formation of ultralaminae-rich kerogen was also supported, in the case of the Göynük oil shale, by compound-specific stable carbon isotope measurements of the aliphatic hydrocarbons generated via catalytic hydropyrolysis of the kerogen (Love et al., 1998).

5.2.2. Selective preservation of materials in protective layers of higher plants

Insoluble, non-hydrolysable, highly aliphatic macromolecular components were also observed in the protective layers of some higher plants. Such materials were first identified in cuticles, i.e. in the thin extracellular layers that cover the aerial part of plants where no secondary growth occurs (Nip et al., 1986) and were subsequently termed cutan (Tegelaar et al., 1989a). It had been documented for a long time (Kolattukudy et al., 1976; Kolattukudy, 1980) that cuticles comprise a soluble lipid fraction (epicuticular waxes) and an insoluble matrix containing hydrolysable macromolecular material with a polyester structure (cutin). In addition, drastic treatment similar to that used for algaenan isolation revealed the presence of an insoluble non-hydrolysable macromolecular material in the cuticle of various species, including gymnosperms and angiosperms (Nip et al., 1986; Tegelaar et al., 1991; de Leeuw and Largeau, 1993). Furthermore, close morphological and chemical similarities were observed between these resistant biomacromolecules isolated from extant higher plants and ancient materials. The latter included Pliocene to Permian fossil cuticles and the cutinite maceral isolated from Carboniferous samples (IN, USA; Nip et al., 1986, 1989; Tegelaar et al., 1991, 1993; van Bergen et al., 1994a, 1995). It thus appeared that the selective preservation of cutan also contributed to kerogen.

Analysis of periderm layers (outer bark and root tissues) in several angiosperms (Tegelaar et al., 1995) also showed the occurrence of a non-hydrolysable, highly aliphatic macromolecular material, termed suberan (Tegelaar et al., 1989a). The suberinite maceral in kerogen probably originates from the selective preservation of such resistant biomacromolecules (Tegelaar et al., 1995). The inner layers of numerous fossil Eocene seed coats of water plants exhibit a well-preserved morphology and are composed of a ''cutan-like'' highly aliphatic macromolecular material (van Bergen et al., 1994b; Plate f(a–f)). Thus, fossilization via the selective preservation pathway probably also occurs for such layers.

5.2.3. Chemical structure of algaenan, cutan and suberan

Numerous studies were carried out on the chemical structure of these biomacromolecules, especially algaenan, so as to carry out precise comparison with fossil materials and to understand the origin of their conspicuous resistance to chemical and microbial attack. Extensive examination was performed on the algaenan isolated from the three chemical races of *B. braunii* (reviewed in Metzger and Largeau, 1999) using a combination of methods, along with analysis of the high molecular weight lipids involved as precursors in algaenan biosynthesis. The algaenan of *B. braunii* contain functional groups, like unsaturations, aldehydes, esters and ether bridges, that should be sensitive to chemical and microbial attack. The conspicuous resistance of these potentially labile groups, unaffected by drastic laboratory hydrolysis and diagenesis, reflects the efficient steric protection provided by the aliphatic macromolecular network.

The algaenan of a number of other freshwater and marine microalgae were also examined with respect to chemical structure (reviews by Derenne et al., 1992b; de Leeuw and Largeau, 1993; Largeau and de Leeuw, 1995; Gelin et al., 1999; see also Blokker et al., 1998, 1999; Allard et al., 2002). These studies were generally based on a combination of spectroscopic and pyrolytic methods. Chemical degradation was also carried out for elucidating the structure of some algaenan examples (Gelin et al., 1996, 1997; Schouten et al., 1998; Blokker et al., 1998, 1999, 2000). For example, HI and RuO_4 oxidation was used to examine the algaenan of two marine microalgae, *Nannochloropsis salina* and *Nannochloropsis* sp., whose macromolecular structure is thought to be based on polyether-linked, long chain alkyl units (Gelin et al., 1996, 1997). All the above examples of algaenan exhibit a highly aliphatic

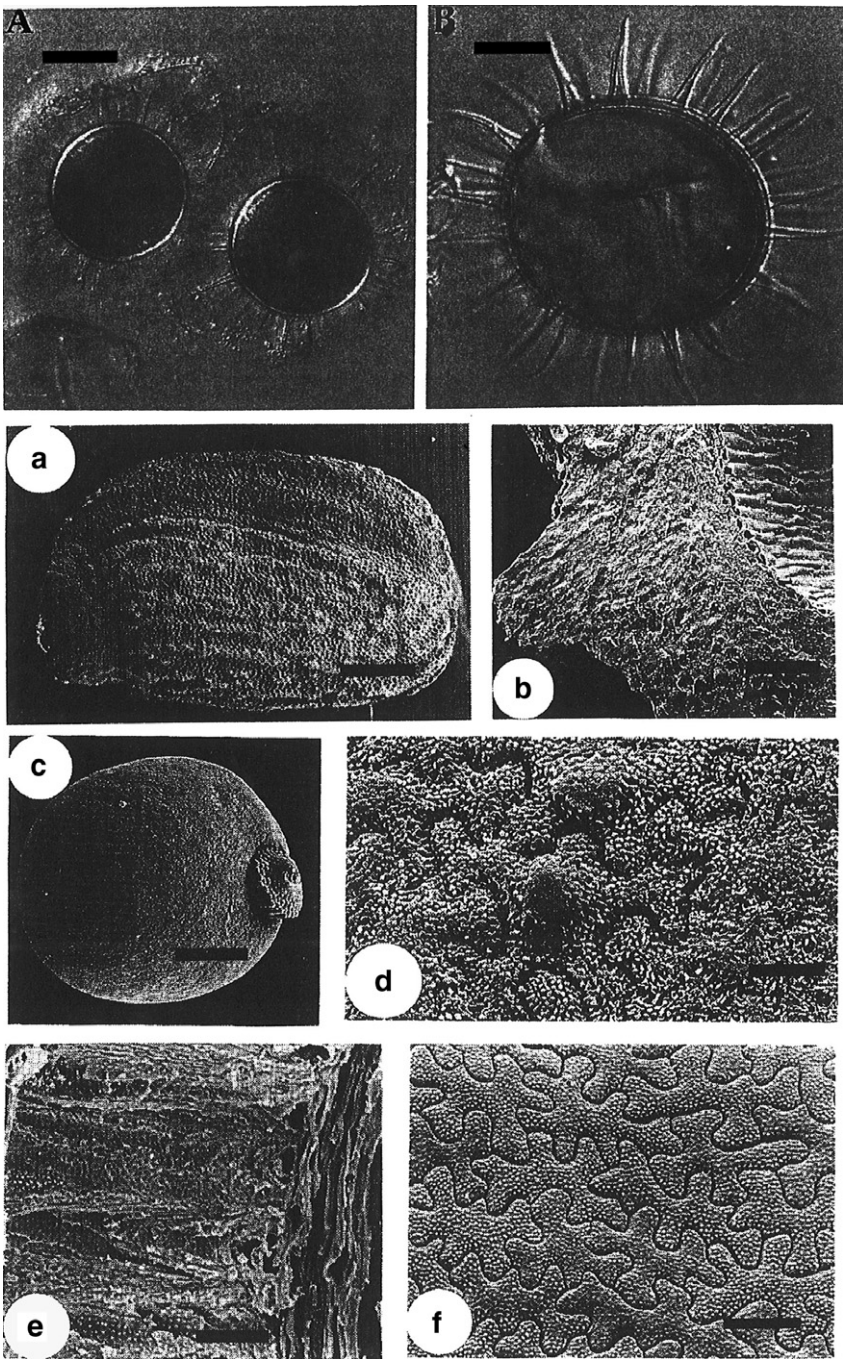

Plate f. A and B: light microscopy observation of resting cysts of the marine Dinoflagellate *Lingulodinium polyedrum*. (A) Living specimens from laboratory cultures, (B) fossil cyst (lower Miocene, France). The cell walls of the extant cysts are composed of an insoluble non-hydrolysable macromolecular material, probably selectively preserved in the fossil cysts. SEM observations of well preserved fossil seed coats and modern counterparts (a–f). Fossil testae of *Stratiotes headonensis*: whole testa (a) and cross-section of testa wall (b). Fossil testae of *Brasenia spinosa*: whole testa (c) and detail of tubercules and micropapillae on testa surface (d). Testae of extant *B. schreberi*: cross-section of testa wall (e) and detail of testa surface (f). Scale bars: A (30 μm), B (15 μm), a (2000 μm), b (120 μm), c (400 μm), d (50 μm), e (35 μm) and f (50 μm). Reprinted with permission from Kokinos et al. (1998, p. 266), Copyright (1998) Pergamon Press for A and B; with permission from van Bergen et al. (1994), p. 3826.

structure, as for *B. braunii* algaenan, and the macromolecular network is based on long to very long (up to C_{80}–C_{120}) alkyl chains (Allard et al., 2002). These chains are usually unbranched. However, a substantial contribution of long isoprenoid chains was observed for the algaenan of the L race of *B. braunii* (review by Metzger and Largeau, 1999) and its fossil counterparts (Derenne et al., 1989, 1997). Phenolic groups, associated with long alkyl chains, occur in the algaenan of the A race of *B. braunii* and their abundance increases with the salinity of the growth medium (Derenne et al., 1992a; Sabelle et al., 1993). Nevertheless, even for the algaenan isolated from "saline" *B. braunii*, long alkyl chains remain by far the main elements of the macromolecular structure.

Among the non-hydrolysable materials isolated from a number of extant microalgae belonging to various classes, a large contribution of aromatic moieties was observed in only two cases: the walls of the vegetative cells of the marine green microalga *Chlorella marina* (Derenne et al., 1996) and the walls of resting cysts of the dinoflagellate *L. polyedrum* (Kokinos et al., 1998) [Plate f(A)]. In agreement with spectroscopic observations, the pyrolysate of the "algaenan" from *C. marina* is dominated by compounds containing a large variety of aromatic groups. The lack of a macromolecular network based on long alkyl chains was also noted for *L. polyedrum* "algaenan" where relatively condensed, mostly aromatic, structures dominate.

Analysis of the cutan of extant plants, via flash pyrolysis and solid state ^{13}C NMR, indicated a highly aliphatic nature (Nip et al., 1986, 1987). A substantial contribution of polysaccharidic moieties was suggested from FTIR spectroscopy (Tegelaar et al., 1989b) but this was not supported by subsequent studies (de Leeuw et al., 1991; McKinney et al., 1996). Further pyrolytic studies of the cutan isolated from *Agave americana* suggested that moieties containing functionalized aromatic rings may also occur (Tegelaar et al., 1989b; McKinney et al., 1996). However, such moieties were no longer observed after extensive purification (Villena et al., 1999). The highly aliphatic nature considered for suberan was mostly based on flash pyrolysis experiments (Tegelaar et al., 1995).

5.2.4. Problems related to algaenan, cutan and suberan isolation

Drastic hydrolysis is required for algaenan, cutan and suberan isolation so as to eliminate all the other insoluble macromolecular components. However, it is well documented that hydrolysis of proteins and/or polysaccharides under drastic laboratory conditions can result in the partial condensation of their degradation products into complex insoluble macromolecules that can withstand subsequent hydrolysis. These insoluble macromolecules, termed melanoidins, are formed by Maillard reactions and show some similarities in chemical structure when compared to humic substances naturally formed from proteins and polysaccharides by degradation–recondensation processes. A detailed study of algaenan isolation from *B. braunii* (Allard et al., 1998) showed that (i) substantial formation of artifactual melanoidin-like material occurred under the classically used hydrolysis conditions and (ii) artifact-free algaenan can be obtained provided that stepwise trifluoroacetic acid (TFA) hydrolysis, with progressive increase in duration and acid concentration, is performed before the usual drastic base and acid hydrolysis (Fig. 23). Accordingly, the abundance of algaenan obtained in previous studies, using the classical treatment, is probably somewhat overestimated due to the formation of melanoidin-type artifacts. Moreover, the presence of these artifacts could hardly be revealed when pyrolysis and solid state ^{13}C NMR were used to characterize the isolated material. Indeed, as shown by the examination of mixtures of reference compounds (Poirier et al., 2000), melanoidin is poorly detected with both methods, in contrast with aliphatic constituents like algaenan.

Stepwise hydrolysis of bacterial biomass with TFA (Allard et al., 1997) showed that the bulk of the so-called bacteran, previously obtained from three species of mycobacteria via classical hydrolysis (Flaviano et al., 1994), in fact corresponded to melanoidin-type artifactual material. Indeed, no significant amount of insoluble non-hydrolyzable constituents was isolated when stepwise hydrolysis was used and, at the moment, there is no clear indication for the presence of non-hydrolysable macromolecular components in bacteria.

5.2.5. Estimate of algaenan, cutan and suberan contribution to kerogen

5.2.5.1. Algaenan. The presence of algaenan has been reported so far in over 30 species of microalgae, chiefly in vegetative cells with very thin trilaminar outer walls (reviewed by Derenne et al., 1992b; Gelin et al., 1999). These algaenan-producing species are found in a large array of genera and in several classes,

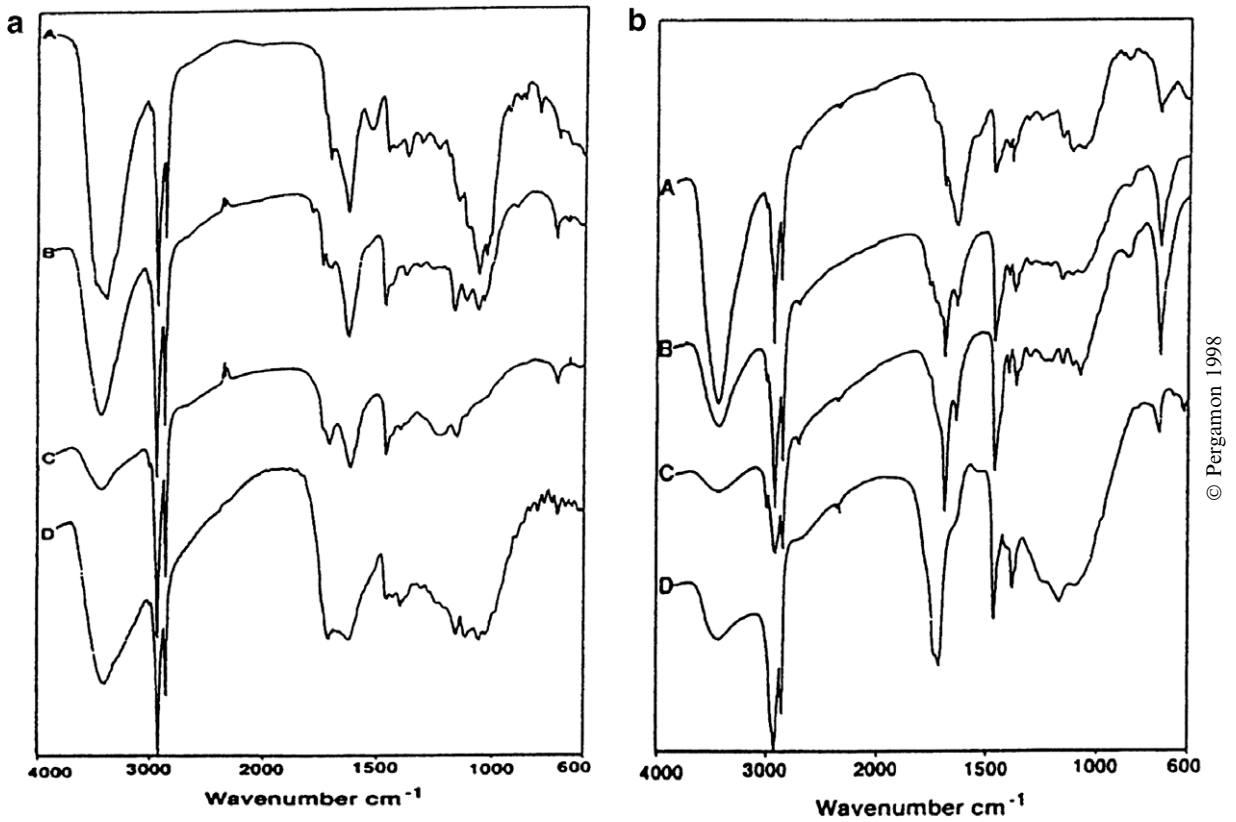

Fig. 23. Algaenan isolation *S. Communis* (a) *B. braunii* (b). FTIR spectra, from top to bottom: material obtained after the first TFA hydrolysis: material obtained after the successive TFA hydrolyses: artifact-free algaenan isolated via the new process and contaminated algaenen obtained through direct drastic saponification and acid hydrolysis. Reprinted with permission from Allard et al. (1998, p. 546).

although most belong to the same class, the Chlorophyceae, i.e. the green microalgae. However, several other types of phytoplanktonic organisms were also tested for the presence of algaenan, including numerous marine species. Algaenan occurrence was thus observed, along with the presence of a very thin trilaminar outer wall, in the four species of Eustigmatophyceae examined by Gelin et al. (1999). Accordingly, algaenan formation is probably a common feature in this class as in the Chlorophyceae. Nevertheless, unlike the diatoms, prymnesiophytes and dinoflagellates, these above classes are not considered as ubiquitous in marine environments and would rarely be a major constituent of marine phytoplankton.

No algaenan was detected in two ubiquitous prymnesiophytes, *Emiliana huxleyi* and *Phaeocystis* sp. or in any of the diatoms tested (Gelin et al., 1999). The diatoms and prymnesiophytes are characterized by the production of mineral exoskeletons and some observations point to an important protective role for algaenan-containing outer walls in living microalgae (Corre et al., 1996). Accordingly, the presence of a protective mineral exoskeleton may account for the lack of algaenan in these two classes. The general lack of algaenan in diatoms is supported by observations on marine sediments underlying upwelling areas off Peru and Mauritania (Eglinton et al., 1994; Zegouagh et al., 1999), where the large primary production is mostly due to diatoms, and the sedimentary OM is thought to be predominantly of diatom origin. Indeed, no significant role was observed for the selective preservation pathway in sediments from these two areas. A non-hydrolysable, highly aliphatic material was identified in the vegetative cells of one dinoflagellate, *Gymnodinium catenatum*, out of three tested (Gelin et al., 1999). However, the location and the morphological features of this macromolecular material and its possible relationship to kerogen components are still to be examined.

Only one case has been reported where the isolated algaenan did not retain the morphology of the cell wall. The algaenan of the Eustigmatophyte *Nannochloropsis salina* appears as an amorphous material with a granular texture when observed with TEM (Gelin et al., 1999). An amorphous nature can therefore be anticipated for the kerogen fraction derived from the selective preservation of this algaenan or of similar examples. Recognition of such a contribution is, however, difficult because kerogen fractions derived from the classical degradation–recondensation pathway are also amorphous with a granular texture (e.g. Zegouagh et al., 1999). Clear-cut chemical differentiation is also difficult because the incorporation of various long chain lipids into kerogen structure occurs via the classical

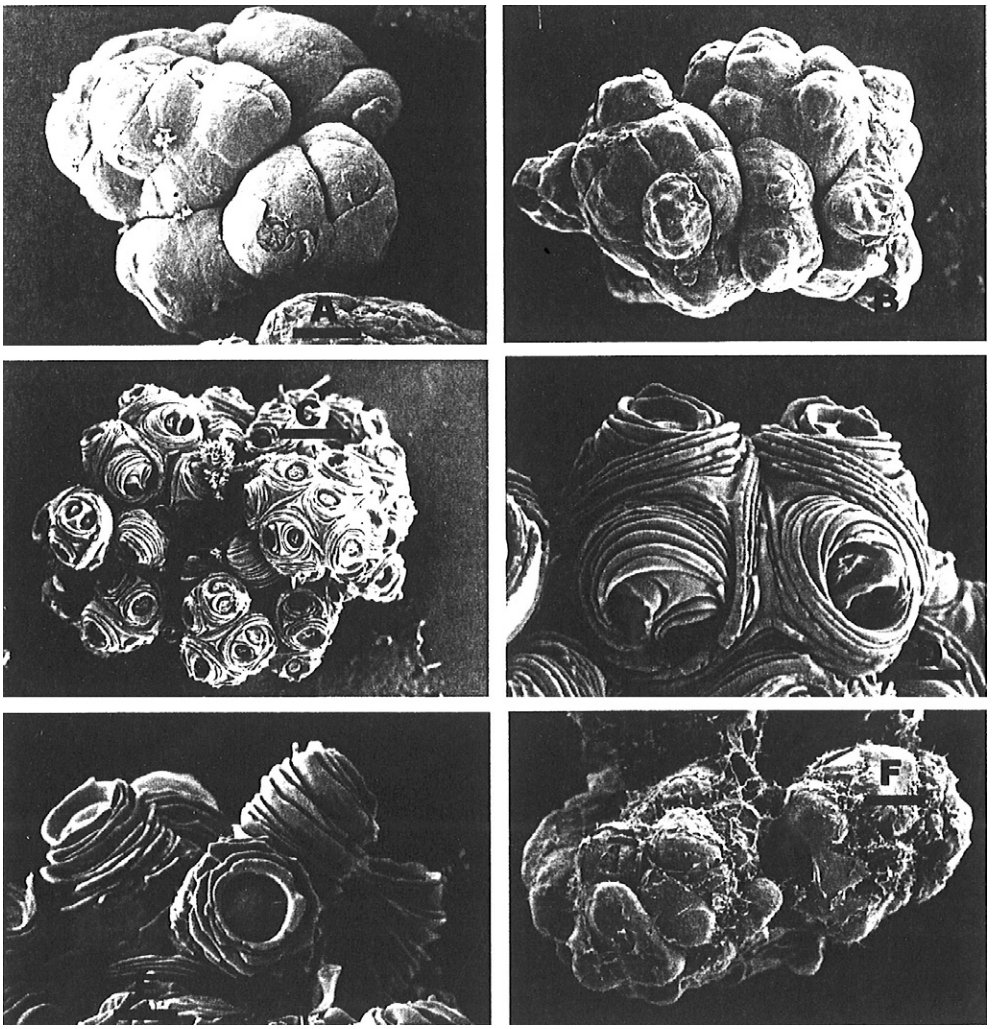

Plate g. SEM observations of *Gloeocapsomorpha prisca* from Kukersite oil shale (Ordovician marine deposit, Estonia) and extant *Botryococcus braunii* grown on "saline" media. A and B: *G. prisca* colonies exhibit a perfectly preserved morphology and TEM observations (not shown, Derenne et al., 1992a) indicated that the cells, appearing now as ghosts, were surrounded by thick walls. These walls were selectively preserved, hence pointing to an algaenan-based composition. Observations on extant *B. braunii* grown on NaCl-containing media (C–F) instead of the NaCl-devoid medium generally used for laboratory cultures of *B. braunii* (in modern environments the species usually thrives in freshwater). Large morphological changes occur for the medium with a NaCl concentration of only 1 g/l: the outer walls are still thicker and exhibit a conspicuous multilayered organization (C–E). When NaCl concentration is raised to 10 g/l further morphological changes are observed (F). The cells are now completely surrounded by the thick multilayered walls and the general morphology of the colonies strongly recalls that of *G. prisca* colonies. Such morphological features, along with associated changes in algaenan composition on "saline" media, point to affinity between Ordovician *G. prisca* and modern *B. braunii.* Scale bars: A, B and F (10 μm), C (25 μm), D and E (5 μm). Reprinted with permission from Derenne et al. (1992) p. 301, for A and B, p. 307 for C–F.

pathway (Tissot and Welte, 1978). Such incorporation would generate moieties whose chemical composition, including pyrolysis products, may mimic the composition of *N. salina* (and related) algaenan. Thus, a contribution from selectively preserved algaenan to some amorphous kerogen fractions cannot at the moment either be completely ruled out or firmly established.

As stressed above, algaenan selective preservation played a prominent role in the formation of some organic-rich deposits composed of accumulations of well recognizable microfossils like Torbanites [Plate a(A and B)] and Messel Oil Shale. Indeed, kerogen in the above samples corresponds mostly to accumulations of algaenan-comprised outer walls of *B. braunii* and *T. minimum*, respectively. The conspicuous role of the selective preservation pathway in the formation of such kerogens reflects the significant amount of algaenan in the source organisms, $>10\%$ of total biomass for *B. braunii* (Allard et al., 1998), in relation to the thickness of the algaenan-comprised outer walls in these two species.

The kerogen of many Ordovician marine source rocks and oil shales is also chiefly composed of the well-preserved remains of a single species of a colonial microorganism, termed *Gloeocapsomorpha prisca* [Plate g(A and B)]. The morphology of these fossil colonies, as revealed using TEM, strongly suggested that the cell walls of *G. prisca* were composed of a highly resistant material and that this Ordovician kerogen was also chiefly formed by selective preservation. Further studies confirmed such an origin and indicated that *G. prisca* was possibly a marine microalga related to *B. braunii* (Derenne et al., 1990, 1992a). Indeed, the latter exhibits large changes in colony morphology (Plate g(C–F)) and in algaenan composition when grown in a saline medium, especially an increasing content of phenolic moieties (particularly of alkyl-1,3-benzenediols) in the algaenan. Due to such changes, close morphological and chemical resemblance to *G. prisca* is observed. The major contribution of *G. prisca* remains to Ordovician source rocks is reflected in the unusual distribution of alkanes observed for both Ordovician oils (e.g. Douglas et al., 1991) and *G. prisca* pyrolysates. The nature and composition of *G. prisca* account for such features: (i) a huge growth of this photosynthetic species in Ordovician seas was favoured, since the major phytoplanktonic groups now dominating marine environments (like diatoms and dinoflagellates) did not exist in the Ordovician and (ii) owing to the presence of thick outer walls composed of aliphatic algaenan, a large part of the total biomass of *G. prisca* was selectively preserved upon fossilization and afforded kerogen with a high oil potential.

Tasmanites are also organic-rich oil prone deposits, Carboniferous to Permian in age, chiefly formed by accumulations of organic microfossils (Revill et al., 1994) termed *Tasmanites punctatus*, and composed of very well preserved thick cell walls. These microfossils show the same morphology as cell walls in the phycoma of modern marine microalgae like *Pachysphaera* sp. and *Halosphaera* sp. (Prasinophyceae). Phycoma, i.e. non-motile stages implicated in the asexual reproduction of Prasinophytes, are sometimes observed in nature but are very difficult to obtain in laboratory cultures. As a result, the assumed relationship between phycoma walls in extant Prasinophytes and *T. punctatus* microfossils in Tasmanites, and hence the formation of these kerogens by selective preservation, has not been ascertained by carrying out comparative studies on their chemical composition.

As expected, the level of resistant material is rather low in all the microalgae that exhibit very thin trilaminar outer walls. Algaenan contents of a few % of the total biomass are observed for these species (Derenne et al., 1992b; Allard et al., 1998). However, contrary to *B. braunii*, each cell division leads to the release of the outer wall of the mother cell. This wall bursts to release the daughter cells that produce their own trilaminar wall. Thus, actively growing populations of such microalgae can produce rather large amounts of algaenan. Fossil ultralaminae derived from the selective preservation of these very thin outer walls are thus abundant in some kerogens [Plate b(D)], as observed for the Rundle and Göynük Oil Shales; however, they often account for only a minor part of the total kerogen (Largeau et al., 1990a).

Fossil dinoflagellates commonly contribute to marine kerogens, as resting cysts with well preserved morphology, back to at least the Trias (Evitt, 1961), and over 400 genera have been identified (Dale, 1983). However, such cysts usually only account for a relatively small fraction of the whole kerogen. The morphology of these ubiquitous microfossils suggests that they originate from the selective preservation of the resistant outermost layer of dinoflagellate cysts. This is supported by microscopic and chemical observations of the presence of an insoluble and non-hydrolysable macromolecular material

in the cell walls of resting cysts, obtained by laboratory culture of the extant dinoflagellate *Lingulodinium polyedrum* [Kokinos et al., 1998; Plate f(A and B)]. However, comparative studies of the chemical composition of this resistant material and of fossil cysts, along with the examination of other extant species, are required to ascertain the implication of the selective preservation pathway in the formation of the dinoflagellate cysts commonly observed in the fossil record. Similarly, the presence of algaenan was observed in the cell walls of the zygospores of the green microalga *Chlamydomonas monoica* (Blokker et al., 1999). However, comparative chemical and/or morphological studies of such spore walls with fossil materials have not been reported.

Taken together, the above results therefore indicate that large variations can be found in (i) the level of resistant macromolecular material of microalgal cell walls depending on the class or species in question and also on the cell type in question (vegetative cells vs. resting cysts or reproductive cells) and (ii) the contribution of the selective preservation pathway to kerogen formation. The resulting implications, on a global scale, are considered in a section below.

Table 11
Modern higher plants where presence of cutan has been reported[a]

Taxon (affinity)
Gymnosperms
Ginkgo biloba (Ginkgoaceae)
Sciadopytis verticillata (Taxodiaceae)
Amentotataxus argotaenia (Taxaceae)
Monocotyledonous angiosperms
Agave americana (Agavaceae)
Clivia miniata (Amaryllidaceae)
Zostera marina (Zosteraceae)
Dicotyledonous angiosperms
Lycopersicon esculentum (Solonaceae)
Citrus limon (Rutaceae)
Salicornia europaea (Chenopodiaceae)
Erica carnea (Ericaceae)
Symplocos paniculata (Symplocaceae)
Hydrangea macrophylla (Saxifragaceae)
Gossypium sp. (Malvaceae)
Prunus laurocerasus (Rosaceae)
Quercus robur (Fagaceae)
Acer platanoides (Aceraceae)
Malus pumila (Rosaceae)
Limonium vulgare (Plumbaginaceae)
Beta vulgaris (Chenopodiaceae)

[a] Reprinted with permission from de Leeuw and Largeau (1993); Copyright (1993) Plenum Press.

5.2.5.2. Cutan and suberan. Previous studies pointed to the presence of cutan in 19 species of higher plants, including both gymnosperms and angiosperms, out of 23 tested (Nip et al., 1986; Tegelaar et al., 1991; de Leeuw and Largeau, 1993; Table 11) and cutan was detected in several drought-adapted plants (Boom et al., 2005). Examination of the outer bark tissues of five angiosperms showed the presence of suberan in all these species (Tegelaar et al., 1995). Therefore, cutan and suberan might be rather common constituents of higher plants. These resistant aliphatic, macromolecules are found, however, in specific tissues, cuticles and suberized layers, respectively, that only account for a very small fraction of the total biomass. In agreement with this low abundance, large accumulations of well recognized remains of such tissues formed by the selective preservation of cutan and suberan, i.e. the cutinite and suberinite macerals, respectively, are seldom observed in kerogen fractions derived from higher plants. A substantial contribution of cutinite was observed in a limited number of samples, like the Upper Carboniferous "paper coals" (IN, USA) where petrographical observations indicated a cutinite content of ca. 7% of total OM (Nip et al., 1989).

5.2.6. Respective contributions of selective preservation and degradation–recondensation pathways to algal kerogen constituents

The importance of the selective preservation pathway on a global scale is still a matter of debate. Estimates of the contribution of algaenan to Types I and II kerogens, largely sourced from microalgal components, has been discussed (Largeau and Derenne, 1993). For a given algal kerogen, the relative importance of the selective preservation and degradation–recondensation pathways will be controlled by (i) the content of algaenan in the primary biomass and (ii) the depositional conditions and the resulting level of mineralization of the non-resistant constituents of this biomass.

Based on studies of extant microalgae, a scale from 0% to 10% was used for the algaenan content, with the zone around 1% corresponding to the level of algaenan expected in a number of algal populations. Species with very high algaenan contents, like *B. braunii*, can be considered as relatively uncommon and are not considered in this global estimate. According to Tissot and Welte (1978), the level of mineralization of the non-resistant constituents is usually extremely high and, on a global scale, only

a tiny fraction (average ca. 0.1%) of the biomass of primary producers is finally transformed into kerogen via the degradation–recondensation pathway. Values up to 4% can be observed in environments where degradation is limited, as in the Black Sea, and larger values would only occur in unusual environments. Accordingly, a scale from 0.1% to 4%, encompassing most depositional conditions, was considered. Using the above two sets of values, a three-dimensional diagram was obtained whose surface represents the contribution of the selective preservation pathway to kerogen formation as a function of the composition of the source organisms and of depositional conditions (Largeau and Derenne, 1993). The zone of this diagram representing the values that are likely to generally prevail for these two parameters corresponds to a contribution of the selective preservation pathway of at least 20%. It therefore appears that selective preservation probably afforded, on a global scale, a substantial contribution to a number of algal kerogens. Such a contribution was also inferred, through compound-specific stable carbon isotopic analysis of aliphatic hydrocarbons in flash pyrolysates, for a set of kerogens corresponding to various depositional conditions and age (Eglinton, 1994). Furthermore, owing to the highly aliphatic nature of algaenan, the kerogen fraction thus formed would largely contribute to the oil potential of the whole kerogen, even if the relative abundance was rather low. This is illustrated by the relationship between the large variation in Rock-Eval HI values and the relative abundance of fossil *B. braunii* vs. terrestrial materials in a large set of samples from an otherwise lithologically homogeneous, maar-type oil shale deposit (Gérce, Pliocene, Hungary; Derenne et al., 2000).

Although algaenan is usually characterized by a highly aliphatic nature, the aforementioned studies on *C. marina* showed that "aromatic algaenan" might also exist. No chemical correlation has been established between this type of "algaenan" and kerogen. However, the observations support results for the Alum Shale (Cambrian, Scandinavia; Horsfield et al., 1992) and the Cerdanya oil shale (Tertiary, Spain; Sinninghe Damsté et al., 1993a) suggesting a large contribution of "aromatic algaenan". They may also account for the occurrence of highly aromatic, although apparently non-biodegraded, crude oils (Tissot and Welte, 1978). Accordingly, we cannot exclude the posssibility that the selective preservation pathway was also significantly responsible, on a global scale, for the aromatic fractions of some kerogens.

5.2.7. Selective preservation of other types of biomacromolecule

The inventory of the main groups of biomacromolecule and their resistance to diagenesis (review in de Leeuw and Largeau, 1993) indicates huge differences in preservation potential. Indeed, a continuum probably exists between highly sensitive, rapidly mineralized components, like storage polysaccharides, and highly resistant biomacromolecules like algaenan. Below we consider some macromolecular components (sporopollenin and lignin) that can exhibit a high resistance to diagenetic degradation under numerous depositional conditions. Proteins are thought to exhibit a high sensitivity to diagenetic degradation and should not be preserved in sedimentary organic matter; further studies have led, however, to reconsideration of the general character of such a feature as discussed below.

5.2.7.1. Sporopollenin. The macromolecular components of the outer walls (exines) of lower plant spores and higher plant pollen exhibit a high resistance to drastic hydrolysis (review by Brooks and Shaw, 1978). The chemical structure of these non-hydrolysable biomacromolecules, termed sporopollenin, is still a matter of debate (e.g. Guilford et al., 1988; Wehling et al., 1989; Hemsley et al., 1993; Gubatz et al., 1993). Unbranched alkyl chains and phenyl propanoid units would be expected to be the main building blocks of sporopollenin (Wiermann et al., 2001, and references therein). In addition, the occurrence of tri- and tetra-substituted phenolic units (Fig. 24) with alkyl, carbonyl, acid or ester groups was reported (Ahlers et al., 1999). The great resistance of sporopollenin to laboratory

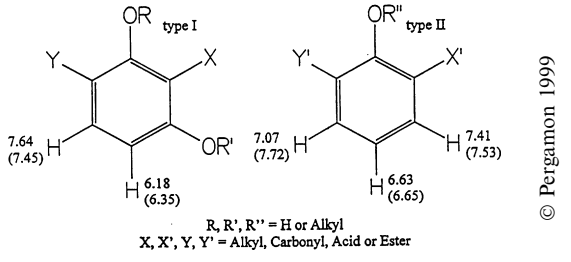

Fig. 24. Phenolic moieties identified via ^{1}H NMR spectroscopy in the purified sporopollenin isolated from *Typha angustifolia* pollen. Reprinted with permission from Ahlers et al. (1999, p. 1096).

hydrolysis is generally paralled by great resistance to diagenetic degradation under natural conditions. A high level of anatomical preservation, including specific ornamentation of the outer part of the exine, is commonly observed in fossil samples, so that the corresponding species can be identified unambiguously, so exines are largely used for palaeoflora reconstruction. Light microscopy showed, however, that the exines of some species can be rapidly degraded during incubation experiments with soils (e.g. Havinga, 1971; Faegri, 1971). The cause(s) of such a low preservation potential, like differences in sporopollenin content and/or composition, have not been determined. The palaeo record of spores and pollen will therefore be biased due to this preferential degradation of some exines.

Spore and pollen exines are widely distributed in fossil OM [Plate a(C)] and the corresponding maceral, sporinite, is ubiquitous in kerogen fractions derived from terrestrial materials. Fossil exines can account for up to half of the total mass in the so-called cannel coals (e.g. Phillips et al., 1985). This abundance reflects the predominance of spore-bearing arborescent lycophytes in Upper Carboniferous coal floras (review in Collinson et al., 1994). Pyrolytic study of fossil exines showed, in agreement with the composition of modern counterparts, the presence of oxygenated aromatic and aliphatic moieties (van Bergen et al., 1993), indicating that such moieties are probably selectively retained upon fossilization.

5.2.7.2. Lignin. After polysaccharides, lignin is the most abundant constituent of vascular plants. This high molecular weight polymer (ca. 600×10^3 kDa) generally accounts for 10–25% of the total mass of

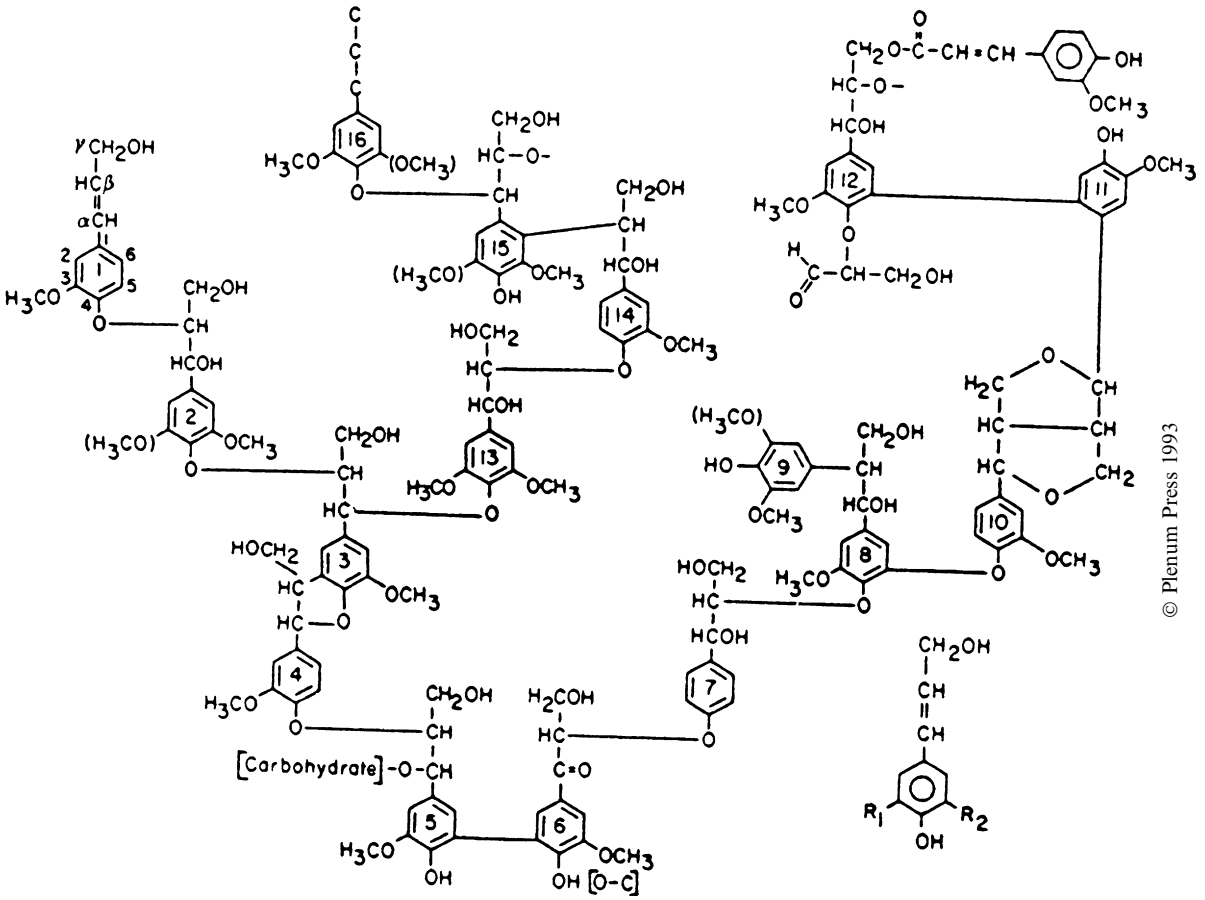

Fig. 25. Structure of monolignols (bottom, right): $R_1 = R_2 = H$, *p*-coumaryl; $R_1 = H$ and $R_2 = OCH_3$, coniferyl alcohol; $R_1 = R_2 = OCH_3$, sinapyl alcohol. Schematic structure of lignin showing the commonly occurring β-O-4 type linkage (e.g. between units 1 and 2), linkage of unit 5 to hemicellulose and esterification of unit 12 to ferulic acid, modified after Adler (1977) and Kirk and Farrell (1987). Reprinted with permission from de Leeuw and Largeau (1993, p. 44).

vascular plants and amounts up to 35% are observed in woody tissue (Higuchi, 1981; Stafford, 1988) The polymeric structure of lignin is based on three phenylpropanoid units, termed "monolignols", that differ in the substitution pattern of the phenyl ring (Fig. 25, Adler, 1977). The monolignols are transformed to phenoxy radicals through enzyme-initiated reactions. Copolymerization of these radicals, via random coupling reactions, finally produces the complex polymeric structure of lignin. Over 10 different types of linkages between the phenylpropanoid units can thus be formed. Among these, aryl–alkyl ether bonds generally dominate and a relatively large contribution from aryl–aryl and aryl–alkyl carbon–carbon bonds is commonly observed. As a result of this formation through random radical copolymerization, lignins are highly heterogeneous cross-linked macromolecules and a number of the condensed units contain several linkages to adjoining units. These features account for the great resistance of lignins to laboratory hydrolysis and the relatively high preservation potential under natural conditions.

The structure of lignin in a given plant is determined by the relative contribution of the monolignol units (Hedges and Mann, 1979; Stafford, 1988). Gymnosperm lignin is generally derived from coniferyl units, whereas coniferyl and sinapyl moieties are implicated in lignin from dicotyledonous angiosperms. In both cases a small contribution from *p*-coumaryl units is usually observed. Coniferyl and *p*-coumaryl units commonly predominate in monocotyledonous angiosperms. The nature and relative abundances of terrigenous sources in marine sediments can therefore be determined via the distribution of the typical phenolic compounds released from these three types of basic units upon lignin cleavage (Hedges et al., 1997). This cleavage is commonly achieved with CuO oxidation (Hedges and Ertel, 1982) or pyrolysis (Saiz-Jimenez and de Leeuw, 1986). Tetramethylammonium hydroxide (TMAH) thermochemolysis affords efficient cleavage of lignin linkages and makes easier the identification of the polar products thus generated (Clifford et al., 1995; Filley et al., 1999, 2000; Mannino and Harvey, 2000). Comparison of conventional pyrolysis and TMAH thermochemolysis of the macromolecular material isolated from a surface sediment off the Danube River Delta (Black Sea) illustrated the usefulness of the latter method and showed a large contribution of lignin from non-woody herbaceous land plants (Garcette-Lepecq et al., 2000, 2001).

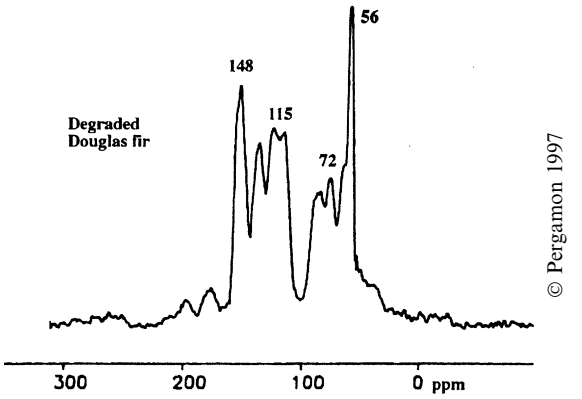

Fig. 26. Solid-state CP/MAS ^{13}C NMR spectrum of a Douglas fir wood "peatified" to the point where most of the cellulose material has been eliminated. Peaks correspond to nearly intact lignin except a small peak (at 72 ppm) reflecting very low contribution from cellulose carbon. Reprinted with permission from Hatcher and Clifford (1997, p. 254).

Lignin and altered (but recognizable) lignin are widely distributed in sedimentary rocks and have been extensively used as markers of terrestrial inputs to marine environments (Hedges et al., 1997). In the fossil record, the abundant contribution of lignin-derived material is reflected in the level of vitrinite that predominates in a number of coals (Hatcher et al., 1982). Under aerobic conditions, extensive degradation by white rot fungi and brown rot fungi takes place and lignin can be rapidly mineralized (Haider, 1992). However, such rapid destruction requires both depolymerase and oxidase activity and a high partial pressure of oxygen (Szklarz and Leonowicz, 1986). As a result, lignin exhibits a high resistance to mineralization under anaerobic conditions (e.g. Kirk and Farrell, 1987) – hence its accumulation in peat and coal (Fig. 26; e.g. Hatcher and Clifford, 1997).

Intact lignin, or parts of lignin macromolecular structure, can be incorporated into fossil OM, as observed via chemical degradation of the kerogen from the Messel Oil Shale and of a Miocene coal (Mycke and Michaelis, 1986). However, in contrast to highly aliphatic macromolecules, like algaenan, the initial structure of lignin commonly undergoes pronounced changes upon diagenesis. The main structural changes associated with the first steps in lignin diagenesis are the elimination of hydroxy groups, the cleavage of some ether linkages and the demethylation of methoxy groups (Hatcher and Clifford, 1997). This alteration is reflected in changes in the relative abundance of some of the products released through CuO oxidation or pyrolysis. From

the variations in relative abundance, several ratios can be calculated, like the syringic to vanillic unit ratio and the aldehyde to acid ratio, that reflect the extent of lignin alteration in modern and fossil materials (e.g. Goñi et al., 1993; van Bergen et al., 1994c; Hatcher et al., 1995).

5.2.7.3. Proteinaceous material. Proteins are the most abundant cellular constituents. However, most are very rapidly degraded during early diagenesis by exoenzymes that cleave peptide bonds, and the released amino acids are then used for microbial metabolism. Accordingly, it was considered for a long time that proteins or weakly altered protein-derived materials did not make a significant contribution to kerogen, and that only water-insoluble structural proteins would exhibit a limited preservation potential (e.g. de Leeuw and Largeau, 1993). In contrast, it is well documented that proteinaceous components can survive on a geological time scale in biominerals like bones and mollusc shells (e.g. Abelson, 1954; Robbins and Brew, 1990; Macko et al., 1993 and references therein; Poinar and Stankiewicz, 1999). During the formation of such materials the mineral phase nucleates on the protein matrix, thus isolating the proteinaceous components from microbial attack, unlike proteins in soft tissue.

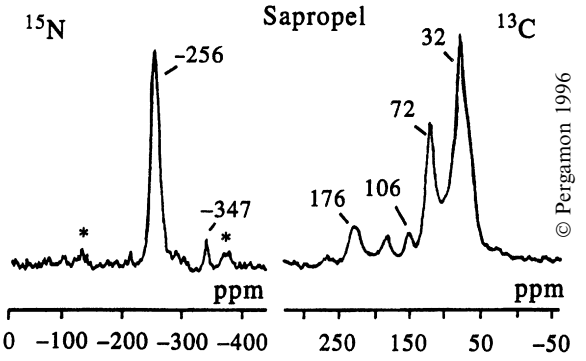

Fig. 27. Solid-state ^{15}N NMR spectrum of ca. 4000 year old algal sapropel (Mangrove Lake, Bermuda). No significant signals were observed in the pyrrolic N (−145 to −240 ppm) and pyridinic N (−40 to −90 ppm) regions. The dominance of the signal at −256 ppm (amide groups) and the peak at −347 ppm (free amino groups) indicates that most of the N occurs in peptide-like structures that survived diagenesis. The ^{13}C NMR spectrum shows a strong signal at 32 ppm reflecting the contribution of selectively preserved algaenan. The peaks at 72 and 106 ppm probably reflect the survival of some carbohydrate and a substantial signal is observed at 176 ppm for carboxylic/amide groups. Reprinted with permission from Knicker et al. (1996, p. 665).

Substantial amounts of nitrogen are found in sedimentary OM (Tissot and Welte, 1984), and it was considered for some time that this nitrogen mostly occurred in heterocyclic aromatic structures (pyrroles and pyridines). This was supported by (i) the low fraction of total nitrogen that could be identified as amino acids after hydrolysis and (ii) examination of recent sediments from the Peru upwelling with X-ray photoelectron spectroscopy (XPS), which showed that heterocyclic nitrogen occurred in a higher proportion than amino nitrogen (Patience et al., 1992). However, further studies led investigators to question the general character of the extensive degradation of proteins during diagenesis. Thus, solid state ^{15}N NMR showed (Fig. 27) that nitrogen occurred in amide groups in a 4000 year old organic-rich sapropelic sediment from Mangrove Lake, Bermuda (Knicker et al., 1996; Knicker and Hatcher, 1997, 2001), and amino acids were identified in the TMAH thermochemolysate of the sediment (Knicker et al., 1996, 2001; Knicker and Hatcher, 1997). Moreover, the production of amino acids, originating from the cleavage of proteinaceous moieties, was also observed upon TMAH thermochemolysis of: (i) kerogen-like OM isolated (by solvent extraction and mineral removal by HF/HCl) from a surface sediment collected off the Danube Delta (Garcette-Lepecq et al., 2001) and (ii) sulfur-rich kerogens from a 140 million year old organic-rich deposit, Kashpir Oil Shale, Volgian, Russia (Mongenot et al., 2001; Riboulleau et al., 2002) and from Tertiary Spanish shales (del Rio et al., 2004).

Hydrophobic and other non-covalent associations would promote preservation of peptide linkages and of proteins in organic matrices (Nguyen and Harvey, 2001). Indeed, studies of Mangrove Lake sediment (Knicker et al., 1996; Knicker and Hatcher, 1997, 2001) and laboratory experiments involving hydrolysis of encapsulated proteins and microbial degradation of *B. braunii* (Zang et al., 2000, 2001) indicated that efficient protection of the proteinaceous moieties resulted from encapsulation in highly aliphatic hydrophobic zones of the organic matrix (Fig. 28), including algaenan components (Nguyen and Harvey, 2003; Nguyen et al., 2003). The same protection process would be implicated with respect to the kerogen from the Kashpir Oil Shale. Moreover, reticulation of the aliphatic units by sulfur possibly afforded further protection to proteinaceous moieties in this sulfur-rich kerogen (Mongenot et al., 2001; Riboulleau et al., 2002) –

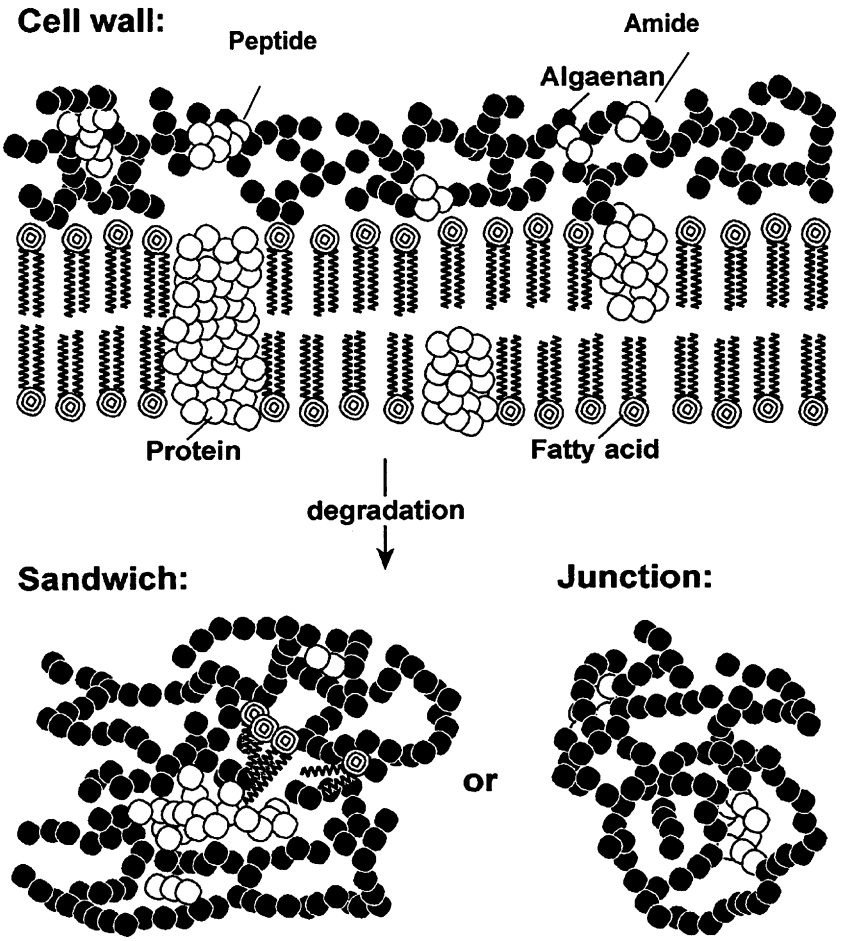

Fig. 28. Scheme proposed to explain the protection of proteinaceous material against diagenetic degradation, through encapsulation into paraffinic network of algaenan. Reprinted with permission from Knicker and Hatcher (2001, p. 742).

hence the conspicuous survival of such moieties in this ancient material. A continuum probably exists in natural samples between proteins (or weakly altered proteinaceous materials), on one hand, and melanoidin-like moieties originating from the random condensation of the degradation products of proteins via degradation–recondensation, on the other. Generally speaking, it seems that protection resulting from OM folding and aggregation, due to its hydrophobicity, has been strongly underestimated (Hedges et al., 2000). Natural materials formed by complexation of potentially labile biomacromolecules can also exhibit a relatively high resistance to diagenesis. Survival of chitin, a polysaccharide which is highly labile on its own, was thus observed in invertebrate cuticles over geological timescales, probably due to complexation with proteins in such cuticles (Baas et al., 1995; Stankiewicz et al., 1997; Flannery et al., 2001).

5.3. Summary

- Two main pathways allow, on the whole, less than 1% of the OM from the initial biomass to escape the biological carbon cycle and enter the sedimentary carbon cycle: (i) the ''degradation–recondensation'' pathway, where biodegradation products of organic constituents from living organisms recondense randomly into protokerogen, (ii) the ''selective preservation'' pathway, where protective macromolecules biosynthesized by some organisms and resistant to microbial enzymes are selectively enriched relative to other, assimilable, constituents.

- Degradation–recondensation is always involved in kerogen preservation, in contrast to selective preservation.
- Selective preservation can afford highly aliphatic kerogen fractions, thereby providing a very high oil potential.
- The respective contribution of these processes to kerogen preservation is probably controlled by environmental conditions, but detailed quantitative information on this point is not presently available.

6. Classification of kerogen by type

Pioneering studies by Down and Himus (1941) initially drew a parallel between some kerogen examples and coal, concluding that there were similarities in their organic precursors on the basis of both light microscopy and the presence of an aromatic core. They attributed kerogen compositional differences to variation in plant sources, depositional environment and bacterial reworking. They tried to describe the chemical structure of various kerogen samples by using controlled oxidation with potassium permanganate and observed large differences in susceptibility to oxidation among the different examples. Later, after concentrating kerogen from marine sedimentary rocks, Forsman and Hunt (1958) performed analysis using different techniques and arrived at conclusions very similar to those of Down and Himus (1941). They recognized the existence of two main types of kerogen, one indistinguishable from coal and the other being more aliphatic. They also showed that changes in elemental composition occur with increasing maturity upon burial.

The modern classification of kerogen stemmed progressively in the 1970s from studies of petroleum provinces and aimed at reconstituting petroleum formation and evolution via analysis of source rock extracts and their related kerogen and generated/expelled oils. Source rocks belonging to the same stratigraphic formation but buried to different depths in various petroleum systems, together with their corresponding crude oils, were made available by oil companies for research. These source rocks were often sampled as cores, thereby enabling work on good quality samples from accurately known depths. Work on cuttings was and is hampered by problems due to poor depth assessment, contamination by drilling mud and the possibility of caving. The first analyses were restricted mainly to the comparison of qualitative and quantitative chemical characteristics of extracts and crude oils, the so-called 'oil-source rock correlation'. However, in the same period, developments in efficient kerogen isolation, pyrolysis methods (including Rock-Eval) and IR spectroscopy made it possible to generate for each source rock a much larger set of analytical parameters for the assessment of maturity, and the comparison of source rock origin and evolution in different petroleum systems. The notions of OM type and maturity are thus inseparable and issue directly from petroleum research.

6.1. Widely accepted classification

Classification of source rock kerogen into three main types and their evolution with maturation under geological conditions were first proposed by Durand and Espitalié (1973). The study was based on elemental analysis of kerogen samples from the Paris Basin and related literature data on various kerogen samples of different age and location (McIver, 1967). The analyses were reported in an atomic H/C vs. O/C diagram, similar to one used earlier (van Krevelen, 1961) for comparing coalification paths of coal macerals (Fig. 29). The elemental analysis of maturity series of kerogen samples from well-characterized petroleum systems studied at the time was also reported in this diagram, allowing definition of "evolution paths" (Durand and Espitalié, 1973; Tissot et al., 1974). Three kerogen types were defined in this 'van Krevelen diagram' (Fig. 29) and associated with the specific depositional environments of these petroleum systems. Elemental analysis of the samples thus defined both kerogen source and evolution with increasing burial. Other source rock examples, although available for only a limited range of maturity, were generally shown to fit well in the diagram with a position related to the predicted depositional environment.

6.1.1. Reference types of kerogen

The source rocks and reference petroleum systems corresponding to the initial definition of Types I–III, ranged in the order of decreasing petroleum potential, and thus of H/C ratio, are described briefly as follows:

(a) The Green River Shale (GRS), the source rock of the primary petroleum system in the Uinta Basin (UT, USA), contains the reference Type

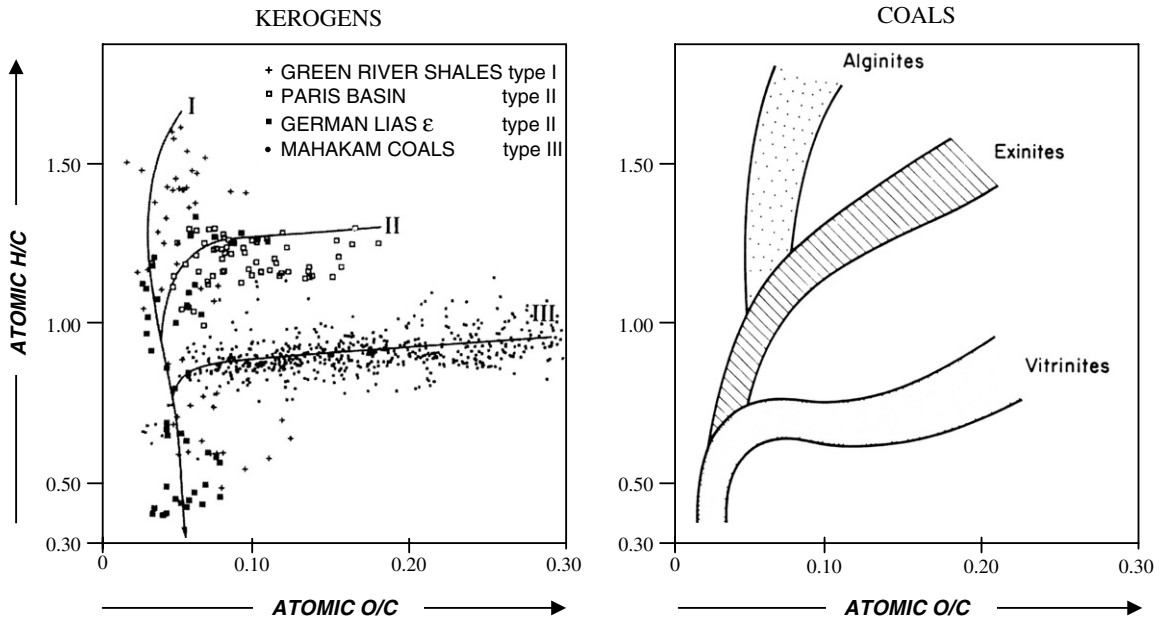

Fig. 29. Coal macerals and kerogen Type: evolution paths upon geological burial in the van Krevelen diagram of H/C vs. O/C atomic element ratios. Closely related depositional environments correspond to kerogen types with similar elemental ratios for a given maturity. Three main types are identified, from I starting at low maturity with high H/C and low O/C to III starting at low maturity with low H/C and high O/C. Modified from Vandenbroucke et al. (1993) and Tissot and Welte (1978).

I kerogen, although some levels in the formation contain classical coal (Tissot et al., 1978). Except for these latter levels, the kerogen of immature samples is highly aliphatic, with an H/C atomic ratio frequently >1.5. The oxygen content is often low, although the O/C atomic ratio for immature samples varies from 0.03 to 0.1. Analysis of oxygen functional groups in immature Mahogany Zone kerogen (Fester and Robinson, 1966) showed a major participation of unreactive oxygen assumed to be located in aliphatic ether bonds. In accordance with the high initial H/C ratio, the extracts, oils or pyrolysis products are rich in long chain *n*-alkanes, extending to >40 carbon atoms, without a marked odd or even predominance. The abundance of iso- and anteiso-alkanes and other microbial biomarkers, such as carotane, led Tissot et al. (1978) to conclude that the initial OM input (probably *Cyanophycea*) had been strongly reworked by bacteria that could have sourced the major part of the finally sedimented OM. It is worth noting that the lacustrine environment associated with most Green River Shale deposition is not freshwater, as it contains unusual alkaline minerals (Smith, 1983), in particular specific carbonates, such as dawsonite [$NaAl(OH)_2CO_3$], nahcolite ($NaHCO_3$) and trona ($NaHCO_3$–Na_2CO_3–H_2O). Robinson (1976), estimated that the mountain streams feeding the shallow lake basins may have contained a total of 460 ppm of dissolved salts, of which >200 ppm were bicarbonate. It should also be recalled that Tissot et al. (1978) studied only the Uinta Basin part of the Green River Formation oil shale; however, the unit also occurs in the Piceance Creek Basin (Colorado) and in the Green River and Washakie Basins of Wyoming. Other Type I kerogen examples such as Autun boghead coal (France), Torbanite (Scotland) or recent materials such as Coorongite (Australia), principally derived from *Botryococcus* remains, were also deposited in a lacustrine setting, although in these cases it was freshwater. The marine kerogen of the organic-rich Tasmanite from Tasmania was also classified as Type I by Tissot and Welte (1978). They explicitly related the aliphatic character of all these kerogen examples to "either a selective accumulation of algal material" for the algal kerogen, "or a severe biodegradation of the OM other than lipids and microbial waxes" for the Green River

examples (Tissot and Welte, 1978, p. 142). The severe biodegradation observed for the GRS was assumed to occur only in lacustrine environments – hence the frequent association of Type I with "lacustrine" OM.

Tissot and Welte (1978) had already pointed out the relatively low occurrence of Type I OM compared to the other types. Numerous geochemical studies of Type I deposits have been performed, not only ancient sedimentary rocks but also recent deposits and relevant cultured source organisms. This is due to the interest in this specific kerogen type for understanding, inter alia, the selective preservation mechanism described above. The geographical and geological extensions of such organic deposits are, however, generally very restricted. Although, they have the highest oil potential among OM types, it was estimated by Klemme and Ulmishek (1991) that they are the source of only 2.7% of the world's original reserves of petroleum and gas. The examples used by Tissot and Welte (1978) for defining this type clearly show that the kerogen from very different organic sources, characterized by a common high aliphaticity, is classified as Type I. Thus, this is not a separate type sensu stricto, since different biological precursors, sedimentary environments and preservation conditions can be implicated.

(b) Type II is based on the lower Toarcian shales of the petroleum system from the Paris Basin (France) and the equivalent Posidonienschiefer (Liassic ε) Formation in Germany. The H/C and O/C atomic ratios of immature kerogen are ca. 1.3 and 0.15, respectively. As shown by group type analysis of kerogen pyrolysates and natural extracts (Tissot and Vandenbroucke, 1983), this OM contains many more cyclic aliphatic moieties than Type I, as well as a large amount of aromatics, whose structure often contains several aliphatic rings that become aromatized with progressive maturation. The *n*-alkane distribution in extracts or pyrolysates is nearly restricted to a range $< C_{25}$, even at low maturity. Sulfur is always associated with this type of OM, either as pyrite and free sulfur, or in the kerogen as aliphatic and thiophenic sulfur. The depositional environment associated with these Toarcian shales, as well as with their analogues in Germany, was a moderately deep marine environment with planktonic input as the primary source. More or less intense reworking by various bacterial communities occurred, depending on the location of the oxic/anoxic boundary. Seawater sulfate provided the oxidant necessary for OM biodegradation via sulfate reducing bacteria. These bacteria released polysulfide, H_2S and native sulfur capable of combining both with Fe from clays, ultimately to form pyrite, and with the OM to produce organosulfur moieties, as discussed in detail in the section on early diagenesis. This Toarcian OM Type was compared to other source rocks from marine deposits in different places in the world (e.g. Devonian of Western Canada, Silurian and Devonian from North Africa). The comparison showed very homogeneous chemical features for kerogens and extracts, and oils and pyrolysates. Differences in kerogen sulfur content were attributed to the different mineralogical compositions of these source rocks, the richest in carbonate being the richest in organic sulfur, because in that case Fe from clays was not available for pyrite formation.

(c) Type III was initially based on the Upper Cretaceous sedimentary rocks of the Douala Basin (Logbaba, Cameroon), sourced by the Niger River palaeo deltaic input, and deposited in a shallow marine environment (Albrecht et al., 1976). This Type of OM is frequently found in deltaic settings and derives from higher plant debris, often highly reworked, given the oxidising transportation conditions associated with detrital sedimentation. In the case of the Logbaba silty clays, no coal beds were found at any depth. Only the most resistant chemical constituents of the terrestrial OM reached the site of sedimentation and, once there, were quickly buried due to large sediment input and high subsidence rate caused by the opening of the South Atlantic Ocean. Under such conditions, strong bacterial degradation could probably not occur and no (or limited) sulfur was available for incorporation into the OM or to form pyrite, even though abundant sulfate was present in seawater. As shown both by chemical and light microscopy analysis, the organic fraction consists in large part, on one hand of ligneous debris with a predominantly aromatic structure, and on the other hand of moieties derived from the protective constituents of higher plants with a predomi-

nantly aliphatic structure based on long chains. This latter part of the terrestrial OM is probably always a minor fraction of the total kerogen. The double contribution explains, however, the apparent discrepancy observed between the mostly aromatic kerogen composition, as seen from elemental analysis, with a H/C atomic ratio less than 0.8 (Durand and Espitalié, 1976), and the highly paraffinic extracts and oils generated by this Type III kerogen compared to Type II kerogen (Vandenbroucke et al., 1976). Other examples of Type III OM were found in the lower Mannville shales of Alberta, Canada.

At one time coal series were often classified separately as a specific Type numbered IV due to their slightly lower position in the van Krevelen diagram (Tissot, 1984). However, Durand et al. (1977b) showed, for a series of kerogen fractions isolated from coals with the usual acid treatment, that Type III OM and coals can be classified together within the same Type.

Extensive studies carried out on the maturity series from the Mahakam Delta (Eocene–Miocene) in Indonesia (Combaz and de Matharel, 1978) showed that pure coals and Type III shales occurring together in these sedimentary rocks are derived from the same precursors. Detailed geochemical study of kerogen from shales and coals of both the Mahakam series and the Gironville series in the Paris Basin (Huc et al., 1986) showed that humin from very immature coals and humin from shales are not equivalent, due to differences in sedimentological conditions. However, no noticeable differences between massive coal and shale evolution were noted, at any maturity stage. Hence, no catalytic effect of clays on kerogen evolution under geological conditions could be observed for the maturity series, as shown in Fig. 30 (Durand et al., 1987). Such a catalytic effect had often been hypothesized on the basis of laboratory experiments (Sieskind and Ourisson, 1972). However, it is only observed during dry open system pyrolysis of some clayey rocks with relatively low OC content, for instance with Rock-Eval pyrolysis as mentioned above (Espitalié et al., 1984).

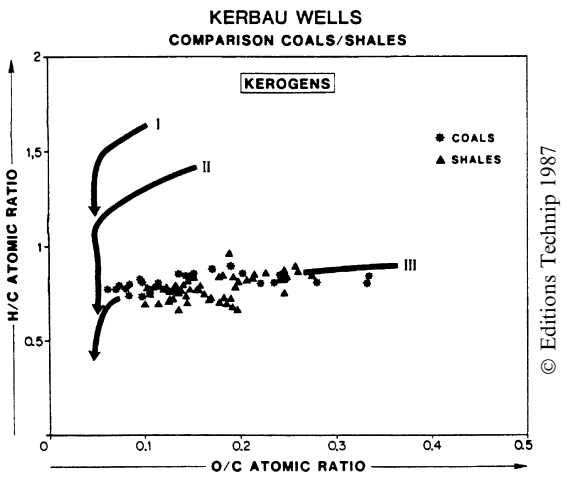

Fig. 30. Comparison of positions in a van Krevelen diagram of kerogens isolated from coals and shales in the Kerbau wells (Mahakam delta, Indonesia) at different maturity. Reprinted with permission from Durand et al. (1987, p. 181).

Resulting from this justified grouping of coals with Type III dispersed OM, massive coal depositional settings, although with contrasting characteristics in comparison to deltaic sedimentation sites, were also associated with Type III OM. In the depositional environment of coals, there is no transportation with detrital sediment under oxic conditions and in situ deposition of an almost pure organic fraction occurs, with moderate alteration due to the sterilizing effect of some OM decomposition products such as phenols. The deposition of large coal beds of Carboniferous age occurred in tropical forest swamps, but similar environments exist today (Van Krevelen, 1993, Chapter 3). Coal beds formed in these swamps may subsequently be affected by erosion and carried with detrital sediment out of their initial site of deposition, thus largely contributing to kerogen-rich sedimentary rocks, as in the case of the Mahakam series (Allen et al., 1979).

Successful petroleum exploration in Tertiary deltaic settings all around the world in the last twenty years has resulted in intensive geochemical studies of good quality cores and cuttings. These studies showed that, contrary to Type I, dispersed Type III OM, associated or not with humic coals, is homogeneous and chemically well defined, like Type II. Type III originates from a terrestrial input of higher plants, although in this case two contrasting depositional environments can be described for the same OM Type as discussed above. It is now becoming more and more clear that the variable oil potential of Type III OM cannot be estimated only from the H/C atomic ratio or the Rock-Eval HI (Isaksen et al., 1998) since either long aliphatic chains ($> C_{24}$) generating waxy oil, or aromatic H and short aliphatic chains ($< C_{18}$) generating mainly gas, may

be predominant. The gas vs. oil potential of Type III results from the variable respective amounts of two main constituents of the kerogen composition: aromatic ligneous debris with mainly gas potential and aliphatic protective coatings with paraffinic oil potential (e.g. Killops et al., 1998 and references therein). However this is not directly related to maceral amounts as vitrinite, for example, may contain a noticeable aliphatic component (Powell et al., 1991). It seems that the varying hydrocarbon potential of Type III OM is controlled by the evolution of plants from the Carboniferous to the Cenozoic, with Cenozoic coals being richer in liptinite, due to an increasing diversification and dominance of angiosperms over gymnosperms (Powell et al., 1991; Petersen and Nytoft, 2006). This view of Type III kerogen composition readily explains why such kerogen can give rise to either oil-prone or gas-prone source rocks.

6.1.2. Influence of kerogen type on petroleum migration

As stressed above, kerogen type will largely influence the chemical composition of the products generated upon burial. It thus has great influence on the solvent soluble compounds generated inside source rock porosity and hence on the mobility of the expelled oil on its way to a reservoir (Penteado and Behar, 2000). Indeed, the composition of Type II petroleum products, very rich in NSO compounds and aromatics, allows good solubilization of naphthenoaromatic molecules and hence fairly rapid pore filling by a viscous oil rich in heavy compounds. In contrast, Types I and III kerogen will produce a paraffinic mobile fluid and, even if aromatics and NSOs are generated together with paraffins, most of these will be barely soluble in the mobile phase, except light aromatics from Type III kerogen. The resulting expelled oil will have a much higher mobility than a Type II oil, as paraffin viscosity decreases strongly with increasing temperature in the range for geological conditions. Natural case studies (Khavari Khorasani and Michelsen, 1991; Clayton et al., 1991; Killops et al., 1998), as well as experimental work (Khavari Khorasani and Michelsen, 1991; Behar et al., 2003), point to very early generation and migration of heavy saturates in oils sourced from Type III kerogen, as shown in Table 12. However, the absolute amount of C_{14+} HCSU (saturated plus unsaturated hydrocarbons with > 14 carbons) obtained in laboratory simulations is quite low, frequently < 10% of the total pyrolysate. Thus, even if saturates are the best candidates for primary migration, their early expulsion does not substantially decrease the petroleum potential as measured by Rock-Eval HI.

Table 12
Comparison of absolute amounts (μg/g C) of saturated and unsaturated hydrocarbons[a] produced by coals with different initial maturity upon preparative open pyrolysis[b]

Coal sample	VR[c] (%)	Final T (°C)	Pr[d]	Σ1[e]	Σ2[f]	Pr/nC$_{18}$	Σ2/Σ1
Wilcox[g]	0.28	400	121	12	57	27.28	4.77
		450	695	376	1028	5.34	2.73
		600	714	1433	1384	1.63	0.97
		Δ450–600	19	1057	356	0.06	0.34
Pennst. Lib. DESC-8	0.37	450	98	40	88	5.88	2.18
		600	266	681	554	1.14	0.81
		Δ450–600	168	641	466	0.78	0.73
Fruitland	0.57	450	150	106	299	4.17	2.83
		600	604	2437	2684	0.74	1.10
		Δ450–600	454	2331	2385	0.59	1.02
Mahakam	0.57	450	56	52	100	3.18	1.93
		600	214	967	833	0.69	0.86
		Δ 450–600	158	915	733	0.54	0.80

[a] Individual saturated and unsaturated hydrocarbons quantified using GC/FID analysis calibrated with standards (Behar et al., 1997).
[b] From 200 °C to variable final temperature at 25 °C/min.
[c] VR, vitrinite reflectance.
[d] Pr, prist-1-ene plus prist-2-ene.
[e] Σ1 = n-C$_{14}$ + n-C$_{16}$ + n-C$_{18}$ alkanes plus n-alk-1-enes.
[f] Σ2 = n-C$_{25}$ + n-C$_{27}$ + n-C$_{29}$ alkanes plus n-alk-1-enes.
[g] Data from Behar et al. (2003).

6.2. Further modifications to the initial classification of kerogen

6.2.1. Difficulties due to extension of classification to other series

It became clear in the mid 1980s that the correlation between a lacustrine environment and Type I kerogen was not exclusive (Kelts, 1988). One example is given by the surficial sediment of the freshwater Lake Tanganyika. Whole sediment and the isolated protokerogen were analyzed using various geochemical methods, including Rock-Eval pyrolysis and elemental analysis (Huc et al., 1990). In this lake, where diatoms, cyanobacteria and Chlorophyceae cyclically represent the major phytoplanktonic input, the sedimentary OM is abundant and displays Type II characteristics, except near the deltaic output of the Ruzizi River where Type III occurs. The variability in lacustrine OM Type was observed in many other places and is discussed in detail by Talbot (1988). In some cases, given the often very good preservation conditions in lacustrine settings, as a result of water stratification and short sedimentation distance, the H/C atomic ratio of immature kerogens reaches 1.4. This position in the van Krevelen diagram led some authors to name them as Types I/II, although they have nothing to do with a marine ecosystem. It now appears, from the numerous published studies, that all the possible types of kerogen can be found in lacustrine sedimentary rocks. Carroll and Bohacs (2001) classify lacustrine facies into three main depositional settings, described as fluvial-lacustrine, fluctuating-profundal and evaporative. This illustrates the variation in OM type associated with such facies.

Type I is usually very low in sulfur, but there are exceptions since some lacustrine environments may contain abundant sulfate from weathering of surrounding rocks or sediments. Such a depositional environment was first recognized for two *Botryococcus*-derived Catalan oil shales (Sinninghe Damsté et al., 1993a), containing kerogen with high H/C atomic ratios characteristic of Type I but also with S/C atomic ratio > 0.05. This kerogen Type was named I-S to distinguish it from the classical S-poor Type I. A third Catalan lacustrine oil shale from the same study (Sinninghe Damsté et al., 1993a) was shown to contain remains of *Pediastrum*, another freshwater alga, and the geochemical parameters for its kerogen unambiguously corresponded to Type II. This example illustrates the high variability in lacustrine deposits, whose ecosystem strongly depends on the chemical composition of water.

Due to the fairly homogeneous composition of unstratified seawater, except in evaporitic settings, many marine kerogen series are located close to the evolution path defined for Type II kerogen. Some source rocks, such as the Monterey Formation (California) exhibit, however, distinct characteristics due to a particularly high amount of sulfur (8–14 wt%) incorporated into the kerogen. Among these, the thermal decomposition of kerogen to oil occurs earlier than for 'normal' Type II kerogen, due to the weakness of S–C bonds, and the resulting 'immature' oil is rich in heavy compounds such as resins and asphaltenes. Given the specific role of sulfur in the kinetics of oil formation and in oil composition, Orr (1986) proposed distinguishing kerogen with a S/C atomic ratio > 0.04 (8 wt% sulfur) as Type II-S. However there should exist a continuum between the kinetic properties of Type II and II-S kerogen in relation to increasing sulfur content. Both Types are sourced from similar marine planktonic organisms. The difference is related to the mineral environment, i.e., to the capacity of the associated minerals to release or not enough Fe to recombine with reduced sulfur to form mineral or organic species, respectively. The occurrence of Type II-S should thus be associated with a major carbonate fraction in sedimentary rocks, although there are very few differences from the classical Type II regarding OM source. It is also possible, although not frequent, to find massive coals with a noticeable organic sulfur content. This may happen if marine incursions flood peat-forming coastal swamps, introducing seawater sulfate and the associated bacterial communities. Several examples of high sulfur coal occurrences, their mode of formation and the different types of organic sulfur compounds identified, can be found in Chou (1990) and other papers in this ACS Symposium 429 Proceedings volume. Sulfur incorporation within sedimentary OM is discussed in detail in the section on kerogen evolution processes.

Separation of kerogen types into sub-types, based on sulfur content, was proposed by Hunt (1996). This separation takes into account differences in kinetic behaviour due to the influence of C–S bonds, and three GRS Type I sub-types and four Type II sub-types were defined on the basis of their kinetic parameters. However, such a classification is no longer related only to depositional environment, as initially defined (Tissot et al.,

Table 13
Post-sedimentary abiotic oxidative alteration of Toarcian outcrops (Paris basin)[a]

Sample depth (m)	Rock parameter				Kerogen parameter		
	TOC (%)	HI (mg/g C)	OI (mg/g C)	T_{max} (°C)	At H/C	At O/C	Pyrite (wt%)
0.5	1.97	134	238	435	1.18	0.235	0.58
1	6.30	397	88	428	1.24	0.186	0.51
3.8	8.06	556	65	419	1.29	0.148	2.01
4.3	13.46	614	27	414	1.28	0.115	2.98
5	9.67	655	26	418	1.31	0.074	20.96

[a] After Nicaise (1977) and IFP data.

1974). Moreover, for the three Type I GRS subtypes, separation based on kinetic parameters was not directly related to sulfur content. Given the large uncertainties in kinetic parameter acquisition, depending on the method used for obtaining the experimental data and for calculating these parameters, the proposed classification should lead to slightly different kinetics for each new kerogen examined, and therefore the "Type" notion loses its predictive capacity. This strongly limits the usefulness of such an extended classification, in contrast to the well-accepted distinction between Type II and Type II-S.

Post–sedimentary abiotic oxidative alteration of OM by air and/or water has frequently been observed, for example in Toarcian outcrops of the Paris Basin (Table 13; Nicaise, 1977; Bordenave et al., 1993), in coal beds (Landais et al., 1984) and in weathered black shales (Petsch et al., 2000). The natural path of oxidative alteration of immature coals, as observed in the Rock-Eval diagrams of HI vs. T_{max} and HI vs. OI, can be reproduced by laboratory heating experiments (Landais et al., 1984 and references therein; Fig. 31). This alteration results in lowering the H/C ratio and increasing the O/C ratio of the kerogen, probably by ether cross linking (Petsch et al., 2000). The location of altered kerogens in a van Krevelen diagram, relative to the initial unaltered material, is thus shifted to an increasingly downward and rightward position as alteration progresses. Weathering is similarly associated with a lowering of the HI, an increase in OI and T_{max}, and an increase in pyrite oxidation, as illustrated by Toarcian outcrop samples taken from various depths under the soil surface (Table 13). The location of an altered Type II kerogen in the van Krevelen diagram thus becomes intermediate between the Type II and Type III evolution paths. This explains the frequent use of a Type II/III classification, even though such a classification has no

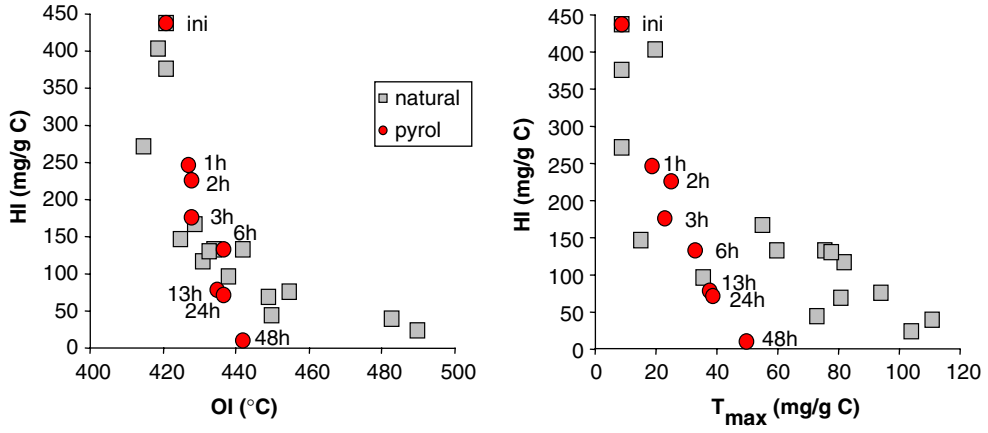

Fig. 31. Oxidative alteration paths of (i) a natural coal series (■) and (ii) laboratory oxidation in air of a same initial coal (●) at 200 °C and increasing duration. Data obtained in the HI vs. OI and HI vs. T_{max} Rock-Eval diagrams show that oxidation in the natural series can be reproduced by laboratory heating experiments. Increasing oxidation results in lowering the HI, and increasing the OI and T_{max}. Modified from Landais et al. (1984).

meaning in terms of type as defined by depositional environment and biological source.

A Type IV was defined by Harwood (1977) in order to characterize a Pennsylvanian humic coal with a low H/C atomic ratio, which was supposed to be immature but capable of generating only dry gas. Type IV was also used in some cases, as mentioned above in relation to defining Type III, to characterize the evolution path of pure humic coals. For strongly altered samples, the type of the original OM cannot be characterized anymore using geochemical analysis unless unaltered equivalents are known, hence their classification sometimes also as Type IV (Tissot, 1984). This new definition would not help, however, in predicting the organic source, evolution path and associated geochemical characteristics of such a kerogen, in contrast to other kerogen types. This ambiguous classification of low petroleum potential OM or humic coals as Type IV was thus progressively abandoned. Nevertheless, some authors continue to use the Type IV nomenclature for unusual low H/C or HI samples, although this does not imply any geochemical characteristics.

6.2.2. Classification based on biological communities in depositional environments

Kerogen classification based on reference types, defined by their position in a van Krevelen diagram, was of great help to oil explorationists in predicting the petroleum generative capacity of source rocks and understanding the chemical characteristics of the generated oils. However the increasing number of geochemical studies on petroleum systems raised some questions about the attribution of a defined type to specific source rocks. This is particularly obvious for Type I, which includes the OM of Eocene Green River shales (microbial waxes?), and that from Ordovician source rocks (*G. prisca*) and different boghead coals (*B. braunii*). Different and almost unique precursors are implicated for these kerogens, as well as different sedimentary environments. These ambiguities are also reflected in the frequent association of two types to account for some of the measured geochemical parameters. An example of this association is *G. prisca*-derived kerogen. Given the presence of aromatic moieties in protective walls, the related kerogen from immature Kukersite has H/C and O/C atomic ratios of 1.48 and 0.14, respectively (Derenne et al., 1990). As a result, it is far from the reference Type I example, the immature GRS kerogen from the Uinta Basin, that peaks at 1.64 for H/C but with only 0.05 for O/C. This is why Derenne et al. (1990) indicated Type II/I OM throughout their study.

One can thus question the adequacy of the present classification, whose initial purpose was to characterize sedimentary OM by its source and depositional environment as expressed by Forsman (1963, p. 165), then by Tissot and Welte (1978, p. 142). Given the frequent lack of a complete maturity suite of source rocks in many case studies, very subtle differences between types may hamper the predictive capacity of such a classification by weakening its underlying purposes, i.e. describing chemical evolution and predicting the amounts and timing of oil and gas generation. A more general and simpler classification of kerogens can be based mainly on the biological specifics of the two main types of primary producers, algae on one hand and higher plants on the other, as initially proposed (Forsman and Hunt, 1958; Forsman, 1963, p. 172). The corresponding kerogen types are then characterized as aquatic or terrestrial; this distinction is similar to the distinction between sapropelic and humic OM as used by petrologists, or between alginite and vitrinite as used by coal scientists. Bacterial reworking takes place on debris from both types of primary producers during sedimentation in aquatic settings. It can be hypothesized that bacterial degradation does not alter significantly the chemical structure of aliphatic and aromatic skeletons in the sedimented plant debris, due to their chemical resistance to enzymatic hydrolysis; rather, it superimposes its own imprint on the kerogen precursors. Differences in the chemical characteristics of hydrocarbon skeletons of aquatic vs. terrestrial kerogens were compared (Vandenbroucke, 1980) in order to derive quantitative structural characteristics of kerogens from bitumen analysis. These chemical features are presented below as a response to environmental conditions, although this deterministic approach is probably a highly simplified view of the reality.

As indicated above, kerogen arising from remains of algal communities in open water environments, such as normal salinity seas and freshwater lakes, includes variable amounts of resistant aliphatic parts of cell walls as well as various recombined lipids. The hydrocarbon potential of the resulting kerogen is characteristic of a Type II (or possibly a low Type I) position in a van Krevelen diagram, depending on the algaenan content and composition of the different algal species. For such

kerogens arising from organisms floating in freshwater or seawater, a feature of the *n*-alkane distribution in the C_6–C_{35} range is a maximum most of the time at below C_{20}. This was demonstrated via numerous pyrolysis GC analyses of immature Type II kerogens (Larter and Horsfield, 1993 and references therein) and by the alkane distributions of low maturity oils resulting from kerogen cracking. It thus seems that long chain aliphatic compounds are not necessary in the aquatic environment for protective purposes, and that lipids based on various C_{16} and C_{18} straight chain fatty acid units, abundant in algae, are well adapted to life in such environments. This would explain the relatively low carbon number distribution of aliphatic moieties in Type II kerogen, reflected in the distribution of *n*-alkanes generated upon maturation.

In contrast to algal communities floating in water, terrestrial primary producers have to live in a drier atmosphere and display their photosynthetic organs towards the sun. The need for an efficient protection against evaporation on one hand, and for a rigid skeleton for rising above other plants to find light for photosynthesis on the other, makes necessary adapted chemical responses through the development of new biosynthetic pathways. Protection against evaporation is achieved by using compounds with long alkyl chains, that are rather inert chemically and resistant to degradation, and thus would be incorporated into kerogen. Pyrolysis of immature terrestrial kerogens thus releases C_6–C_{35} *n*-alkanes, whose distribution often shows a more or less dominant C_{25+} fraction (depending on maturity; Behar and Vandenbroucke, 1988). A rigid skeleton, absent from aquatic plants, is obtained via the aromatic rings of lignin. Ligneous debris, like protective tissues, is fairly resistant to oxic degradation during transport of terrestrial OM to sedimentation sites and is also incorporated into kerogen. However, lignin has almost no oil potential, except for a few aromatic molecules and some gas. Lignin will thus not contribute substantially to petroleum generation, but the high aromaticity of the related kerogen can easily be observed using solid state ^{13}C NMR (Hatcher, 1987). This situation results in aromatic kerogens with an H/C atomic ratio <1, although such a kerogen can generate highly paraffinic oil. Moreover, as mentioned above, the oil vs. gas potential of such a kerogen will depend on the relative contents of aliphatic protective tissues and ligneous debris.

6.3. Summary

- Elemental analysis of low maturity kerogen examples from reference petroleum systems, plotted in an atomic H/C vs. O/C diagram similar to that used by van Krevelen (1961) for coal macerals, can trace the biological sources and depositional environment of these kerogens. Three main kerogens Types were defined, from I to III in the order of decreasing H/C ratio; coals were later shown to be a form of Type III OM.
- Further analysis of the kerogens from other natural series showed that Type II can be associated with planktonic OM in open marine and freshwater lacustrine environments, and Type III to higher plants from a terrestrial input into lacustrine or marine settings. In contrast, Type I kerogen, uncommon in source rocks, can be sourced from various highly specific biological precursors in very different sedimentary environments.
- The definition of different Types, even if it may appear to be a strong simplification of biological precursor and depositional environment diversity, was of great help in petroleum exploration. Except for situations where kerogen is subjected after deposition to major incorporation of sulfur

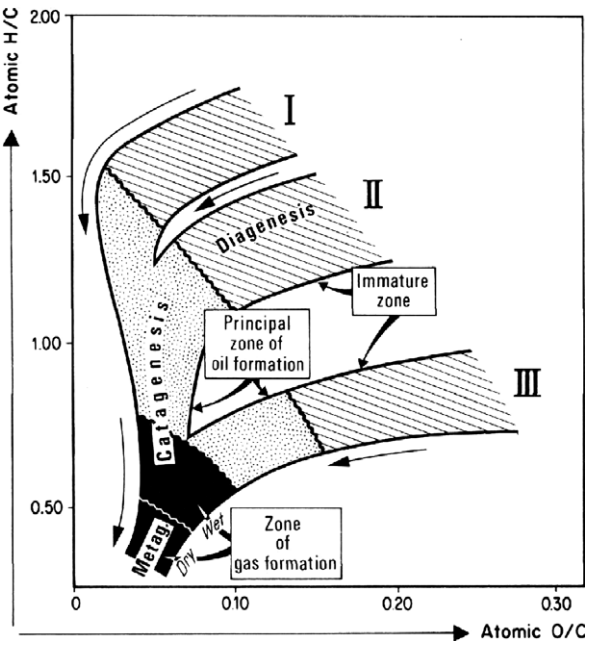

Fig. 32. General scheme of kerogen evolution from diagenesis to metagenesis in the van Krevelen diagram. Modified from Tissot and Welte (1978, p. 186).

<table>
<tr><th colspan="5">KEROGEN</th><th colspan="3">COAL</th></tr>
<tr><th>Tissot & Welte (1978)</th><th>Vassoevitch (1969, 1974)</th><th>Main HC generated</th><th>VR</th><th>LOM</th><th>ICCP (1971)</th><th>Rank USA</th><th>Rank Germany</th></tr>
<tr><td rowspan="2">Diagenesis</td><td>Diagenesis</td><td rowspan="2">Methane</td><td rowspan="9">0.5
1.3
1.5
2
2.5
3.5
4</td><td rowspan="9">2
4
6
8
10
12
14
16
18
20</td><td>Peat</td><td>Peat</td><td>Peat</td></tr>
<tr><td>Protocatagenesis</td><td rowspan="2">Brown coal</td><td>Lignite</td><td rowspan="2">Braun-kohle</td></tr>
<tr><td rowspan="3">Catagenesis</td><td rowspan="3">Mesocatagenesis</td><td rowspan="2">Oil</td><td>Sub bituminous</td></tr>
<tr><td rowspan="5">Hard coal</td><td>High Volatile bituminous</td><td rowspan="4">Stein-kohle</td></tr>
<tr><td>Wet gas</td><td>Med. vol. bit.</td></tr>
<tr><td rowspan="2">Metagenesis</td><td rowspan="3">Apocatagenesis</td><td rowspan="3">Methane</td><td>Low vol. bit.</td></tr>
<tr><td>Semi anthracite</td><td rowspan="2">Anthracite</td></tr>
<tr><td>Anthracite</td></tr>
<tr><td>Metamorphism</td><td colspan="3"></td><td>Meta anthrac.</td><td>Meta-anthracite</td></tr>
</table>

Fig. 33. Maturity scales for sedimentary OM and coal evolution. Modified from Tissot and Welte (1978, p. 71).

or oxygen, such defined Types can be directly related to total hydrocarbon potential, oil chemistry and kinetics of hydrocarbon generation.

7. Kerogen evolution upon sediment burial

The classical maturity zones for OM evolution were defined by Vassoevitch et al. (1969) and then renamed by Tissot and Welte (1978, 1984) in order to separate the main zones of petroleum formation in the van Krevelen diagram (Fig. 32). The comparison of these maturity zones with those based on vitrinite reflectance, on the LOM (level of organic metamorphism) scale (Hood et al., 1975) and on coal rank, is shown in Fig. 33.

Elemental analysis, besides its role in the classification of kerogen type, was also from the beginning used to study maturity by way of the definition of evolution paths reflecting changes in kerogen chemical structure and associated main zones of oil and gas generation with increasing burial (Tissot et al., 1974). With the van Krevelen diagram being based on O/C and H/C atomic ratios, the maturity stages were separated according to element losses, first oxygen, then hydrogen. These three elements, accounting for the bulk of coal, provided a complete description of coal evolution upon geological maturation. However, this is generally not the case for marine kerogen precursors that contain substantial amounts of labile nitrogen. Studies of humic fractions from marine recent sediments, including humin, led to the definition of a first specific stage, referred to as early diagenesis, for kerogen evolution in a sediment, associated with nitrogen loss. Other element concentrations may also change in protokerogen during this early stage as detailed below.

It is worth remembering that all the steps in the change in elemental composition upon sediment burial correspond in fact to net losses from kerogen, as shown by a continuous decrease in TOC content with increasing maturity in homogeneous sedimentary series.

7.1. Early diagenesis

Algal organic debris settling on surficial sediments is relatively rich in nitrogen and is highly reactive, particularly when the organic input is abundant. Moreover, under specific environmental conditions, elements such as sulfur or oxygen from inorganic sources may react with freshly incorporated sedimentary OM. It is thus necessary to consider an initial transformation step for sedimented organic debris to account for these changes in elemental composition. This first evolution stage, referred to as early diagenesis (Tissot and Welte, 1978, p. 70), differs from the succeeding ones by way of two characteristics. First, it occurs in a very restricted depth range, usually down to a few meters below the water–sediment interface. Second, living organisms and biochemical reactions can participate, directly

via biodegradation processes or indirectly via reaction of sedimented OM with their metabolic products, in the chemical changes in the protokerogen structure. Nitrogen loss always occurs during this stage. In sulfate-rich depositional environments, sulfur incorporation may take place in both mineral and organic sediment fractions, sometimes with a noticeable increase in the S/C atomic ratio of the kerogen. Finally, under conditions alternating between oxic and anoxic at the water/sediment interface, partial oxidation of the sedimented OM may take place. This decreases the TOC content and leaves a material depleted in hydrogen and enriched in oxygen that reticulates organic structures via ether bonds. These early diagenetic transformations, changing chemical bond types and N/C, S/C and O/C atomic ratios in sedimented OM, may become extensive in some cases, having tremendous implications for the future petroleum potential of the kerogen in terms of kinetics and/or amounts generated (Orr, 1986).

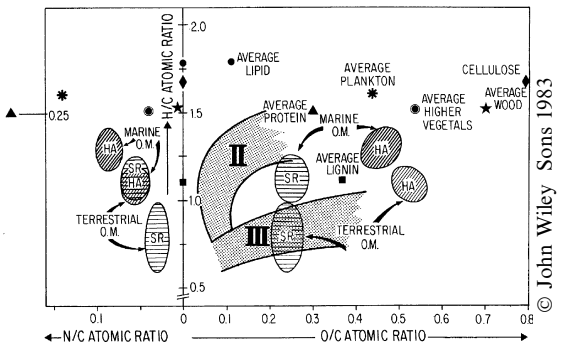

Fig. 34. Comparison of average C, H, O, N composition, as atomic ratios to C, of some living organisms, biopolymers, humic acids (HA) and humins (SR) from marine and terrestrial sedimentary OM. Reprinted with permission from Pelet et al. (1983, p. 243).

Table 14
Evolution of C and N contents upon early diagenesis in sediment cored in the Sukra transect (Oman Sea) under 830 m water depth[a]

Sample depth (cm)	Total sediment			Humin	
	TOC (wt%)	N (wt%)	At N/C	C (% TOC)	At N/C
0–2	7.07	0.96	0.117	86.2	0.117
2–4	6.98	0.97	0.119	87.3	0.119
10–12	6.70	0.86	0.110	88.1	0.111
20–22	6.30	0.80	0.109	87.5	0.110
100	2.54	0.30	0.101	83.8	0.099
300	1.83	0.174	0.081	77.4	0.081
400	1.72	0.158	0.079	77.4	0.081
500	2.06	0.183	0.076	80.8	0.080

[a] After Jocteur-Monrozier and Jeanson (1981).

7.1.1. Nitrogen content: atomic N/C decrease

Early diagenesis is the stage involving the main loss in N, which is not accounted for in the classical van Krevelen diagram. It is clearly observed by considering the evolution of the N/C atomic ratio of humin with increasing sample depth. However, the starting point for the N/C ratio is not the same for all OM types, as it depends on the amino acid content of the source organisms (Pelet et al., 1983). Terrestrial plants generally have a N/C ratio < 0.05 for a H/C ratio around 1.0, whereas planktonic organisms have N/C ratio > 0.08 for H/C ratio ranging from 1.3 to 1.5 (Fig. 34).

Because biomass degradation occurs mainly via hydrolysis reactions, N elimination takes place chiefly in the form of amino acids and NH_4^+ (Schnitzer, 1985). This results in a decrease in TOC and N content in the sediment and in the humin fraction, as shown in Table 14 for the Sukra transect in the Oman sea (Jocteur-Monrozier and Jeanson, 1981). The relative elimination rates of N and C, reflected in the decrease in N/C atomic ratio, depend on the nature of the minerals associated with the OM. Thus, clay minerals significantly lower N loss during early diagenesis, due to their sorptive capacity and resulting protection of OM (Jocteur-Monrozier and Jeanson, 1981). As indicated above in the section on preservation processes, labile N moieties can also be protected by steric encapsulation into a resistant organic matrix. In algaenan obtained after drastic acid hydrolysis of living algae such as *B. braunii* (Derenne et al., 1998), or in OM of very immature sediments a few thousand years old, such as algal sapropel from Mangrove Lake, Bermuda (Knicker et al., 1996), N is mainly present as amide groups. However, in the immature (a few million years old) sedimentary OM derived from *B. braunii*, pyrrole units have already become the main form of N (Derenne et al., 1998).

The end of early diagenesis is defined by the stage when N in humin is no longer hydrolysable. The N content of kerogen will not change much after this stage until the end of petroleum and natural gas formation. It is only during the late stage in CH_4 formation that N will be released from kerogen in the form of N_2 gas (e.g. Littke et al., 1995; Gillaizeau et al., 1997). This does not mean, however, that

Table 15
N speciation (XPS analysis) in two immature Argonne Premium coals and two kerogens, and their artificially matured residues after pyrolysis[a,b]

Sample	Nature	At O/C	Pyridinic (mole%)	Amino (mole%)	Pyrrolic (mole%)	Quaternary (mole%)
Beulah Zap coal	Fresh	0.188	26	⩽5	58	16
	Pyr. char	0.075	31	⩽5	60	9
Wyodak coal	Fresh	0.169	25	⩽5	60	15
	Pyr. char	0.100	32	⩽5	62	6
Green River kerogen	Fresh	0.026	28	11	53	8
	Pyr. char	0.039	31	⩽5	54	15
Bakken kerogen	Fresh	0.101	25	6	53	16
	Pyr. char	0.050	41	⩽5	51	9

[a] After Kelemen et al. (1999).
[b] 510 °C for 30 s.

Table 16
S content of some reference crude oils (IFP analysis) from GEOCHIM database[a]

Crude oil	Source rock type	S content (wt%)
Minas	I	0.085
Duri	I biodegraded	0.12
Boscan	II	5.35
Safanyia	II	2.85
Arabian light	II	1.81
Cold Lake	II biodegraded	4.62
Hamaca	II biodegraded	3.77
El Pao	II biodegraded	3.78
Arjuna	III	0.094
Handil	III	0.11

[a] Note high sulfur amount in marine-sourced (Type II) crudes, increasing with decreasing maturity or biodegradation, in contrast with low sulfur content of Types I and III sourced crudes.

the structural forms of N do not vary. In fact, N speciation in kerogen and coal changes with increasing maturity, as shown by various studies using spectroscopic methods such as XPS (Patience et al., 1992; Kelemen et al., 1994, 1999) or solid state ^{15}N NMR (Knicker et al., 1996; Derenne et al., 1998). For example, N speciation deduced from XPS analysis of artificially matured coal and kerogen (Kelemen et al., 1999; Table 15) showed that some N still occurs in amide/amine groups for immature samples, in amounts reflecting the difference in N content of the source OM. Pyrrole and pyridine N structures become predominant during petroleum formation, as also observed for soluble nitrogenous compounds in crude oil (Schmitter et al., 1980; Dorbon et al., 1984). A minor contribution of quaternary N is always observed, generally decreasing with increasing maturity; this could be due to interaction between pyridine structures and residual OH groups in kerogen (Kelemen et al., 1994).

7.1.2. Sulfur incorporation into organic and mineral sediment fractions

Sulfur is often the most abundant hetero element in marine-sourced crude oils (Table 16) and a more or less high content is commonly observed for marine kerogen (Orr, 1978; Tissot and Welte, 1984). The extent of S incorporation into kerogen is commonly assessed from the S_{org}/C atomic ratio obtained through elemental analysis. Estimates can also be obtained via pyrolysis experiments. Thus, the ratio for some low molecular weight pyrolysis products, like the 2-methylthiophene/toluene ratio, was used by Eglinton et al. (1990, 1994).

Sulfur is found in source rocks in both soluble and insoluble OM fractions and in associated minerals. Pyrite microcrystals and pyritic framboids are often incorporated within sedimented OM, thus remaining with the kerogen after concentration by non-oxidant acid treatment. As indicated above, it is considered that S-rich kerogens (mainly Type II-S) are those where the S/C atomic ratio is > 0.04. S-rich deposits occur back to the Precambrian, and contents around 15 wt% (at. S/C = 0.10) are found in extremely S-rich kerogen (e.g. Orr and Sinninghe Damsté, 1990) such as some samples from the Orbagnoux Oil Shale (Kimmeridgian, Jura; Mongenot et al., 2000). The wide occurrence of marine S-rich kerogens contrasts, as discussed below, with the rare occurrence of lacustrine S-rich kerogen (Sinninghe Damsté et al., 1993a).

7.1.2.1. The S cycle: organic vs. mineral transformations and implication of bacteria. The S cycle is closely related to the C cycle, thereby exerting a major regulating influence on the levels of oxygen in the atmosphere and of dissolved C and S in the oceans (Berner, 1987). Consequently, the S cycle in marine environments was studied in a large number of publications starting in the 1960s (e.g. Kaplan et al., 1963; Berner, 1964; Goldhaber and Kaplan, 1974 and references therein). The role of biological processes in this cycle was soon considered, on the basis of changes in S stable isotope ratio (Kaplan et al., 1963). Dissimilatory sulfate reduction is performed in anaerobic environments by sulfate reducing bacteria (SRB) belonging mostly to the *Desulfovibrio* genus in marine settings. The overall reaction for this complex process, implicating several bacterial consortia, shows that two C atoms are used to reduce one sulfate ion (Berner, 1984). SRB dispersed in anoxic water remineralize a large part of the descending metabolizable OM, but the resulting concentration of reduced sulfur products in the water column is always low because sulfate-rich seawater acts as a buffer. However, even when the whole water column is oxic, the redox conditions change below the water/sediment interface since the OM is concentrated and its composition can be enriched in highly labile particulate organic substrate, which escaped mineralization thanks to a high sedimentation rate and low surface to volume ratio. Decomposable OM in this zone is thus not only the carbon source for bacteria, but is also the agent bringing about anoxic conditions (Berner, 1984). Anoxia and OM concentration just beneath the sediment surface are favourable for the proliferation of SRB. On the basis of data from chemical and isotopic analysis for the Santa Barbara Basin (Kaplan et al., 1963), the number of SRB was estimated to be around 4×10^8 cells/cm^3 in the upper 10 cm of sediment. These bacteria are responsible for the consumption of 16% of the OM deposited at the interface.

Once in the sediment, a part of the deposited OM is oxidized by these bacteria, using SO_4^{2-} dissolved in pore water. Sulfide (mainly as HS^-), polysulfide and H_2S are thus produced and there is a marked decrease in SO_4^{2-}, along with a related increase in H_2S, in sediment pore water below a few cm depth.

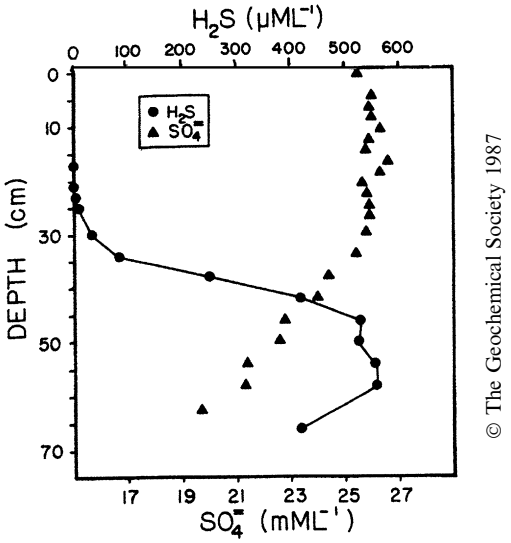

Fig. 35. Pore water sulfide (●) and sulfate (▲) concentration at various depths (cm) in recent sediments from a core collected in the Jervis Inlet fjord, British Columbia, where oxic conditions occur up to the water–sediment contact. H_2S production by bacterial sulfate reduction appears only below 30 cm and increases strongly in the 30–45 cm zone. Reprinted with permission from François (1987, p. 21).

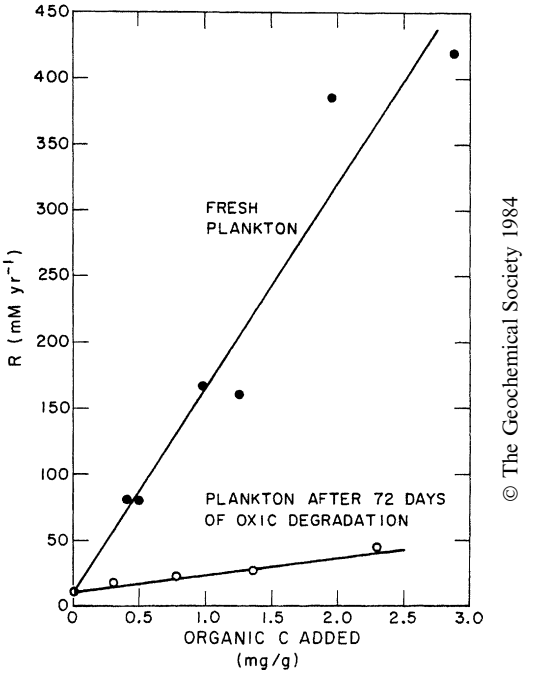

Fig. 36. Comparison of rate of sulfate reduction vs. concentration of organic C in fresh plankton and in plankton-derived material remaining after 72 day of oxic degradation. The rate increase is directly proportional to the amount of plankton added, but the reactivity of fresh plankton to bacterial reduction is much higher that that of degraded plankton for a given C amount added. Similar results were obtained with OM degraded anoxically. Reprinted with permission from Berner (1984, p. 607).

An example of this evolution in sediments from Jervis Inlet, British Columbia, cored under 650 m of oxic seawater (François, 1987), is shown in Fig. 35. Reduced S can be incorporated into the sediment in larger amounts than the S from the initial porewater SO_4^{2-} due to ion diffusion, seawater circulation and possible recycling by burrowing organisms (Berner, 1964; Goldhaber and Kaplan, 1974). The major factor controlling the rate of bacterial reduction is not SO_4^{2-} concentration when this is > 5 millimole, as in most marine sediments (Berner, 1984), but the amount and more importantly the reactivity of the OM, as shown by data from Westrich (in Berner, 1984; Fig. 36). In consequence, OM source, either terrestrial or marine, primary productivity and depth of the water column are expected to influence the degradative activity of SRB (Goldhaber and Kaplan, 1975).

7.1.2.2. Conditions for incorporation of mineral and organic S into sediments as shown by studies of recent sediments. Large amounts of pyrite are frequently present in marine sediments, both as isolated microscopic cubic crystals and as framboidal spherules often embedded in OM. The close association between pyrite framboids and sedimentary OM has led to numerous studies aimed at understanding how and when such pyrite framboids are formed in sediments (Goldhaber and Kaplan, 1974; Berner, 1984 and references therein). Studies of recent sediment cores and laboratory simulations showed that iron oxide and hydroxide coatings on detritic minerals, or goethite ($FeO \cdot OH$) in laboratory experiments, can react rapidly at low pH with dissolved H_2S, producing first a metastable iron sulfide amorphous phase ($FeS_{0.9}$) that precipitates. A spherical texture is developed when this precipitate is transformed into spherical greigite (Fe_3S_4), and finally converted by internal nucleation of pyrite crystals ($FeS_{1.8-2}$) into framboids (Goldhaber and Kaplan, 1974).

In SO_4^{2-}-rich environments, reactive Fe is usually considered to outcompete OM for S incorporation, due to faster formation of pyrite (Berner, 1984, 1985; Sinninghe Damsté et al., 1989; Hartgers et al., 1997). Accordingly, extensive OM sulfurization is generally thought to occur only when the production of reduced S species exceeds the amount of reactive Fe, i.e. when terrestrial detrital input is low. Thus, abundant supply of reactive Fe would account for negligible OM sulfurization in the Bonarelli black shales (Cenomanian, Italy) although

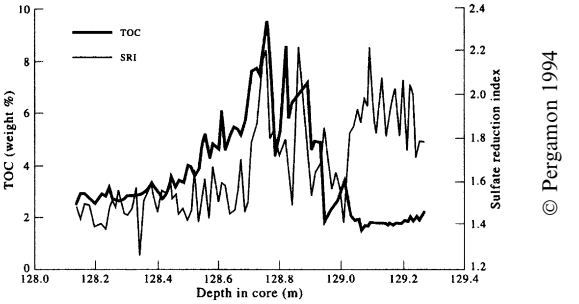

Fig. 37. Correlation between organic productivity and sulfate reduction in a cyclic organic sequence from the Marton 87 well, Kimmeridge clay, Yorkshire, UK: relationship between sulfate reduction index and TOC. Reprinted with permission from Bertrand et al. (1994, p. 514).

intense sulfate reducing activity took place during deposition (Salmon et al., 1997). In contrast, deposition in a lagoonal setting on a shallow carbonate platform with negligible detrital input would have promoted OM sulfurization for the Orbagnoux deposit (Kimmeridgian, Jura; Mongenot et al., 2000). However, this general view about competition between iron and OM was challenged, in the case of lacustrine and estuarine recent sediments, by studies showing the co-occurrence of high concentrations of pyrite and of organic sulfur in some intervals (Bates et al., 1995; Brüchert and Pratt, 1996; Urban et al., 1999). It was suggested (Filley et al., 2002a) that such a feature would reflect the co-sulfurization of OM and of Fe triggered by reaction between reactive Fe (as hydroxides) and sulfide. This reaction would induce both the formation of pyrite and of polysulfides, the latter reacting with OM to generate polysulfide-rich components.

Primary productivity influences SO_4^{2-} reduction and OM sulfurization, as clearly observed, for example, in the extensively studied organic microcycle of the Kimmeridge Clay Formation from the Marton 87 borehole (Kimmeridgian, UK). Thus, the OM degradation intensity, measured by the sulfate reduction index (SRI = % initial C_{org}/% residual C_{org}) and the TOC exhibit similar profiles along the core interval corresponding to a whole microcycle (ca. 30 kyr sedimentation; Bertrand et al., 1994; Fig. 37). Higher productivity is associated with greater SO_4^{2-} reduction, TOC and HI, as well as with a greater abundance of orange, nanoscopically amorphous OM when observed by light and transmission electron microscopy, respectively, reflecting increasing sulfurization (Boussafir et al., 1995).

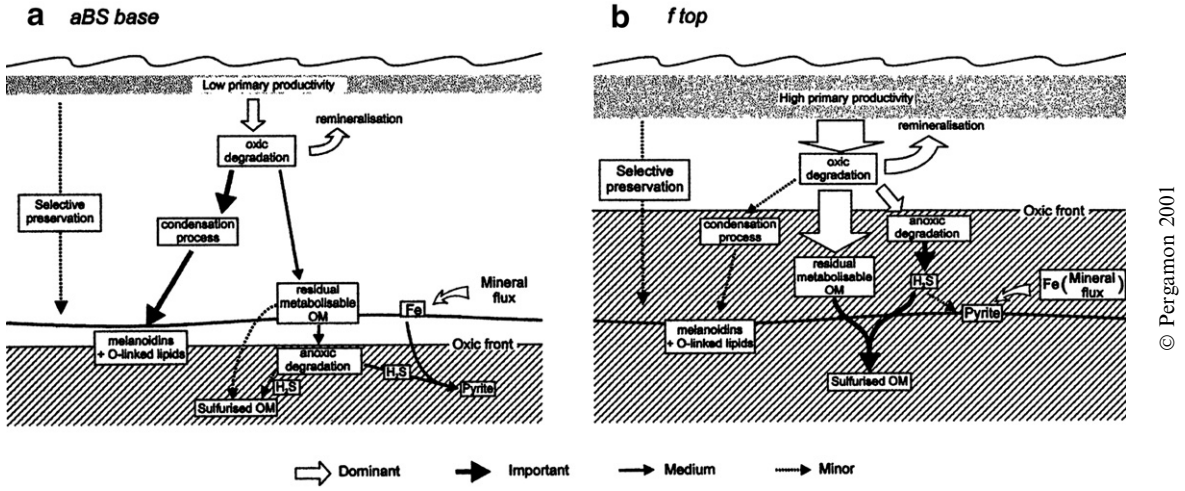

Fig. 38. Scheme proposed to account for conspicuous differences in kerogen abundance and composition observed for Kashpir Oil Shale (late Tithonian, Russia). Here, differences in primary productivity are thought to have played a major role in these contrasting features. Other factors such as depth of water column, nature of the minerals and their adsorptive capacities and the distribution of OM between particulate and soluble forms were probably of importance in other deposits. Reprinted with permission from Riboulleau et al. (2001, p. 661).

A large supply of SO_4^{2-} is always available in marine settings but seldom in lacustrine ones (Gransch and Posthuma, 1974); hence the more common occurrence of marine S-rich kerogens, compared to lacustrine S-rich kerogens. The first example of lacustrine S-rich kerogen was only reported in the 1990s for the Ribesalbes Oil Shale (Miocene, Catalonia; Sinninghe Damsté et al., 1993a). This kerogen was deposited under unusual conditions due to weathering of surrounding gypsum rocks that afforded a large SO_4^{2-} contribution to the lake, promoting extensive growth of SRB. In addition to SO_4^{2-} and reactive Fe abundance, other parameters are implicated in the control of the extent of S incorporation into OM, such as primary productivity in surface water and water column depth. The importance of the latter factors can be illustrated by the differences observed between recent marine sediments from the Peru and the Mauritania upwelling regions: incorporation is important for the Peruvian samples while it is minor for the Mauritanian ones (Eglinton et al., 1994; Zegouagh et al., 1999). These striking differences reflect a relatively lower primary productivity and a much deeper water column in the latter area, so that markedly lower amounts of metabolizable OM reach the anoxic zone and no prolific growth of SRB takes place. Similarly, large differences in primary productivity account for the conspicious differences in kerogen composition (Fig. 38) observed (Riboulleau et al., 2001) between different levels of the stratotype sections of the Volgian stage (Gorodische section, Jurassic, Russian Platform).

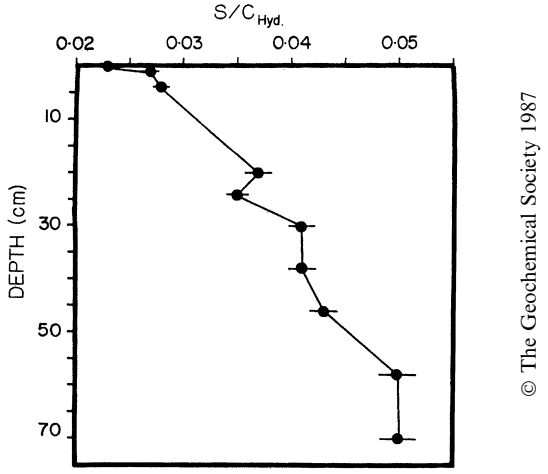

Fig. 39. S/C ratio (wt/wt) in HAs after hydrolysis in 5 N HCl for 5 h at 120 °C; S = total S content and C hyd = TOC of hydrolyzed HAs. Reprinted with permission from François (1987, p. 23).

Sulfur incorporation into OM occurs at the early stages of sediment burial. This is reflected in (i) regular increase in S content with sample depth in both kerogen (Eglinton et al., 1994) and humic fractions (François, 1987) and (ii) molecular studies (e.g. Kohnen et al., 1989; Kenig and Huc, 1990; Wake-

Table 17
Evolution with depth of C, N and S contents in sediments cored on Peruvian margin, and H/C, N/C and S_{org}/C atomic ratios of corresponding kerogen[a]

Sample depth (m)	Sediment					Kerogen		
	Total C wt%	TOC wt%	Total N wt%	Total S wt%	Atomic total S/total C	At H/C	At N/C	At Sorg/C
0	13.34	12.47	1.65	1.09	0.031	1.420	0.112	0.012
0.02	12.16	11.40	1.49	1.21	0.037	1.478	0.111	0.017
0.06	12.73	11.53	1.50	1.10	0.032	1.486	0.110	0.017
0.1	11.48	9.71	1.30	0.99	0.032	1.448	0.110	0.017
0.7	8.40	8.36	1.03	0.89	0.039	1.461	0.100	0.023
2.3	2.58	2.58	0.28	0.87	0.127	1.32	0.082	0.038
2.9	2.68	2.26	0.25	0.87	0.122	1.375	0.078	0.041
3.7	3.37	3.09	0.30	1.84	0.205	1.876	0.068	0.067
6	3.11	2.83	0.24	1.26	0.152	1.446	0.063	0.094
20.2	2.61	2.62	0.21	1.92	0.276	1.397	0.056	0.076
80.1	3.08	2.81	0.20	1.74	0.212	1.351	0.053	0.092
92.9	3.61	3.47	0.26	1.57	0.163	1.486	0.052	0.090

[a] After Eglinton et al. (1994).

ham et al., 1995). As shown in Fig. 39 (François, 1987), S is incorporated into hydrolyzed humic fractions, thereby becoming non-hydrolyzable and bonded to C. However, sulfurization takes place only after OM burial under a sediment depth of a few tens of centimeters, necessary for the concentration of reduced sulfur species in pore water (Fig. 35). Studies of core samples from sediments underlying the Peru upwelling region (Eglinton et al., 1994), collected in the area where the oxygen minimum zone impinges on the shelf, showed that S incorporation into OM extends several meters below the surface and may continue for several tens of meters (Table 17). In fact, pyrolysis/gas chromatography/mass spectrometry (GC–MS) of the protokerogen isolated from a surface sample showed the presence of only negligible amounts of S-containing compounds. A similar situation was found for the protokerogen from a surface sample from the Cariaco Basin (Aycard-Giorgi et al., 2001), although environmental conditions in this basin are especially favourable for sulfurization (bottom water euxinic for ca. 600 m in the zone sampled). These observations point to a relatively slow rate for S incorporation. However, examination of core samples from the Cariaco Basin, ranging in age from 900 to 6000 year, showed a faster sulfurisation for carbohydrate moeties than for alkyl moieties (Aycard et al., 2003).

The bacterial reduction of SO_4^{2-} ($\delta^{34}S$ +15 to +25‰) in the upper centimeters of sediment produces sulfide with $\delta^{34}S$ around −20‰, and S incorporation into OM and/or pyrite does not change

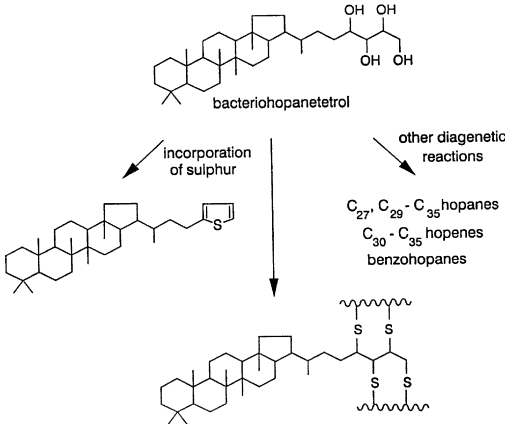

Fig. 40. Scheme illustrating intra-and intermolecular diagenetic incorporation of S in bacteriohopanetetrol. Reprinted with permission from de Leeuw and Sinninghe Damsté (1990, p. 436).

this value much (Kaplan et al., 1963; Goldhaber and Kaplan, 1980). This demonstrates that sedimented OM reacts with bacterially reduced forms of S via abiotic reactions. Nevertheless, the nature and detailed mechanism of S incorporation in OM is still a pending question (Adam et al., 1998, 2000; Kok et al., 2000b; Werne et al., 2000) and the mechanism would depend on the nature of the sulfurized functional groups (Amrani and Aizenshtat, 2004a). Bacterial biomass can contribute to this sedimented OM, but does not constitute by itself a S source since its S/C ratio (wt/wt) is in the 0.01–0.02 range, i.e. much lower than that measured for the sedimented OM after burial for a few meters (François, 1987).

7.1.2.3. Sulfurization modes and related chemical structures. Reduced sulfur can be incorporated into various OM functional groups, including alkenes, ketones and aldehydes (e.g. Vairavamurthy and Mopper, 1987; Sinninghe Damsté and de Leeuw, 1990; Sinninghe Damsté et al., 1990; Rowland et al., 1993; Schouten et al., 1993, 1994; Krein and Aizenshtat, 1994; Amrani and Aizenshtat, 2004b). Laboratory simulations suggest that alcohol functional groups may also be implicated (Gelin et al., 1998). S can be incorporated via intra- and intermolecular reactions (Fig. 40; e.g. Sinninghe Damsté et al., 1988). The former process results in the formation of cyclic alkyl sulfides (like thiolanes, thianes and thiophenes; e.g. Brassell et al., 1986). Subsequently, thiolanes and thianes can become stabilized as thiophenes with increasing diagenesis (Sinninghe Damsté et al., 1990). Intermolecular sulfurization corresponds to the formation of (poly)sulfide linkages between alkyl chains (e.g. Richnow et al., 1993; Schaeffer et al., 1995b). Their occurrence can be revealed by chemical degradation with Li/$EtNH_2$, a reagent that cleaves sulfide bonds (e.g. Schaeffer et al., 1995a). Further studies indicate that S incorporation into carbohydrate moieties also occurs (Hartgers et al., 1997; van Kaam-Peters et al., 1998; Sinninghe Damsté et al., 1998a,b; Kok et al., 2000a; van Dongen et al., 2003), generating (poly)sulfide cross-linked carbohydrate skeletons. Such incorporation is reflected in (i) the abundant presence of short-chain (C_1–C_4) alkyl thiophenes with a linear carbon skeleton in kerogen pyrolysates (Fig. 41) and (ii) ^{13}C enrichment in organosulfur compounds (OSCs) due to the isotopically heavy nature of carbohydrates relative to alkyl moieties (van Kaam-Peters et al., 1998; Riboulleau et al., 2000).

The structure of S-rich kerogens has been extensively examined using chemical degradation and/or pyrolysis (e.g. Sinninghe Damsté et al., 1993b; Eglinton et al., 1994; Gelin et al., 1995; Schaeffer et al., 1995a; van Kaam-Peters and Sinninghe Damsté, 1997; Schaeffer-Reiss et al., 1998; Höld et al., 1998; Mongenot et al., 1999; Riboulleau et al., 2000). Pyrolysis generates a wide range of low

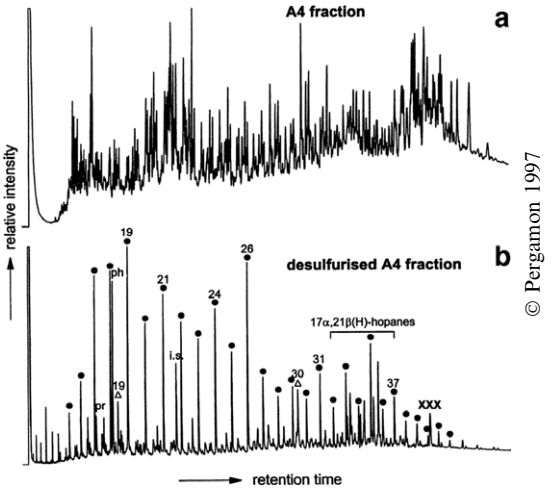

Fig. 42. GC traces of "thiophenic" sub-fraction isolated via column chromatography and thin layer chromatography from bitumen of a sulfur-rich sample from Orbagnoux deposit (upper Kimmeridgian, France) and of desulfurised sub-fraction. These traces illustrate the complexity of the bitumen in such samples and the usefulness of Raney nickel desulfurization for revealing the nature of the hydrocarbon skeletons in complex mixtures of organosulfur compounds. Circles: *n*-alkanes, triangles: 9-methylalkanes, pr, pristane; ph, phytane. Reprinted with permission from van Kaam-Peters and Sinninghe Damsté (1997, p. 374).

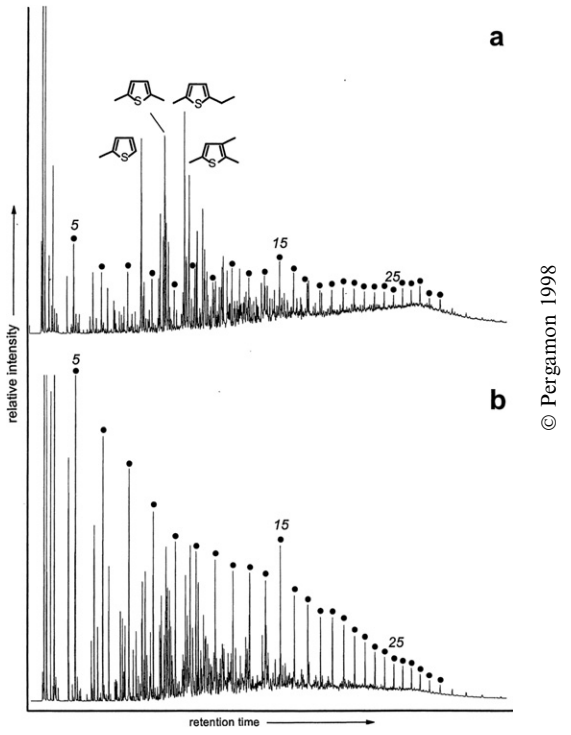

Fig. 41. GC trace of pyrolysate of a sulfur-rich kerogen (Jurf ed Darawish Oil Shale, Maastrichtian, Jordan), obtained using micro-scale sealed vessel pyrolysis at 300 °C for 24 h. The abundant production of "short chain" alkyl thiophenes reflects the substantial contribution of carbohydrate sulfurization to this kerogen. Reprinted with permission from Sinninghe Damsté et al. (1998a, p. 1897).

molecular weight alkylated OSCs, including the same sulfur species as in bitumen (Fig. 42). In addition, the pyrolysates of such kerogens commonly contain large amounts of non-GC-amenable products, like the high molecular weight macromolecular fraction of sediment extracts. Subsequent chemical degradation of such products is useful for obtaining detailed information on kerogen structure, as shown for the Orbagnoux deposit (Mongenot et al., 1999).

In agreement with observations of simultaneous attachment via O and S in some macromolecular components of sediment extracts and crude oils, the occurrence of moieties linked both by sulfide and ether bridges was observed for various kerogens (Richnow et al., 1992; Höld et al., 1998; Schaeffer-Reiss et al., 1998; Riboulleau et al., 2000). The ether bridges might be partly derived from diagenetic incorporation of O, and competition between S and O incorporation into OM should occur at the oxic-anoxic interface (Jenisch-Anton et al., 1999). This O incorporation should promote subsequent OM sulfurization due to an increase in reactivity towards reduced S (Schouten et al., 1994; Carmo et al., 1997).

The common occurrence of thiophenes in the pyrolysates of S-rich kerogen does not necessarily reflect a ubiquitous contribution of thiophenic moieties to kerogen structure. Such aromatic OSCs may originate, at least partly, from secondary transformation of (poly)sulfide-containing moieties (Sinninghe Damsté et al., 1990). In fact, heating (poly)sulfide-linked macromolecules resulted in the rapid formation of thiophenic compounds (Krein and Aizenshtat, 1994; Schouten et al., 1994; Tomic et al., 1995). Secondary thermal reactions of (poly)sulfide-bound linear carbon skeletons, derived fom carbohydrate sulfurization, were shown to yield C_1–C_4 linear alkyl thiophenes upon kerogen pyrolysis (Sinninghe Damsté et al., 1998a). XANES can afford direct information on S speciation in kerogen and the presence of native thiophenic moieties can thus be tested. Only a limited number of kerogens have been examined with this method so far. The bulk of S corresponds to alkyl sulfides and, to a lesser extent, di(poly)sulfides in Monterey and Kashpir Oil Shale kerogens (Eglinton et al., 1994; Nelson et al., 1995; Riboulleau et al., 2000), whereas thiophene S affords a relatively low contribution. A reverse distribution was observed for the Orbagnoux kerogen (Sarret et al., 2002), and thiophenes are now believed to be the main native S form in that kerogen. Such features reflect major differences

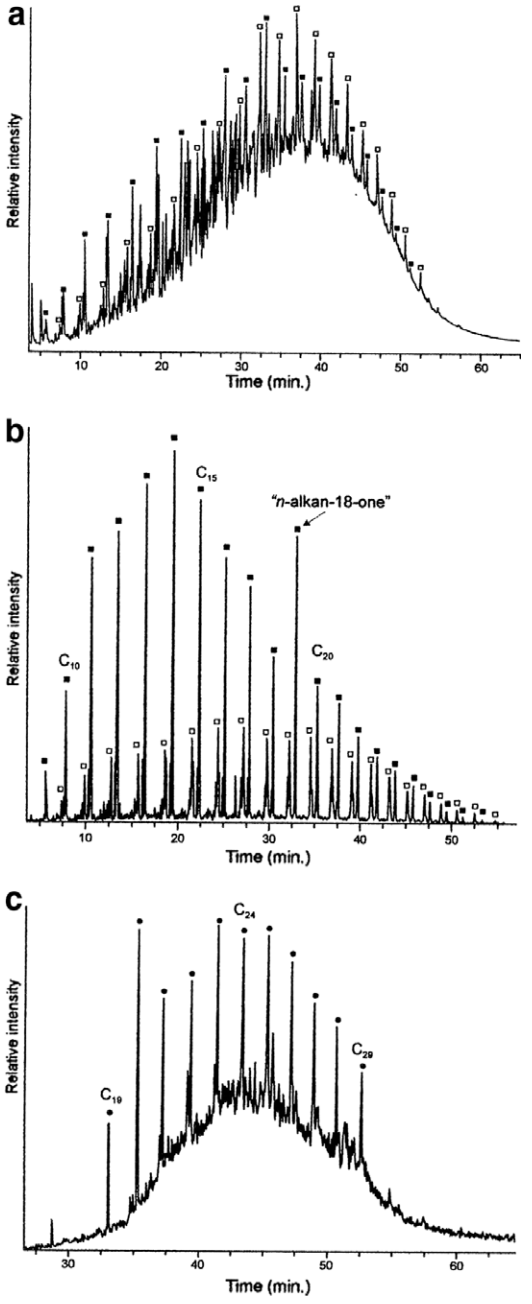

Fig. 43. GC trace of medium polarity (toluene elution) fraction of off-line pyrolysate at 400 °C of an O-rich kerogen from Kashpir Oil Shale (late Tithonian, Russia) (a), ion chromatogram of $m/z = 58$ showing distribution of *n*-alkan-2-ones and "mid-chain" ketones (b). Additional ion chromatograms [e.g. $m/z = 267$(c)] showed that the latter correspond to a complex mixture of *n*-alkanones with the C=O group on any carbon atom from C-2 to C-13. Their abundance and diversity reflect the effect of the oxidative reticulation on this kerogen. Reprinted with permission from Riboulleau et al. (2001, p. 654).

in the extent of intermolecular vs. intramolecular S incorporation in these two cases.

7.1.3. Oxygen incorporation

As discussed above, post-sedimentary abiotic oxidation of OM can alter the characteristics of kerogen type. Such oxidation may occur at the early diagenesis stage for some kerogens. It causes both a decrease in the OM amount in the sediment (generally measured by TOC), and an increase in the O/C atomic ratio of kerogen. Oxidation thus corresponds to partial degradation of immature OM, whereas the residual organic fraction is enriched in O. Such a situation was described by Riboulleau et al. (2001) for the kerogen of a relatively organic-poor (TOC 2.3%) and highly bioturbated level from the Kashpir Oil Shale (Volgian, Russia). This kerogen is characterized by a high O content (O/C atomic ratio 0.27) and the abundant production of O-containing compounds on pyrolysis, especially long chain *n*-alkanones up to C_{30} (Fig. 43). The latter correspond to a complex mixture of isomeric compounds, with the C=O group located on any carbon atom of the alkyl chain, and originate from the thermal cleavage of ether bridges. These features reflect intense O incorporation and cross linking via ether bridges. This incorporation probably took place largely at C=C bonds originating from diagenetic isomerisation and random migration. Previous observations also showed the formation of long chain *n*-alkanones upon pyrolysis of various kerogens and recent samples (Gatellier et al., 1993; Gillaizeau et al., 1996; Kruge et al., 1997; Salmon et al., 1997; Riboulleau et al., 2000), although amounts seemed less important than in the above case. The extensive O incorporation observed for some levels of the Kashpir Oil Shale kerogen is probably related to early diagenesis under oxic conditions, as reflected in intense bioturbation and well developed nectonic and benthic flora (Riboulleau et al., 2001). Polymerization under oxygenated conditions of alkenyl resorcinols, contained in cell walls or sheaths, was thought to be implicated in the formation of *G. Prisca* microfossils in Ordovician kerogens (Blokker et al., 2001). The oxidative polymerization of unsaturated fatty acids was considered for the fossilization of motile forms of dinoflagellates (Jatta Gypsum Formation, Eocene, Pakistan; Versteegh et al., 2004). In contrast to S incorporation, O incorporation may occur at any stage in kerogen evolution. Oxidative alteration during the first stages of deposition was observed, for example, for the different facies of the Orbagnoux deposit (Kimmeridgian, Jura), due to frequent temporary emergence episodes that affected the upper sediment, as indicated by analysis of redox-sensitive trace elements (Mongenot et al., 2000). As stressed above, extensive post-depositional abiotic oxidation, due to air and/or oxygen dissolved in meteoritic water, occurs also for kerogen in uplifted sedimentary rocks, especially at outcrops (Nicaise, 1977; Espitalié and Bordenave, 1993; Petsch et al., 2000, 2001a).

7.2. Diagenesis

Diagenesis occurs over a much larger depth range in sediments than the previous stage of early diagenesis. It may take place over an interval >1000 m, depending on the geothermal gradient and burial rate. Diagenesis sensu stricto is a stage where kerogen loses large amounts of oxygen, mainly as CO_2 and H_2O. Simultaneously, the amount of extractable humic and fulvic acids continuously decreases. According to Tissot and Welte (1978, 1984), the end of diagenesis corresponds to the time when humic and fulvic acid amounts are negligible.

During this stage, humin and kerogen become progressively similar with increasing sediment burial. In contrast to N, some loss of O from kerogen, with a related decrease in the absolute O content (wt%) and the O/C atomic ratio, is still observed during further catagenesis, particularly for Type III kerogen. After early diagenesis, kerogen transformation at depth is driven by cracking reactions

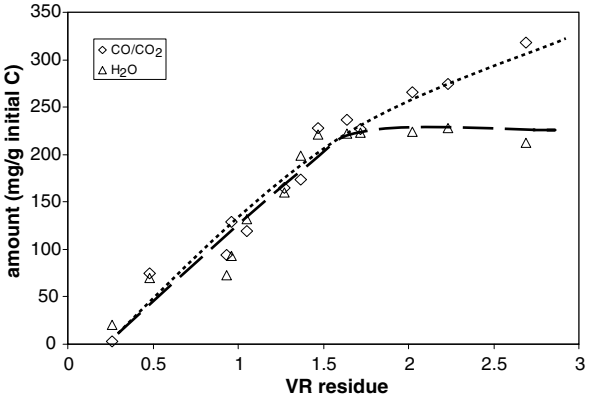

Fig. 44. Comparison of CO/CO_2 and H_2O production upon confined pyrolysis of immature Morwell coal as a function of vitrinite reflectance of residual coal. After Behar et al. (1995).

dependent on increasing temperature and time. Therefore, these transformations and the resulting products can be reproduced by experimental simulation in the laboratory, using higher temperature to compensate for long geological time periods. For example, artificial maturation of different types of immature kerogen was performed with an open system coupled to a mass spectrometer, and the gaseous effluent was analysed and quantified (Durand-Souron et al., 1982). Although open system pyrolysis tends to overestimate H_2O production at the expense of CH_4 formation (Landais et al., 1984; Lorant and Behar, 2002), the results confirm that H_2O and CO_2 are major products in the effluent both before and during the main stage of hydrocarbon generation. Artificial maturation of the Morwell coal, a very immature brown coal (vitrinite reflectance 0.26), was performed using isothermal confined system pyrolysis at various temperatures, weight and elemental balances being obtained (Behar et al., 1995). Water and CO/CO_2 production from this coal (Fig. 44) showed parallel and regular increases with maturation to a point located far into the catagenesis stage (vitrinite reflectance 1.47%), where total H_2O production reached a plateau but CO and CO_2 continued to be produced. This reflects the large range of oxygen-containing functional groups giving rise to these oxygenated species, some being quite resistant to thermal degradation.

There is thus an overlap between generation of these products and hydrocarbon release. Accordingly, this observation supports the restriction by Tissot and Welte (1978, 1984) of the end of diagenesis stage to the disappearance of humic acids and not to the end of O/C decrease.

7.3. Catagenesis

Catagenesis is the main stage of H (and C) loss from kerogen and, as a consequence, is the stage of petroleum formation. This stage takes place over a depth range that frequently reaches > 2000 m. Considering a general formula of generated hydrocarbons as $(CH_2)_n$, two H atoms are lost for one C atom, so the H/C atomic ratio of the residual kerogen decreases in a van Krevelen diagram, reflecting increasing aromatization (cf. Figs. 29 and 32). As shown by natural samples from petroleum case studies and laboratory thermal simulation, compounds with lower and lower molecular weight are formed during this stage, ending with gases. At the beginning of catagenesis, a large part of the oil components generated correspond to asphaltenes and resins containing hetero elements, the major being O. Beside further loss of CO/CO_2, this is the reason why the O/C atomic ratio continues to decrease at the beginning of catagenesis.

Defining the onset of catagenesis is not straightforward as it depends on the parameter used for this definition. A widely used parameter is vitrinite reflectance, by analogy with the maturity scale defined for coal series (cf. Fig. 33). Vitrinite reflectance is related to the presence of π electrons in kerogen aromatic structures and increases with aromatization, thus reflecting maturation. This parameter was therefore used by Tissot and Welte (1978, 1984) to separate the three maturity stages on the kerogen evolution paths. The beginning of catagenesis is often set at a vitrinite reflectance of 0.5. However, vitrinite is only present as a major maceral in Type III kerogen. The difficulty for other types is to find true vitrinite, which is allochthonous with respect to the major OM constituents but has undergone the same maturation history from the beginning. The risks are to (i) measure reflectance on macerals other than vitrinite, with a different aromaticity, thereby providing a different reflectance value for the same thermal history (Durand, 1975), (ii) have too few or very dispersed data points, or (iii) find vitrinite with a thermal maturation different from that of the bulk OM. Among Rock-Eval parameters, T_{max} is not always a good maturity indicator, particularly for Type I kerogen, since the petroleum formation kinetics lead to a

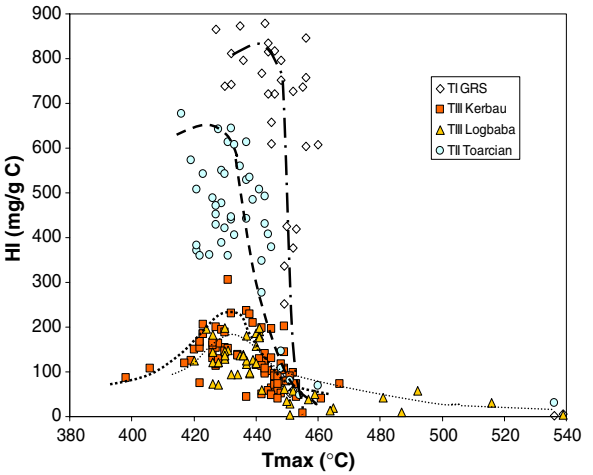

Fig. 45. Evolution with increasing maturity of Rock-Eval HI vs. T_{max} value for reference kerogen types (IFP analyses from GEOCHIM database).

high and almost constant T_{max} during the whole range of hydrocarbon generation. For Type II and Type III kerogens, the onset of catagenesis is often taken at a T_{max} of 435 °C (Espitalié and Bordenave, 1993). The best parameter for defining the beginning of catagenesis as the main zone of petroleum formation is the hydrogen index, using the HI vs. T_{max} diagram as reported in Fig. 45 for maturity series of reference kerogens.

During diagenesis, the loss of O-containing molecules results in a concentration of potential hydrocarbon generating structures, and hence an increase in HI. This relative increase depends on O abundance in the kerogen: it is high for Type III kerogen and hardly visible for Types I and II. The beginning of catagenesis thus corresponds to the beginning of HI decrease. As catagenesis progresses, the transition from oil to condensate takes place around a T_{max} of 455 °C and the main wet gas production ends around a T_{max} of 470 °C (Espitalié and Bordenave, 1993). However, there is still some gas, more and more enriched in CH_4, produced beyond this limit. The HI vs. T_{max} diagram shows (Fig. 45) that the decrease in HI in the gas zone is more progressive for Type III kerogen than for the other types. This difference should not be due to kerogen (primary) cracking because all types exhibit similar chemical structures at this stage and produce gas by cracking of short chain alkylated polyaromatics (Lorant and Behar, 2002). This latter feature was confirmed by closed system pyrolysis of kerogens of different type at the dry gas generation stage: similar absolute amounts of late CH_4 are generated at 550 °C for 24 h (Behar et al., 1997). In fact, the slower HI decrease for Type III kerogen could be due to the high initial aromaticity of the kerogen network. This network may very tightly trap some petroleum products that are only released through production by secondary reactions of gaseous compounds, whose size is small enough to escape the aromatic network of the kerogen structure.

At the end of catagenesis, conventionally taken at a H/C atomic ratio of 0.5 or a vitrinite reflectance of 2% (Tissot and Welte, 1978, p. 72), all types plot in the same region of the van Krevelen diagram. Chemical analysis cannot anymore allow distinction between types at this maturity stage. However, this distinction can still be achieved by electron diffraction imaging techniques, first used for studies of natural coalification and artificial carbonization (Oberlin et al., 1999). Aromatic

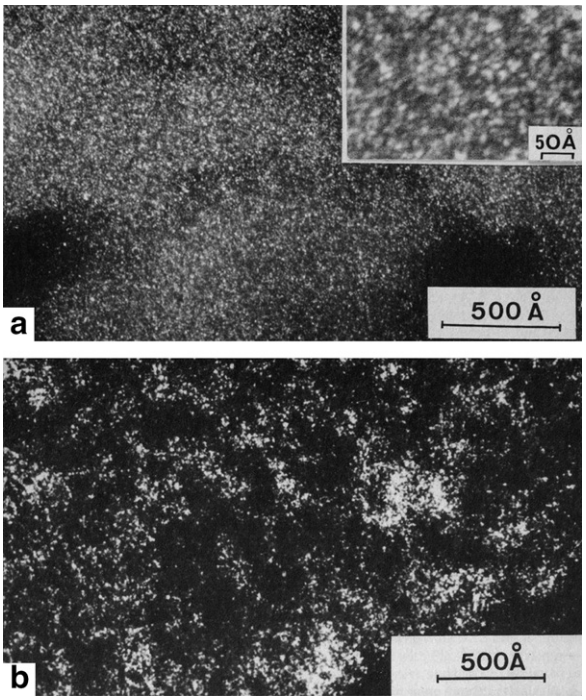

Fig. 46. Dark field imaging (0.0.2 mode) of aromatic stacks in Type II kerogen from electron diffraction; each bright dot is a stack of aromatic molecules seen edge-on. (a) At a low catagenesis stage (H/C = 1.32); (b) at the metagenesis stage (H/C = 0.44). Modified from Oberlin et al. (1980).

stacks with a diameter corresponding at least to coronene (7.1 Å, seven fused rings) appear as bright spots when kerogen is observed using dark field electron microscopy (Oberlin et al., 1980), and their size can be measured. Smaller aromatic molecules that may exist in kerogen, but cannot stack face to face, are not detected. Bright spots corresponding to aromatic stacks can be observed even at a low maturity. Their abundance increases with increasing maturity, but the increase cannot be quantified precisely. During catagenesis, the diameter of the aromatic domains is always < 8 Å, corresponding to fewer than 10 fused rings, piled up into stacks of two and sometimes three aromatic layers, regardless of the Type. Aromatic stacks are homogeneously distributed within the kerogen and randomly orientated, as shown by similar bright spot abundance when the sample is rotated (Fig. 46a).

The only changes observed upon increasing catagenesis, up to the peak of oil formation, are the increase in bright spot abundance and the decrease in interlayer spacing spreading due to elimination of defects, i.e. non-aromatic moieties. After this

peak, around a H/C atomic ratio of 0.7, individual aromatic stacks tend to orientate themselves parallel to each other in local clusters of bright spots and are therefore no longer homogeneously distributed. Up to the end of catagenesis (H/C atomic ratio 0.5), the amount of aromatic clusters increases, resulting in more contrasted images, but the diameter of individual bright spots does not change significantly (Oberlin et al., 1980). From this stage, the orientation of aromatic domains does not change further. These transformations would be similar to what is observed during carbonisation of non-graphitizing carbons (Van Krevelen, 1993, p. 237). Like coal, low maturity kerogen can be considered as a plastic substance, with aromatic stacks suspended in a metaplast made of mobile aliphatic parts. The latter are progressively removed by thermal cracking upon catagenesis, up to the transition to metagenesis where a brittle solid is obtained (Oberlin et al., 1999).

7.4. Metagenesis

Metagenesis is the stage of reorganization of the aromatic network of the residual kerogen. It is associated with an aromaticity increase, mainly by elimination of aromatic CH_3 groups as CH_4, but also by release of hetero elements as CO_2, N_2 and H_2S. As indicated above, all types at the onset of metagenesis have a similar elemental composition and hence a similar location in the van Krevelen diagram. Confined system pyrolysis also showed that the only hydrocarbon generated at this stage is CH_4, with a similar potential around 50 mg/g C (Behar et al., 1997), indicating a similar ratio of aliphatic to aromatic C for all types. However, at the transition from catagenesis to metagenesis (H/C = 0.5 and C = 93%), the size of the aromatic clusters in the solid structure depends on type: around 50 Å for Type III, 100–200 Å for Type II and up to 1000 Å for Type I (Oberlin et al., 1980). This difference may seem surprising because at this stage all types have similar chemical parameters. In fact, the extent of parallel formation of aromatic stacks depends on the elimination efficiency of low molecular weight moieties during catagenesis. This allows more or less free rotation of individual aromatic stacks, depending on the ratio between residual aliphatic and aromatic moieties and on the amount of residual hetero elements, that markedly decrease from Type III to Type II and to Type I, i.e. according to kerogen type.

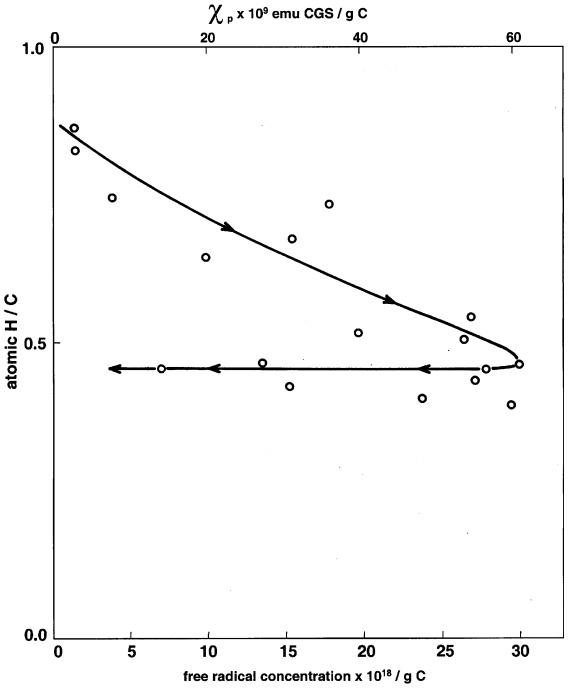

Fig. 47. Evolution with increasing maturity of concentration of free radicals (χ_p) in kerogen from Logbaba series (Type III), measured using EPR. Adapted from Marchand and Conard (1980).

During metagenesis, gases are expelled from kerogen as shown by experimental simulation of maturation on Types II and III kerogen using open and closed system pyrolysis (Lorant and Behar, 2002). According to the different steps for CH_4 formation proposed in the above study, the first step in forming it plus higher homologues has already taken place in the catagenesis zone. A second step, occurring at the metagenesis stage, is demethylation of methyl aromatics together with cleavage of aromatic ether bridges, yielding gases such as CH_4, CO and CO_2, and also some N_2 as observed by Behar et al. (2000). At this stage, ring condensation increases in the residual kerogen, as observed with dark field imaging, by an increasing diameter of aromatic stacks (Fig. 46b). This is confirmed using electron paramagnetic resonance (EPR): in a diagram of paramagnetic susceptibility vs. H/C atomic ratio (Fig. 47) the number of free radicals in kerogen, which increases during catagenesis, begins to decrease due to radical recondensation (Durand et al., 1977a).

The last step for gas generation, occurring in the late metagenesis zone, would be the opening of some aromatic rings. Cleavage of C–H bonds and

auto hydrogenation, yielding CH_4 besides CO and CO_2, can be observed for both kerogen and model aromatic compounds, during high temperature pyrolysis. However, it was stressed that this reaction is unlikely in sedimentary basins due to the required temperature range (Lorant and Behar, 2002).

7.5. Pyrolysis as a tool for modelling geological maturation of kerogen

It is now widely accepted that, after early diagenesis, where biological processes are largely involved, further kerogen transformation is influenced only by thermal cracking reactions due to the temperature increase associated with sediment burial. Accordingly, after the development of isolation procedures, pyrolysis immediately became a major technique for geochemical studies of kerogen, both for characterization of its molecular building blocks and for kinetic studies. Given the chemical complexity of kerogen and petroleum products, a huge number of reactions are involved in kerogen transformation, taking place in parallel and/or in succession with ongoing kerogen cracking in source rocks. The main steps in kerogen cracking to oil were first described (Tissot, 1969; Tissot and Pelet, 1971) on the basis of those explaining the formation of coal pyrolysis products upon thermal conversion (de Poncins, 1950 and Chermin and van Krevelen, 1957; cited by Van Krevelen, 1993, p. 705). The first kinetic models were calibrated using only the evolution with burial of amounts of extract in source rocks from reference petroleum systems. For all kerogens, bulk thermal decomposition could be represented by a nearly first order kinetic law, with a rate constant related to temperature by the Arrhenius equation. Reproducing such transformation is thus possible under laboratory conditions by increasing the temperature to compensate for long geological times, provided that the same reaction mechanisms take place under both geological and laboratory conditions (e.g., with no catalytic cracking or no thermal cracking of C–H bonds). Besides time compensation to allow laboratory simulation, the main advantage of using pyrolysis to mimic thermal cracking under geological conditions is to have access to the amounts of generated compounds, such as gases and light hydrocarbons, that most of the time cannot be recovered quantitatively from geological samples (e.g. Monthioux et al., 1985). It is thus possible to obtain a full mass

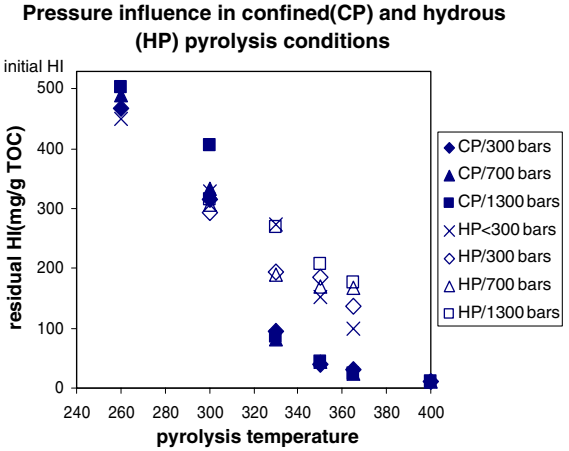

Fig. 48. Comparison of Rock-Eval HI of extracted pyrolysis residues of Woodford shale after confined (CP) and hydrous (HP) pyrolysis over 72 h at various temperatures and pressures. Modified from Michels et al. (1995).

and atomic balance for the remaining kerogen and its cracking products at various transformation stages with, for some of these products, a possible control by geological samples. Then, the main geological factors that may influence kerogen transformation can be discussed. Analytical pyrolysis methods that give insights into specific molecular families of compounds, but do not allow a mass balance of kerogen cracking products to be obtained, are not considered here. For a review of pyrolysis techniques and their applications, we refer the reader to Larter and Horsfield (1993) and references therein.

Among the factors that influence kerogen transformation under geological conditions, it is widely accepted that the type largely influences both the amount and the chemical composition of the cracking products for a given maturity stage. It is also well documented that S incorporation into a kerogen decreases average bond strengths, making it more thermally labile and justifying addition of "-S" to the Type name to account for this lability. Since kerogens show a continuous range of S content, there should also be a continuous shift in kinetic parameters. Thus, given the fairly large number of kinetic distributions now available for various Type II-S kerogens (Hunt and Hennet, 1992, and references therein), it should be possible, although not yet reported to the best of our knowledge, to calculate directly activation energies and frequency factors as a function of the S content obtained from elemental analysis of kerogen.

Pressure increase has been shown (Fig. 48) to delay kerogen cracking in hydrous pyrolysis experiments (pressure transmitted by the liquid phase), whereas such a delay is hardly observable with confined medium experiments (pressure transmitted by the solid phase) with or without added water (Lewan et al., 1979; Michels et al., 1995 and references therein). Pressure also modifies some reaction pathways and favours aromatization. The recombination of hydrogen and alkyl radicals is also promoted (hence the absence of unsaturates) in both hydrous and non-hydrous closed system experiments. The nature of the pressurizing medium, liquid water for hydrous pyrolysis or solid confinement for non-hydrous closed system pyrolysis, probably plays an important role by changing the main source of hydrogen radicals, water or OM, respectively (Michels et al., 1995). The importance of the role of pressure under geological conditions is, however, far from being ascertained, and it is generally considered as a secondary parameter for kerogen cracking, relative to temperature. It is indeed difficult to estimate the real pressure applied to kerogen in source rocks. In fine-grained sediments, i.e. those favourable for OM accumulation and preservation, the fluids contained in the pore volume support part of the overburden charge during burial. The pressure inside a pore will depend on the relative burial rate and may vary, even at constant depth, with geological time. The pressure applied to kerogen thus ranges from hydrostatic to lithostatic pressure (e.g., from 300 to 800 bar at 3000 m depth), but the value is not precisely known. The nature of the pressurizing medium under geological conditions should be close to that of a confined system since kerogen is embedded in the mineral matrix of the source rock, whereas water is contained in the pores. Water could, however, have more influence on secondary cracking reactions, because the products generated as a result of kerogen maturation are stored in source rock pores before expulsion. Further studies are clearly needed to quantify the role of pressure on cracking reactions under geological conditions.

The influence of water on kerogen cracking has been examined by using heavy water (D_2O) in hydrous pyrolysis experiments at low transformation rate (Hoering, 1984). The resulting saturated hydrocarbons show multiple extents of deuteriation. This reflects the occurrence of free radical chain reactions involving D_2O, through deuterium exchange with hydrogen both in the kerogen structure and during chain propagation reactions. Such exchange could also occur under geological conditions. However, a number of further studies indicated that only some hydrogen atoms in kerogen (like those linked to hetero atoms or located in a position α to carbonyl groups) are exchangeable with hydrogen from water (e.g. Sessions et al., 2004), whereas most hydrogen atoms linked to aliphatic carbon are isotopically not exchangeable and would be retained over geological time (e.g. Schimmelmann et al., 1999; Sessions et al., 2004). In fact, the net effect of water on the yield and composition of the products generated upon kerogen thermal degradation is still unclear, because the chemical reactivity of water changes very quickly with increasing temperature (Michels et al., 1995). Indeed, it has been observed, when comparing hydrous and non-hydrous pyrolysis experiments on the same sample (Behar et al., 2003), that CO_2 and NSO yields are higher in the former case, both in relative and absolute proportion, possibly due in part to a delay in primary cracking under hydrous conditions. Moreover, differences in CO_2 and NSO yields between hydrous and non-hydrous pyrolysis increase sharply with temperature in the 300–350 °C range, independently of heating time, probably as a result of increasing hydrolysis efficiency in the case of the hydrous experiments.

Although discussions appear from time to time about the catalytic influence of minerals on secondary cracking of petroleum products (Kissin, 1987; Mango and Hightower, 1997), such an influence on primary cracking of kerogen under geological conditions can be ruled out. First, this primary cracking occurs mainly within the organic network of kerogen, where minerals are absent. Second, as discussed above (see Fig. 30), studies on Type III kerogens at any stage during natural maturation have never shown any difference between massive coals and dispersed OM (Huc et al., 1986), although detrital minerals predominating in the latter exhibit especially high catalytic activity if dehydrated. Non-catalytic cracking mechanisms are also confirmed, for other OM types, by the lack of difference among kinetic parameters for kerogen from source rocks from the same formation but with widely different TOC values. The exception, for low TOC samples ($< 1\%$), is clearly due to alteration during deposition or outcropping, as discussed above. Note that, were this not the case, the notion of OM Type would lose its predictive capacity.

7.6. Summary

- The main stages for kerogen evolution in sedimentary rocks are, except for the very first stage, triggered by thermal cracking associated with sediment burial and associated geothermal heating. They are, in order of increasing maturity, as follows:
  (i) Early diagenesis, with a major loss of N as amino acids and NH_4^+, due mostly to biological processes, and ending when N in humin/protokerogen is no longer hydrolyzable. This stage may also be, but not always, the time for inorganic S and O incorporation into the kerogen.
  (ii) Diagenesis sensu stricto, with a major loss of oxygen as H_2O, CO_2, humic and fulvic acids, ending when these acids cannot be extracted from sedimentary rocks.
  (iii) Catagenesis, with a major loss of H and C (oil and wet gas) and ending when all kerogen evolution paths merge into a single path on the van Krevelen diagram, around a H/C atomic ratio of 0.5.
  (iv) Metagenesis, with reorganization of the aromatic network in residual kerogen and production of CH_4 (dry gas) and non-hydrocarbon gases such as CO_2, H_2S and N_2.
- Kerogen transformation after early diagenesis can be simulated by carrying out pyrolysis experiments, insofar as the reaction mechanisms, influenced by pressure, minerals, water and temperature range, are similar under both geological and laboratory conditions.

8. Structure modelling: why and how

8.1. Significance of chemical models

The general term 'kerogen' cannot represent a defined chemical structure, unlike other terms such as 'protein'. Indeed, the latter corresponds to macromolecules sensu stricto, whereas kerogen is a complex combination, via numerous bond types, of a large number of molecular moieties encompassing a wide range of composition and molecular weight. As discussed above, immature kerogen should be viewed as a mixture of various macromolecular structures comprising both resistant biomacromolecules and recombined biodegradation products in unknown proportions. The chemical features of this immature material, which depend on biological precursors and depositional conditions, will change continuously during natural evolution as a result of sediment burial. The resulting changes originate from both thermal cracking of previously insoluble OM and formation of new insoluble OM by condensation reactions. It is possible, however, to estimate a lower limit for the molecular weight of kerogen constituents from the properties of the solvents used for kerogen isolation. Kerogen is defined operationally by its insolubility and the most common solvents used for bitumen extraction: CH_2Cl_2, $CHCl_3$ and mixtures thereof with CH_3OH or acetone. Mass spectrometric techniques (field ionization or field desorption) and gel permeation chromatography, when applied to the heaviest bitumen fractions thus obtained, i.e. asphaltenes, showed an average molecular weight of < 5000 Da. The insolubility limit for kerogen macromolecular units in typical organic solvents, depending on their polarity, may thus be expected to be around values of 5000–10,000 Da.

In fact, "true" macromolecular components of kerogen cannot be represented because their molecular composition is not known. Only chemical structures like those of synthetic polymers, where a small sub-unit repeats the whole structure, can be represented by a detailed chemical structure. The same representation is possible for biopolymers such as proteins or nucleotides, where the number of building blocks is limited to a few chemical species and bonding types. Even in the latter case, the task is difficult and needed advanced analytical methods that became available only in the 1990s. Kerogen chemical structures drawn at the atomic scale, with a molecular weight around 25,000 Da, relate to an incredibly small amount of kerogen concentrate since the corresponding molecular weight is divided by Avogadro's number (6.02×10^{23}), so that it represents about $2–4 \times 10^{-20}$ g of analyzed product. Because any analytical technique presently used for kerogen characterisation works on amounts in the microgram to milligram range, any analytical result is already an average of a large number of kerogen macromolecular components. Thus a "true" representation of the chemical structure of kerogen based on such analyses has no meaning, and only conceptual models representing at best the largest possible set of physicochemical analytical data, but also including many assumptions, can be obtained.

Nevertheless, this is not a reason for giving up the idea of building chemical models for insoluble sedimentary OM. Accordingly, coal scientists began to

construct molecular models for coal as far back as the 1940s. Even a hypothetical average structure of coal or kerogen, accounting for extensive information from various sources, can provide a synthetic view of the main resemblances and differences among sedimentary OM samples and types. Such a structure may also serve as a starting point for new studies if the model does not fit the analytical data, or for new analyses which could improve its representativity. A suitable model should thus synthesize in the best possible way physical and/or chemical structural information arising from a number of analyses. Depending on the properties of interest, several types of representation can be used, e.g., based on elemental/molecular composition, aromatic sheet distances, swelling properties, and cracking reactions and products, so that detailed molecular formulae are not always necessary.

The main steps in coal structure representation are reviewed below. Modelling of soluble macromolecular organic constituents, such as humic acids or asphaltenes, is not considered, since this approach is contemporaneous with (and often derived from) kerogen modelling. The section then focusses on molecular models of kerogen, in order to show how kerogen Type and maturity can account for the variety in amount and composition of oil (including extracts and pyrolysates) generated during thermal cracking under geological and laboratory conditions.

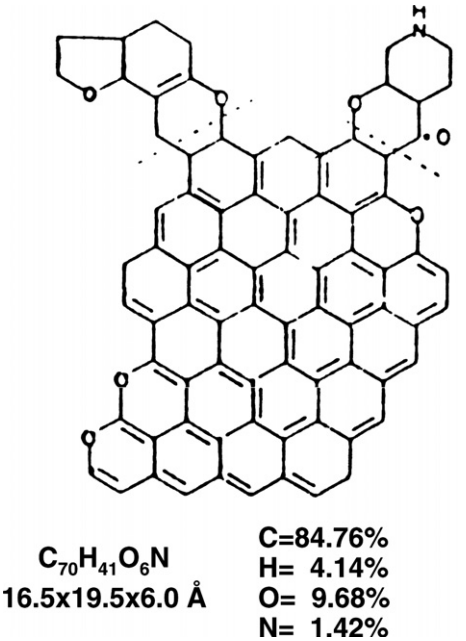

Fig. 49. Molecular model of an averaged bituminous coal molecule, explaining intermediate radical formation upon pyrolysis. Adapted from Fuchs and Sandhoff (1942).

8.2. Coal modelling

A review of molecular modelling of coal structure can be found in Van Krevelen (1993, Chapter 25). The main findings are described here in order to enable comparison with kerogen models. In consequence, only a few among numerous published models are presented.

8.2.1. Models based mainly on coal liquefaction products

To the best of our knowledge, the first attempt to build a molecular model of coal (Fig. 49) was carried out by Fuchs and Sandhoff (1942). Their aim was to explain experimental results of coal pyrolysis by modelling the different chemical processes involved, using thermodynamic calculations to classify bond strengths at various temperatures. This remarkable paper accounted correctly for the composition and order of appearance of cracking products, mechanism of coke formation (the concept of a free radical process was a new one at that time) and compositional differences between boghead coals and regular coking coals. However, the different

Table 18
Comparison of analytical parameters for vitrinite of a bituminous coal with those calculated from its model in Fig. 50[a]

Property	Coal vitrinite analysis	Model parameter
C (wt%)	82.3	82.1
H (wt%)	5.0	5.2
O (wt%)	10.9	10.7
N (wt%)	1.8	1.9
Atomic H/C	0.73	0.76
Model molecular formula		$C_{102}H_{78}O_{10}N_2$
Model molecular weight (uma)		1490
CH_{aro}/CH_{ali}	0.18–0.20	0.26
C atoms in aromatic clusters	16 (ave.)	12–19
Average number of intercluster linkages		3.5/cluster
Ratios CH_3:CH_2:CH:C	2:20:[b]:[b]	2:23:3:2
O as hydroxyl (wt%)	6.1	6.25
O as carbonyl (wt%)	4.0	4.15

[a] After Given (1960).
[b] Not available.

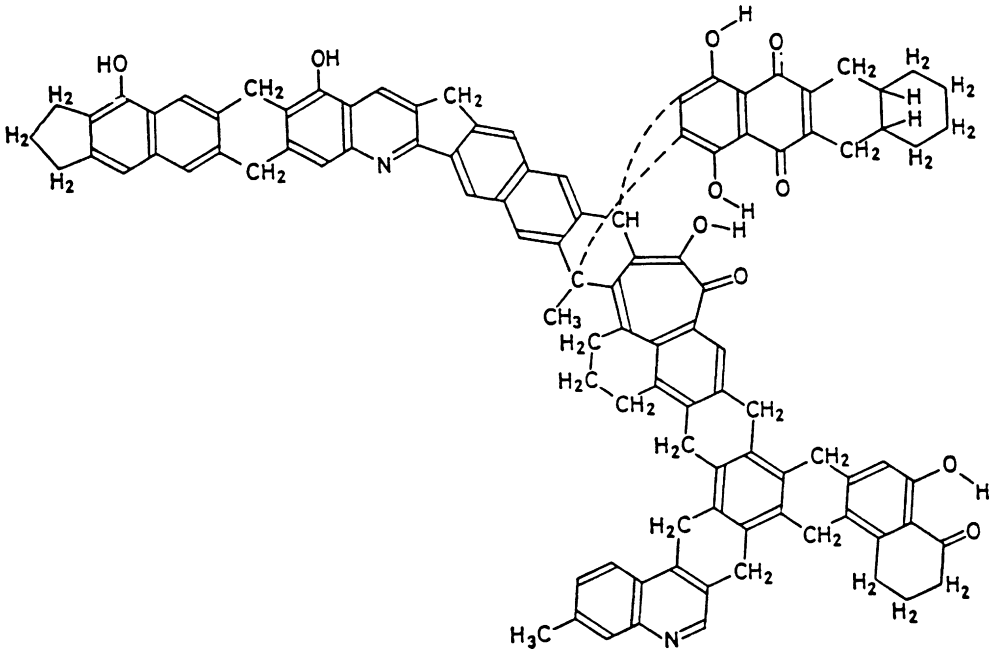

Fig. 50. Model structure of vitrinite of a bituminous coal. Reprinted from Given (1960, p. 150).

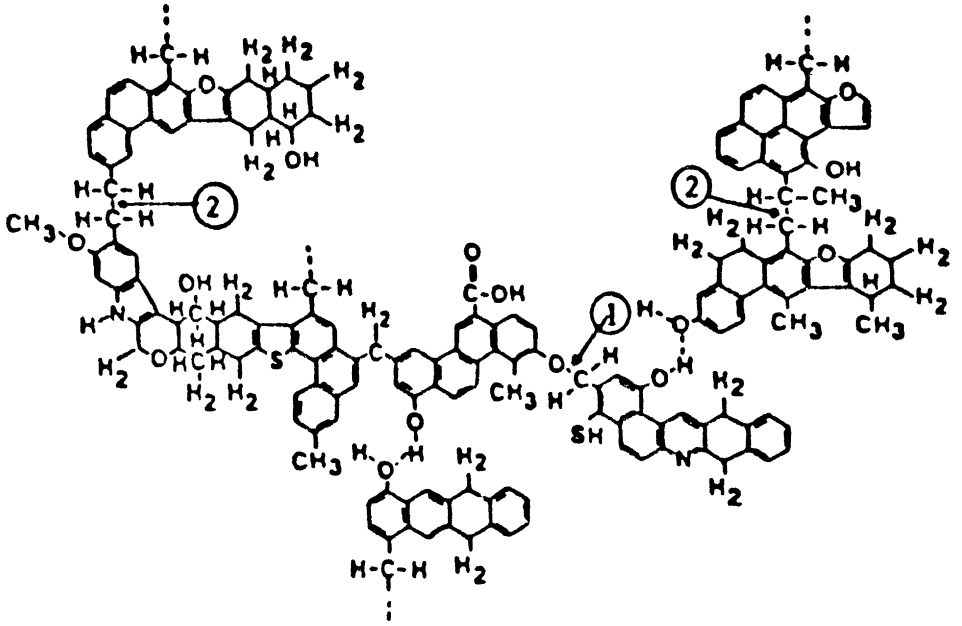

Fig. 51. Functional group model of a bituminous coal molecule constructed from structural groups of its gaseous pyrolysis products and elemental analysis data. Adapted from Serio et al. (1987).

structural models proposed were based on almost planar, highly condensed cyclic structures, with low H/C ratio and oxygen was assumed to be exclusively in the form of ether bonds.

A new step in coal modelling was reached in the 1960s thanks to improvements in X-ray analysis, which showed that aromatic clusters in coals up to the catagenesis stage contain no more than two to

four condensed rings. The coal model of Given (1960, Fig. 50), accounted not only for such a degree of condensation, but also for new results for oxygen functional group analysis from IR and NMR spectroscopy (Table 18). This lower aromatic condensation degree allowed for a better representation of the non-planar structure of coal, in line with observed microporosity at the molecular scale. Hetero elements, particularly oxygen, were also represented by a variety of functional groups (Fig. 50); a better account of the nature, amount and timing of formation of coal cracking products was therefore obtained.

Several structural models built for the same purpose as those of Fuchs and Sandhoff (1942), but using updated data for coal and its thermal degradation products, were published in the 1980s. They accounted not only for the initial structure of coal, but also for structures and amounts of cracking products. The hypothetical molecular structure of a bituminous coal (Solomon, 1981), using as starting point the functional group cracking model of Solomon's team (Serio et al., 1987 and references therein), is shown in Fig. 51. The chemical parameters of coal structure were focussed on quantitative distribution of functional groups, carbon–carbon bond types and related kinetic parameters for cracking, constrained by experimental results from coal pyrolysis. Coal structures at different initial ranks were assumed to differ only in their content of these functional groups, as considered also by Gavalas et al. (1981). The chemical structure depicted in Fig. 51 is structurally quite similar to that of Given (1960), but H bonds are thought to bind some structural elements.

The bituminous coal model of Shinn (1984, Fig. 52a) was based on detailed chemical analysis of several coals and their liquefaction products. It correctly accounted for the distribution of single and two stage liquefaction products. However, the author considered that improvements could be obtained by using other analyses on aliphatic groups, 3D structure and bonding sites, and structural information derived from pyrolysis. This model synthesizes previous ones, and uses chemical information obtained from analysis of low molecular weight hydrogenolysis products to reconstruct coal building blocks. The detailed characterization of hydrogenolysis products in terms of molecular weight, aromaticity, elemental analysis and functional groups is matched with crosslink reactivity under liquefaction conditions, in order to reconstruct the coal initial structure. This coal model has a larger unit size than previous ones, consistent with the insolubility constraints defined previously (MW > 10,000). Furthermore, a 20 wt% proportion of building blocks was considered as a mobile phase, held into the macromolecular network by H bonds and steric trapping, in agreement with extraction data obtained using strong electron donor solvents like pyridine. The presence of a significant proportion of low molecular weight components in the macromolecular network of coal was also reflected in ^{1}H NMR observations (Marzec and Kisielow, 1983; Marzec et al., 1983). Compounds in the 200–600 Da range, accounting for up to 30–40 wt% of the total coal, were thus considered as tightly trapped within the macromolecular network of bituminous coals, due to steric inaccessibility in relation to micropore size and to complexation via electronic interactions. These values, estimated from the proportion of protons having a high rotational mobility, were considered by some scientists as being too high in comparison with other observations (Derbyshire et al., 1989). However, the hypothetical structure of bituminous coals, based on a 3D macromolecular network entrapping significant amounts of low molecular weight molecules, was not disputed. That was also supported by studies of swelling and extractability properties of coals in various solvents (Larsen et al., 1985), showing that the macromolecular network of such coals is highly reticulated by H bonds from OH groups. These H bonds can be up to five times more abundant than covalent bonds and are responsible for the trapping properties and brittleness of bituminous coals. Pyridine, with its ability to break H bonds, can strongly expand the macromolecular structure and so extract large amounts of trapped low molecular weight compounds (see Fig. 52a).

Due to increasing computer power in the 1990s it became possible to build and visualize 3D molecular structures of coals and to apply molecular mechanics and dynamics to calculate minimum energy configurations, using force field approximation algorithms. After potential energy minimization, the 3D structure is much more compact (Fig. 52b and c) for the coal model of Shinn (1984), demonstrating the importance of van der Waals interactions and H bonding. The density and microporosity of this minimum energy structure are consistent with experimental values (Carlson, 1992).

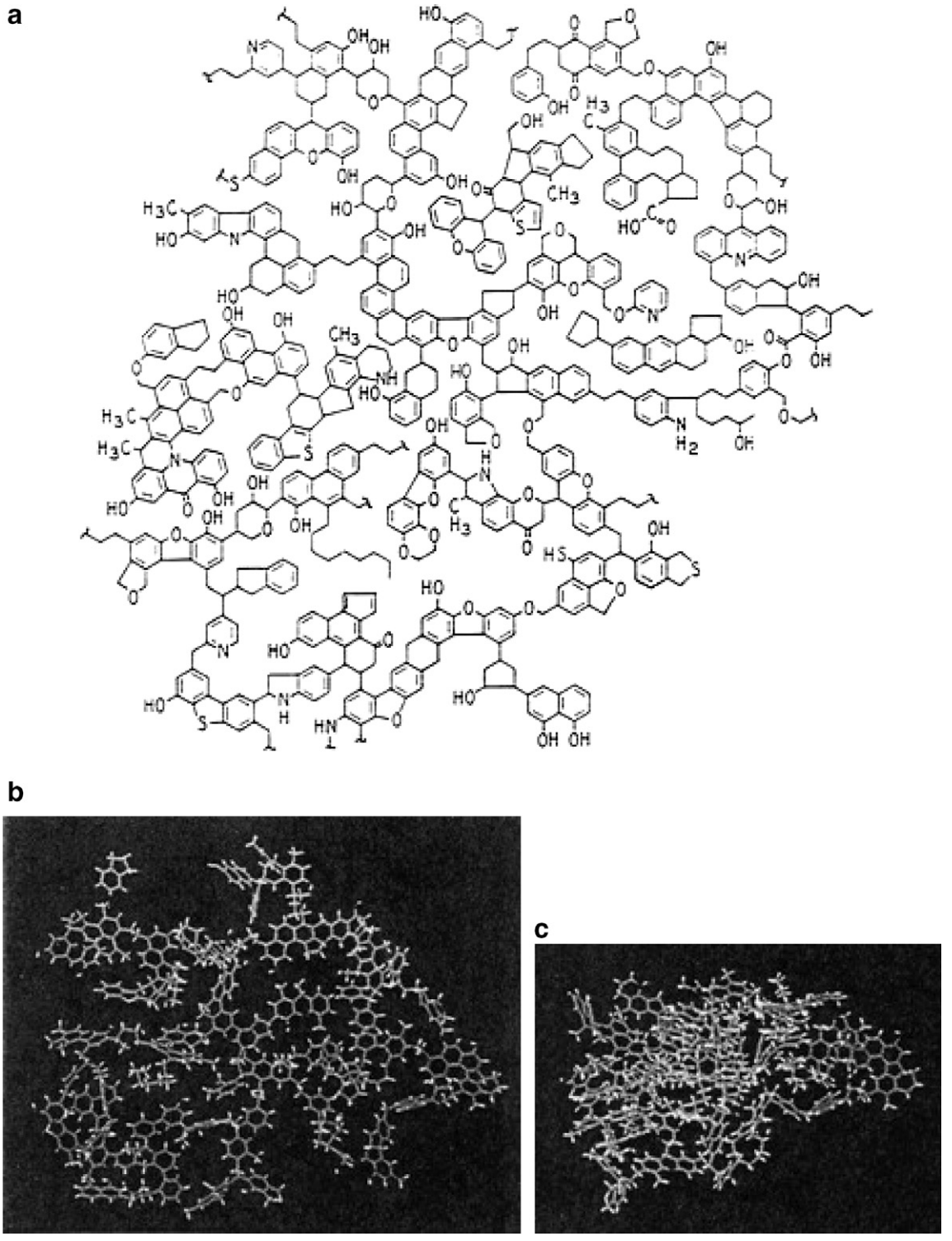

Fig. 52. (a) Molecular model of a bituminous coal by Shinn (1984); (b) and (c) 3D structure of Shinn's model constructed using computer assisted modelling software before (b) and after (c) energy minimization (Carlson, 1992). The molecular formula of the model is $C_{661}H_{561}O_{74}N_4S_6$, of which 455 C_{aro} and 171 H_{aro}, the corresponding molecular weight is 10,023 Da. Adapted from Shinn (1984) for a and Carlson (1992) for b and c.

8.2.2. Models accounting for coal physicochemical properties

Other coal models published in the same period considered specific structural features associated with bond types other than covalent bonds. The aim was to explain NMR results on proton mobility, implying the occurrence of moieties with highly different molecular sizes in coals on one hand, and extractibility and swelling properties on the other hand. The 3D structures constructed by Spiro (1981) according to these models, and later extended to coals of increasing rank (Spiro and Kosky, 1982), aimed at explaining coal properties such as plasticity, porosity, anisotropy, and their evolution with thermal maturation. Coal structure was, however, represented as predominantly macromolecular in all of these models, despite the fairly high extractability observed for bituminous coals.

Solid state spectroscopic techniques, like X-ray and electron spectroscopy or ^{13}C and ^{15}N solid state NMR, have made great progress during the last ten years, both in sensitivity and quantification accuracy. Information resulting from these analyses, although it represents average properties and has the same limitations as discussed above for building molecular models, could also improve understanding of coal chemical and physical features.

8.3. Kerogen modelling

The first ideas regarding the average structure of kerogen arose from analysis of soluble fractions generated upon thermal cracking under geological conditions on one hand, and of degradation products on the other. The main structural elements of kerogen were discussed by Forsman (1963) on the basis of functional group analysis and degradative studies, including permanganate oxidation, hydrogenolysis and pyrolysis. Although only a few kerogen examples were studied at the time, Forsman (1963, p. 177) already recognized two kerogen types, described as "coaly" and "non-coaly". The coal type was viewed as "a macromolecule consisting of condensed aromatic rings interconnected by ether, alkoxy, and perhaps sulfur bridges. Attached to the aromatic nuclei are hydroxyl groups, methoxyl groups, and perhaps esterified carboxyl groups". In contrast, the non-coaly type was viewed as "a more nearly open chain structure, with some cycloparaffin or mononuclear aromatic rings attached. Oxygen, and possibly nitrogen and sulfur atoms may act as connecting links". Although no chemical structure was shown, this view of kerogen building blocks and the indications that (i) resistant portions of living organisms could participate in the

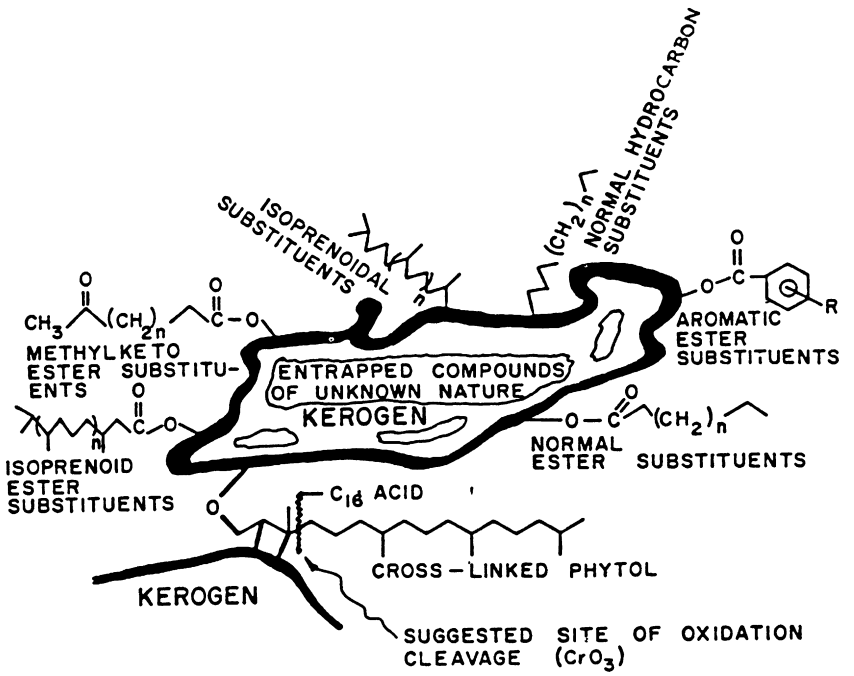

Fig. 53. Representation of some building blocks of kerogen structure in Green River shale, as deduced from kerogen oxidative cleavage using CrO_3. Reprinted from Burlingame et al. (1969, p. 126).

structure and (ii) kerogen structure should change with rank as observed for coals, were particularly perspicacious.

8.3.1. Precursor models: Green River Shale (GRS) kerogen

During the 1960s, a number of analytical studies were performed on OM structure in oil shales. GRS kerogen was studied extensively by Robinson and coworkers and its main structural components were described quantitatively (summarized by Robinson, 1969b). However, the first kerogen model to be published (Fig. 53) was that of Burlingame et al. (1969). It did not represent a full chemical structure of the GRS kerogen, but only some of its building blocks as released by CrO_3 oxidation and possible bonding sites. Already at the time, the presence of compounds trapped within the macromolecular network was suggested. A fairly similar representation of GRS kerogen by Djuricić et al. (1971) was based on the analysis of the products formed using alkaline permanganate oxidation. Given the high yield (70%) of aliphatic mono- and dicarboxylic acids obtained, these authors concluded that the structure of the kerogen was comprised mainly of polymethylene moieties including long *n*-alkyl and isoprenoid chains, with aromatic structures being only minor.

The first detailed molecular representation of GRS kerogen was published by Yen (1976). In line with the aims of Given (1960) when drawing his coal model, the purpose was to build for kerogen "a conceptual model to accomodate the accumulated physical and chemical evidence". This model was based on the results gained via extensive studies of asphaltene structure. In opposition to the above structural models, it accounted not only for the structure of the chemical degradation compounds but also for the spectroscopic features of the kerogen obtained using X-ray diffraction, IR spectroscopy, electron spectroscopy for chemical analysis (ESCA) and electron spin resonance (ESR). A simplified representation of the structure (Fig. 54a), together with the description of the chemical family of each of its components (Fig. 54b), were used for building a 3D model with a molecular construction kit (Fig. 54c). Such a representation was intended to be a conceptual model of only a small part of the kerogen molecular network since, as mentioned above, any analytical result on kerogen is only an average value for a very large number of its constitutive moieties. This 3D model (Fig. 54c), with a

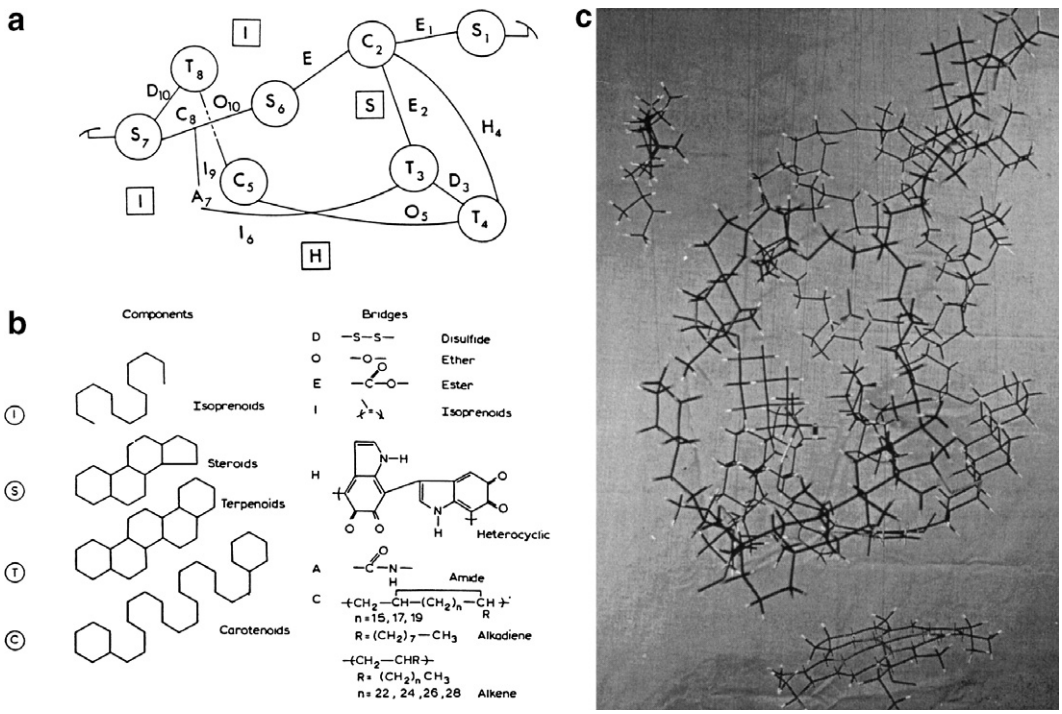

Fig. 54. Structural and 3D molecular models for Green River shale kerogen: (a) hypothetical structural model; (b) abbreviations and related chemical structures for constituents of model a; (c) 3D construction corresponding to $C_{235}H_{397}O_{13}N_3S_5$. Adapted from Yen (1976).

Table 19
Functional analysis of two Type I kerogen concentrates from oil shales[a]

Total element (for 100 °C) and functional group proportion	Rundle Ramsay Crossing	Green River Shale
Total O for 100 °C	9.2	3.0
Carboxylic acid	2.3	0.2
Ester/carboxylate	1.1	1.8
Ketone/aldehyde	1.4	0
Phenol	0	0
Alcohol	0.6	0.5
Ether (by diff.)	3.8	0.5
Total N for 100 °C	1.8	2.2
Pyrrole	0.3	0.5
Unhindered basic N	0.1	0.3
Hindered basic N	0.9	0.8
N-substituted pyrrole (by diff.)	0.5	0.6
Total S for 100 °C (thiophenic)	0.7	0.7
H/C atomic ratio	1.61	1.56
Aromatic C for 100 °C	16	22

[a] After Siskin et al. (1995).

bulk formula of $C_{235}H_{397}O_{13}N_3S_5$ and an atomic weight of 3627 Da, failed to reproduce the measured density (0.2 for the model as constructed instead of about 0.8 measured). Such a large discrepancy was partly due to the fact that (i) molecular conformations were not those of minimal energy and (ii) the atomic construction assembly tended to deform and flatten due to its own weight. It is interesting to note that Yen (1976) also indicated, probably on the basis of his knowledge of asphaltene structure, that (i) loosely held bitumen molecules may be entrapped within the kerogen matrix and (ii) kerogen structure contains not only covalent bonding, but also inter- and intramolecular hydrogen bonding as well as charge transfer bonding.

Finally, a later publication by Siskin et al. (1995) on modelling of oil shale kerogen concerned not only the GRS but also the Rundle Ramsay Crossing Shale (Qld., Australia). The most interesting aspect of this paper lies in the use of solid state ^{13}C and ^{29}Si NMR combined with selective chemical derivatization of kerogen, along with detailed mass spectrometry and NMR studies of kerogen pyrolysates. The result is a much better quantitation of the various structural constituents in these oil shales, particularly for O- and N-containing functional groups (Table 19), than previously obtained using classical functional

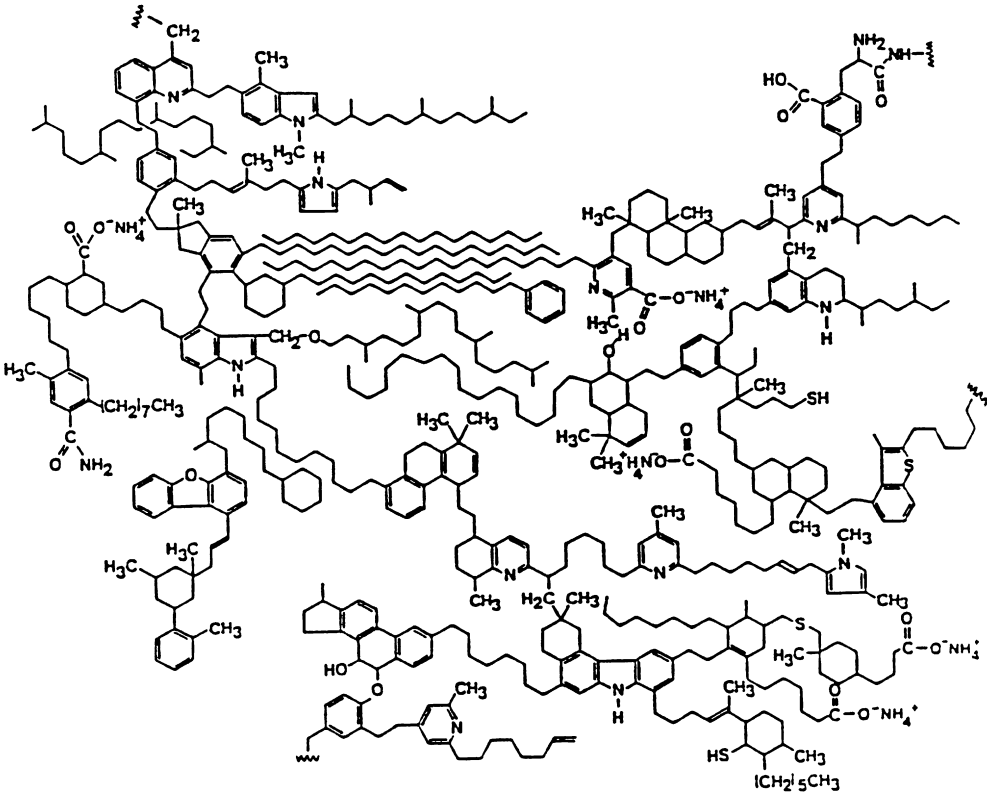

Fig. 55. Structural model of Green River oil shale kerogen. Reprinted from Siskin et al. (1995, p. 157).

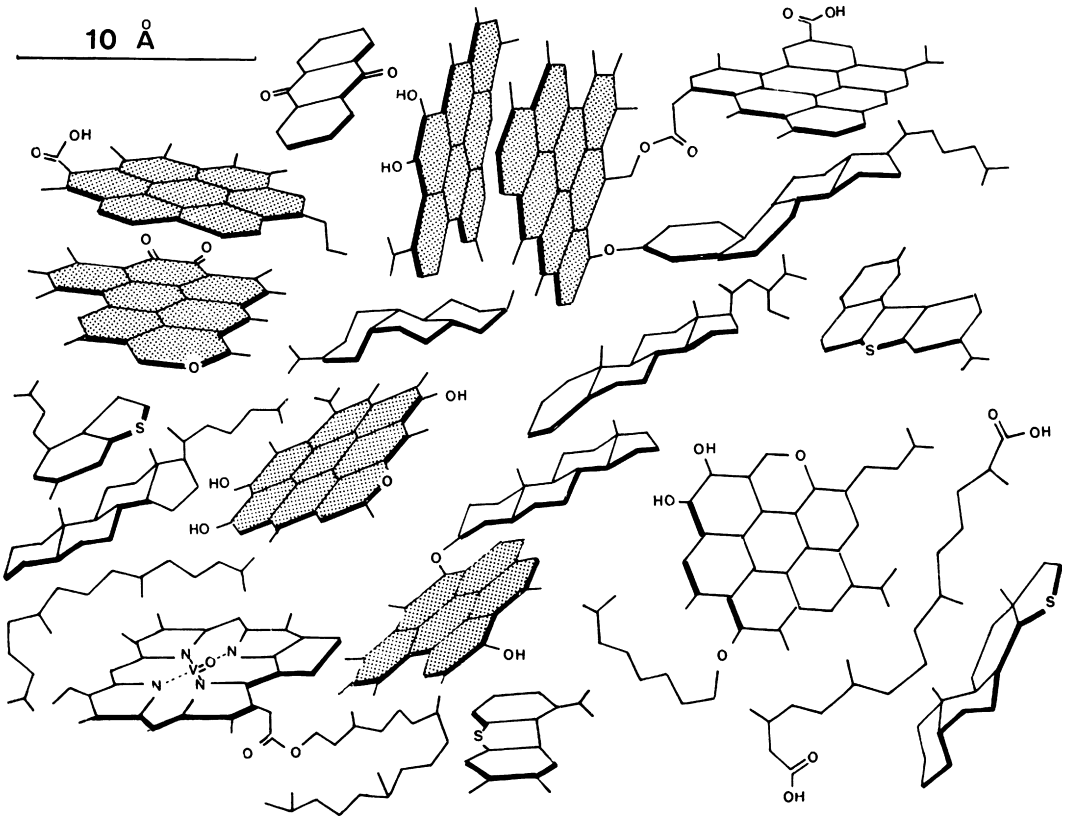

Fig. 56. Structural scheme for a Type II kerogen at an evolution stage corresponding to beginning of catagenesis. Note that bonds between elemental bricks are not represented, the scheme aiming to show how aromatic stacks should be piled up to produce bright spots upon dark field imaging electron microscopy. Adapted from Oberlin et al. (1980).

group analysis. The resulting chemical structure for GRS kerogen is shown in Fig. 55.

8.3.2. Kerogen models accounting for differences in type and evolution

The main differences in the structural components of kerogens according to type, at the onset of the oil window, were first described by Vandenbroucke (1980) on the basis of bitumen composition. Simultaneously, a structure for Type II kerogen was reported by Oberlin et al. (1980), Fig. 56, using complementary data on kerogen building blocks. However, it rapidly became clear that such a structure could not represent kerogen, because the bulk molecule would have been readily soluble in $CHCl_3$. Nevertheless, it provided a starting point for attempts to build a complete series of structures representing the different types kerogens at various maturity stages. The idea was not, as stressed above, to represent in a rigorous way the exact chemical structure of kerogen, since this is not realistic. It was rather to present in a synthetic way the main chemical and physical characteristics related to type and maturity, in order to allow for easy comparisons (Behar and Vandenbroucke, 1986, 1987). The way these models were built was essentially similar to, although done independently from, that used by the coal scientists cited above. A combination of quantitative atomic and molecular information resulting from analysis of kerogens and of their degradation products was used, and the consistency of the analytical results obtained for a given parameter using different techniques was checked. The atomic information counts up atoms or atomic groups, including their nearest chemical environment, and was mostly derived from elemental analysis, solid state ^{13}C NMR, XANES and functional group analysis. The molecular information counts up structural building blocks on the basis of analysis of natural extracts, pyrolysates and chemical degradation products. Starting for the three types with a similar number of

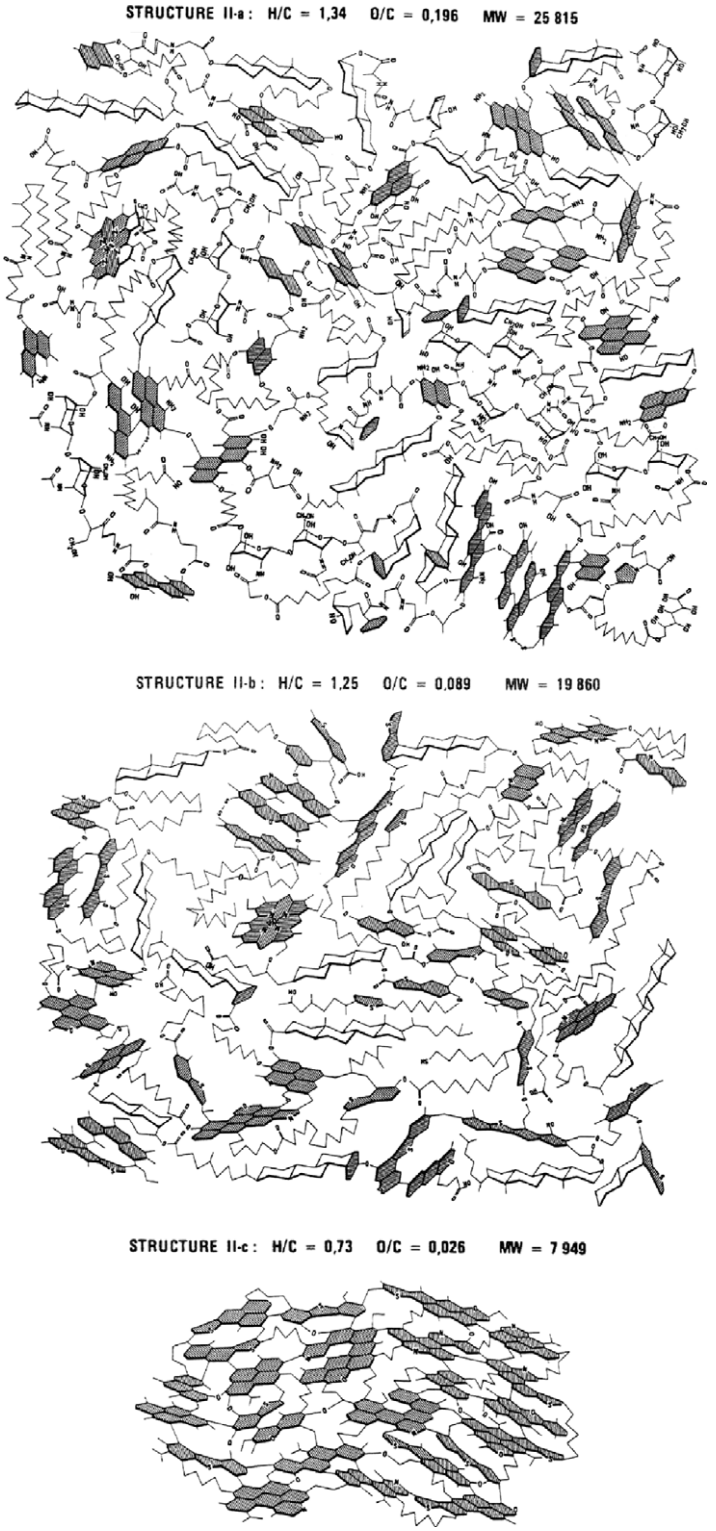

Fig. 57. Structural representation of Type II kerogen (analytical data from Paris Basin Toarcian series) at increasing maturity stages, corresponding to given atomic H/C and O/C ratios. Structure IIa: beginning of diagenesis; structure IIb: beginning of catagenesis; structure IIc: end of catagenesis. Adapted from Behar and Vandenbroucke (1987).

carbon atoms at the diagenesis stage, corresponding to molecular weights ranging from 20,000 to 25,000 Da, the structure size upon maturation was constrained by weight loss from each type measured using thermogravimetry (Durand-Souron, 1980). The ring number and orientation of aromatic clusters were derived from dark field imaging electron microscopy (Oberlin et al., 1980). The structures were built by trial and error: functional groups and molecular building blocks selected through molecular analysis were connected by covalent bonds in order to fit elemental analysis and solid–state ^{13}C NMR results, removing or adding building blocks and functional groups to improve fitting at each further step in the construction. Although trapping of saturates (Behar and Vandenbroucke, 1988) and other bitumen constituents had been demonstrated, these kerogen structures deliberately omitted trapped compounds because kerogen sensu stricto should be totally free of soluble compounds. A 3D-like representation of individual cyclic building blocks was preferred to the traditional chemical representation in order to better visualize the differences in structure according to type and maturity. An example of the structural transformations of the model for Type II kerogen with increasing maturity is shown in Fig. 57. The GRS kerogen model at low maturity is shown in Fig. 58 for comparison with the model by Siskin et al. (1995, Fig. 55).

In view of the extensive knowledge acquired on kerogen examples after the publication of these models, and thanks to studies of new samples and developments with analytical tools, today one can question their representativity at the molecular scale, although as indicated above, they were intended only to present in a synthetic way the main chemical and physical characteristics related to type and maturity. Thus, the Type I model is likely to be valid only for some Type I kerogens related to an alkaline depositional environment, like the GRS. In fact, since Type I OM results from eutrophication conditions, its chemical composition should be closely related to chemical changes in its depositional environment. Moreover, even among the

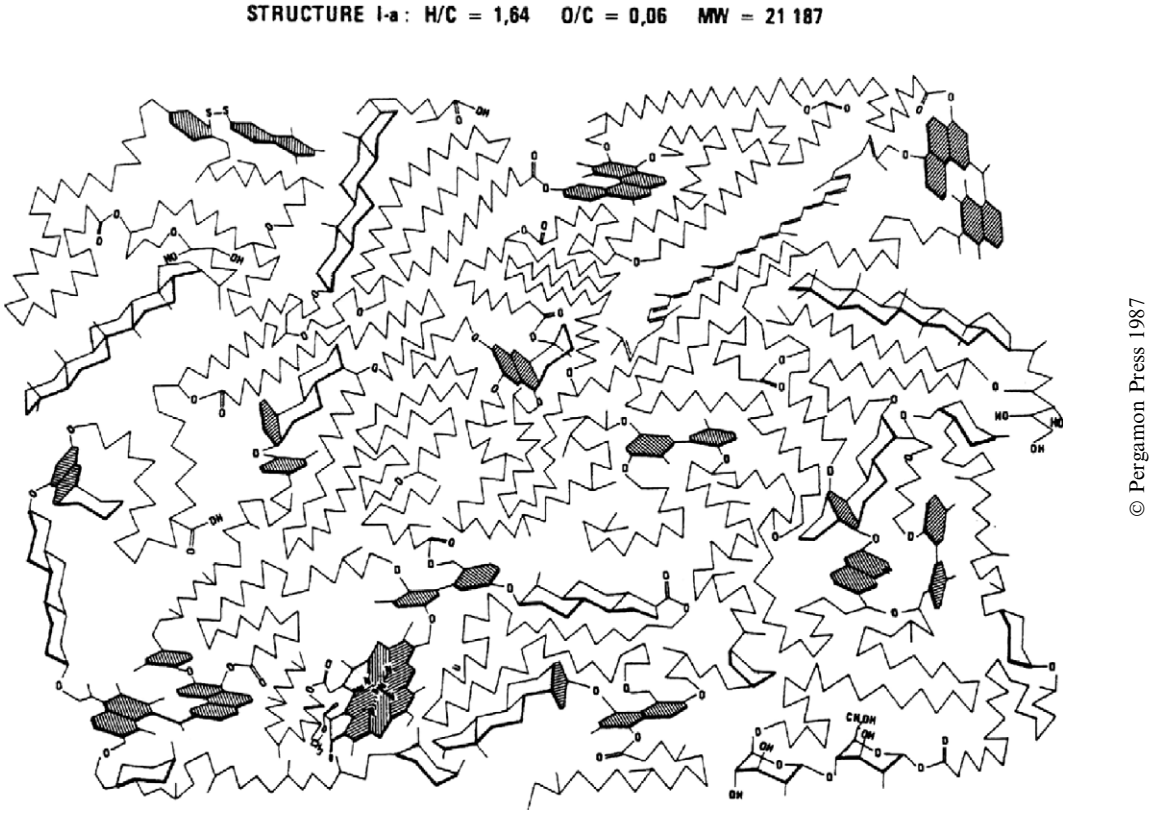

Fig. 58. Structural model of low maturity Type I kerogen from Green River shale. Compare with the model by Siskin et al. in Fig. 55. Reprinted from Behar and Vandenbroucke (1987, p. 16).

GRS samples, a fairly large variability in composition was observed, both laterally and vertically, for immature examples (Tissot et al., 1978). This is probably all the more true when comparing Type I kerogen from the GRS to *Botryococcus*-derived Type I kerogen. Moreover, although non-extractable, a large amount of long chain constituents such as those observed using high temperature GC (Hsieh and Philp, 2001 and references therein) are probably trapped in Type I kerogen by physical entanglement, and are not linked by covalent bonds to the kerogen structure. The Type II model may have a broader representativity up to a limit of S content at 8 wt%, where the kerogen is considered as Type II-S (Orr, 1986). The molecular representation of coals and Type III kerogens by averaged chemical structure cannot be realistic. In fact, it was shown from light microscopy observations of coals (Stopes, 1935) that their main constituents are physically completely separated at the microscopic level, hence a fortiori separated at the macromolecular level. Given the common precursors of coal and Type III kerogen, a similar separation of aromatic and aliphatic constituents exists for the latter (Vandenbroucke, 1980). This may partly explain the very early generation and migration of heavy saturates in oils sourced by some Type III kerogens, as found in several case studies (Khavari Khorasani and Michelsen, 1991; Clayton et al., 1991).

Further studies on kerogen composition are thus needed in order to propose new representations of its structure at the molecular scale. However without new microscopic techniques reaching this molecular level, scientists are unable at present to represent correctly kerogen macromolecules at various evolution stages.

8.4. Computer aided structural modelling

One of the first applications of computers to the structural elucidation of moieties from sedimentary OM was published by Oka et al. (1977). In this paper, the systematic construction of possible coal-derived liquefaction products was obtained on the basis of experimental data from ^{1}H NMR and elemental analysis. Because of the computer power available at the time, such modelling was limited to low molecular weight compounds (<400 Da), for which a systematic construction of all possible structures could be achieved. Moreover, 3D representation of these structures was not attempted,

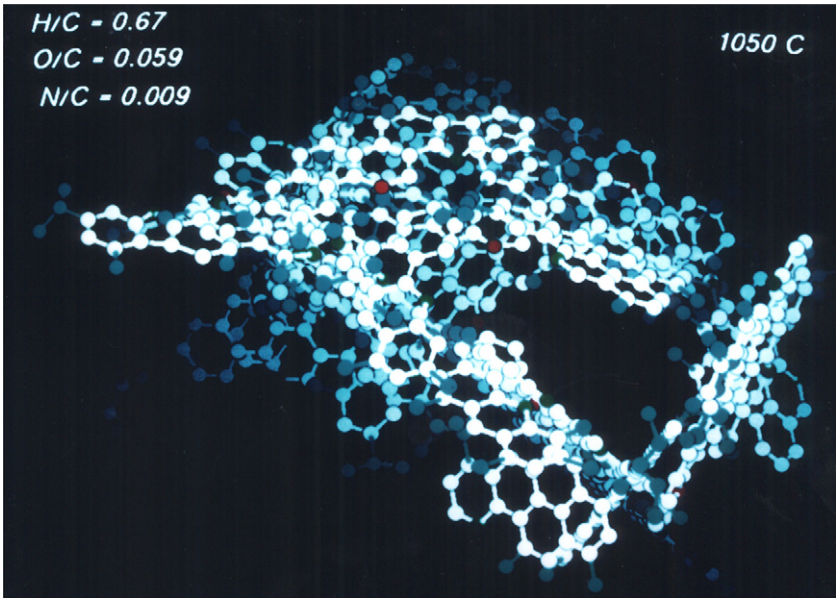

Plate h. 3D representation, using the XMol software, of a Type III kerogen structure at the end of catagenesis. Only C atoms (aromatic in white, aliphatic in blue), O atoms (in dark green), N atoms (in red) are represented. Published lengths and directions for covalent bonds are used, but energy minimization calculations are not performed on the resulting structure. However, it is expected to make little difference due to its high aromaticity. Reprinted with permission from Vandenbroucke (2003, p. 265).

because it was not useful for the authors' particular purpose.

A systematic construction is not possible for kerogen. Indeed, although the structural constituents (molecular building blocks, functional groups and bond types) can be identified through analysis, the number of possible combinations is so high that only a limited part of these combinations can be constructed. However 3D constructions can be informative for eliminating unrealistic structures, as shown by space filling coal models of Spiro (1981). A computational tool for building 3D kerogen models, based on those of Behar and Vandenbroucke (1987), was elaborated by Faulon et al. (1990). Starting from atomic and molecular analytical data and from 3D basic chemical structures in a library, the nature and amount of building blocks and bonds were first calculated. To this end, an intermediate kerogen structure was used where hetero elements were replaced by equivalent C configurations. Then, 3D carbon skeletons of kerogen were constructed by connecting successively these building blocks by bonds randomly picked in the library, assuming that any building block is connected by one or two covalent bonds. Final models were obtained by replacing carbons by hetero elements according to atomic and functional group analysis. A possible structure obtained in this way for a Type III kerogen at the end of catagenesis is shown on Plate h. The microporosity observed in this structure does not represent input data; it results from the construction, with building blocks respecting bond lengths and directions.

The computer program used in the above work was not compatible with molecular modelling software enabling calculations based on molecular mechanics and dynamics; this type of software became commercially available later. Therefore, Faulon (1995) proposed a new compatible program for generating statistically representative subsets of 3D chemical models. This program, in conjunction with commercial software like BIOSYM, was used to estimate macromolecule physical characteristics such as density, porosity distribution, surface area, solvent and/or solute interactions and thermoplastic behaviour. These calculations were applied to many other materials in addition to kerogen, including polymers, coals, asphaltenes, petroleum heavy ends and coal liquefaction products. However, apart from the easier handling brought about by computerized calculation of structural elements, this 3D representation was not found to provide much additional information on kerogen conceptual models. The immediate comparison of structures representing various types and maturity, in terms of chains vs. rings, aliphatics vs. aromatics, hetero element amounts and functional types, was easier using the models of Behar and Vandenbroucke (1986) than those of Faulon et al. (1990). Continuous increase in computer speed makes available more powerful 3D modelling and molecular mechanics calculations, that brought new insights into the types of bonding that are responsible for the rigidity of coal structures (Carlson, 1992). Further efforts in 3D modelling of fossil OM constituents have been generally devoted to asphaltene structure (Kowalewski et al., 1996; Murgich et al., 1996), petroleum heavy ends and coal combustion products (Jones et al., 1999) rather than to kerogen type. However, coal modelling is still an active reseach domain for computer modelling using molecular mechanics. For example, microporosity and true density can be now represented and calculated in 3D structures, in good agreement with measured data (Faulon et al., 1993); stabilisation of coal structures by water, inorganic ions and metallic complexes has also been demonstrated by using such models (Domazetis and James, 2006).

8.5. Summary

- As kerogen is not a polymer, it is impossible to represent its chemical macromolecular structure by a set of a limited number of chemical moieties; a molecular representation can thus only account for the statistical representativity of analytical data.
- The first chemical models for coal were published as early as 1942 and were aimed at supporting kinetic modelling of thermal cracking. Structural and molecular models were proposed for the GRS in the 1970s. Conceptual models visualizing chemical differences in kerogen type and evolution stages were published only ten years later.
- New knowledge on kerogen obtained since then led to the idea that kerogen macromolecular structure contains both organized building blocks inherited from selective preservation and random structures issued from recondensation processes. Accordingly, averaged models constructed from analytical data can at best reflect

random structures, but may be not appropriate when a single type of selectively preserved moieties constitutes the major organic source for a particular kerogen in question.

9. Future research on kerogen

A wealth of information has been accumulated since the 1980s on kerogen. However, a number of important points still have to be elucidated and significant advances can be expected in the near future, especially in relation to progress in using specific analytical tools. Indeed, increasing possibilities in molecular analysis and microscopy have been responsible for most of the advances in the past. Degradative chemical techniques and pyrolysis were also of prime interest for the study of complex macromolecular systems such as kerogen. These advances took advantage not only of improvements in analytical techniques, but also of their coupling, allowing separate analysis of selected individual compounds in complex mixtures. Besides the foreseen development of new, often coupled, analytical methods, discussed below, a general trend can be observed towards absolute quantification of given molecular species, formerly studied using qualitative techniques. Quantification enables not only universally-scaled parameters to be obtained, but also determination of the representativity of molecular species arising from thermal or chemical degradation of kerogen.

Kerogen study will remain an active and prolific field in the coming years. It should be largely promoted using multidisciplinary approaches, including biological studies and OM studies of modern environments, along with the development of new analytical tools, including pin-point analysis. In turn, the information obtained on kerogen could give new insights into the traditional geochemical applications, but also into other fields like palaeoenvironment and palaeoclimate reconstruction and the global carbon cycle.

The following discussion is focussed on topics currently in progress. In each case, starting from the latest available studies, we try to bring out some trends for future research, in the short to medium term. After a brief discussion on possible improvements in kerogen isolation methods suitable for very low maturity samples, the first part is devoted to the potential of recent developments in analytical techniques for obtaining better knowledge of the chemical structure of kerogen and of its interactions with minerals in sediments. Then, the pathways leading from biomolecules to kerogen and related chemical transformations are considered as another possible area for important developments.

9.1. Kerogen isolation and analytical tools

Suitable conditions for kerogen isolation from ancient samples are now well established. Moreover, maceral separation from isolated kerogens has been accomplished through the technique of density gradient centrifugation (Han et al., 1995; Stankiewicz et al., 1994, 1996), thereby allowing better characterization of kerogen components. In contrast, problems are still encountered for "protokerogen" isolation from recent sediments. This is due to the lability of a large part of the insoluble OM in such samples when submitted to the classical HF/HCl treatment. Similar problems are encountered for soil OM but, in that case, they can be largely overcome by using diluted HF (Skjemstad et al., 1994; Zegouagh et al., 2004). An efficient method has been developed for the demineralization of recent sediments as described in the kerogen isolation section. This method results in extensive elimination of minerals, while OM losses and alteration are limited. Moreover, efficient removal of paramagnetic metals is achieved so that the quality of the solid state CP/MAS ^{13}C NMR spectra of the isolated materials is highly improved (Gélinas et al., 2001). Further gains in the organic enrichment factor obtained with this method could probably result from improvements in the sequence of acid treatments for reducing ash content, and in using desalting by resins for increasing dissolved OM recovery.

Kerogen studies should rapidly benefit not only from the development of new analytical methods, but also from greater use of some of the existing tools which have so far been rarely employed for the analysis of fossil macromolecular OM. Thus, examination of kerogen ultrastructure using SEM and TEM should become more general, in combination with geochemical analyses, along with microscopic observations coupled to spectroscopic analysis with micro-FTIR and elemental mapping. Other pin–point methods should also be useful, such as energy filtering TEM and electron energy loss spectroscopy, as applied by Furukawa, 2000 to a study of OM/clay

mineral interactions. Furthermore, as shown by Greenwood et al. (1998, 2000) and Arouri et al. (1999), important information on the composition of individual organic particles could be obtained through kerogen examination with light microscopy coupled to laser micropyrolysis GC–MS. The use of high resolution TEM should also be developed, especially for studies concerned with the identification and characterization of highly aromatic particles, such as black carbon (BC) particles, as well as with OM/mineral interactions.

Pyrolytic methods have been used extensively for kerogen studies. However, relatively low yields of liquid effluents and relatively low weight losses are obtained (except for low maturity Type I kerogen) when using conventional pyrolysis. Improvement and additional information on complex natural macromolecular materials can be obtained with double shot pyrolysis (Quénéa et al., 2006a). Yield improvement can also be achieved using catalytic hydropyrolysis and, as mentioned above, TMAH thermochemolysis. Important additional information can be obtained with the latter approach using other tetramethylammonium salts, with different base strengths, like acetate (TMAAc) or carbonate ($TMACO_3$; e.g. Joll et al., 2004; Deport et al., 2006) or by using ^{13}C labelled reagents such as ^{13}C TMAH (Filley et al., 2002b). Catalytic hydropyrolysis, i.e. pyrolysis under high H_2 pressure with a Mo catalyst, was first developed for coal liquefaction and to increase shale oil production upon retorting (Snape et al., 1994). This method has been applied successfully, inter alia, to the study of kerogen composition and has afforded useful information on aliphatic moieties (Love et al., 1995, 1998) and organic sulfur speciation (Mitchell et al., 1994; Brown et al., 1997). However, all the above improvements have been applied so far only in a limited number of cases and future pyrolytic studies should largely benefit from their more general use.

Selective chemical degradation has also been applied extensively to derive information on the chemical structure of kerogen (e.g. Forsman, 1963; Vitorović et al., 1984; Michaelis et al., 1989; Rullkötter and Michaelis, 1990; Adam et al., 1991; Amblès et al., 1996; Blokker et al., 2000; Yoshioka and Ishiwatari, 2005). Such experiments usually suffer from low yields of released products being obtained. Kerogen conversion to up to 80 wt% of soluble material has been achieved through stepwise chemical degradation of some Type II-S kerogen examples (Schaeffer-Reiss et al., 1998; Höld et al., 1998), although such high yields are only obtained from S-rich samples owing to the relatively easy cleavage of sulfur linkages using chemical treatment. Great advances in the development of new reagents and/or more suitable experimental conditions are still needed to obtain satisfactory yields from other kerogen types via chemical degradation. In this respect, high degradation yield and differentiation between ester and ether moieties have been obtained, for example, for the Messel oil shale by using an alkaline hydrolysis/RuO_4 oxidation/alkaline hydrolysis sequence (Dragojlović et al., 2005).

Developments in mass spectrometry should promote direct structural studies of kerogen. Temperature-resolved, in-source pyrolysis mass spectrometry was shown to be a powerful tool for the examination of various types of macromolecules and for marine high molecular weight (HMW) OM (e.g. Boon, 1992; Boon et al., 1998). Ionization methods such as matrix-assisted laser desorption ionization (MALDI) and electrospray ionization (ESI) were developed for studies on biomacromolecules and are efficient for proteins with molecular weight $> 100{,}000$ Da (McLafferty et al., 1999). Such techniques are therefore highly promising for the characterization of kerogen and of HMW kerogen precursors and degradation products. However, limitation in interpretation may arise from the great complexity of these materials. ESI combined with quadrupole time-of-flight (QqTOF) mass spectrometry and with FT (Fourier transformed ion cyclotron resonance (FT-ICR)) mass spectrometry was used for the characterization of humic substances (Kujawinski et al., 2002) and of polar NSO compounds in various oils (Hughey et al., 2004; Kim et al., 2005). High resolution was thus achieved, with resolving power $> 80{,}000$ and mass accuracy < 1 ppm, for compounds with m/z up to 3000 and exact molecular formulae could be obtained.

Advances in spectroscopic studies could be achieved through new developments in NMR. A solid state 2D double cross polarization, magic angle spinning, ^{13}C ^{15}N NMR study has been reported for ^{13}C- and ^{15}N-enriched humic substances and microbially degraded biomass (Zang et al., 2001; Knicker, 2002). High resolution, magic angle spinning ^{13}C ^{1}H NMR has been used for structural studies of cutan (Deshmukh et al., 2005). XANES spectroscopy proved to be an efficient tool for sulfur speciation in kerogen (e.g.

Riboulleau et al., 2000). Studies on carbonaceous material charring (Turner et al., 1997) suggest that oxygen K-edge XANES could also be useful for oxygen speciation in kerogen.

The development of compound-specific isotopic analysis (CSIA) for carbon (Matthews and Hayes, 1978) has resulted in major advances in geochemical studies. Measurements of $\delta^{13}C$ values were thus extensively performed for individual compounds in sediment extracts and for the identification of sources, as well as for palaeoenvironment and palaeoclimate reconstruction (e.g. Hayes et al., 1990; Freeman et al., 1990). Parallel CSIA measurements for radiocarbon ($\Delta^{14}C$) were performed in a few cases to distinguish between modern and fossil sources for *n*-alkanes in marine sediments (Pearson and Eglinton, 2000). It was only in the late 1990s that CSIA for ^{13}C started to be used for studies of HMW materials. Thus, *n*-alkanes in pyrolysates of asphaltenes from biodegraded oils were examined with respect to oil-source rock correlation (Xiong and Geng, 2000). CSIA was also performed, along with GC–MS, to examine pyrolysis products from peat (Kracht and Gleixner, 2000), total OM from soil (Gleixner et al., 1999, 2002), OM concentrated from soil by way of extensive extraction and removal of minerals with HF (Loiseau et al., 2002; Dignac et al., 2004) and the non-hydrolysable macromolecular organic fractions isolated from forest and cultivated soils (Poirier et al., 2006). The first (and it seems so far the only) CSIA study on alkanes generated from kerogen pyrolysis was reported by Eglinton (1994) and pointed to a large contribution from the selective preservation of resistant aliphatic structures. CSIA of pyrolysates of kerogens from lacustrine source rocks (Cretaceous, West Africa) allowed distinction between alkyl benzene biomarkers sourced from microalgae and green sulfur bacteria, respectively, thus providing palaeoenvironmental information on photic zone euxinia (Pedentchouk et al., 2004). CSIA was developed later for D/H ratios (Burgoyne and Hayes, 1998) and has been applied to the examination of lipid biomarkers in sedimentary rocks as a proxy for environmental and climatic studies (Sauer et al., 2001) and of alkanes in crude oils for oil-source correlation and palaeoenvironment reconstruction (Li et al., 2001). Systematic use of CSIA for determining $\delta^{13}C$ values and D/H ratios should provide a powerful tool for deciphering the origin of a number of constitutive moieties in kerogens.

9.2. From biomolecules to kerogen

9.2.1. Biological studies

Determining the composition of the refractory macromolecular compounds that occur in the cell walls of extant microbial species is a prerequisite for the recognition of their fossil counterparts in kerogen. As mentioned above, the ubiquitous occurrence of dinoflagellate cysts in marine kerogens and observations on the cyst walls of a modern species point to the presence of refractory biomacromolecules in such walls and a contribution to kerogen via selective preservation. Comparison of these fossil and modern macromolecular materials is now needed to elucidate their chemical features and investigate the above assumptions. A further step will be to test the general character of these observations through study of cysts from other cultured dinoflagellate species. However, such studies are at present hampered by the difficulties encountered in laboratory experiments in culturing dinoflagellates to achieve cyst formation. Similarly, it is commonly considered that the organic microfossils that form the bulk of kerogen in Tasmanites originate from the selective preservation of thick walls from cysts of microalgae identical (or closely related) to the extant marine genera *Halosphaera* and *Pachysphaera*. Such an origin is based on morphological similarities and may account for the specific composition observed for biomarkers in the bitumen of these Late Paleozoic organic-rich deposits (e.g. Revill et al., 1994; Azevedo et al., 2001). Production of thick walled cysts from species of these two genera through laboratory cultures is required to test these assumptions. Generally speaking, better assessment of the contribution of the selective preservation pathway to kerogen formation is largely dependent on the availability of new microbial strains for laboratory culture and on the elucidation of the growth conditions that control their different life stages, including cyst formation.

9.2.2. Diagenetic stability of biomolecules

Additional information is needed on the fate of non-hydrolysable biomacromolecules, like algaenan, under natural conditions. In fact, as discussed above, it is well documented that such components can remain virtually unaffected upon diagenesis and so contribute significantly to kerogen through the selective preservation pathway. However, it is still unclear whether such preservation is effective

under any (or most) depositional conditions usually encountered in aquatic environments and, if not, under which range of conditions a direct contribution of these preserved biomacromolecules to kerogen occurs. All of the studies performed so far on sedimentary OM have shown a close parallel between a high resistance of some biomacromolecules to drastic laboratory hydrolysis and a high degree of survival to diagenetic alteration. However, a different situation is found for soil (Poirier et al., 2001, 2003, 2006; Quénéa et al., 2006b), an environment characterized by especially active degradation processes due to the highly oxic conditions, intense reworking and highly diverse micro- and macrofauna. Contrary to numerous aquatic settings (e.g. Hedges et al., 1997), intense degradation of lignin has thus been observed for arable soil (e.g. van Bergen et al., 1997; Gleixner et al., 2002). Accordingly, decoupling resistance to drastic laboratory hydrolysis from survival under natural conditions may also occur when diagenesis takes place under depositional conditions (to be determined) that promote extensive degradation.

Further information on the composition and resistance to diagenesis of complex HMW lipids is also needed. In fact, as observed in the case of *B. braunii*, such lipids could be important for kerogen, both as algaenan precursors and through condensation upon diagenesis (e.g. Metzger and Largeau, 1999). Studies of the structure and diagenetic fate of lipid-containing biomolecules are also essential. Indeed, as noted for protein/polysaccharide complexes in chitin, the complexation of lipids with other components, for example in glycolipids, may induce a greater resistance to diagenetic degradation and hence a greater contribution to kerogen moieties. The hydrophobic nature of such complexes should also be assessed because a few observations, reviewed by Hedges et al. (2000), point to a major role for hydrophobicity in resistance to diagenetic degradation.

9.2.3. Study of OM in soil and recent sediments

Parallel examination of OM in soil and recent sediments is of prime importance for kerogen studies. Indeed, the latter should largely benefit from advances in the elucidation of the structure, sources and transformations of the OM occurring in these modern environments, especially of the so-called ''molecularly-uncharacterized component'' (Hedges et al., 2000) that represents a major part of the total organic fraction. Such ''uncharacterized'' components should largely originate from the diagenetic transformation of the deposited bioproducts. However, observations on sediments also point to additional contributions, sometimes in substantial amounts, of other types of materials, like weathered fossil OM and black carbon. The input of such materials to sedimentary rocks could have important consequences for the abundance and composition of the eventually formed kerogen.

The weathering of ancient OM is considered a major process in the global carbon cycle and in the control of the composition of the Earth's atmosphere (e.g. Petsch and Berner, 1998). The changes in kerogen abundance and composition, associated with the first steps in weathering, were examined in various formations (Petsch et al., 2000, 2001a, and references therein). Extensive mineralization generally occurs during weathering and, as shown by radiocarbon measurements, some of the generated products are used as carbon sources by bacteria (Petsch et al., 2001b). However, a significant part of the weathered kerogen can escape complete degradation to CO_2 and be buried again in sediments. The presence of ancient OM has thus been detected in various modern sediments through global, molecular and isotopic studies (e.g. Eglinton et al., 1997; Leithold and Blair, 2001 and references therein; Dickens et al., 2004). The total amount of ancient OM thus reburied remains largely unknown; it is controlled by several factors, including the rate of physical erosion and the rate of transport to the new depositional setting. Materials derived from kerogen weathering may account for a substantial part of the ''uncharacterized'' (or poorly characterized) OM in sedimentary rocks and thus significantly influence the quantitative and qualitative features of kerogen.

The bulk of the OM carried by rivers to the sea is derived from soil through leaching or erosion (Hedges et al., 1994; Hedges and Oades, 1997, and references therein). Global budgets and distribution estimates pointed to extensive mineralization of this terrestrial material at sea through (a) mechanism(s) that is (are) largely unknown (Hedges et al., 1997). However, examination of Quaternary sediments from the Niger and Congo deep sea fans showed that SOM contribution to marine sediments can be abundant at least for continental margins; the nature of this contribution and its extent relative to marine OM are thought to be climate driven (Holtvoeth et al., 2005).

Black carbon (BC) has probably remained unnoticed or greatly underestimated in the study of various kerogen samples so far. As stressed below, this is due to specific analytical difficulties in relation to BC definition and nature. In fact, BC is a collective term for the residues of incomplete combustion of organic materials. These complex polyaromatic structures are formed by wood and fossil fuel burning and by natural vegetation fires. BC is widely distributed over the entire surface of the earth and might play a major role as a sink in the global C cycle via burial in marine sediments (Kuhlbusch and Crutzen, 1995; Lim and Cachier, 1996; Gustafsson and Gschwend, 1998). OM analysis of a number of marine sediments pointed to a highly variable proportion of BC, from only 2% up to 90% of TOC (e.g. Lim and Cachier, 1996; Gustafsson and Gschwend, 1998; Massiello and Druffel, 1998; Middelburg et al., 1999). However, BC quantification is difficult (e.g. Gustafsson et al., 2001; Quénéa et al., 2006c), and such a wide span may partly (or even mostly) reflect differences in analytical methods. Indeed, different methods applied to complex environmental matrices such as marine sediments afford variable BC contents as shown by intercomparison (e.g. Middelburg et al., 1999; Schmidt et al., 2001). BC exhibits a relatively high resistance to diagenetic degradation, as shown by studies of soil OM (e.g. Poirier et al., 2000, 2001, 2003; Quénéa et al., 2005) and is found in sedimentary rocks as old as Devonian (see Schmidt and Noack, 2000 for a review). However, degradation of charcoal particles was observed, via analysis of the generated water-soluble products using ultrahigh resolution mass spectrometry, over a period of 100 years in a temperate forest soil (Hockaday et al., 2006). As a result of the problems encountered with BC quantification, the extent of its contribution to total OM both in recent sediments and in kerogen is largely unknown. Furthermore, such highly aromatic and condensed material is detected inefficiently with the tools (like conventional solid state CP/MAS ^{13}C NMR and pyrolysis) classically used for kerogen studies (e.g. Derenne et al., 1987; Smernik et al., 2006). This drawback is especially important when BC occurs along with aliphatic products as illustrated by studies of mixtures of model compounds (Poirier et al., 2000). Carbon atoms in polyaromatic materials can be detected by way of Bloch decay measurements but this method is time consuming and so is not systematically used (e.g. Maroto-Valer et al., 1996; Preston, 1996). Therefore, BC remains probably unnoticed or greatly underestimated in the study of various kerogen samples. However, aromatic C detection using CP/MAS ^{13}C NMR can be improved by using a high spinning rate and ramped amplitude (Simpson and Hatcher, 2004; Knicker et al., 2005).

9.3. Physical protection

Several important points related to this topic have still to be elucidated. Protection by minerals could result from adsorption on to mineral grains and/or within nanopores or from alternating organic and clay nanolayers. The features that control the implications of these different processes, such as the composition of clay minerals and of deposited OM and sedimentation conditions, are still unclear. Moreover, the monolayer/adsorption model has been challenged, based on calculation, bulk analysis and TEM results (Ransom et al., 1997, 1998) and on studies of recent marine sediments using density fractionation and XPS (Bock and Mayer, 2000; Arnarson and Keil, 2001). Simple sorption to minerals was considered in the latter studies to play only a minor role in OM protection by clay in continental sediment margins (see also Pichevin et al., 2004). In fact, formation of organo-mineral aggregates is probably implicated, along with a patchy distribution of the OM at discrete spots on mineral surfaces.

In addition to simple physical protection, minerals could be implicated in OM preservation via other types of processes. Thus, it was considered (Petrovich, 2001) that adsorption of Fe^{2+} to potentially labile structural biopolymers, like cellulose and collagen, would promote preservation through (i) inhibition by the adsorbed ions to further bacterial degradation and (ii) formation of a coating of clay minerals by nucleation with these ions. Such a process would account for the perfect morphological preservation of soft tissues observed in various formations such as the Burgess Shale (middle Cambrian, Canada). Finally, protection of potentially labile units by encapsulation in resistant organic material has been put forward to account for the survival of proteinaceous materials. The general character of this type of protection and its consequences for kerogen preservation and composition are also important open questions.

10. General conclusions

The study of kerogen has remained a very active field since the publication of the last comprehensive review on this topic edited by Durand (Kerogen, Insoluble Organic Matter from Sedimentary Rocks, Editions Technip, Paris, 1980) and there have been major advances regarding the main questions related to kerogen, such as sources and chemical composition. Great strides were also achieved on understanding preservation processes, especially with the recognition of the selective preservation pathway, and their relationship with depositional environments. The application to kerogen of a large array of new analytical methods, including solid-state ^{13}C NMR spectroscopy, electron microscopy and isotopic studies, played a prominent role in most of these advances.

Kerogen studies also largely benefitted from interaction with other fields, especially biology, owing to increasing knowledge on the chemical composition and ecology of wide groups of living organisms, in particular microbial organisms. In return, kerogen studies provided useful information for a number of other fields, such as studies involving palaeoclimate and palaeoenvironment reconstruction. Such studies are rapidly developing in relation to concerns about present and future climate and modern ecosystems, and with climate influence on OM preservation and the global C cycle. More classically, kerogen studies also continue to be tightly interrelated with oil and natural gas exploration and production. In addition, kerogen degradation under the type of thermal stress that would be associated with the long term disposal of high activity nuclear waste, upon burial in geological formations, and the possible influence of the generated compounds on the effectiveness of the geological barrier, may become an important topic (Deniau et al., 2005a,b).

Continuation and even amplification of the above trends can be foreseen for future work on kerogen. For example, genetic studies of microbial consortia in various environments should afford essential information to help in deciphering the fate of deposited OM in the water column and upper sediment. Along with continuous progress with analytical methods, increasing emphasis should also be put on microscopic analysis for dealing with the morphological, molecular and isotopic features of OM in sedimentary rocks. Such information might be obtained using new microscopy techniques at the molecular scale, coupled with elemental analysis. All this should help organic geochemists to cope with important questions on kerogen that are far from being clarified, such as its molecular structure at different stages in its sedimentary evolution.

In other respects, the information and methods related to kerogen should be essential for developing studies in two fields that encompass major and highly disputed questions: (i) the origin of life on the Earth, via examination of the insoluble organic fraction of the most ancient sedimentary rocks, and (ii) the origin and formation of extraterrestrial organic matter, via the study of the insoluble fraction of meteorites and other extraterrestrial materials (e.g. Sephton and Gilmour, 2001; Binet et al., 2004; Remusat et al., 2005, 2006). In both cases the insoluble macromolecular fraction markedly predominates over the soluble fraction. Furthermore, the problems related to contamination, like migration of OM from relatively younger rocks in studies about early life, are much more easily overcome when considering the insoluble fraction rather than the soluble one.

Finally, kerogen studies will remain of prime importance in relation to the search for new oil and natural gas fields. Indeed, these studies may even become more and more important as explorationists are faced with increasing difficulties due to progressive exhaustion of relatively easily discovered and relatively cheaply produced resources. Pyrolysis techniques have been presented in this paper as a tool for the analysis of kerogen moieties. However they are also widely applied to the reconstruction of petroleum generation in source rocks, by comparing kerogen pyrolysis products with their equivalents obtained upon geological maturation. Kinetic models derived from pyrolysis data at elevated temperature and short duration in the laboratory can be extrapolated to mild heating during long periods of time under geological conditions. It is all the more necessary for modelling the composition and amounts of generated gases, as they can easily migrate out of source rocks and reservoirs, and it is difficult to recover them quantitatively without specific sampling devices. The problem is that the domain in which extrapolation from the laboratory to geological conditions is possible, without changing the chemical reactions of kerogen transformation into oil and gas, is the subject of many discussions. Any improvement in knowledge of kerogen composition and structure may increase the reliability of kinetic models in predicting the amount and composition of generated petroleum products.

This would be very useful for making better estimates of the nature and amounts of hydrocarbon resources before drilling new petroleum plays. In parallel, kerogen studies should be more and more tightly interrelated with other fields such as plate tectonics, palaeoclimate reconstruction and modelling, and the biology of ancient organisms.

Acknowledgements

The authors gratefully acknowledge the help of F. Behar, B. Durand, P. Hatcher and A.Y. Huc for making many constructive comments on earlier versions of the manuscript. Special thanks are due to J.A. Curiale, J.R. Maxwell and L.R. Snowdon for help in editing and reviewing the manuscript, and for being so patient during its long term gestation, the project being initiated at the end of 1999. The review is dedicated to Bernard Durand with whom MV collaborated for many years on research upon kerogen, and to all colleagues and students who worked with us to bring their contributions to the kerogen puzzle.

Associate Editor—**J.R. Maxwell**

Appendix

List of abbreviations

BC Black carbon
BSEM SEM in backscattered electron mode
CP-MAS Cross polarization–magic angle spinning
CSIA Compound-specific isotopic analysis
EDS Electron dispersive spectrometry
EPR Electron paramagnetic resonance
ESCA Electron spectroscopy for chemical analysis
ESI Electrospray ionization
ESR Electron spin resonance
FA Fulvic acids
FT-ICR Fourier transform ion cyclotron resonance
FTIR Fourier transform infrared
GRS Green river shales
HA Humic acids
HI Hydrogen index
HMW High molecular weight
IR Infra red
LOM Level of organic metamorphism
MALDI Matrix-assisted laser desorption ionization
MS Mass spectrometry
NMR Nuclear magnetic resonance
NSO/NSOs Nitrogen sulfur oxygen containing compounds
OC Organic carbon
OI Oxygen index
OM organic matter
OSCs Organosulfur compounds
QqTOF Quadrupole time of flight
SEM Scanning electron microscopy
SRB Sulfate reducing bacteria
TEM Transmission electron microscopy
TFA Trifluoroacetic acid
TMAH Tetramethylammonium hydroxide
TOC Total organic carbon
UV Ultraviolet
VR Vitrinite reflectance
XANES X-ray absorption near edge spectroscopy
XPS X-ray photoelectron spectroscopy

References

Abelson, P.H., 1954. Organic constituents of fossils. Carnegie Institution of Washington Yearbook 53, 97–101.

Acholla, F.V., Orr, W.L., 1993. Pyrite removal from kerogen without altering organic matter: the chromous chloride method. Energy and Fuels 7, 406–410.

Adam, P., Schmid, J.C., Connan, J., Albrecht, P., 1991. 2α and 3β Steroid thiols from reductive cleavage of macromolecular petroleum fraction. Tetrahedron Letters 32, 2955–2958.

Adam, P., Philippe, E., Albrecht, P., 1998. Photochemical sulfurization of sedimentary organic matter: a widespread process occurring at early diagenesis in natural environments?. Geochimica et Cosmochimica Acta 62 265–271.

Adam, P., Schneckenburger, P., Schaeffer, P., Albrecht, P., 2000. Clue to early diagenesis sulfurization process from mild chemical cleavage of labile sulfur-rich macromolecules. Geochimica et Cosmochimica Acta 64, 3485–3503.

Adler, E., 1977. Lignin chemistry. Past, present and future. Wood Science and Technology 11, 169–218.

Ahlers, F., Thom, I., Lambert, J., Kuckuk, R., Wiermann, R., 1999. ^{1}H NMR analysis of sporopollenin from *Typha angustifolia*. Phytochemistry 50, 1095–1098.

Albrecht, P., Vandenbroucke, M., Mandengué, M., 1976. Geochemical studies on the organic matter from the Douala Basin (Cameroon)-I. Evolution of the extractable organic matter and the formation of petroleum. Geochimica et Cosmochimica Acta 40, 791–799.

Allard, B., Templier, J., Largeau, C., 1997. Artifactual origin of mycobacterial bacteran. Formation of melanoidin-like artifactual macromolecular material during the usual isolation process. Organic Geochemistry 26, 691–703.

Allard, B., Templier, J., Largeau, C., 1998. An improved method for the isolation of artifact-free algaenans from microalgae. Organic Geochemistry 28, 543–548.

Allard, B., Rager, M.-N., Templier, J., 2002. Occurrence of high molecular weight lipids (C_{80+}) in the trilaminar outer walls of some freshwater microalgae. A reappraisal of algaenan structure. Organic Geochemistry 33, 789–801.

Alldredge, A.L., Cohen, Y., 1987. Can microscale chemical patches persist in the sea? Microelectrode study of marine snow, fecal pellets. Science 235, 689–691.

Allen, G., Laurier, D., Thouvenin, J., 1979. Etude sédimentologique du delta de la Mahakam. Notes et Mémoires N° 15, Compagnie Française des Pétroles, Paris.

Alpern, B., 1980. Pétrographie du kérogène. In: Durand, B. (Ed.), Kerogen. Editions Technip, Paris, pp. 339–383.

Amblès, A., Grasset, L., Dupas, G., Jacquesy, J.C., 1996. Ester- and ether-bond cleavage in immature kerogens. Organic Geochemistry 24, 681–690.

Amrani, A., Aizenshtat, Z., 2004a. Mechanisms of sulfur introduction are chemically controlled: $\delta^{34}S$ imprint. Organic Geochemistry 35, 1319–1336.

Amrani, A., Aizenshtat, Z., 2004b. Reaction of polysulfide anions with α, β unsaturated isoprenoid aldehydes in aquatic media: simulation of oceanic conditions. Organic Geochemistry 35, 909–924.

Arnarson, T.S., Keil, R.G., 2001. Organic–mineral interactions in marine sediments studied using density fractionation and X-ray photoelectron spectroscopy. Organic Geochemistry 32, 1401–1415.

Arouri, K., Greenwood, P.F., Walter, M.R., 1999. A possible chlorophycean affinity of some Neoproterozoic acritarchs. Organic Geochemistry 30, 1323–1337.

Aycard-Giorgi, M., Derenne, S., Largeau, C., Tribovillard, N., Baudin, F., 2001. Preservation processes of sedimentary organic matter along a core in a euxinic upwelling-influenced basin: The Cariaco Trough (Venezuela), In: 20th International Meeting on Organic Geochemistry, Nancy, France, Abstracts vol. 2, pp. 137–138.

Aycard, M., Derenne, S., Largeau, C., Mongenot, T., Tribovillard, N., Baudin, F., 2003. Formation pathways of protokerogens in Holocene sediments of the upwelling influenced Cariaco Trench, Venezuela. Organic Geochemistry 34, 701–718.

Azevedo, D.A., Zinu, C.J.A., Aquino Neto, F.R., Simoneit, B.R.T., 2001. Possible origin of acyclic (linear and isoprenoid) and tricyclic terpane methyl ketones in a Tasmanian tasmanite bitumen. Organic Geochemistry 32, 443–448.

Baas, M., Briggs, D.E.G., van Heemst, J.D.H., Kear, A.J., de Leeuw, J.W., 1995. Selective preservation of chitin during the decay of shrimp. Geochimica et Cosmochimica Acta 59, 94–951.

Baldock, J.A., Skjemstad, J.O., 2000. Role of the soil matrix and minerals in protecting natural organic materials against biological attack. Organic Geochemistry 31, 697–710.

Bates, A.L., Spiker, E.C., Hatcher, P.G., Stout, S.A., Weintraub, V.C., 1995. Sulfur geochemistry of organic-rich sediments from Mud Lake, Florida, USA. Chemical Geology 121, 245–262.

Behar, F., Vandenbroucke, M., 1986. Représentation chimique de la structure des kérogènes et des asphaltènes en fonction de leur origine et de leur degré d'évolution. Revue de l'Institut Français du Pétrole 41, 173–188.

Behar, F., Vandenbroucke, M., 1987. Chemical modelling of kerogens. Organic Geochemistry 11, 15–24.

Behar, F., Vandenbroucke, M., 1988. Characterization and quantification of saturates trapped inside kerogen: implications for pyrolysate composition. In: Mattavelli, L., Novelli, L. (Ed.), Advances in Organic Geochemistry 1987. Organic Geochemistry 13, 927-938.

Behar, F., Vandenbroucke, M., Teerman, S., Hatcher, P., Leblond, C., Lerat, O., 1995. Experimental simulation of gas generation from coals and a marine kerogen. Chemical Geology 126, 247–260.

Behar, F., Vandenbroucke, M., Tang, Y., Marquis, F., Espitalié, J., 1997. Thermal cracking of kerogen in open and closed systems: determination of kinetic parameters and stoichiometric coefficients for oil and gas generation. Organic Geochemistry 26, 321–339.

Behar, F., Gillaizeau, B., Derenne, S., Largeau, C., 2000. Nitrogen distribution in the pyrolysis products of a type II kerogen (Cenomanian, Italy). Timing of molecular nitrogen production versus other gases. Energy & Fuels 14, 431–440.

Behar, F., Beaumont, V., De Barros-Penteado, H.L., 2001. Rock-Eval 6 technology: performances and developments. Oil & Gas Science and Technology. Revue de l'Institut Français du Pétrole 56, 111–134.

Behar, F., Lewan, M.D., Lorant, F., Vandenbroucke, M., 2003. Comparison of artificial maturation of lignite in hydrous and nonhydrous conditions. Organic Geochemistry 34, 575–600.

Belin, S., 1992a. Application of backscattered electron imaging to the study of source rock microtextures. Organic Geochemistry 18, 333–346.

Belin, S., 1992b. Distribution microscopique de la matière organique disséminée dans les roches-mères. Technique d'étude. Interprétation des conditions de dépôt et de diagenèse, Ph.D. Thesis, Orsay.

Benson, S.W., 1960. The Foundations of Chemical Kinetics. McGraw-Hill Book Company, New York.

Berkaloff, C., Casadevall, E., Largeau, C., Metzger, P., Peracca, S., Virlet, J., 1983. The resistant polymer of the walls of the hydrocarbon-rich alga *Botryococcus braunii*. Phytochemistry 22, 389–397.

Berner, R.A., 1964. Distribution and diagenesis of sulfur in some sediments from the Gulf of California. Marine Geology 1, 117–140.

Berner, R.A., 1984. Sedimentary pyrite formation: an update. Geochimica et Cosmochimica Acta 48, 605–615.

Berner, R.A., 1985. Sulphate reduction, organic matter decomposition and pyrite formation. Philosophical Transactions of the Royal Society of London A 315, 25–38.

Berner, R.A., 1987. Models for carbon and sulfur cycles and atmospheric oxygen: application to Paleozoic geologic history. American Journal of Science 287, 177–196.

Berner, R.A., 1994. GEOCARBII: a revised model of atmospheric CO_2 over Phanerozoic time. American Journal of Science 294, 56–91.

Bertrand, P., Lallier-Vergès, E., Boussafir, M., 1994. Enhancement of accumulation and anoxic degradation of organic matter controlled by cyclic productivity: a model. Organic Geochemistry 22, 511–520.

Binet, L., Gourier, D., Derenne, S., Robert, F., Ciofini, I., 2004. Occurrence of abundant diradicaloid moieties in the insoluble organic matter from the Orgueil and Murchison meteorites: a fingerprint of its extraterrestrial origin? Geochimica et Cosmochimica Acta 68, 881–891.

Blokker, P., Schouten, S., van den Ende, H., de Leeuw, J.W., Hatcher, P.G., Sinninghe Damsté, J.S., 1998. Chemical structure of algaenans from the fresh water algae *Tetraedron minimum*, *Scenedesmus communis* and *Pediastrum boryanum*. Organic Geochemistry 29, 1453–1468.

Blokker, P., Schouten, S., de Leeuw, J.W., Sinninghe Damsté, J.S., van den Hende, H., 1999. Molecular structure of the resistant biopolymers in the zygospore cell wall of *Chlamydomonas monoica*. Planta 207, 539–543.

Blokker, P., Schouten, S., de Leeuw, J.W., Sinninghe Damsté, J.S., van den Hende, H., 2000. A comparative study of fossil and extant algaenans using ruthenium tetroxide degradation. Geochimica et Cosmochimica Acta 64, 2055–2065.

Blokker, P., van Bergen, P., Pancost, R., Collinson, M.E., de Leeuw, J.W., Sinninghe Damsté, J.S., 2001. The chemical structure of *Gloeocapsomorpha prisca* microfossils: implications for their origin. Geochimica et Cosmochimica Acta 65, 885–900.

Bock, M.J., Mayer, L.M., 2000. Mesodensity organo-clay associations in a nearshore sediment. Marine Geology 163, 65–75.

Boom, A., Sinninghe Damsté, J.S., de Leeuw, J.W., 2005. Cutan, a common aliphatic biopolymer in cuticles of drought-adapted plants. Organic Geochemistry 36, 595–601.

Boon, J.J., 1992. Analytical pyrolysis mass spectrometry: new vistas opened by temperature-resolved in-source Py-MS. International Journal of Mass spectrometry and Ion processes (118/119), 755–787.

Boon, J.J., Klap, V.A., Eglinton, T.I., 1998. Molecular characterization of microgram amounts of oceanic colloidal organic matter by direct temperature-resolved ammonia chemical ionization mass spectrometry. Organic Geochemistry 29, 1051–1061.

Bordenave, M.L., Espitalié, J., Leplat, P., Oudin, J.L., Vandenbroucke, M., 1993. Screening techniques for source rock evaluation. In: Bordenave, M.L. (Ed.), Applied Petroleum Geochemistry. Editions Technip, Paris, pp. 219–278.

Boussafir, M., Gelin, F., Lallier-Vergès, E., Derenne, S., Bertrand, P., Largeau, C., 1995. Electron microscopy and pyrolysis of kerogens from the Kimmeridge Clay Formation, U.K.: source organisms, preservation processes and origin of microcycles. Geochimica et Cosmochimica Acta 59, 3731–3747.

Brassell, S.C., Lewis, C.A., de Leeuw, J.W., de Lange, F., Sinninghe Damsté, J.S., 1986. Isoprenoid thiophenes: novel products of sediment diagenesis? Nature 320, 160–162.

Breger, I.A., 1960. Diagenesis of metabolites and a discussion of the origin of petroleum hydrocarbons. Geochimica et Cosmochimica Acta 19, 297–308.

Brooks, J., Shaw, G., 1978. Sporopollenin: a review of its chemistry, palaeobiochemistry and geochemistry. Grana 17, 91–97.

Brown, S.D., Sirkecioglu, O., Snape, C.E., Eglinton, T.I., 1997. Speciation of the organic sulphur forms in a recent sediment and type I and II-S kerogens by high pressure temperature programmed reduction. Energy & Fuels 11, 532–538.

Brüchert, V., Pratt, L.M., 1996. Contemporaneous early diagenetic formation of organic and inorganic sulfur in estuarine sediments from St. Andrew Bay, Florida, USA. Geochimica et Cosmochimica Acta 60, 2325–2332.

Brukner, A., Vetö, I., 1983. Extracts from the open and closed pores of an upper Triassic sequence from W.Hungary: a contribution to studies of primary migration. In: Bjøroy, M. et al. (Eds.), Advances in Organic Geochemistry 1981. Wiley Heiden Ltd., Chichester, pp. 175–182.

Burges, A., Hurst, H.M., Walkden, B., 1964. The phenolic constituents of humic acid and the relation to the lignin of the plant cover. Geochimica et Cosmochimica Acta 28, 1547–1554.

Burgoyne, T.W., Hayes, J.M., 1998. Quantitative production of H_2 by pyrolysis of gas chromatographic effluents. Analytical Chemistry 70, 5136–5141.

Burlingame, A.L., Haug, P.A., Schnoes, H.K., Simoneit, B.R., 1969. Fatty acids derived from the Green River Formation oil shale by extractions and oxidations – a review. In: Schenck, P.A., Havenaar, I. (Eds.), Advances in Organic Geochemistry 1968. Pergamon Press, Oxford, pp. 85–129.

Burnham, A.K., Braun, R.L., 1999. Global kinetic analysis of complex materials. Energy & Fuels 13, 1–22.

Calvert, S.E., Pedersen, T.F., 1992. Organic carbon in marine sediments: is anoxia important? In: Whelan, J., Farrington, J.W. (Eds.), Organic Matter – Productivity, Accumulation and Preservation in Recent and Ancient Sediments. Columbia University Press, New York, pp. 231–263.

Carlson, G.A., 1992. Computer simulation of the molecular structure of bituminous coal. Energy & Fuels 6, 771–778.

Carmo, A.M., Stankiewicz, B.A., Mastalerz, M., Pratt, L.M., 1997. Factors controlling the abundance of organic sulfur in flash-pyrolyzates of Upper Cretaceous kerogens from Sergipe Basin, Brazil. Organic Geochemistry 26, 587–603.

Carroll, A.R., Bohacs, K.M., 2001. Lake-type controls on petroleum source rock potential in nonmarine basins. American Association of Petroleum Geologists Bulletin 85, 1033–1053.

Carruthers, R.G., Caldwell, W., Steuart, D.R., 1912. The Oil Shales of the Lothians. HMSO, Edinburgh, 201pp.

Chermin, H.A.G., van Krevelen, D.W., 1957. Chemical structure and properties of coal XVII – a mathematical model of coal pyrolysis. Fuel 36, 85–104.

Chou, C.L., 1990. Geochemistry of sulfur in coal. In: Orr, W.L., White, C.M. (Eds.), Geochemistry of Sulfur in Fossil Fuels, ACS Symposium Series, vol. 429. American Chemical Society, Washington, DC, pp. 30–52.

Clayton, J.L., Rice, D.D., Michael, G.E., 1991. Oil-generating coals of the San Juan Basin, New Mexico and Colorado, USA. Organic Geochemistry 17, 735–742.

Clifford, D.J., Carson, D.M., McKinney, D.E., Bortiatynski, J.M., Hatcher, P.G., 1995. A new rapid technique for the characterization of lignin in vascular plants: thermochemolysis with tetramethylammonium hydroxide (TMAH). Organic Geochemistry 23, 167–175.

Collins, M.J., Bishop, A.N., Farrimond, P., 1995. Sorption by mineral surfaces: rebirth of the classical condensation pathway for kerogen formation? Geochimica et Cosmochimica Acta 59, 2387–2391.

Collinson, M.E., van Bergen, P.F., Scott, A., de Leeuw, J.W., 1994. The oil-generating potential of plants from coal and coal-bearing strata through time: a review with new evidence from Carboniferous plants. In: Scott, A.C., Fleet, A.J. (Eds.), Coal and Coal-bearing Strata as Oil-prone Source Rocks, vol. 77. Geological Society Special Publications, pp. 31–67.

Combaz, A., 1980. Les kérogènes vus au microscope. In: Durand, B. (Ed.), Kerogen. Editions Technip, Paris, pp. 55–111.

Combaz, A., de Matharel, M., 1978. Organic sedimentation and genesis of petroleum in Mahakam delta, Borneo. American Association of Petroleum Geologists Bulletin 62, 1684–1695.

Corre, G., Templier, J., Largeau, C., Rousseau, B., Berkaloff, C., 1996. Influence of cell wall composition on the resistance of two Chlorella species (Chlorophyta) to detergents. Journal of Phycology 32, 584–590.

Dale, B., 1983. Dinoflagellate resting cysts: benthic plankton. In: Fryxell, G.A. (Ed.), Survival Strategies of the Algae. Cambridge University Press, Cambridge, pp. 69–136.

de Leeuw, J.W., Sinninghe Damsté, J.S., 1990. Organic sulfur compounds and other biomarkers as indicators of palaeosalinity. In: Orr, W.L., White, C.M. (Eds.), Geochemistry of Sulfur in Fossil Fuels, American Chemical Society Symposium Series, vol. 429. American Chemical Society, Washington, DC, pp. 417–443.

de Leeuw, J.W., van Bergen, P.F., van Aarsen, B.G.K., Gatellier, J.P.L.A., Sinninghe Damsté, J.S., Collinson, M.E., 1991. Resistant biomacromolecules as major contributors to kerogen. Philosophical Transactions of the Royal Society of London Series B 333, 329–337.

de Leeuw, J.W., Largeau, C., 1993. A review of macromolecular compounds that comprise living organisms and their role in kerogen, coal and petroleum formation. In: Engel, M.H., Macko, S.A. (Eds.), Organic Geochemistry – Principles and Applications. Plenum Press, New York, pp. 23–72.

de Poncins, P., 1950. La chimie des macromolécules. Son application à l'étude de la composition chimique des houilles, des cokes et des brais. In: Association Technique de l'Industrie du Gaz en France (Ed.), Compte rendu du 66e Congrès de l'Industrie du Gaz. Barnéoud frères et Cie, Laval, pp. 590–596.

del Rio, J.C., Olivella, M.A., Knicker, H., de las Heras, F.X.C., 2004. Preservation of peptide moieties in three Spanish sulfur-rich Teriary kerogens. Organic Geochemistry 35, 993–999.

Demaison, G.J., Moore, G.T., 1980. Anoxic environments and oil source bed genesis. American Association of Petroleum Geologists Bulletin 64, 1179–1209.

Deming, J.W., Baross, J.A., 1993. The early diagenesis of organic matter: bacterial activity. In: Engel, M.H., Macko, S.A. (Eds.), Organic Geochemistry – Principles and Applications. Plenum Press, New York, pp. 119–144.

Deniau, I., Derenne, S., Beaucaire, C., Pitsch, H., Largeau, C., 2001. Morphological and chemical features of a kerogen from the underground Mol laboratory (Boom Clay Formation, Oligocene, Belgium): structure, source organisms and formation pathways. Organic Geochemistry 32, 1343–1356.

Deniau, I., Derenne, S., Beaucaire, C., Pitsch, H., Largeau, C., 2004. Occurrence and nature of thermolabile compounds in the Boom Clay kerogen (Oligocene, underground Mol Laboratory, Belgium). Organic Geochemistry 35, 91–107.

Deniau, I., Derenne, S., Beaucaire, C., Pitsch, H., Largeau, C., 2005a. Simulation of thermal stress influence on the Boom Clay kerogen (Oligocene, Belgium) in relation to long-term storage of high activity nuclear waste. I – study of generated soluble compounds. Applied Geochemistry 20, 587–597.

Deniau, I., Behar, F., Largeau, C., De Cannière, P., Beaucaire, C., Pitsch, H., 2005b. Determination of kinetic parameters and simulation of early CO_2 production from the Boom Clay kerogen under low thermal stress. Applied Geochemistry 20, 2097–2107.

Deport, C., Lemée, L., Amblès, A., 2006. Comparison between humic substances from soil and peats using TMAH and TEAAc thermochemolysis. Organic Geochemistry 37, 649–664.

Derbyshire, F., Marzec, A., Schulten, H.R., Wilson, M.A., Davis, A., Tekely, P., Delpuech, J.J., Jurkiewicz, A., Bronnimann, C.E., Wind, R.A., Maciel, G.E., Narayan, R., Bartle, K., Snape, C., 1989. Molecular structure of coals: a debate. Fuel 68, 1091–1106.

Derenne, S., Largeau, C., Casadevall, E., Lauprêtre, F., 1987. The quantitative analyse of coals and kerogens by ^{13}C CP/MAS NMR. Journal de Chimie Physique 84, 754–756.

Derenne, S., Largeau, C., Casadevall, E., Berkaloff, C., 1989. Occurrence of a resistant biopolymer in the *L* race of *Botryococcus braunii*. Phytochemistry 28, 1137–1142.

Derenne, S., Largeau, C., Casadevall, E., Sinninghe-Damsté, J.S., Tegelaar, E.W., de Leeuw, J.W., 1990. Characterization of Estonian Kukersite by spectroscopy and pyrolysis: evidence for abundant alkyl phenolic moieties in an Ordovician, marine, type II/I kerogen. In: Durand, B., Behar, F. (Eds.), Advances in Organic Geochemistry 1989, Organic Geochemistry, vol. 16. Pergamon Press, Oxford, pp. 873–888.

Derenne, S., Largeau, C., Casadevall, E., Berkaloff, C., Rousseau, B., 1991. Chemical evidence of kerogen formation in source rocks and oil shales via selective preservation of thin resistant outer walls of microalgae: origin of ultralaminae. Geochimica et Cosmochimica Acta 55, 1041–1050.

Derenne, S., Metzger, P., Largeau, C., van Bergen, P.F., Gatellier, J.P., Sinninghe Damsté, J.S., de Leeuw, J.W., 1992a. Similar morphological and chemical variations of *Gloeocapsomorpha prisca* in Ordovician sediments and cultured *Botryococcus braunii* as a response to changes in salinity. Organic Geochemistry 19, 299–313.

Derenne, S., Largeau, C., Berkaloff, C., Rousseau, B., Wilhelm, C., Hatcher, P.G., 1992b. Non-hydrolysable macromolecular constituents from outer walls of *Chlorella fusca* and *Nanochlorum eucaryotum*. Phytochemistry 31, 1923–1929.

Derenne, S., Largeau, C., Hatcher, P.G., 1992c. Structure of *Chlorella fusca* algaenan: relationships with ultralaminae in lacustrine kerogens; species- and environment-dependent variations in the composition of fossil ultralaminae. Organic Geochemistry 18, 417–422.

Derenne, S., Le Berre, F., Largeau, C., Hatcher, P.G., Connan, J., Raynaud, J.F., 1992d. Formation of ultralaminae in marine kerogens via selective preservation of thin resistant outer walls of microalgae. Organic Geochemistry 19, 345–350.

Derenne, S., Largeau, C., Hatcher, P.G., 1996. First example of an algaenan yielding an aromatic-rich pyrolysate. Possible geochemical implications on marine kerogen formation. Organic Geochemistry 24, 617–627.

Derenne, S., Largeau, C., Hetényi, M., Brukner-Wein, A., Connan, J., Lugardon, B., 1997. Chemical structure of the organic matter in a Pliocene maar-type oil shale. Implicated *Botryococcus* races and formation pathways. Geochimica et Cosmochimica Acta 61, 1879–1889.

Derenne, S., Knicker, H., Largeau, C., Hatcher, P.G., 1998. Timing and mechanisms of changes in nitrogen functionality during biomass fossilization. In: Stankiewicz, B.A., van Bergen, P.F. (Eds.), Nitrogen-Containing Macromolecules in the Bio- and Geosphere, American Chemical Society Symposium Series, vol. 707. American Chemical Society, Washington, DC, pp. 243–253.

Derenne, S., Largeau, C., Brukner-Wein, A., Hetenyi, M., Bardoux, G., Mariotti, A., 2000. Origin of variations in organic matter abundance and composition in a lithologically

homogeneous maar-type oil shale deposit (Gérce, Pliocene, Hungary). Organic Geochemistry 31, 787–798.

Deshmukh, A.P., Simpson, A.J., Hadad, C.M., Hatcher, P.G., 2005. Insights in the structure of cutin and cutan from. Agave americana leaf cuticle using HRMAS NMR spectroscopy. Organic Geochemistry 36, 1072–1085.

Dickens, A.F., Masiello, C.A., Gélinas, Y., Hedges, J.I., 2004. Reburial of fossil carbon in marine sediments. Nature 427, 336–339.

Dignac, M.-F., Zegouagh, Y., Loiseau, L., Bardoux, G., Baruiso, E., Largeau, C., Derenne, S., Mariotti, A., 2004. Pyrolytic study of the non-extractable residues of ^{13}C-atrazine in soil size fractions and soil humin. In: Ghabbour, E., Davies, G. (Eds.), Humic Substances: Nature's Most Versatile Materials. Taylor & Francis Inc., New York, pp. 161–172.

Djuricić, M., Murphy, R.C., Vitorović, D., Biemann, K., 1971. Organic acids obtained by alkaline permanganate oxidation of kerogen from the Green River (Colorado) shale. Geochimica et Cosmochimica Acta 35, 1201–1207.

Domazetis, G., James, B.D., 2006. Molecular models of brown coal containing inorganic species. Organic Geochemistry 37, 244–259.

Dorbon, M., Schmitter, J.M., Garrigues, P., Ignatiadis, I., Ewald, M., Arpino, P., Guiochon, G., 1984. Distribution of carbazole derivatives in petroleum. Organic Geochemistry 7, 111–120.

Douglas, A.G., Sinninghe Damsté, J.S., Fowler, M.G., Eglinton, T.I., de Leeuw, J.W., 1991. Flash pyrolysis of Ordovician kerogens: unique distributions of hydrocarbons and sulphur compounds released from the fossilized alga *Gloeocapsomorpha prisca.*. Geochimica et Cosmochimica Acta 55, 275–291.

Down, A.L., Himus, G.W., 1941. A preliminary study of the chemical constitution of kerogen. Journal of the Institute of Petroleum 27, 426–445.

Dragojlović, V., Bajc, S., Amblès, A., Vitorović, D., 2005. Ether and ester moieties in Messel shale kerogen examined by hydrolysis/ruthenium tetroxide oxidation/hydrolysis. Organic Geochemistry 36, 1–12.

Durand, B., Espitalié, J., 1973. Evolution de la matière organique au cours de l'enfouissement des sédiments. Compte rendus de l'Académie des Sciences (Paris) 276, 2253–2256.

Durand, B., 1975. Indices optiques, potentiel pétrolier et histoire thermique des sédiments. In: Alpern, B. (Ed.), Pétrographie de la Matière Organique des Sédiments, Relations avec la Paléotempérature et le Potentiel Pétrolier Editions du CNRS (Centre National de la Recherche Scientifique), Paris, pp. 205–215.

Durand, B., Espitalié, J., 1976. Geochemical studies on the organic matter from the Douala Basin (Cameroon)-II. Evolution of kerogen. Geochimica et Cosmochimica Acta 40, 801–808.

Durand, B., Marchand, A., Amiell, J., Combaz, A., 1977a. Etude de kérogènes par résonance paramagnétique électronique. In: Campos, R., Goñi, J. (Eds.), Advances in Organic Geochemistry 1975. ENADIMSA, Madrid, pp. 753–779.

Durand, B., Nicaise, G., Roucaché, J., Vandenbroucke, M., Hagemann, H.W., 1977b. Etude géochimique d'une série de charbons. In: Campos, R., Goñi, J. (Eds.), Advances in Organic Geochemistry 1975. ENADIMSA, Madrid, pp. 601–631.

Durand, B., 1980. Sedimentary organic matter and kerogen. Definition and quantitative importance of kerogen. In: Durand, B. (Ed.), Kerogen, Insoluble Organic Matter from Sedimentary Rocks. Editions Technip, Paris, pp. 13–34.

Durand, B., Nicaise, G., 1980. Procedures of kerogen isolation. In: Durand, B. (Ed.), Kerogen, Insoluble Organic Matter from Sedimentary Rocks. Editions Technip, pp. 35–53.

Durand, B., Monin, J.C., 1980. Elemental analysis of kerogens. In: Durand, B. (Ed.), Kerogen, Insoluble Organic Matter from Sedimentary Rocks. Editions Technip, Paris, pp. 113–142.

Durand, B., Huc, A.Y., Oudin, J.L., 1987. Oil saturation and primary migration: observations in shales and coals from the Kerbau wells, Mahakam delta, Indonesia. In: Doligez, B. (Ed.), Proceedings of the 3rd Institut Français du Pétrole Exploration Research Conference, Carcans France. Editions Technip, Paris, pp. 173–195.

Durand, B., 1988. Understanding of HC migration in sedimentary basins (present state of knowledge). Organic Geochemistry 13, 445–459.

Durand-Souron, C., 1980. Thermogravimetric analysis and associated techniques applied to kerogens. In: Durand, B. (Ed.), Kerogen, Insoluble Organic Matter from Sedimentary Rocks. Editions Technip, Paris, pp. 143–161.

Durand-Souron, C., Boulet, R., Durand, B., 1982. Formation of methane and hydrocarbons by pyrolysis of immature kerogens. Geochimica et Cosmochimica Acta 46, 1193–1202.

Duval, B.C., Cramez, C., Vail, P.R., 1998. Stratigraphic cycles and major marine source rocks. In: de Graciansky, P.C., Hardenbol, J., Jacquin, T., Vail, P.R. (Ed.), Mesozoic and Cenozoic Sequence Stratigraphy of European Basins. SEPM (Society for Sedimentary Geology) Special Publication 60, Tulsa, pp. 43–51.

Eglinton, T.I., Sinninghe Damsté, J.S., Kohnen, M.E.L., de Leeuw, J.W., 1990. Rapid estimation of organic sulfur content of kerogens, coals and asphaltenes by flash pyrolysis-gas chromatography. Fuel 69, 1394–1404.

Eglinton, T.I., 1994. Carbon isotopic evidence for the origin of macromolecular aliphatic structure in kerogen. Organic Geochemistry 21, 721–735.

Eglinton, T.I., Irvine, J.E., Vairavamurthy, A., Zhou, W., Manowitz, B., 1994. Formation and diagenesis of macromolecular organic sulfur in Peru margin sediments. Organic Geochemistry 22, 781–799.

Eglinton, T.I., Benitez-Nelson, B.C., Pearson, A., McNichol, A.P., Bauer, J.E., Drufell, E.R.M., 1997. Variability in organic carbon ages of individual organic compounds from marine sediments. Science 277, 769–799.

Espitalié, J., Madec, M., Tissot, B., Mennig, J.J., Leplat, P., 1977. Source rock characterization method for petroleum exploration. Paper OTC (Offshore Technology Conference) 2935, pp. 439–444.

Espitalié, J., Senga-Makadi, K., Trichet, J., 1984. Role of the mineral matrix during kerogen pyrolysis. In: Schenck, P.A., de Leeuw, J.W., Lijmbach, G.W.M. (Eds.), Advances in Organic Geochemistry 1983, Organic Geochemistry 6, 365-382.

Espitalié, J., Deroo, G., Marquis, F., 1985. La pyrolyse Rock-Eval et ses applications. Revue de l'Institut Français du Pétrole, Part I 40, 563–578, Part II, 40, 755–784; Part III, 41, 73–89.

Espitalié, J., Bordenave, M.L., 1993. Rock-Eval pyrolysis. In: Bordenave, M.L. (Ed.), Applied Petroleum Geochemistry. Editions Technip, Paris, pp. 237–261.

Eusterhues, K., Rumpel, C., Kleber, M., Kögel-Knabner, I., 2003. Stabilisation of soil organic matter by interactions

with minerals as revealed by mineral dissolution and oxidative degradation. Organic Geochemistry 34, 1591–1600.

Evitt, W.R., 1961. Observations on the morphology of fossil dinoflagellates. Micropaleontology 7, 385–420.

Faegri, K., 1971. The preservation of sporopollenin membranes under natural conditions. In: Brooks, J., Grant, P., Muir, M.D., Shaw, G., van Gijzel, P. (Eds.), Sporopollenin. Academic Press, London, pp. 256–272.

Faulon, J.L., Vandenbroucke, M., Drappier, J.M., Behar, F., Romero, M., 1990. 3D chemical model for geological macromolecules. In: Durand, B., Behar, F. (Eds.), Advances in Organic Geochemistry 1989, Organic Geochemistry, vol. 16. Pergamon Press, Oxford, pp. 981–993.

Faulon, J.L., Hatcher, P.G., Carlson, G.A., Wenzel, K.A., 1993. A computer-aided molecular model for high volatile bituminous coal. Fuel Processing Technology 34, 277–293.

Faulon, J.L., 1995. Unraveling complex molecules. Chemtech January 1995, 16–23.

Fester, J.I., Robinson, W.E., 1966. Oxygen functional groups in Green River oil-shale kerogen and trona acids. In: Gould, R.F. (Ed.), Coal Science. American Chemical Society, Washington, DC, pp. 22–31.

Filley, T.R., Minard, R.D., Hatcher, P.G., 1999. Tetramethylammonium hydroxide (TMAH) thermochemolysis: proposed mechanisms based upon the application of ^{13}C-labeled TMAH to a synthetic model lignin dimer. Organic Geochemistry 30, 607–621.

Filley, T.R., Hatcher, P.G., Shortle, W.C., Praseuth, R.T., 2000. The application of ^{13}C-labeled tetramethylammonium hydroxide (^{13}C-TMAH) thermochemolysis to the study of fungal degradation of wood. Organic Geochemistry 31, 181–198.

Filley, T.R., Freeman, K.T., Wilkins, R.T., Hatcher, P.G., 2002a. Biogeochemical controls on reaction of organic matter and aqueous sulfites in Holocene sediments of Mud Lake, Florida. Geochimica et Cosmochimica Acta 66, 937–954.

Filley, T.R., Cody, G.D., Goodell, B., Jellison, J., Noser, C., Ostrofsky, A., 2002b. Lignin demethylation and polysaccharide decomposition in spruce sapwood degraded by brown rot fungi. Organic Geochemistry 33, 111–124.

Flaig, W., 1966. The chemistry of humic substances. In: The Use of Isotopes in Soil Organic Matter Studies. Pergamon, New York, pp. 103–127.

Flaig, W., Beutelspacher, H., Rietz, E., 1975. Chemical composition and physical properties of humic substances. In: Gieseking, J.E. (Ed.), Soil Components, Organic Components, vol. 1. Springer Verlag, New York, pp. 1–211.

Flaig, W., 1988. Generation of model chemical precursors. In: Frimmel, F.H., Christman, R.F. (Eds), Humic Substances and their Role in the Environment. Dahlem Workshop Reports, Wiley, Chichester, pp. 75–92.

Flannery, M.B., Stott, A.W., Briggs, D.E.G., Evershed, R.P., 2001. Chitin in the fossil record: identification and quantification of D-glucosamine. Organic Geochemistry 32, 745–754.

Flaviano, C., Le Berre, F., Derenne, S., Largeau, C., Connan, J., 1994. First indications of the formation of kerogen amorphous fractions by selective preservation. Role of non-hydrolysable macromolecular constituents of eubacterial cell walls. Organic Geochemistry 22, 759–771.

Foriel, J., Philippot, P., Susini, J., Dumas, P., Somogyl, A., Salomé, M., Khodia, H., Ménez, B., Fouquet, Y., Moreira, D., López-García, P., 2004. High-resolution imaging of sulfur oxidation states, trace elements, and organic molecules distribution in individual microfossils and contemporary microbial filaments. Geochimica et Cosmochimica Acta 68, 1561–1569.

Forsman, J.P., 1963. Geochemistry of kerogen. In: Breger, I.A. (Ed.), Organic Geochemistry, Earth Series Monograph, vol. 16. Pergamon Press, Oxford, pp. 148–182.

Forsman, J.P., Hunt, J.M., 1958. Insoluble organic matter (kerogen) in sedimentary rocks. Geochimica et Cosmochimica Acta 15, 170–182.

François, R., 1987. A study of sulphur enrichment in the humic fraction of marine sediments during early diagenesis. Geochimica et Cosmochimica Acta 51, 17–27.

François, R., 1990. Marine sedimentary humic substances: structure, genesis and properties. Aquatic Sciences 3, 41–80.

Freeman, K.H., Hayes, J.M., Trendel, J.-M., Albrecht, P., 1990. Evidence from carbon isotope measurements for diverse origins of sedimentary hydrocarbons. Nature 343, 254–256.

Froelich, P.N., Klinkhammer, G.P., Bender, M.L., Luedtke, N.A., Heath, G.R., Cullen, D., Dauphin, P., Hammond, D., Hartman, B., Maynard, V., 1979. Early oxidation of organic matter in pelagic sediments of the Eastern equatorial Atlantic: Suboxic diagenesis. Geochimica et Cosmochimica Acta 43, 1075–1090.

Fuchs, W., Sandhoff, A.G., 1942. Theory of coal pyrolysis. Industrial and Engineering Chemistry 34, 567–571.

Furukawa, Y., 2000. Enegy-filtering transmission electron microscopy (EFTEM) and electron energy-loss spectroscopy (EELS) investigations of clay-organic matter aggregates in aquatic sediments. Organic Geochemistry 31, 735–744.

Garcette-Lepecq, A., Derenne, S., Largeau, C., Bouloubassi, I., Saliot, A., 2000. Origin and formation pathways of kerogen-like organic matter in recent sediments off the Danube Delta (northwestern Black Sea). Organic Geochemistry 31, 1663–1683.

Garcette-Lepecq, A., Derenne, S., Largeau, C., Bouloubassi, I., Saliot, A., 2001. Thermally assisted hydrolysis and methylation of kerogen-like organic matter in a recent sediment off the Danube delta (northwestern Black Sea). Journal of Analytical and Applied Pyrolysis 61, 147–164.

Gatellier, J.P., de Leeuw, J.W., Sinninghe-Damsté, J.S., Derenne, S., Largeau, C., Metzger, P., 1993. A comparative study of macromolecular substances of a Coorongite and cell walls of the extant alga *Botryococcus braunii*. Geochimica et Cosmochimica Acta 57, 2053–2068.

Gavalas, G.R., Jain, R., Cheong, P.H., 1981. Model of coal pyrolysis. 2. Quantitative formulation and results. Industrial and Engineering Chemistry Fundamentals 20, 122–132.

Gelin, F., Sinninghe Damsté, J.S., Harrison, W.N., Maxwell, J.R., de Leeuw, J.W., 1995. Molecular indicators for paleoenvironmental changes in a Messinian evaporitic sequence (Vena del Geso, Italy): III. Stratigraphic changes in the molecular structure of kerogen in a single marl bed as revealed by flash pyrolysis. Organic Geochemistry 23, 555–566.

Gelin, F., Boogers, I., Nooderloos, A.A.M., Sinninghe Damsté, J.S., Hatcher, P.G., de Leeuw, J.W., 1996. Novel, resistant microalgal polyethers: an important sink in the marine environment? Geochimica et Cosmochimica Acta 60, 1275–1280.

Gelin, F., Boogers, I., Noordeloos, A.A.M., Sinninghe Damsté, J.S., Riegman, R., de Leeuw, J.W., 1997. Resistant biomacromolecules in marine microalgae of the classes Eustigmatophyceae and Chlorophyceae: Geochemical implications. Organic Geochemistry 26, 659–675.

Gelin, F., Kok, M.D., de Leeuw, J.W., Sinninghe Damsté, J.S., 1998. Laboratory sulfurisation of the marine microalga *Nannochloropsis salina*. Organic Geochemistry 29, 1837–1848.

Gelin, F., Volkman, J.K., Largeau, C., Derenne, S., Sinninghe Damsté, J.S., de Leeuw, J.W., 1999. Distribution of aliphatic, nonhydrolysable biopolymers in marine microalgae. Organic Geochemistry 30, 147–159.

Gélinas, Y., Baldock, J.A., Hedges, J.I., 2001. Demineralization of marine and freshwater sediments for CP/MAS ^{13}C NMR analysis. Organic Geochemistry 32, 677–693.

Gillaizeau, B., Derenne, S., Largeau, C., Berkaloff, C., Rousseau, B., 1996. Source organisms and formation pathway of the kerogen of the Göynük Oil Shale (Oligocene, Turkey) as revealed by electron microscopy, spectrometry and pyrolysis. Organic Geochemistry 24, 671–679.

Gillaizeau, B., Behar, F., Derenne, S., Largeau, C., 1997. Nitrogen fate during laboratory maturation of a type I kerogen (Oligocene, Turkey) and related algaenan: nitrogen mass balances and timing of N_2 production versus other gases. Energy & Fuels 11, 1237–1249.

Given, P.H., 1960. The distribution of hydrogen in coals and its relation to coal structure. Fuel 39, 147–153.

Gleixner, G., Bol, R., Balesdent, J., 1999. Molecular insight into soil carbon turnover. Rapid Communications in Mass Spectrometry 13, 1278–1283.

Gleixner, G., Poirier, N., Bol, R., Balesdent, J., 2002. Molecular dynamics of organic matter in a cultivated soil. Organic Geochemistry 33, 357–366.

Goldhaber, M.B., Kaplan, I.R., 1974. The sulfur cycle. In: Goldberg, E.D. (Ed.), The Sea, Marine Chemistry, vol. 5. Wiley and Sons, New York, pp. 569–655.

Goldhaber, M.B., Kaplan, I.R., 1975. Controls and consequences of sulfate reduction rates in recent marine sediments. Soil Science 119, 42–55.

Goldhaber, M.B., Kaplan, I.R., 1980. Mechanisms of sulfur incorporation and isotope fractionation during early diagenesis in sediments of the Gulf of California. Marine Chemistry 9, 95–143.

Goñi, M.A., Nelson, B., Blanchette, R.A., Hedges, J.I., 1993. Fungal degradation of wood lignins: geochemical perspectives from CuO-derived phenolic dimers and monomers. Geochimica et Cosmochimica Acta 57, 3985–4002.

Goth, K., de Leeuw, J.W., Püttmann, W., Tegelaar, E.W., 1988. Origin of Messel Oil Shale kerogen. Nature 36, 759–761.

Gransch, J.A., Posthuma, J., 1974. On the origin of sulphur in crudes. In: Tissot, B., Bienner, F. (Eds.), Advances in Organic Geochemistry 1973. Editions Technip, Paris, pp. 727–739.

Graubau, A.W., 1936. Oscillation or pulsation. In: International Geological Congress, Report of the 16th session, vol. 1, pp. 539–553.

Greenwood, P.F., George, S.C., Hall, K., 1998. Applications of laser micropyrolysis–gas chromatography–mass spectrometry. Organic Geochemistry 29, 1075–1089.

Greenwood, P.F., Guthrie, E.A., Hatcher, P.G., 2000. The in situ analytical pyrolysis of two different organic components of a synthetic environmental matrix doped with (4,9-^{13}C) pyrene. Organic Geochemistry 31, 635–643.

Gubatz, S., Rittscher, M., Meuter, A., Nagler, A., Wiermann, R., 1993. Tracer experiments on sporopollenin biosynthesis. Grana 1 (Suppl.), 12–17.

Guilford, W.J., Schneider, D.M., Labovitz, J., Opella, S.J., 1988. High resolution solid-state ^{13}C NMR investigation of sporopollenin from different plant taxa. Plant Physiology 86, 134–136.

Gustafsson, O., Gschwend, Ph.M., 1998. The flux of black carbon to surface sediments on the New England continental shelf. Geochimica et Cosmochimica Acta 62, 465–472.

Gustafsson, O., Bucheli, T.D., Kukulska, Z., Andersson, M., Largeau, C., Rouzaud, J.-N., Reddy, C.M., Eglinton, T.I., 2001. Evaluation of a protocol for the quantification of black carbon in sediments, soils and aquatic particles. Global Biogeochemical Cycles 15, 881–890.

Haider, K., Martin, J.P., 1967. Synthesis and transformation of phenolic compounds by *Epicoccum nigrum* in relation to humic acid formation. Soil Science Society of America Proceedings 31, 766–771.

Haider, K., 1992. Problems related to the humification processes in soils of temperate climates. In: Stokzky, G., Bollag, J.M. (Eds.), Soil Biochemistry. Marcel Dekker Inc., New York, pp. 55–93.

Han, Z., Kruge, M.A., Crelling, J.C., Stankiewicz, B.A., 1995. Organic geochemical characterization of the density fractions of a Permian torbanite. Organic Geochemistry 21, 39–50.

Hartgers, W.A., Sinninghe Damsté, J.S., Requejo, A.G., Allan, J., Hayes, J.M., Ling, Y., Xie, T.-M., Primack, J., de Leeuw, J.W., 1994. Evidence for only minor contribution from bacteria to sedimentary organic carbon. Nature 369, 224–227.

Hartgers, W.A., Lopez, J.F., Sinninghe Damsté, J.S., Reiss, C., Maxwell, J.R., Grimalt, J.O., 1997. Sulfur-binding in recent environments: II. Speciation of sulfur and iron and implications for the occurrence of organo-sulfur compounds. Geochimica et Cosmochimica Acta 61, 4769–4788.

Harvey, G.R., Boran, D.A., 1985. Geochemistry of humic substances in seawater. In: McKnight, D.M., Aiken, G.R., Wershaw, R.L., MacCarthy, P. (Eds.), Humic Substances in Soil, Sediment and Water: Geochemistry, Isolation and Characterization. Wiley & Sons, New York, Chichester, pp. 233–247.

Harvey, G.R., Boran, D.A., Chesal, L.A., Tokar, J.M., 1983. The structure of marine fulvic and humic acids. Marine Chemistry 12, 119–132.

Harwood, R.J., 1977. Oil gas generation by laboratory pyrolysis of Kerogen. American Association of Petroleum Geologists Bulletin 61, 2082–2102.

Hatcher, P.G., Breger, I.A., Szeverenyi, N., Maciel, G.E., 1982. Nuclear magnetic resonance studies of ancient buried wood : II. Observations on the origin of coal from lignite bituminous coal. Organic Geochemistry 4, 9–18.

Hatcher, P.G., Spiker, E.C., Szeverenyi, M., Maciel, G.E., 1983. Selective preservation and origin of petroleum-forming aquatic kerogen. Nature 305, 498–501.

Hatcher, P.G., Breger, I.A., Maciel, G.E., Szeverenyi, N.M., 1985. Geochemistry of humin. In: McKnight, D.M., Aiken, G.R., Wershaw, R.L., MacCarthy, P. (Eds.), Humic Substances in Soil, Sediment and Water: Geochemistry, Isolation and Characterization. Wiley, New York, Chichester, pp. 275–302.

Hatcher, P.G., 1987. Chemical structural studies of natural lignin by dipolar dephasing solid-state ^{13}C nuclear magnetic resonance. Organic Geochemistry 11, 31–39.

Hatcher, P.G., Spiker, E.C., 1988. Selective degradation of plant biomolecules. In: Frimmel, F.H., Christman, R.F. (Eds.), Humic Substances and their Role in the Environment, Dahlem Workshop Reports. Wiley, Chichester, pp. 59–74.

Hatcher, P.G., Nanny, M.A., Minard, R.D., Dible, S.D., Carson, D.M., 1995. Comparison of two thermochemolytic methods for the analysis of lignin in decomposing gymnosperm wood: the CuO oxidation method and the method of thermochemolysis with tetramethylammonium hydroxide (TMAH). Organic Geochemistry 23, 881–888.

Hatcher, P.G., Clifford, D.J., 1997. The organic geochemistry of coal: from plant materials to coal. Organic Geochemistry 27, 251–274.

Havinga, A.J., 1971. An experimental investigation into the decay of pollen and spores in various soil types. In: Brooks, J., Grant, P., Muir, M.D., Shaw, G., van Gijzel, P. (Eds.), Sporopollenin. Academic Press, London, pp. 446–479.

Hay, W.W., 1995. Paleocenography of marine organic-carbon-rich sediments. In: Huc, A.H. (Ed.), Paleogeography, Paleoclimate and Source Rocks, American Association of Petroleum Geologists Studies in Geology no. 40. American Association of Petroleum Geologists, Tulsa, pp. 21–59.

Hayes, J.M., Freeman, K.H., Popp, B.N., Hoham, C.H., 1990. Compound-specific isotopic analysis: a novel tool for reconstruction of ancient biogeochemical processes. In: Durand, B., Behar, F. (Eds.), Advances in Organic Geochemistry 1989, Organic Geochemistry, vol. 16. Pergamon Press, Oxford, pp. 1115–1128.

Hedges, J.I., Mann, D.C., 1979. The characterization of plant tissues by their cupric oxide oxidation products. Geochimica et Cosmochimica Acta 43, 1803–1807.

Hedges, J.I., Ertel, J.R., 1982. Characterization of lignin by capillary gas chromatography of cupric oxide oxidation products. Analytical Chemistry 54, 174–178.

Hedges, J.I., 1988. Polymerization of humic substances in natural environments. In: Frimmel, F.H., Christman, R.F. (Eds.), Humic Substances and their Role in the Environment, Dahlem Workshop Reports. Wiley, Chichester, pp. 45–58.

Hedges, J.I., Ertel, J.R., Richey, J.E., Quay, P.D., 1994. Origin and processing of organic matter in the Amazon River as indicated by carbohydrates and amino acids. Limnology and Oceanography 39, 743–761.

Hedges, J.I., Keil, R.G., 1995. Sedimentary organic matter preservation: an assessment and speculative synthesis. Marine Chemistry 49, 81–115.

Hedges, J.I., Oades, J.M., 1997. Comparative organic geochemistries of soils and marine sediments. Organic Geochemistry 27, 319–361.

Hedges, J.I., Keil, R.G., Benner, R., 1997. What happens to terrestrial organic matter in the oceans? Organic Geochemistry 27, 195–212.

Hedges, J.I., Eglinton, G., Hatcher, P.G., Kirchman, D.L., Arnosti, C., Derenne, S., Evershed, R.P., Kögel-Knaber, I., de Leeuw, J.W., Littke, R., Michaelis, W., Rullkötter, J., 2000. The molecularly-uncharacterized component of nonliving organic matter in natural environments. Organic Geochemistry 31, 945–958.

Heinrichs, S.M., 1993. Early diagenesis of organic matter: the dynamics (rates) of cycling of organic compounds. In: Engel, M.H., Macko, S.A. (Eds.), Organic Geochemistry – Principles and Applications. Plenum Press, New York, pp. 101–117.

Hemsley, A.R., Barrie, P.J., Chaloner, W.G., Scott, A.C., 1993. The composition of sporopollenin and its use in living and fossil plant systematics. Grana 1 (Suppl.), 2–11.

Higuchi, T., 1981. Lignin structure and morphological distribution in plant cell walls. In: Kirk, T., Higuchi, T., Chang, H. (Eds.), Lignin Biodegradation: Microbiology, Chemistry and Potential Applications. CRC Press, Boca Raton, pp. 1–70.

Hill, R.J., Bence, A.E., Behar, F., Curry, D.J., Symington, W.A., Vandenbroucke, M., Lacombre, D., 1999. The effects of retention and secondary cracking on the composition of migratable petroleum. In: 19th International Meeting on Organic Geochemistry – Abstracts Part I. Tübitak Marmara Research Center, Turkey, pp. 69–70.

Himus, G.W., 1951. Observations on the composition of kerogen rocks and the chemical constitution of kerogen. In: Second Oil Shale and Cannel Coal Conference. Institute of Petroleum, London, pp. 1–22.

Hitchon, B., Holloway, L.R., Bayliss, P., 1976. Formation of ralstonite during low-temperature acid digestion of shales. Canadian Mineralogist 14, 391–392.

Hockaday, W.C., Grannas, A.M., Sunghwan, K., Hatcher, P.G., 2006. Direct molecular evidence for the degradation and mobility of black carbon in soils from ultrahigh-resolution mass spectral analysis of dissolved organic matter from a fire-impacted forest soil. Organic Geochemistry 37, 501–510.

Hoering, T.C., 1984. Thermal reactions of kerogen with added water, heavy water and pure organic substances. Organic Geochemistry 5, 267–278.

Hollander, D., Behar, F., Vandenbroucke, M., Bertrand, P., McKenzie, J.A., 1990. Geochemical alteration of organic matter in eutrophic Lake Greifen: implications for the determination of organic facies and the origin of lacustrine source rocks. In: Huc, A.Y. (Ed.), Deposition of Organic Facies, American Association of Petroleum Geologists Studies in Geology 30. American Association of Petroleum Geologists, Tulsa, Oklahoma, pp. 181–194.

Höld, I.M., Brussee, N.J., Schouten, S., Sinnighe Damsté, J.S., 1998. Changes in the molecular structure of a type II-S kerogen (Monterey Formation, USA) during sequential chemical degradation. Organic Geochemistry 29, 1403–1417.

Holtvoeth, F.J., Kolonic, S., Wagner, T., 2005. Soil organic matter as an important contributor to late Quaternary sediments of the tropical West African continental margin. Geochimica et Cosmochimica Acta 69, 2031–2041.

Hood, A., Gutjahr, C.C.M., Heacock, R.L., 1975. Organic metamorphism and the generation of petroleum. American Association of Petroleum Geologists Bulletin 59, 986–996.

Horsfield, B., Bharati, S., Larter, S.R., Leistner, F., Littke, R., Schenk, H.J., Dypvik, H., 1992. On the typical petroleum-generating characteristics of alginite in the Cambrian Alum shale. In: Schidlowski, M. (Ed.), Early Organic Evolution: Implications for Mineral and Energy Resources. Springer, Berlin, pp. 257–266.

Hsieh, M., Philp, R.P., 2001. Ubiquitous occurrence of high molecular weight hydrocarbons in crude oils. Organic Geochemistry 32, 955–966.

Huc, A.Y., Durand, B., 1974. Etude des acides humiques et de l'humine de sédiments récents considérés comme précurseurs des kérogènes. In: Tissot, B., Bienner, F. (Eds.), Advances in

Organic Geochemistry 1973. Editions Technip, Paris, pp. 53–72.

Huc, A.Y., Durand, B., 1977. Occurrence and significance of humic acids in ancient sediments. Fuel 56, 73–80.

Huc, A.Y., 1980. Origin and formation of organic matter in recent sediments and its relation to kerogen. In: Durand, B. (Ed.), Kerogen, Insoluble Organic Matter from Sedimentary Rocks. Editions Technip, Paris, pp. 445–474.

Huc, A.Y., Durand B., Roucache J., Vandenbroucke M., Pittion J.L., 1986. Comparison of three series of organic matter of continental origin. In: Leythaeuser, D., Rullkotter, J. (Ed.), Advances in Organic Geochemistry 1985. Organic Geochemistry 10, 65–72.

Huc, A.Y., 1988. Aspects of depositional processes of organic matter in sedimentary basins. Organic Geochemistry 13, 263–272.

Huc, A.Y., 1990. Understanding organic facies: a key to improved quantitative petroleum evaluation of sedimentary basins. In: Huc, A.Y. (Ed.), Deposition of Organic Facies, American Association of Petroleum Geologists Studies in Geology 30. American Association of Petroleum Geologists, Tulsa, Oklahoma, pp. 1–11.

Huc, A.Y., Le Fournier, J., Vandenbroucke, M., Bessereau, G., 1990. Northern Lake Tanganyika. An example of organic sedimentation in an anoxic rift lake. In: Katz, B.J. (Ed.), Lacustrine Basin Exploration – Case Studies and Modern Analogs American Association of Petroleum Geologists – Memoir 50. American Association of Petroleum Geologists, Tulsa, Oklahoma, pp. 169–185.

Huc, A.Y., Van Buchem, F.S.P., Colletta, B., 2005. Stratigraphic control on source rock distribution: first and second order scale. In: Harris, N.B. (Ed.), The Deposition of Organic-Carbon-Rich Sediments: Models, Mechanisms and Consequences. SEPM (Society for Sedimentary Geology) Special Publication 82, Tulsa, Oklahoma, pp. 225–242.

Hughey, C.A., Rodgers, R.P., Marshall, A.G., Walters, C.C., Kuangnan, Q., Mankiewicz, P., 2004. Acidic and neutral polar NSO compounds in Smackover oils of different thermal maturity revealed by electrospray high field Fourier transform ion cyclotron resonance mass spectrometry. Organic Geochemistry 35, 863–880.

Hunt, J.M., 1972. Distribution of carbon in crust of earth. American Association of Petroleum Geologists Bulletin 56, 2273–2277.

Hunt, J.M., Hennet, R.J-C., 1992. Modeling petroleum generation in sedimentary basins. In: Whelan, J.K., Farrington, J.W. (Eds.), Organic Matter: Productivity, Accumulation, and Preservation in Recent and Ancient Sediments. Columbia University Press, New York, pp. 20–52.

Hunt, J.M., 1996. Petroleum Geochemistry and Geology, second ed. Freeman, New York.

Hutton, A.C., 1987. Petrographic classification of oil shales. International Journal of Coal Geology 8, 203–231.

Ingalls, A.E., Aller, R.C., Lee, C., Wakeham, S.G., 2004. Organic matter diagenesis in shallow water carbonate sediments. Geochimica et Cosmochimica Acta 68, 4363–4379.

Isaksen, G.H., Curry, D.J., Yeakel, J.D., Jenssen, A.I., 1998. Controls on the oil and gas potential of humic coals. Organic Geochemistry 29, 23–44.

Ishiwatari, R., 1985. Geochemistry of humic substances in lake sediments. In: McKnight, D.M., Aiken, G.R., Wershaw, R.L., MacCarthy, P. (Eds.), Humic Substances in Soil, Sediment and Water: Geochemistry, Isolation and Characterization. Wiley & Sons, New York & Chichester, pp. 147–180.

Jenisch-Anton, A., Adam, P., Schaeffer, P., Albrecht, P., 1999. Oxygen-containing subunits in sulfur-rich nonpolar macromolecules. Geochimica et Cosmochimica Acta 63, 1059–1074.

Jocteur-Monrozier, L., Jeanson, P., 1981. Caractères généraux et évolution de l'azote organique dans les sédiments superficiels. In: Orgon IV. Editions du CNRS (Centre National de la Recherche Scientifique), Paris, pp. 503–528.

Jokic, K., Wang, M.C., Lui, C., Frenkel, A.I., Huang, P.M., 2004. Integration of the polyphenol and Maillard reactions into a unified abiotic pathway for humification in nature: the role of δ -MnO_2. Organic Geochemistry 35, 747–762.

Joll, C.A., Couton, D., Heitz, A., Kagi, R.I., 2004. Comparison of reagents for off-line thermochemolysis of natural organic matter. Organic Geochemistry 35, 47–59.

Jones, J.M., Pourkashanian, M., Rena, C.D., Williams, A., 1999. Modelling the relationship of coal structure to char porosity. Fuel 78, 1737–1744.

Kaiser, K., Guggenberger, G., 2000. The role of DOM sorption to mineral surfaces in the preservation of organic matter in soils. Organic Geochemistry 31, 711–725.

Kaplan, I.R., Emery, K.O., Rittenberg, S.C., 1963. The distribution and isotopic abundance of sulphur in recent marine sediments off southern California. Geochimica et Cosmochimica Acta 27, 297–331.

Keil, R.G., Tsamakis, E., Fuh, C.B., Giddings, J.C., Hedges, J.I., 1994. Mineralogical and textural controls on the organic composition of coastal marine sediments: hydrodynamic separation using SPLITT-fractionation. Geochimica et Cosmochimica Acta 58, 879–893.

Kelemen, S.R., Gorbaty, M.L., Kwiatek, P.J., 1994. Quantification of nitrogen forms in Argonne Premium coals. Energy & Fuels 8, 896–906.

Kelemen, S.R., Freund, H., Gorbaty, M.L., Kwiatek, P.J., 1999. Thermal chemistry of nitrogen in kerogen and low-rank coal. Energy & Fuels 13, 529–538.

Kelts, K., 1988. Environments of deposition of lacustrine petroleum source rocks: an introduction. In: Fleet, A.J., Kelts, K., Talbot, M.R. (Eds.), Lacustrine Petroleum Source Rocks. Geological Society Special Publication No. 40. Blackwell Scientific Publications, Oxford, pp. 3–26.

Kenig, F., Huc, A.Y., 1990. Early sulfur incorporation in recent sedimentary organic matter within Abu Dhabi carbonate environment. In: Orr, W.L., White, O.M. (Eds.), Geochemistry of Sulfur in Fossil Fuels, American Chemical Society Symposium series, vol. 429. American Chemical Society, Washington, DC, pp. 170–185.

Khavari Khorasani, G., Michelsen, J.K., 1991. Geological and laboratory evidence for early generation of large amounts of liquid hydrocarbons from suberinite and subereous components. Organic Geochemistry 17, 849–863.

Kiem, R., Kögel-Knabner, I., 2002. Refractory organic carbon in particle-size fractions of arable soils II: organic carbon in relation to mineral surface area and iron oxides in fraction <6 μm. Organic Geochemistry 33, 699–1713.

Killops, S.D., Funnell, R.H., Suggate, R.P., Sykes, R., Peters, K.E., Walters, C., Woolhouse, A.D., Weston, R.J., Boudou, J.-P., 1998. Predicting generation and expulsion of paraffinic oil from vitrinite-rich coals. Organic Geochemistry 29, 1–21.

Kim, S., Stanford, L.A., Rodgers, R.P., Marshall, A.G., Walters, C.C., Kuangnan, Q., Wenger, L.M., Mankiewicz, P., 2005. Microbial alteration of the acidic and neutral polar NSO compounds revealed by Fourier transform ion cyclotron resonance mass spectrometry. Organic Geochemistry 36, 1117–1134.

Kirk, T.K., Farrell, R.L., 1987. Enzymatic "combustion: the microbial degradation of lignin. Annual Reviews of Microbiology 41, 465–505.

Kissin, Y., 1987. Catagenesis and composition of petroleum: origin of *n*-alkanes and isoalkanes in petroleum crudes. Geochimica et Cosmochimica Acta 51, 2445–2457.

Klemme, H.D., Ulmishek, G.F., 1991. Effective petroleum source rocks of the world: stratigraphic distribution and controlling depositional factors. American Association of Petroleum Geologists Bulletin 75, 1809–1851.

Knicker, H., Scaroni, A.W., Hatcher, P.G., 1996. ^{13}C and ^{15}N spectroscopic investigation on the formation of fossil algal residues. Organic Geochemistry 24, 661–669.

Knicker, H., Hatcher, P.G., 1997. Survival of protein in an organic-rich sediment: possible protection by encapsulation in organic matter. Naturwissenschaften 84, 231–234.

Knicker, H., Hatcher, P.G., 2001. Sequestration of organic nitrogen in the sapropel from Mangrovre Lake, Bermuda. Organic Geochemistry 32, 733–744.

Knicker, H., del Rio, J.C., Hatcher, P.G., Minard, R.D., 2001. Identification of protein remnants in insoluble geopolymers using TMAH thermochemolysis/GC-MS. Organic Geochemistry 32, 397–409.

Knicker, H., 2002. The feasibility of using DCPMAS ^{15}N ^{13}C NMR spectroscopy for a better characterization of immobilized ^{15}N during incubation of ^{13}C- and ^{15}N-enriched plant material. Organic Geochemistry 33, 237–246.

Knicker, H., Totsche, K.U., Almendros, G., Gonzalez-Vila, F.J., 2005. Condensation degree of burnt peat and plant residues and the reliability of solid-state VACP MAS ^{13}C NMR spectra obtained from pyrogenic humic material. Organic Geochemistry 36, 1359–1377.

Kohnen, M.E.L., Sinninghe Damsté, J.S., ten Haven, H.L., de Leeuw, J.W., 1989. Early incorporation of polysulphides in sedimentary organic matter. Nature 341, 640–641.

Kok, M.D., Schouten, S., Sinninghe Damsté, J.S., 2000a. Formation of insoluble, nonhydrolyzable, sulfur-rich macromolecules via incorporation of inorganic sulfur species into algal carbohydrates. Geochimica et Cosmochimica Acta 64, 2689–2699.

Kok, M.D., Rijpstra, W.I.C., Roberston, L., Volkman, J.K., Sinninghe Damsté, J.S., 2000b. Early steroid sulfurisation in surface sediments of a permanently stratified lake (Ace Lake, Antarctica). Geochimica et Cosmochimica Acta 64, 1425–1436.

Kokinos, J.P., Eglinton, T.I., Goñi, M.A., Boon, J.J., Martoglios, P.A., Anderson, D.A., 1998. Characterization of a highly resistant biomacromolecular material in the cell walls of a marine dinoflagellate resting cyst. Organic Geochemistry 28, 265–288.

Kolattukudy, P.E., Croteau, R., Buckner, J.S., 1976. Biochemistry of plant waxes. In: Kolattukudy, P.E. (Ed.), Chemistry and Biochemistry of Natural Waxes. Elsevier, Amsterdam, pp. 289–347.

Kolattukudy, P.E., 1980. Biopolyester membranes of plants: cutin and suberin. Science 208, 890–1000.

Kononova, M.M., 1966. Soil Organic Matter. Pergamon Press, New York.

Kowalewski, I., Vandenbroucke, M., Huc, A.Y., Taylor, M.J., Faulon, J.L., 1996. Preliminary results on molecular modelling of asphaltenes using structure elucidation programs in conjunction with molecular simulation programs. Energy & Fuels 10, 97–107.

Kracht, O., Gleixner, G., 2000. Isotope analysis of pyrolysis products from Sphagnum peat and dissolved organic matter from bog water. Organic Geochemistry 31, 645–654.

Krein, E.B., Aizenshtat, Z., 1994. The formation of isoprenoid sulfur compounds during diagenesis: simulated sulfur incorporation and thermal transformation. Organic Geochemistry 21, 1015–1025.

Kruge, M.A., Landais, P., Bensley, D.F., Stankiewicz, B.A., Elie, M., Ruau, O., 1997. Separation and artificial maturation of macerals from type II kerogens. Energy & Fuels 11, 503–514.

Kuhlbusch, T.A.J., Crutzen, P.J., 1995. Toward a global estimate of black carbon in residues of vegetation fires representing a sink of atmospheric CO_2 and a source of O_2. Global Biogeochemical Cycles 9, 491–501.

Kujawinski, E.B., Freitas, M.A., Zang, X., Hatcher, P.G., 2002. The application of electrospray mass spectrometry (ESI MS) to the structural characterization of natural organic matter. Organic Geochemistry 33, 171–180.

Lafargue, E., Marquis, F., Pillot, D., 1998. Rock-Eval 6 applications in hydrocarbon exploration, production and soils contamination studies. Oil & Gas Science and Technology – Revue de l'Institut Français du Pétrole 53, 421–437.

Lallier-Vergès, E., Bertrand, P., Huc, A.Y., Bückel, D., Tremblay, P., 1993. Control of the preservation of organic matter by productivity and sulphate reduction in Kimmeridgian shales from Dorset (UK). Marine and Petroleum Geology 10, 600–605.

Landais, P., Monthioux, M., Meunier, J.D., 1984. Importance of the oxidation/maturation pair in the evolution of humic coals. Organic Geochemistry 7, 249–260.

Landais, P., Rochdi, A., Largeau, C., Derenne, S., 1993. Chemical characterization of Torbanites by Transmission Micro-FTIR spectroscopy. Origin and extent of compositional heterogeneities. Geochimica et Cosmochimica Acta 57, 2529–2539.

Largeau, C., Casadevall, E., Kadouri, A., Metzger, P., 1984. Formation of *Botryococcus braunii* kerogens. Comparative study of immature Torbanite and of the extant alga *Botryococcus braunii.*. In: Schenck, P.A., de Leeuw, J.W., Lijmbach, G.W.M. (Eds.), Advances in Organic Geochemistry 1983, Organic Geochemistry, vol. 6. Pergamon Press, Oxford, pp. 327–332.

Largeau, C., Derenne, S., Casadevall, E., Kadouri, A., Sellier, N., 1986. Pyrolysis of immature Torbanite and of the resistant biopolymer (PRB A) isolated from extant alga *Botryoccocus braunii*. Mechanism of formation and structure of Torbanite. In: Leythauser, D., Rullkötter, J. (Eds.), Advances in Organic Geochemistry 1985, Organic Geochemistry, vol. 10. Pergamon Press, Oxford, pp. 1023–1032.

Largeau, C., Derenne, S., Casadevall, E., Berkaloff, C., Corolleur, M., Lugardon, B., Raynaud, J.F., Connan, J., 1990a. Occurrence and origin of "ultralaminar" structures in "amorphous kerogens of various source rocks and oil shales. In: Durand, B., Behar, F. (Eds.), Advances in Organic Geo-

chemistry 1989, Organic Geochemistry, vol. 16. Pergamon Press, Oxford, pp. 889–895.

Largeau, C., Derenne, S., Clairay, C., Casadevall, E., Raynaud, J.F., Lugardon, B., Berkaloff, C., Corolleur, M., Rousseau, B., 1990b. Characterization of various kerogens by Scanning Electron Microscopy (SEM) and Transmission Electron Microscopy (TEM) – Morphological relationships with resistant outer walls in extant microorganisms. Mededelingen Rijks Geology Dienst 45, 91–101.

Largeau, C., Derenne, S., 1993. Relative efficiency of the selective preservation and degradation recondensation pathways in kerogen formation. Source and environment influence on their contributions to type I and II kerogens. Organic Geochemistry 20, 611–615.

Largeau, C., de Leeuw, J.W., 1995. Insoluble, non-hydrolysable, aliphatic macromolecular constituents of microbial cell walls. In: Gwynfryn Jones, J. (Ed.), Advances in Microbial Ecology, vol. 14. Plenum Press, New York, pp. 77–118.

Larsen, J.W., Green, T.K., Kovac, J., 1985. The nature of the macromolecular network structure of bituminous coals. Journal of Organic Chemistry 50, 4729–4735.

Larsen, J.W., Pan, C.S., Shawver, S., 1989. Effect of demineralization on the macromolecular structure of coals. Energy & Fuels 3, 557–561.

Larter, S., Horsfield, B., 1993. Determination of structural components of kerogens by the use of analytical pyrolysis methods. In: Engel, M.H., Macko, S.A. (Eds.), Organic Geochemistry – Principles and Applications. Plenum Press, New York, pp. 271–287.

Leithold, E.L., Blair, N.E., 2001. Watershed control on the carbon loading of marine sedimentary particles. Geochimica et Cosmochimica Acta 65, 2231–2240.

Lewan, M.D., Winters, J.C., McDonald, J.H., 1979. Generation of oil-like pyrolyzates from organic-rich shales. Science 203, 897–899.

Li, M., Huang, Y., Obermayer, M., Jiang, C., Snowdon, L.R., Fowler, M.G., 2001. Hydrogen isotopic composition of individual alkanes as a new approach to petroleum correlation: case study from the Western Canada Sedimentary Basin. Organic Geochemistry 32, 1387–1399.

Lim, B., Cachier, H., 1996. Determination of black carbon by chemical oxidation and thermal treatment in recent marine and lake sediments and Cretaceous–Tertiary clays. Chemical Geology 131, 143–154.

Lin, R., Ritz, G., 1993. Reflectance FT-IR microspectroscopy of fossil algae contained in organic-rich shales. Applied Spectroscopy 47, 265–271.

Littke, R., Krooss, B., Idiz, E., Frielingsdorf, J., 1995. Molecular nitrogen in natural gas accumulations: generation from sedimentary matter at high temperatures. American Association of Petroleum Geologists Bulletin 79, 410–430.

Loiseau, L., Zegouagh, Y., Bardoux, G., Barruiso, E., Derenne, S., Mariotti, A., Chenu, C., Largeau, C., 2002. Etude du devenir de l'atrazine dans des sols limono-argileux du Bassin Parisien par la combinaison de méthodes isotopiques et pyrolytiques. Bulletin de la Société Géologique de France 173, 271–280.

Lorant, F., Behar, F., 2002. Late generation of methane from mature kerogens. Energy & Fuels 16, 412–427.

Love, G.D., Snape, C.E., Carr, A.D., Houghton, R.C., 1995. Release of covalently-bound alkane biomarkers in high yields from kerogen via catalytic hydropyrolysis. Organic Geochemistry 23, 981–986.

Love, G.D., Snape, C.E., Fallick, A.E., 1998. Differences in the mode of incorporation and biogenicity of the principal aliphatic constituents of a Type I oil shale. Organic Geochemistry 28, 797–811.

Macko, S.A., Engel, M.H., Parker, P.L., 1993. Early diagenesis of organic matter in sediments: assessment of mechanisms and preservation by the use of isotopic molecular approaches. In: Engel, M.H., Macko, S.A. (Eds.), Organic Geochemistry – Principles and Applications. Plenum Press, New York, pp. 211–224.

Maillard, L.C., 1912a. Action des acides aminés sur les sucres; formation des mélanoïdines par voie méthodique. Comptes Rendus de l'Académie des Sciences (Paris) 154, 66–68.

Maillard, L.C., 1912b. Formation d'humus et de combustibles minéraux sans intervention de l'oxygène atmosphérique, des microorganismes, des hautes températures, ou des fortes pressions. Comptes Rendus de l'Académie des Sciences (Paris) 155, 1554–1556.

Maillard, L.C., 1916. Synthèse des matières humiques par action des acides aminés sur les sucres réducteurs. Annales de Chimie, 9 ème série, tome V, 258–317.

Mango, F.D., Hightower, J., 1997. The catalytic decomposition of petroleum into natural gas. Geochimica et Cosmochimica Acta 61, 5347–5350.

Mannino, A., Harvey, H.R., 2000. Terrigenous dissolved organic matter along an estuarine gradient and its flux to the coastal ocean. In: Yalçin, N., Inan, S. (Eds.), Advances in Organic Geochemistry 1999, Organic Geochemistry, vol. 31. Pergamon, Oxford, pp. 1611–1625.

Marchand, A., Conard, J., 1980. Electron paramagnetic resonance in kerogen studies. In: Durand, B. (Ed.), Kerogen, Insoluble Organic Matter from Sedimentary Rocks. Editions Technip, Paris, pp. 243–270.

Maroto-Valer, M.M., Atkinson, C.J., Willmers, R.R., Snape, C.E., 1996. Characterization of partially carbonized coals by solid-state ^{13}C NMR and optical microscopy. Energy & Fuels 12, 833–842.

Martin, J.P., Haider, K., 1971. Microbial activity in relation to soil humus formation. Soil Science 111, 54–63.

Marzec, A., Kisielow, W., 1983. Mechanism of swelling and extraction and coal structure. Fuel 62, 977–979.

Marzec, A., Jurkiewicz, A., Pislewski, N., 1983. Application of ^{1}H pulse n.m.r. to the determination of molecular and macromolecular phases in coals. Fuel 62, 996–998.

Massiello, C.A., Druffel, E.R.M., 1998. Black carbon in deep-sea sediments. Science 280, 1911–1913.

Mastalerz, M., Hower, J.C., 1996. Elemental composition and molecular structure of *Botryococcus* alginite in Westphalian cannel coals from Kentucky. Organic Geochemistry 24, 301–308.

Mastalerz, M., Hower, J.C., Carmo, A., 1998. *In situ* FTIR and flash pyrolysis/GC-MS characterization of *Protosalvinia* (Upper Devonian, Kentucky, USA): implications for maceral classification. Organic Geochemistry 28, 57–66.

Matthews, D.E., Hayes, J.M., 1978. Isotope-ratio-monitoring gas chromatography–mass spectrometry. Analytical Chemistry 50, 1465–1473.

Mayer, L.M., Rahaim, P.T., Guerin, W., Macko, S.A., Watling, L., Anderson, F.E., 1985. Biological and granulometric controls on sedimentary organic matter of an intertidal

mudflat. Estuarine Marine and Coastal Shelf Science 20, 491–503.

Mayer, L.M., 1993. Organic matter at the sediment–water interface. In: Engel, M.H., Macko, S.A. (Eds.), Organic Geochemistry – Principles and Applications. Plenum Press, New York, pp. 171–184.

Mayer, L.M., 1994a. Surface area control of organic carbon accumulation in continental shelf sediments. Geochimica et Cosmochimica Acta 58, 1271–1284.

Mayer, L.M., 1994b. Relationships between mineral surfaces and organic carbon concentrations in soils and sediments. Chemical Geology 114, 347–363.

Mayer, L.M., Schick, L.L., Hardy, K.R., Wagal, R., McCarthy, J., 2004. Organic matter in small mesospores in sediments and soil. Geochimica et Cosmochimica Acta 68, 3863–3872.

McIver, R.D., 1967. Composition of kerogen. Clue to its role in the origin of petroleum. In: Seventh World Petroleum Congress Proceedings, vol. 2, pp. 25–36.

McKinney, D.E., Bortiatynski, J.M., Carson, D.M., Clifford, D.J., de Leeuw, J.W., Hatcher, P.G., 1996. Tetramethylammonium hydroxide (TMAH) thermochemolysis of the aliphatic biopolymer cutan: insights into the chemical structure. Organic Geochemistry 24, 641–650.

McLafferty, F.W., Fridriksson, E.K., Horn, M.D., Lewis, M.A., Zubarev, R.A., 1999. Biomolecule mass spectrometry. Science 284, 1289–1290.

Metzger, P., Largeau, C., 1999. Chemicals of *Botryococcus braunii*. In: Cohen, Z. (Ed.), Chemicals from Microalgae. Taylor & Francis, London, pp. 205–260.

Michaelis, W., Richnow, H.H., Jenisch, A., 1989. Structural studies of marine and riverine humic matter by chemical degradation. Science of the Total Environment 81/82, 41–50.

Michels, R., Landais, P., Torkelson, B.E., Philp, R.P., 1995. Effects of effluents and water pressure on oil generation during confined pyrolysis and high-pressure hydrous pyrolysis. Geochimica et Cosmochimica Acta 59, 1589–1604.

Middelburg, J.J., Nieuwenhuize, J., van Breugel, P., 1999. Black carbon in marine sediments. Marine Chemistry 65, 245–252.

Mitchell, S.C., Snape, C.E., Garcia, R., Ismail, K., Bartle, K.D., 1994. Determination of organic sulfur forms in some coals and kerogens by high pressure temperature-programmed reduction. Fuel 73, 1159–1166.

Mongenot, T., Boussafir, M., Derenne, S., Lallier-Vergès, E., Largeau, C., Tribovillard, N.P., 1997. Sulfur-rich organic matter from bituminous laminites of Orbagnoux (France, Upper kimmeridgian). The role of early vulcanization. Bulletin de la Société Géologique de France 168, 331–341.

Mongenot, T., Derenne, S., Largeau, C., Tribovillard, N.P., Lallier-Vergès, E., Dessort, D., Connan, J., 1999. Spectroscopic, kinetic and pyrolytic studies of kerogen from the dark parallel laminae facies of the sulphur-rich Orbagnoux deposit (Upper Kimmeridgian, Jura). Organic Geochemistry 30, 39–56.

Mongenot, T., Tribovillard, N.P., Arbey, F., Lallier-Vergès, E., Derenne, S., Largeau, C., Pichon, R., Dessort, D., Connan, J., 2000. Comparative studies of high resolution samples from the Orbagnoux deposit (Upper Kimmeridgian, Jura) via petrographic and bulk geochemical methods. Extent and origin of interfacies and intrafacies variations. Bulletin de la Société Géologique de France 171, 23–36.

Mongenot, T., Riboulleau, A., Garcette-Lepecq, A., Derenne, S., Pouet, Y., Baudin, F., Largeau, C., 2001. Occurrence of proteinaceous moieties in S- and O-rich Late Tithonian kerogen (Kashpir oil shales, Russia). Organic Geochemistry 32, 199–203.

Monin, J.C., Durand, B., Vandenbroucke, M., Huc, A.Y., 1980. Experimental simulation of the natural transformation of kerogen. In: Douglas, A.G., Maxwell, J.R. (Eds.), Advances in Organic Geochemistry 1979. Pergamon Press, Oxford, pp. 517–530.

Monthioux, M., Landais, P., Monin, J.C., 1985. Comparison between natural and artificial maturation series of humic coals from the Mahakam delta, Indonesia. Organic Geochemistry 8, 275–292.

Murgich, J., Rodriguez, J., Aray, Y., 1996. Molecular recognition and molecular mechanics of micelles of some model asphaltenes and resins. Energy & Fuels 10, 68–76.

Mycke, B., Michaelis, W., 1986. Molecular fossils from chemical degradation of macromolecular organic matter. In: Leythauser, D., Rullkötter, J. (Eds.), Advances in Organic Geochemistry 1985. Pergamon Press, Oxford, Organic Geochemistry 10, pp. 847–858.

Nelson, B.C., Eglinton, T.I., Seewald, J.S., Vairavamurthy, M.A., Miknis, F.P., 1995. Transformations in organic sulfur speciation during maturation of Monterey shale: constraints from laboratory experiments. In: Vairavamurthy, M.A., Schoonen, M.A.A. (Eds.), Geochemical Transformation of Sedimentary Sulfur, American Chemical Society Symposium Series, vol. 612. American Chemical Society, Washington, DC, pp. 138–166.

Nguyen, R.T., Harvey, H.R., 2001. Preservation of proteins in marine systems: hydrophobic and other noncovalent associations as major stabilizing forces. Geochimica et Cosmochimica Acta 65, 1467–1480.

Nguyen, R.T., Harvey, H.R., 2003. Preservation via macromolecular associations during *Botryococcus braunii* decay: proteins in the Pula kerogen. Organic Geochemistry 34, 1391–1403.

Nguyen, R.T., Harvey, H.R., Zang, X., van Heemst, J.D.H., Hetényi, M., Hatcher, P.G., 2003. Preservation of algaenan and proteinaceous material during the oxic decay of *Botryococcus braunii* as revealed by pyrolysis-gas chromatography/mass spectrometry and ^{13}C NMR spectroscopy. Organic Geochemistry 34, 483–497.

Nicaise, G., 1977. Etude d'un phénomène d'altération naturelle en surface sur des échantillons prélevés à Fécocourt. IFP (Institut Français du Pétrole) report n° 24792.

Nip, M., Tegelaar, E.W., Brinkhuis, H., de Leeuw, J.W., Schenck, P.A., Holloway, P.J., 1986. Analysis of modern and fossil plant cuticles by Curie point Py-GC and Curie point Py-GC–MS: recognition of a new highly aliphatic and resistant biopolymer. In: Leythauser, D., Rullkötter, J. (Eds.), Advances in Organic Geochemistry 1985, Organic Geochemistry, vol. 10. Pergamon Press, Oxford, pp. 769–778.

Nip, M., de Leeuw, J.W., Holloway, P.J., Jensen, J.P.T., Sprenkels, J.C.M., de Poorter, M., Sleeckx, J.J.M., 1987. Comparison of flash pyrolysis, differential scanning calorimetry, ^{13}C NMR and IR spectroscopy in the analysis of a highly aliphatic biopolymer from plant cuticles. Journal of Analytical Applied Pyrolysis 11, 287–295.

Nip, M., de Leeuw, J.W., Schenck, P.A., Winding, W., Meuzelaar, H.L.C., Crelling, J.C., 1989. A flash pyrolysis

and petrographic study of cutinite from the Indiana paper coal. Geochimica et Cosmochimica Acta 53, 671–683.

Nissenbaum, A., Kaplan, I.R., 1972. Chemical and isotopic evidence for the *in situ* origin of marine humic substances. Limnology and Oceanography 17, 570–582.

Oades, M., 1995. An overview of processes affecting the cycling of organic carbon in soils. In: Zepp, R.G., Sonntag, Ch. (Eds.), The Role of Nonliving Organic Matter in the Earth's Carbon Cycle. Dahlem Conference Reports. John Wiley & Sons, New York, pp. 293–303.

Oberlin, A., Boulmier, J.L., Villey, M., 1980. Electron microscopic study of kerogen microtexture. Selected criteria for determining the evolution path and evolution stage of kerogen. In: Durand, B. (Ed.), Kerogen, Insoluble Organic Matter from Sedimentary Rocks. Editions Technip, Paris, pp. 191–241.

Oberlin, A., Bonnamy, S., Rouxhet, P.G., 1999. Colloidal and supramolecular aspects of carbon. In: Thrower, P.A., Radovic, L.R. (Eds.), Chemistry and Physics of Carbon, vol. 26. Marcel Dekker Inc., New York, p. 48pp.

Oka, M., Chang, H.C., Gavalas, G.R., 1977. Computer-assisted molecular structure construction for coal-derived compounds. Fuel 56, 3–8.

Orr, W.L., 1978. Sulphur in heavy oils, oil sands and oil shales. In: Strausz, O.P., Lown, E.M. (Eds.), Oil Sand and Oil Shale Chemistry. Verlag Chemie International, Berlin, pp. 223–243.

Orr, W.L., 1986. Kerogen/asphaltene/sulfur relationships in sulphur-rich Monterey oils. In: Leythauser, D., Rullkötter, J. (Eds.), Advances in Organic Geochemistry 1985, Organic Geochemistry, vol. 10. Pergamon Press, Oxford, pp. 499–516.

Orr, W.L., Sinninghe Damsté, J.S., 1990. Geochemistry of sulfur in petroleum systems. In: Orr, W.L., White, C.M. (Eds.), Geochemistry of Sulfur in Fossil Fuels, American Chemical Society Symposium Series, vol. 429. American Chemical Society, Washington, DC, pp. 2–49.

Ourisson, G., Albrecht, P., Rohmer, M., 1984. The microbial origin of fossil fuels. Scientific American 251, 34–41.

Patience, R.L., Baxby, M., Bartle, K.D., Perry, D.L., Rees, A.G.W., Rowland, S.J., 1992. The functionality of organic nitrogen in some recent sediments from the Peru upwelling region. Organic Geochemistry 18, 161–169.

Pearson, A., Eglinton, T.I., 2000. The origin of *n*-alkanes in Santa Monica basin surface sediments: a model based on compound-specific $\Delta^{14}C$ and $\delta^{13}C$ data. Organic Geochemistry 31, 1103–1116.

Pedentchouk, N., Freeman, K.H., Harris, N.B., Clifford, D.J., Grice, K., 2004. Sources of alkylbenzenes in Lower Cretaceous lacustrine source rocks, West African rift basins. Organic Geochemistry 35, 33–45.

Pelet, R., 1983. Preservation of sedimentary organic matter. In: Bjøroy et al. (Eds.), Advances in Organic Geochemistry 1981. Wiley Heiden Ltd., Chichester, pp. 241–250.

Penteado, H.L.B., Behar, F., 2000. Geochemical characterization and compositional evolution of the Gomo Member source rocks in the Reconcavo Basin, Brazil. In: Mello, M.R., Katz, B.J. (Eds.), Petroleum Systems of South Atlantic Margins. AAPG (American Association of Petroleum Geologists) Memoir 73, pp. 179–194.

Peters, K.E., Moldowan, J.M., 1993. The Biomarker Guide: Interpreting Molecular Fossils in Petroleum and Ancient Sediments. Prentice-Hall, Englewood Cliffs, NJ.

Peters, K.E., Walters, C.C., Moldowan, J.M., 2004. The Biomarker Guide, second ed. Cambridge University Press.

Petersen, H.I., Nytoft, H.P., 2006. Oil generation capacity of coals as a function of coal age and aliphatic structure. Organic Geochemistry 37, 558–583.

Petrovich, R., 2001. Mechanisms of fossilization of the soft-bodied and lightly armored faunas of the Burgess Shale and of some other classical localities. American Journal of Science 301, 683–726.

Petsch, S.T., Berner, R.A., 1998. Coupling the geochemical cycles of C, P, Fe, and S: The effect on atmospheric O_2 and the isotopic records of carbon and sulfur. American Journal of Science 298, 246–262.

Petsch, S.T., Berner, R.A., Eglinton, T.I., 2000. A field study of the chemical weathering of ancient sedimentary organic matter. Organic Geochemistry 31, 475–487.

Petsch, S.T., Smernik, R.J., Eglinton, T.I., Oades, J.M., 2001a. A solid-state ^{13}C NMR study of kerogen degradation during black shale weathering. Geochimica et Cosmochimica Acta 65, 1867–1882.

Petsch, S.T., Eglinton, T.I., Edwards, K.J., 2001b. ^{14}C-dead living biomass: evidence for microbial assimilation of ancient organic carbon during shale weathering. Science 292, 1127–1131.

Phillips, T.L., Peppers, R.A., DiMichele, W.A., 1985. Stratigraphic and interregional changes in Pennsylvania coal-swamp vegetation: Environmental inferences. International Journal of Coal Geology 5, 43–109.

Philp, R.P., Calvin, M., 1976. Possible origin for insoluble organic (kerogen) debris in sediments from insoluble cell-wall materials of algae and bacteria. Nature 262, 134–136.

Pichevin, L., Bertrand, P., Boussafir, M., Disnar, J.R., 2004. Organic matter accumulation and preservation controls in a deep sea modern environment: an example from Namibian slope sediments. Organic Geochemistry 35, 543–559.

Poinar, H.N., Stankiewicz, B.A., 1999. Protein preservation and DNA retrieval from ancient tissues. Proceedings of the National Academy of Sciences of the United States of America 96, 8426–8431.

Poirier, N., Derenne, S., Rouzaud, J.N., Largeau, C., Mariotti, A., Balesdent, J., Maquet, J., 2000. Chemical structure and sources of the macromolecular, resistant, organic fraction isolated from a forest soil (Lacadée, south-west France). Organic Geochemistry 31, 813–827.

Poirier, N., Derenne, S., Balesdent, J., Rouzaud, J.-N., Mariotti, A., Largeau, C., 2001. Abundance and composition of the refractory organic fraction of an ancient, tropical soil (Pointe Noire, Congo). Organic Geochemistry 33, 383–391.

Poirier, N., Derenne, S., Balesdent, J., Mariotti, A., Massiot, A., Largeau, C., 2003. Isolation and analysis of the non-hydrolysable fraction of a forest soil (Lacadée, southwest France). European Journal of Soil Science 54, 243–255.

Poirier, N., Derenne, S., Balesdent, J., Chenu, C., Bardoux, G., Mariotti, A., Largeau, C., 2006. Dynamics and origin of the non-hydrolysable organic fraction in a forest and a cultivated temperate soil, as determined by isotopic and microscopic studies. European Journal of Soil Science 57, 719–730.

Powell, T.G., Boreham, C.J., Smyth, M., Russel, N., Cook, A.C., 1991. Petroleum source rock assessment in non-marine sequences: pyrolysis and petrographic analysis of Australian coals and carbonaceous shales. Organic Geochemistry 17, 375–394.

Pradier, B., Landais, P., Rochdi, A., Davis, A., 1992. Chemical basis of fluorescence alteration of crude oils and kerogens-II. Fluorescence and infrared micro-spectrometric analysis of vitrinite and liptinite. Organic Geochemistry 18, 241–248.

Preston, C.M., 1996. Applications of NMR to soil organic matter: history and prospects. Soil Science 161, 144–166.

Quénéa, K., Derenne, S., Gonzàlez-Vila, F.J., Mariotti, A., Rouzaud, J.N., Largeau, C., 2005. Study of the composition of the macromolecular refractory fraction from an acidic sandy forest soil (Landes de Gascogne, France) using chemical degradation and electron microscopy. Organic Geochemistry 36, 1151–1162.

Quénéa, K., Derenne, S., Gonzalez-Vila, F.J., Gonzalez-Pérez, J.A., Mariotti, A., Largeau, C., 2006a. Double-shot pyrolysis of the non-hydrolysable organic fraction isolated from a sandy forest soil (Landes de Gascogne, South-West France). Comparison with classical Curie point pyrolysis. Journal of Analytical and Applied Pyrolysis 76, 271–279.

Quénéa, K., Derenne, S., Largeau, C., Rumpel, C., Mariotti, A., 2006b. Influence of change in land use on the refractory organic macromolecular fraction of a sandy spodosol (Landes de Gascogne, France). Geoderma 136, 136–151.

Quénéa, K., Derenne, S., Rumpel, C., Rouzaud, J.N., Gustafsson, O., Carcaillet, C., Mariotti, A., Largeau, C., 2006c. Black carbon quantification in forest and cultivated sandy soils (Landes de Gascogne, France). Influence of change in land-use. Organic Geochemistry 37, 1185–1189.

Ransom, B., Bennett, R.H., Baerwald, R., 1997. In situ organic matter in recent marine sediment: a TEM investigation of organic matter preservation on continental margins and the monolayer hypothesis. Marine Geology 138, 1–9.

Ransom, B., Kim, D., Kastner, M., Wainwright, S., 1998. Organic matter preservation on continental slopes: importance of mineralogy and surface area. Geochimica et Cosmochimica Acta 62, 1329–1345.

Read, H.H., Watson, J., 1968. Introduction to Geology, second ed. MacMillan & Co Ltd., London.

Remusat, L., Derenne, S., Robert, F., 2005. New insight on aliphatic linkages in the macromolecular organic fraction of Orgueil and Murchison meteorites through ruthenium tetroxide oxidation. Geochimica et Cosmochimica Acta 69, 4377–4386.

Remusat, L., Palhol, F., Robert, F., Derenne, S., France-Lanord, C., 2006. Enrichment of deuterium in insoluble organic matter from primitive meteorites: a solar system origin?. Earth and Planetary Science Letters 243 15–25.

Revill, A.T., Volkman, J.K., O'Leary, T., Summons, R.E., Boreham, C.J., Banks, M.R., Denwer, K., 1994. Hydrocarbon biomarkers, thermal maturity, and depositional setting of tasmanite oil shales from Tasmania, Australia. Geochimica et Cosmochimica Acta 58, 3803–3822.

Riboulleau, A., Derenne, S., Sarret, G., Largeau, C., Baudin, F., Connan, J., 2000. Pyrolytic and spectroscopic study of a sulphur-rich kerogen from the "Kashpir oil shales" (Upper Jurassic, Russian Platform). In: Yalçin, N., Inan, S. (Eds.), Advances in Organic Geochemistry 1999, Organic Geochemistry, vol. 31. Pergamon Press, Oxford, pp. 1641–1661.

Riboulleau, A., Derenne, S., Largeau, C., Baudin, F., 2001. Origin of contrasted features and preservation pathways in kerogens from the Kashpir oil shales (Upper Jurassic, Russian Platform). Organic Geochemistry 32, 647–665.

Riboulleau, A., Mongenot, T., Baudin, F., Derenne, S., Largeau, C., 2002. Factors controlling the survival of proteinaceous material in Late Tithonian kerogens (Kashpir oil shales, Russia). Organic Geochemistry 33, 1127–1130.

Richnow, H.H., Jenisch, A., Michaelis, W., 1992. Structural investigations of sulphur-rich macromolecular oil fractions and a kerogen by *sequential* chemical degradation. In: Eckardt, C.B., Maxwell, J.R., Larter, S.R., Manning, D.A.C. (Eds.), Advances in Organic Geochemistry 1991, Organic Geochemistry, vol. 19. Pergamon Press, Oxford, pp. 351–370.

Richnow, H.H., Jenisch, A., Michaelis, W., 1993. The chemical structure of macromolecular fractions of a sulfur-rich oil. Geochimica et Cosmochimica Acta 57, 2767–2780.

Robbins, L.L., Brew, K., 1990. Proteins from the organic matrix of core-top and fossil planktonic foraminifera. Geochimica et Cosmochimica Acta 54, 2285–2292.

Robert, P., 1979. Classification des matières organiques en fluorescence. Application aux roches mères pétrolières. Bulletin du CR Exploration-Production Elf Aquitaine 3, 223–263.

Robinson, W.E., 1969a. Isolation procedures for kerogens and associated soluble organic materials. In: Eglinton, G., Murphy, M.T.J. (Eds.), Organic Geochemistry – Methods and Results. Springer-Verlag, Berlin Heidelberg, New York, pp. 181–195.

Robinson, W.E., 1969b. Kerogen of the Green River Formation. In: Eglinton, G., Murphy, M.T.J. (Eds.), Organic Geochemistry – Methods and Results. Springer-Verlag, Berlin Heidelberg, New York, pp. 619–637.

Robinson, W.E., 1976. Origin and characteristics of Green River oil shale. In: Yen, T.F., Chilingarian, G.V. (Eds.), Oil Shale, Developments in Petroleum Science, vol. 5. Elsevier, Amsterdam, pp. 61–79.

Robl, T.L., Davis, B.H., 1993. Comparison of the HF-HCl and HF-BF_3 maceration techniques and the chemistry of resultant organic concentrates. Organic Geochemistry 20, 249–255.

Rochdi, A., Landais, P., Largeau, C., 1991. Fourier transform-infrared microspectroscopy of fossilized organic matter: Principles, semiquantitative aspects and applications. Spectroscopy International 3, 37–42.

Rowland, S., Rockey, C., Al-Lihaibi, S.S., Wolf, G.A., 1993. Incorporation of sulphur into phytol derivatives during simulated early diagenesis. Organic Geochemistry 20, 1–15.

Rullkötter, J., Michaelis, W., 1990. The structure of kerogen and related materials. A review of recent progress and future trends. In: Durand, B., Behar, F. (Eds.), Advances in Organic Geochemistry 1989, Organic Geochemistry, vol. 16. Pergamon Press, Oxford, pp. 829–852.

Sabelle, S., Oliver, E., Metzger, P., Derenne, S., Largeau, C., 1993. Variability in phenol moieties in the resistant biomacromolecules of the A and B races of *Botryococcus braunii*. Geochemical implications, In: Øygard, K. (Ed.), Organic Geochemistry, Poster sessions from the 16th International Meeting on Organic Geochemistry. Falch Hurtigtrykk, Oslo, pp. 558–562.

Saiz-Jimenez, C., de Leeuw, J.W., 1986. Lignin pyrolysis products: their structure and their significance as biomarkers. Organic Geochemistry 10, 869–876.

Salmon, V., Derenne, S., Largeau, C., Beaudoin, B., Bardoux, G., Mariotti, A., 1997. Kerogen chemical structure and source organisms in a Cenomanian organic-rich black shale (Central

Italy) – Indications for an important role of the "sorptive protection" pathway. Organic Geochemistry 27, 423–438.

Salmon, V., Derenne, S., Lallier-Vergès, E., Largeau, C., Beaudoin, B., 2000. Protection of organic matter by mineral matrix in a Cenomanian black shale. Organic Geochemistry 31, 463–474.

Sarret, G., Mongenot, T., Connan, J., Derenne, S., Kasrai, M., Bancroft, G.M., Largeau, C., 2002. Sulfur speciation in kerogens of the Orbagnoux deposit (Upper Kimmeridgian, Jura) by XANES spectroscopy and pyrolysis. Organic Geochemistry 33, 877–895.

Sauer, P.E., Eglinton, T.I., Hayes, J.M., Schimmelmann, A., Sessions, A.L., 2001. Compound-specific D/H ratios of lipid biomarkers from sediments as a proxy for environmental and climatic conditions. Geochimica et Cosmochimica Acta 65, 213–222.

Saxby, J.D., 1970. Isolation of kerogens in sediments by chemical methods. Chemical Geology 6, 173–184.

Schaeffer, P., Harrison, W.N., Keely, B.J., Maxwell, J.R., 1995a. Product distributions from chemical degradation of kerogens from a marl from a Miocene evaporitic sequence (Vena del Gesso, N. Italy). Organic Geochemistry 23, 541–554.

Schaeffer, P., Reiss, C., Albrecht, P., 1995b. Geochemical study of macromolecular organic matter from sulfur-rich sediments of evaporitic origin (Messinian of Sicily) by chemical degradation. Organic Geochemistry 23, 567–581.

Schaeffer-Reiss, C., Schaeffer, P., Putschew, A., Maxwell, J.R., 1998. Stepwise chemical degradation of immature S-rich kerogens from Vena del Gesso (Italy). Organic Geochemistry 29, 1857–1873.

Schenk, H.J., Horsfield, B., Krooss, B., Schaefer, R.G., Schwochau, K., 1997. Kinetics of petroleum formation and cracking. In: Welte, D.H., Horsfield, B., Baker, D.R. (Eds.), Petroleum and Basin Evolution. Springer, Berlin, pp. 233–269.

Schimmelmann, A., Lewan, M.D., Wintsch, R.P., 1999. D/H isotope ratios of kerogen, oil, and water in hydrous pyrolysis of source rocks containing kerogen types I, II, IIS, and III. Geochimica et Cosmochimica Acta 63, 3751–3766.

Schmidt, M.W.I., Noack, A.G., 2000. Black carbon in soils and sediments: analysis, distribution, implications, and current challenges. Global Biogeochemical Cycles 14, 777–793.

Schmidt, M.W.I., Skjemstad, J.O., Czimczik, C.I., Glaser, B., Prentice, K.M., Gélinas, Y., Kulbusch, T.A.J., 2001. Comparative analysis of black carbon in soil. Global Biogeochemical Cycles 15, 163–167.

Schmitter, J.M., Vajta, Z., Arpino, P.J., 1980. Investigation of nitrogen containing bases in petroleum. In: Douglas, A., Maxwell, J. (Eds.), Advances in Organic Geochemistry 1979. Pergamon Press, Oxford, pp. 67–76.

Schnitzer, M., Neyroud, J.A., 1975. Alkanes and fatty acids in humic substances. Fuel 54, 17–19.

Schnitzer, M., 1978. Humic substances: chemistry and reactions. In: Schnitzer, M., Khan, S.U. (Eds.), Soil Organic Matter. Elsevier, Amsterdam, pp. 1–64.

Schnitzer, M., Barr, M., Hartenstein, M., 1984. Kinetics and characteristics of humic acids produced from simple phenols. Soil Biology and Biochemistry 16, 371–375.

Schnitzer, M., 1985. Nature of nitrogen in humic substances. In: Mc Knight, D.M., Aiken, G.R., Wershaw, R.L., MacCarthy, P. (Eds.), Humic Substances in Soil, Sediment and Water: Geochemistry, Isolation and Characterization. Wiley & Sons, New York & Chichester, pp. 303–325.

Schouten, S., van Driel, G.B., Sinninghe Damsté, J.S., de Leeuw, J.W., 1993. Natural sulphurization of ketones and aldehydes: A key reaction in the formation of organic sulphur compounds. Geochimica et Cosmochimica Acta 57, 5111–5116.

Schouten, S., de Graaf, W., van Driel, G.B., Sinninghe Damsté, J.S., de Leeuw, J.W., 1994. Laboratory simulation of natural sulphurization: II. Reaction of multifunctionalized lipids with inorganic polysulphides at low temperature. In: Telnaes, N., van Graas, G., Øygard, K. (Eds.), Advances in Organic Geochemistry 1993, Organic Geochemistry, vol. 22. Pergamon Press, Oxford, pp. 25–834.

Schouten, S., Moerkerken, P., Gelin, F., Baas, M., de Leeuw, J.W., Sinninghe Damsté, J.S., 1998. Structural characterization of aliphatic, non-hydrolyzable biopolymers in freshwater algae and a leaf cuticle using ruthenium tetroxide degradation. Phytochemistry 49, 987–993.

Senga-Makadi, K., 1982. Etude expérimentale des interactions entre matière organique – matrice minérale au cours de la pyrolyse. PhD Thesis, Université d'Orléans, France.

Sephton, M., Gilmour, I., 2001. Pyrolysis-gas chromatography-isotope ratio mass spectrometry of macromolecular material in meteorites. Planetary and Space Science 49, 465–471.

Serio, M.A., Hamblen, D.G., Markham, J.R., Solomon, P.R., 1987. Kinetics of volatile product evolution in coal pyrolysis: experiment and theory. Energy & Fuels 1, 138–152.

Sessions, A.L., Sylva, S.P., Summons, R.E., Hayes, J.M., 2004. Isotopic exchange of carbon-bound hydrogen over geologic timescales. Geochimica et Cosmochimica Acta 68, 1545–1559.

Shinn, J.H., 1984. From coal to single-stage and two-stage products: a reactive model of coal structure. Fuel 63, 1187–1196.

Sieskind, O., Ourisson, G., 1972. Hydrocarbures formés par le craquage thermocatalytique de l'acide stéarique en présence de montmorillonite. Comptes Rendus de l'Académie des Sciences (Paris) 274, 2186–2189.

Simpson, M.J., Hatcher, P.G., 2004. Determination of black carbon in natural organic matter by chemical oxidation and solid-state ^{13}C nuclear magnetique resonance spectroscopy. Organic Geochemistry 35, 923–935.

SinninghеDamsté, J.S., Rijpstra, W.I.C., de Leeuw, J.W., Schenck, P.A., 1988. Origin of organic sulphur compounds and sulphur-containing high molecular weight substances in sediments and immature crude oils. In: Mattavelli, L., Novelli, L. (Eds.), Advances in Organic Geochemestry 1987, Organic Geochemistry, vol. 13. Pergamon Press, Oxford, pp. 593–606.

Sinninghe Damsté, J.S., Rijpstra, W.I.C., de Leeuw, J.W., Schenck, P.A., 1989. The occurrence and identification of series of organic sulphur compounds in oils and sediment extracts, II. Their presence in samples from hypersaline and non-hypersaline palaeoenvironments and possible application as source, palaeoenvironmental and maturity indicators. Geochimica et Cosmochimica Acta 53, 1323–1341.

Sinninghe Damsté, J.S., Eglinton, T.I., Rijpstra, W.I.C., de Leeuw, J.W., 1990. Charaterization of organically bound sulfur in high molecular weight, sedimentary organic matter using flash pyrolysis and Raney Ni desulfurization. In: Orr, W.L., White, C.M. (Eds.), Geochemistry of Sulfur in Fossil Fuels, American Chemical Society Symposium Series, vol. 429. American Chemical Society, Washington, DC, pp. 486–528.

Sinninghe Damsté, J.S., de Leeuw, J.W., 1990. Analysis, structure and geochemical significance of organically-bound sulphur in the geosphere: State of the art and future research. In: Durand, B., Behar, F. (Eds.), Advances in Organic Geochemistry 1989, Organic Geochemistry, vol. 16. Pergamon Press, Oxford, pp. 1077–1101.

Sinninghe Damsté, J.S., de las Heras, F.X.C., van Bergen, P.F., de Leeuw, J.W., 1993a. Characterization of tertiary Catalan lacustrine oil shale: Discovery of extremely organic sulphur-rich type I kerogens. Geochimica et Cosmochimica Acta 57, 389–415.

Sinninghe Damsté, J.S., Hartgers, W.A., Baas, M., de Leeuw, J.W., 1993b. Characterization of high molecular weight organic matter in marls of the salt IV Formation of the Mulhouse Basin. Organic Geochemistry 20, 1237–1251.

Sinninghe Damsté, J.S., Kohnen, M.E., Horsfield, B., 1998a. Origin of low-molecular-weight alkylthiophenes in pyrolysates of sulfur-rich kerogens as revealed by micro-scale sealed vessel pyrolysis. Organic Geochemistry 29, 1891–1904.

Sinninghe Damsté, J.S., Kok, M.D., Köster, J., Schouten, S., 1998b. Sulfurized carbohydrates: an important sink of organic matter? Earth and Planetary Science Letters 164, 7–13.

Siskin, M., Scouten, C.G., Rose, K.D., Aczel, T., Colgrove, S.G., Pabst Jr., R.E., 1995. Detailed structural characterization of the organic material in Rundle Ramsay Crossing and Green River oil shales. In: Snape, C. (Ed.), Composition, Geochemistry and Conversion of Oil Shales. Kluwer Academic Publishers, Dordrecht, pp. 143–158.

Skjemstad, J.O., Clarke, P., Taylor, J.A., Oades, J.M., Newman, R.H., 1994. The removal of magnetic materials from surface soils. A solid-state ^{13}C CP/MAS n.m.r study. Australian Journal of Soil Research 32, 1215–1229.

Smernik, R.J., Schwark, L., Schmidt, M.W.I., 2006. Assessing the quantitative reliability of solid-state ^{13}C NMR spectra of kerogens. Solid State Nuclear Magnetic Resonance 29, 312–321.

Smith, J.W., 1961. Ultimate composition of organic material in Green River oil shale. United States Bureau of Mines Report 5725.

Smith, J.W., 1983. The chemistry that formed Green River Foundation oil shales. In: Miknis, F.P., Mckay, J.F. (Eds.), Geochemistry and Chemistry of Oil Shales, ACS Symposium Series 230. American Chemical Society, Washington D.C., pp. 225–248.

Snape, C.E., Lafferty, C.J., Eglinton, G., Robinson, N., Collier, R., 1994. The potential of hydropyrolysis as a route for coal liquefaction. International Journal of Energy Research 18, 233–242.

Solomon, P.R., 1981. New Approaches in Coal ChemistryACS (American Chemical Society) Symposium Series, vol. 169. American Chemical Society, Washington, DC, pp. 61–71.

Souron, C., Boulet, R., Espitalié, J., 1977. Etude par spectrométrie de masse de la décomposition thermique de roches sédimentaires contenant de la matière organique de deux types différents et comparaison avec les kérogènes correspondants. In: Campos, R., Goñi, J. (Eds.), Advances in Organic Geochemistry 1975. Enadimsa, Madrid, pp. 797–820.

Spiro, C.L., 1981. Space-filling models for coal: a molecular description of coal plasticity. Fuel 60, 1121–1126.

Spiro, C.L., Kosky, P.G., 1982. Space-filling models for coal. 2. Extension to coals of various ranks. Fuel 61, 1080–1087.

Stach, E., 1975. Coal Petrology. Gebruder Borntraeger, Stuttgart.

Stafford, H.A., 1988. Proanthocyanidins and the lignin connection. Phytochemistry 27, 1–6.

Stainforth, J.G., Reinders, J.E.A., 1990. Primary migration of hydrocarbons by diffusion through organic matter networks, and its effect on oil and gas generation. In: Durand, B., Behar, F. (Eds.), Advances in Organic Geochemistry 1989, Organic Geochemistry, vol. 16. Pergamon Press, Oxford, pp. 61–74.

Stankiewicz, B.A., Kruge, M.A., Crelling, J.C., Salmon, G.L., 1994. Density gradient centrifugation: application to the separation of macerals of Type I, II and III sedimentary organic matter. Energy & Fuels 8, 1513–1521.

Stankiewicz, B.A., Kruge, M.A., Mastalerz, M., Salmon, G.L., 1996. Geochemistry of the alginite and amorphous organic matter from type II-S kerogens. Organic Geochemistry 24, 495–509.

Stankiewicz, B.A., Briggs, D.E.G., Evershed, R.P., Flannery, M.B., Wuttke, M., 1997. Preservation of chitin in 25 million-year-old fossils. Science 276, 1541–1543.

Stasiuk, L.D., 1999. Confocal laser scanning fluorescence microscopy of *Botryococcus* alginite from boghead oil shale, Boltysk, Ukraine: selective preservation of various micro-algal components. Organic Geochemistry 30, 1021–1026.

Stevenson, F.J., Butler, J.H.A., 1969. Chemistry of humic acids and related pigments. In: Eglinton, G., Murphy, M.T.J. (Eds.), Organic Geochemistry. Springer-Verlag, Berlin, Heidelberg & New York, pp. 534–557.

Stopes, M., 1935. On the petrology of banded bituminous coals. Fuel 14, 4–13.

Stuermer, D.H., Peters, K.E., Kaplan, I.R., 1978. Source indicators of humic substances and protokerogen. Stable isotope ratios, elemental compositions and electronic spin resonance spectra. Geochimica et Cosmochimica Acta 42, 989–997.

Suess, E., 1973. Interaction of organic compounds with calcium carbonate II. Organo-carbonate associations in recent sediments. Geochimica et Cosmochimica Acta 37, 2435–2447.

Suess, E., 1980. Particulate organic carbon flux in the oceans. Surface productivity and oxygen utilization. Nature 288, 260–263.

Summons, R.E., 1993. Biogeochemical cycles: a review of fundamental aspects of organic matter formation, preservation and composition. In: Engel, M.H., Macko, S.A. (Eds.), Organic Geochemistry – Principles and Applications. Plenum Press, New York, pp. 3–21.

Swain, F.M., 1963. Geochemistry of humus. In: Breger, I.A. (Ed.), Organic Geochemistry, Earth Series monograph no, vol. 16. Pergamon Press, Oxford, pp. 87–147.

Szklarz, G., Leonowicz, A., 1986. Cooperation between fungal laccase and glucose oxidase in the degradation of lignin derivatives. Phytochemistry 25, 2537–2539.

Talbot, M.R., 1988. The origins of lacustrine oil source rocks: evidence from the lakes of tropical Africa. In: Fleet, A.J., Kelts, K., Talbot, M.R. (Eds.), Lacustrine Petroleum Source Rocks. Geological Society Special Publication N° 40. Blackwell Scientific Publications, Oxford, pp. 3–26.

Tanoue, E., Handa, N., 1979. Differential sorption of organic matter by various sized sediments particles in Recent sediment from the Bering Sea. Journal of the Oceanographic Society of Japan 35, 199–208.

Taylor, G.H., Teichmüller, M., Davis, A., Diessel, C.F.K., Littke, R., Robert, P., 1998. Organic Petrology. Gebrüder Borntraeger, Berlin.

Tegelaar, E.W., de Leeuw, J.W., Derenne, S., Largeau, C., 1989a. A reappraisal of kerogen formation. Geochimica et Cosmochimica Acta 53, 3103–3106.

Tegelaar, E.W., de Leeuw, J.W., Largeau, C., Derenne, S., Schulten, H.R., Müller, R., Boon, J.J., Nip, M., Sprenkels, J.C.M., 1989b. Scope and limitations of several pyrolysis methods in the structural elucidation of a macromolecular plant constituent in the leaf cuticle of *Agave americana L.* Journal of Analytical Applied Pyrolysis 15, 29–54.

Tegelaar, E.W., Kerp, H., Visscher, H., Schenck, P.A., de Leeuw, J.W., 1991. Bias of the paleobotanical record as a consequence of variations in the chemical composition of higher vascular plant cuticles. Paleobiology 17, 133–144.

Tegelaar, E.W., Wattendorff, J., de Leeuw, J.W., 1993. Possible effects of chemical heterogeneity in higher land plant cuticles on the preservation of its ultrastructure upon fossilization. Reviews of Paleobotany and Palynology 77, 149–170.

Tegelaar, E.W., Hollman, G., van der Vegt, P., de Leeuw, J.W., Holloway, P.J., 1995. Chemical characterization of periderm tissue of some angiosperm species: recognition of an insoluble, non-hydrolyzable, aliphatic biomacromolecule (Suberan). Organic Geochemistry 23, 239–250.

Teichmüller, M., 1989. The genesis of coal from the standpoint of coal petrology. International Journal of Coal Geology 12, 1–87.

Thomas, B.M., 1981. Land–plant source rocks for oil and their significance in Australian basins. Australian Petroleum Exploration Association Journal 22, 164–178.

Tissot, B., 1969. Premières données sur les mécanismes et la cinétique de la formation du pétrole dans les sédiments – Simulation d'un schéma réactionnel sur ordinateur. Revue de l'Institut Français du Pétrole 24, 470–501.

Tissot, B., Pelet, R., 1971. Nouvelles données sur les mécanismes de genèse et de migration du pétrole – Simulation mathématique et application à la prospectionProceedings of the Eighth World Petroleum Congress, vol. 2. Applied Science Publishers, London, pp. 35–46.

Tissot, B., Durand, B., Espitalié, J., Combaz, A., 1974. Influence of nature and diagenesis of organic matter in formation of petroleum. American Association of Petroleum Geologists Bulletin 58, 499–506.

Tissot, B.P., Welte, D.H., 1978. Petroleum Formation and Occurrence, first ed. Springer Verlag, Berlin.

Tissot, B., Deroo, G., Hood, A., 1978. Geochemical study of the Uinta Basin: formation of petroleum from the Green River formation. Geochimica et Cosmochimica Acta 42, 1469–1485.

Tissot, B., 1979. Effects on prolific petroleum source rocks and major coal deposits caused by sea-level changes. Nature 277, 463–465.

Tissot, B., Pelet, R., 1981. Sources and fate of organic matter in ocean sediments. Oceanologica Acta, Proceedings 26th International Geological Congress 1980, special issue, 97–103.

Tissot, B., Vandenbroucke, M., 1983. Geochemistry and pyrolysis of oil shales. In: Miknis, F.P., McKay, J.F. (Eds.), Geochemistry and Chemistry of Oil Shales, ACS Symposium Series, vol. 230. American Chemical Society, Washington D.C, pp. 1–11.

Tissot, B.P., 1984. Recent advances in petroleum geochemistry applied to hydrocarbon exploration. American Association of Petroleum Geologists Bulletin 68, 545–563.

Tissot, B.P., Welte, D.H., 1984. Petroleum Formation and Occurrence, second ed. Springer Verlag, Berlin.

Tomic, J., Behar, F., Vandenbroucke, M., Tang, Y., 1995. Artificial maturation of Monterey kerogen (Type II-S) in a closed system and comparison with Type II kerogen: implications on the fate of sulfur. Organic Geochemistry 23, 647–660.

Trager, E.A., 1924. Kerogen and its relation to the origin of oil. American Association of Petroleum Geologists Bulletin 8, 301–311.

Turner, J.A., Thomas, K.M., Russell, A.E., 1997. The identification of oxygen functional groups in carbonaceous materials by oxygen K-edge XANES. Carbon 35, 983–992.

Tyson, R.V., 1995. Sedimentary Organic Matter – Organic Facies and Palynofacies. Chapman & Hall, London.

Tyson, R.V., 2005. Productivity versus preservation controversy: cause, flaws, and resolution. In: Harris, N.B. (Ed.), The Deposition of Organic Carbon-Rich Sediments: Models, Mechanisms and Consequences. SEPM (Society for Sedimentary Geology) Special Publication 82, Tulsa, Oklahoma, pp. 17–34.

Ungerer, P., 1993. Modelling of petroleum generation and migration. In: Bordenave, M.L. (Ed.), Applied Petroleum Geochemistry. Editions Technip, Paris, pp. 395–442.

Urban, N.R., Ernst, K., Bernasconi, S., 1999. Addition of sulfur to organic matter during early diagenesis of lake sediments. Geochimica et Cosmochimica Acta 63, 521–533.

Vail, P.R., Mitchum, R.M., Thompson, S.I., 1977. Seismic stratigraphy and global changes of sea level, Part 4: Global cycles of relative changes of sea level. In: Payton, C.E. (Ed.), Seismic Stratigraphy Applications to Hydrocarbon Exploration. American Association of Petroleum Geologists memoir 26, pp. 83–97.

Vairavamurthy, A., Mopper, K., 1987. Geochemical formation of organosulphur compounds (thiols) by addition of H_2S to sedimentary organic matter. Nature 329, 623–625.

van Bergen, P.F., Collinson, M.E., de Leeuw, J.W., 1993. Chemical composition and ultrastructure of fossil and extant salvinialean microspore massulae and megaspores. Grana 1 (Suppl.), 18–30.

van Bergen, P.F., Scott, A.C., Barrie, P.J., de Leeuw, J.W., Collinson, M.E., 1994a. The chemical composition of upper Carboniferous pteridosperm cuticles. Organic Geochemistry 21, 107–112.

van Bergen, P.F., Collinson, M.E., Hatcher, P.G., de Leeuw, J.W., 1994b. Lithological control on the state of preservation of fossil seed coats of water plants. In: Telnaes, N., van Graas, G., Øygard, K. (Eds.), Advances in Organic Geochemistry 1993, Organic Geochemistry, vol. 22. Pergamon Press, Oxford, pp. 683–702.

van Bergen, P.F., Goñi, M., Collinson, M.E., Barrie, P.J., Sinninghe Damsté, J.S., de Leeuw, J.W., 1994c. Chemical and microscopic characterization of outer seed coats of fossil and extant water plants. Geochimica et Cosmochimica Acta 58, 3823–3844.

van Bergen, P.F., Collinson, M.E., Briggs, D.E.G., de Leeuw, J.W., Scott, A.C., Evershed, R.P., Finch, P., 1995. Resistant biomacromolecules in the fossil record. Acta Botanica Neerlandica 44, 319–342.

van Bergen, P.M., Bull, I.D., Poulton, P.R., Evershed, R.P., 1997. Organic geochemical studies of soils from the Rothamsted Classical Experiments-I. Total lipid extracts, solvent insoluble residues and humic acids from Broadbalk Wilderness. Organic Geochemistry 26, 117–135.

van Buchem, F.S.P., Knox, R.W., 1998. Lower and middle Liassic depositional sequences of Yorkshire. In: Mezozoic and Cenozoic Sequence Stratigraphy of European Basins. SEPM (Society for Sedimentary Geology) Special Publication 60, Tulsa, Oklahoma, pp. 545–559.

van Buchem, F.S.P., Huc, A.Y., Pradier, B., Stefani, M., 2005. Stratigraphic patterns in carbonate source-rock distribution: second-order to fourth-order control and sediment flux. In: Harris, N.B. (Ed.), The Deposition of Organic Carbon-Rich Sediments: Models, Mechanisms and Consequences. SEPM (Society for Sedimentary Geology) Special Publication 82, Tulsa, Oklahoma, pp. 191–224.

Vandenbroucke, M., Albrecht, P., Durand, B., 1976. Geochemical studies on the organic matter from the Douala Basin (Cameroon). 3- Comparison with the early Toarcian shales, Paris Basin, France. Geochimica et Cosmochimica Acta 40, 1241–1249.

Vandenbroucke, M., 1980. Structure of kerogens as seen by investigations on soluble extracts. In: Durand, B. (Ed.), Kerogen, Insoluble Organic Matter from Sedimentary Rocks. Editions Technip, Paris, pp. 415–443.

Vandenbroucke, M., Pelet, R., Debyser, Y., 1985. Geochemistry of humic substances in marine sediments. In: McKnight, D.M., Aiken, G.R., Wershaw, R.L., MacCarthy, P. (Eds.), Humic Substances in Soil, Sediment and Water: Geochemistry, Isolation and Characterization. Wiley & Sons, New York, Chichester, pp. 249–273.

Vandenbroucke, M., Debyser, Y., Fabre, M., Montacer, M., Pillon, P., Jocteur-Monrozier, L., Jeanson, P., 1987. Géochimie de la matière organique du sondage MISEDOR. In: Géochimie Organique des Sédiments Plio-quaternaires du Delta de la Mahakam (Indonésie). Le sondage MISEDOR. Editions Technip, Paris, pp. 257–292.

Vandenbroucke, M., Bordenave, M.L., Durand, B., 1993. Transformation of organic matter with increasing burial of sediments and the formation of petroleum in source rocks. In: Bordenave, M.L. (Ed.), Applied Petroleum Geochemistry. Editions Technip, Paris, pp. 101–122.

Vandenbroucke, M., 2003. Kerogen: from types to models of chemical structure. Oil & Gas Science and Technology – Rev. IFP (Institut Français du Pétrole) 58, 243–269.

van Dongen, B.E., Schouten, S., Baas, M., Geenevasen, A.J., Sinninghe Damsté, J.S., 2003. An experimental study of the low-temperature sulfurization of carbohydrates. Organic Geochemistry 34, 1129–1144.

van Kaam-Peters, H.M.E., Sinninghe Damsté, J.S., 1997. Characterization of an extremely organic sulfur-rich 150 Ma old carbonaceous rock: palaeoenvironmental implications. Organic Geochemistry 27, 371–397.

van Kaam-Peters, H.M.E., Schouten, S., Köster, J., Sinninghe Damsté, J.S., 1998. Controls on the molecular and carbon isotopic composition of organic matter deposited in a Kimmeridgian euxinic shelf sea: evidence for preservation of carbohydrates through sulfurisation. Geochimica et Cosmochimica Acta 62, 3259–3283.

van Krevelen, D.W., 1961. Coal: Typology – Chemistry – Physics – Constitution, first ed. Elsevier, The Netherlands.

Van Krevelen, D.W., 1993. Coal: Typology – Chemistry – Physics – Constitution, third ed. Elsevier, The Netherlands.

Vassoevitch, N.B., Korchagina, Yu.I., Lopatin, N.V., Chernyshev, V.V., 1969. Principal phase of oil formation. Moscow University Vestnik 6, 3–37 (in Russian). English translation: International Geology Review 12, 1276–1296.

Versteegh, G.J.M., Blokker, P., Wood, G.D., Collinson, M.E., Sinninghe Damsté, J.S., de Leeuw, J.W., 2004. An example of oxidative polymerisation of unsaturated fatty acids as a preservation pathway for dinoflagellate organic matter. Organic Geochemistry 35, 1129–1139.

Villena, J.F., Dominguez, E., Stewart, D., Heredia, A., 1999. Characterization and biosynthesis of non-degradable polymers in plant cuticules. Planta 208, 181–187.

Vitorović, D., Amblès, A., Djordjević, M., 1984. Relationship between kerogens of various structural types and the products of their multistep oxidative degradation. Organic Geochemistry 6, 333–342.

Wakeham, S.G., Lee, C., 1993. Production, transport and alteration of particulate organic matter in the marine water column. In: Engel, M.H., Macko, S.A. (Eds.), Organic Geochemistry – Principles and Applications. Plenum Press, New York, pp. 145–169.

Wakeham, S.G., Sinninghe Damsté, J.S., Kohnen, M.E.L., de Leeuw, J.W., 1995. Organic sulfur compounds formed during early diagenesis in Black Sea sediments. Geochimica et Cosmochimica Acta 59, 521–533.

Wehling, K., Niester, C., Boon, J.J., Willemste, M.T.M., Wiermann, R., 1989. *p*-Coumaric acid – a monomer in the sporopollenin skeleton. Planta 179, 376–380.

Welte, D., 1974. Recent advances in organic geochemistry of humic substances and kerogen. A review. In: Tissot, B., Bienner, F. (Eds.), Advances in Organic Geochemistry 1973. Editions Technip, Paris, pp. 3–13.

Werne, J.P., Hollander, D.J., Behrens, A., Schaeffer, P., Albrecht, P., Sinninghe Damsté, J.S., 2000. Timing of early diagenetic sulfurization of organic matter: a precursor-product relationship in Holocene sediments of the anoxic Cariaco Basin, Venezuela. Geochimica et Cosmochimica Acta 64, 1741–1751.

Weser, G., Suess, E., Blazer, W., Liebeziet, G., Muller, P.J., Ungerer, C.A., Zenk, W., 1982. Fluxes of biogenic components from sediment trap deployment in circumpolar waters of the Drake Passage. Nature 299, 145–147.

Whelan, J.K., Thompson-Rizer, C.L., 1993. Chemical methods for assessing kerogen and protokerogen types and maturity. In: Engel, M.H., Macko, S.A. (Eds.), Organic Geochemistry – Principles and Applications. Plenum Press, New York, pp. 289–353.

White, W.D., 1915. Some relations in origin between coal and petroleum. Journal of the Washington Academy of Science 5, 189–212.

White, C.M., Douglas, L.J., Anderson, R.R., Schmidt, C.E., Gray, R.J., 1990. Organosulfur constituents in Rasa coal. In: Orr, W.L., White, C.M. (Eds.), Geochemistry of Sulfur in Fossil Fuels, ACS Symposium Series, vol. 429. American Chemical Society, Washington, DC, pp. 261–286.

Wiermann, R., Ahlers, F., Schmitz-Thom, I., 2001. Sporopollenin. In: Hofrichter, M., Steinbüchel, A. (Eds.), Biopolymers, Lignin, Humic Substances and Coal, vol. 1. Wiley-VCH, Weinheim, Germany, pp. 210–228.

Williams, M., Barghoorn, E.S., 1963. Biochemical aspects of the formation of marine carbonates. In: Breger, I.A. (Ed.),

Organic Geochemistry, Earth Series Monograph, vol. 16. Pergamon Press, Oxford, pp. 596–604.

Xiong, Y., Geng, A., 2000. Carbon isotopic composition of individual n-alkanes in asphaltene pyolysates of biodegraded crude oils from the Liaohe Basin, China. Organic Geochemistry 31, 1441–1449.

Yen, T.F., 1976. Structural aspects of organic components in oil shales. In: Yen, T.F., Chilingarian, G.V. (Eds.), Oil Shale, Developments in Petroleum Science, vol. 5. Elsevier, Amsterdam, pp. 129–148.

Yoshioka, H., Ishiwatari, R., 2005. An improved ruthenium tetroxide oxidation of marine and lacustrine kerogens: possible origin of low molecular weight acids and benzenecarboxylic acids. Organic Geochemistry 36, 83–94.

Zang, X., van Heemst, J.D.H., Dria, K.J., Hatcher, P.G., 2000. Encapsulation of protein in humic acid from a histosol as an explanation for the occurrence of organic nitrogen in soil and sediment. Organic Geochemistry 31, 679–695.

Zang, X., Nguyen, R.T., Harvey, H.R., Knicker, H., Hatcher, P.G., 2001. Preservation of proteinaceous material during the degradation of the green alga *Botryococcus braunii*: a solid-state 2D ^{15}N ^{13}C NMR spectroscopy study. Geochimica et Cosmochimica Acta 65, 3299–3305.

Zegouagh, Y., Derenne, S., Largeau, C., Bertrand, Ph., Sicre, M.-A., Saliot, A., Rousseau, B., 1999. Refractory organic matter in sediments from the North-West African upwelling system: abundance, chemical structure and origin. Organic Geochemistry 30, 101–117.

Zegouagh, Y., Derenne, S., Dignac, M-F., Barruiso, E., Mariotti, A., Largeau, C., 2004. Demineralisation of a crop soil by mild hydrofluoric acid treatment. Influence on organic matter composition and pyrolysis. Journal of Analytical and Applied Pyrolysis 71, 119–135.

Zimmerman, A.R., Goyne, K.W., Chorover, J., Komarneni, S., Brantley, S.L., 2004. Mineral mesospore effects on nitrogenous organic matter adsorption. Organic Geochemistry 35, 355–375.